IB/04/ 2252

PA 1232621

THE UNITED STATES OF AMERICA

TO ALL TO WHOM THESE PRESENTS SHALL COME:

UNITED STATES DEPARTMENT OF COMMERCE

United States Patent and Trademark Office

October 05, 2004

THIS IS TO CERTIFY THAT ANNEXED HERETO IS A TRUE COPY FROM THE RECORDS OF THE UNITED STATES PATENT AND TRADEMARK OFFICE OF THOSE PAPERS OF THE BELOW IDENTIFIED PATENT APPLICATION THAT MET THE REQUIREMENTS TO BE GRANTED A FILING DATE UNDER 35 USC 111.

APPLICATION NUMBER: ***60/505,161***
FILING DATE: ***September 24, 2003***

PRIORITY DOCUMENT
SUBMITTED OR TRANSMITTED IN COMPLIANCE WITH RULE 17.1(a) OR (b)

By Authority of the
COMMISSIONER OF PATENTS AND TRADEMARKS

L. Edelen

L. EDELEN
Certifying Officer

17667 U.S. PTO

09/24/03

PROVISIONAL APPLICATION COVER SHEET

This is a request for filing a PROVISIONAL APPLICATION under 37 CFR 1.53(c).

19587 U.S. PTO
60/505161
09/24/03

Docket Number 243238US0PROV

INVENTOR(s)/APPLICANT(s)

LAST NAME	FIRST NAME	MIDDLE INITIAL	RESIDENCE (CITY AND EITHER STATE OR FOREIGN COUNTRY)
AGOU	Fabrice		Paris, France
COURTOIS	Gilles		Paris, France
ISRAEL	Alain		Paris, France
VERON	Michel		Paris, France

■ Additional inventors are named on separately numbered sheets attached hereto.

TITLE OF THE INVENTION (280 CHARACTERS MAX)

SELECTIVE INHIBITION OF NF-KB ACTIVATION BY PEPTIDES DESIGNED TO DISRUPT NEMO OLIGOMERIZATION

CORRESPONDENCE ADDRESS

Customer Number
22850

Phone: (703) 413-3000

Fax: (703) 413-2220

ENCLOSED APPLICATION PARTS

■ Specification *Number of Pages:* 142 ☐ CD(s), Number

■ Drawing(s) *Number of Sheets:* 45 ■ Other (specify): Application Data Sheet
White Advance Serial Number Card

METHOD OF PAYMENT

☐ Applicant claims small entity status. See 37 CFR 1.27.

■ A check or money order is enclosed to cover the Provisional Filing Fees

☐ Credit card payment form is attached to cover the Provisional Filing Fees in the amount of ____

☐ The Director is hereby authorized to charge filing fees and credit any overpayment to Deposit Account Number 15-0030

PROVISIONAL FILING FEE AMOUNT $160.00

The invention was made by an agency of the United States Government or under a contract with an agency of the United States Government.

■ No.

☐ Yes, the name of the U.S. Government agency and the Government contract number are:

Respectfully Submitted,

9/24/03
DATE

Norman F. Oblon
Registration Number: 24,618

PROVISIONAL APPLICATION FILING ONLY

Vincent K. Shier, Ph. D.
Registration Number 50,552

The PTO did not receive the following listed item(s) - 1 Page(s) of Drawings

PROVISIONAL APPLICATION COVER SHEET

This is a request for filing a PROVISIONAL APPLICATION under 37 CFR 1.53(c).

			Docket Number 243238US0PROV
INVENTOR(s)/APPLICANT(s) Continued			
LAST NAME	FIRST NAME	MIDDLE INITIAL	RESIDENCE (CITY AND EITHER STATE OR FOREIGN COUNTRY)
TRAINCARD	Francois		Issy-les-Moulineaux, France
YAMAOKA	Shoji		BUNKYO-KU, Japan

General Description of the Technology

The present inventors have proven that NEMO constitutes a preferential target for the search for drugs inhibiting the NF-κB signaling path, because this protein acts upstream from the NF-κB activation path. The role of NEMO and its various domains was partially studied and published in the following article, *"NEMO trimerizes through its coiled-coil C-terminal domain."* J Biol Chem, 2002 May 17;277(20):17464-75. Agou F. et al., a copy of which is incorporated by reference and is filed herewith.

In the present invention, the inventors have synthesized peptides which mimic either the oligomerization domain (CC2 domain = approx. 40 residues), or the LZ motif (LZ domain = approx. 40 residues). The combination of these peptides alters either the oligomerization of NEMO or the combining thereof with the proteinic effector, in both cases inhibiting the NF-κB pathway.

In an aspect of the present invention, peptide drugs have been chemically combined with a peptide of 16 amino-acids in length (penetratin/antennapedia), thereby enabling intracellular transport thereof possible. The resulting peptides also may be chemically coupled with a fluorescent tracer in order to monitor internalization into B lymphocyte cell lines through FACS.

The action of these peptides was tested directly on B lymphocytes having stably integrated the beta-galactosidase carrier gene also bearing upstream from its promoter several NF-κB transcription factor (Clone C3) activation sites.

The present inventors have successfully been able to monitor the inhibitory effect of these peptides by measuring the same following stimulation of the B lymphocytes by LPS.

The results as a whole reveal that the presence of the peptide mimicking the "CC2" motif reduces the NF-κB activity by 70% as compared with a control peptide at a relatively

low dose of 20 μM. At this concentration, the effect of the "Leucine zipper" peptide is still more significant, since its presence in the medium completely eliminates cell response.

These new inhibitors of the NF-kB cellular signalling path offer a major advantage as anti-inflammatory compounds and also as anti-tumor compounds, which may be used for the treatment and/or prevention of cancers and other disorders.

The present invention relates to compounds, peptides, or compositions that are used for modulating the oligomerization of NEMO. In particular, the peptide compounds described in the manuscript entitled "Selective inhibition of NF-κB activation by peptides designed to disrupt NEMO oligomerization" by Agou et al, which constitutes in significant part the context of the present invention and is incorporated by reference in its entirety. The peptides may be in an isolated or coupled form with or without a vectorizing agent.

It is to be understood that the present invention also embraces peptides having at least 70% homology to those described in Agou et al, so long as the homologs possess said inhibitory activity. Methods for assessing activity are provided in the attached and incorporated references. The peptides of the present invention and the doses thereof are deemed to possess inhibitory activity when the NF-κB activity is reduced by at least 70% as compared with a control peptide.

The present invention also relates to pharmaceutical compositions containing said peptides, especially for the preparation of medicines used for the treatment of cancer.

Also embraced by the present invention are methods of obtaining, making, and identifying peptides and compounds that inhibit the NF-κB signaling pathway, in particular by means of the 70Z/3-C3 cellular line filed with the CNCM.

All of the contents of the references and papers submitted herewith are incorporated in their entirety in the present application and form the basis for the present invention.

Poster

Analyse du domaine d'oligomérisation de la protéine NEMO impliquée dans la régulation de la voie NF-κB

F. Traincard[1], B. Vinet[1], G. Courtois[2], A. Israël[2], M. Véron[1] & F. Agou[1]

[1]Unité de Régulation Enzymatique des Activités Cellulaires, CNRS URA 2185, [2]Unité de Biologie Moléculaire de l'Expression Génique, CNRS URA 2582, Institut Pasteur, 25 rue du Dr. Roux 75724 Paris cedex 15.

Email : traincar@pasteur.fr

La protéine NEMO (*NF-κB essentiel modulator*) qui joue un rôle crucial dans l'activation de la voie NF-κB (1), est associée aux protéines kinases IKK-α et -β pour former le complexe multiprotéique IKK. Bien que le mode d'activation d'IKK reste encore peu compris, l'activation des kinases implique probablement une phosphorylation en trans des deux kinases induite par l'oligomérisation de NEMO. Nous avons montré que le domaine C-terminal (résidus 241-388) est le domaine de trimérisation de NEMO (2). L'examen de la séquence polypeptidique indique que ce domaine est composé de deux motifs coiled-coils en tandem (CC2 et LZ), d'un motif riche en proline et d'un motif en doigt de zinc (ZF) situé à l'extrémité C-terminale de la chaine polypeptidique.

Nous avons produit chez *E. coli*, et purifié à homogénéité, des formes tronquées de NEMO contenant des combinaisons de ces motifs et nous avons comparé leurs propriétés d'assemblage par des expériences de filtration sur gel et de sédimentation à l'équilibre. Les résultats indiquent que le motif riche en proline et le motif ZF ne participent pas à l'oligomérisation de NEMO puisque le segment "CC2-LZ", délété de ces deux éléments, présente une constante d'association trimérique identique à celle de la protéine sauvage. Nous avons alors recherché lequel des motifs "coiled-coil" gouverne l'homo-association en utilisant des peptides de synthèse mimant les motifs CC2 ou LZ. Le peptide CC2 forme un homotrimère de 12,5 kDa, alors que le peptide LZ s'associe en homodimère de 10 kDa. Leurs constantes d'association sont cependant très fortement diminuées par rapport à celle du segment CC2-LZ (100 fois pour CC2 et 40 fois pour LZ), suggérant que le motif LZ participe à la formation du trimère CC2-LZ. Lorsque que les deux peptides CC2 et LZ sont combinés, ils forment un hétérohexamère stable. Leur interaction a été confirmée par polarisation de fluorescence au moyen de peptides couplés au Bodipy.

L'ensemble de ces résultats indique que le domaine de trimérisation de NEMO est un hétérohexamère résultant d'interactions homo- et hétérotypiques des coiled-coils LZ et CC2. La parenté structurale de cette protéine qui participe à la réponse immunitaire avec la famille des ecto-domaines des protéines d'enveloppes virales de type I sera discutée.

(1) S. Yamaoka et al., 1998 *Cell* 93, 1231-1240.

(2) F. Agou et al. 2002. *J.Biol.Chem.* 277, 17464-17475.

■ Protéomique de la microsporidie encephalitozoon cuniculi : application à la recherche de nouvelles protéines pariétales
C Texier , L Kuhn , D Brosson , J Garin et C Vivares

■ Membrane adsorbers: powerful tools for rapid protein purification in single spin columns et multiwell formats
R. Zeidler, A. Kocourek, C. Naumann, K. Kitzler, C. Kasper, O. Reif et C. Tinet

■ Analyse du domaine d'oligomérisation de la protéine NEMO impliquée dans la régulation de la voie NF-kB
F. Traincard, E. Vinolo, G. Courtois, A. Israël, M. Véron et F. Agou

■ Contrôle de la production de facteurs de virulence chez *Streptococcus pneumoniae*
Sabine Chapuy-Regaud, José Echenique, Marie-Claude Trombe

■ Remodelage de la népcarzinostatine
Magali Nicaise, Marielle Valerio, Philippe Minard et Michel Desmadril

■ Discussion du mécanisme de la chitine synthase à l'aide d'un analogue de substrat N-trifluoroacétylé et d'un test d'activité non radioactif.
Anne Vidal-Cros, Annie Piffeteau, Hubert Becker, Annie Thelland, Patricia Busca et Olivier Martin

■ Puces à protéines : développements technologiques
V. Dugas, S. Vigneron, JP. Cloarec, J. Wallach, MC. Ducloe, V. Bulone, E. Vnuk, M. Jaber, M. Cabrera, E. Souteyrand, JR. Martin

■ Etude de l'altération fonctionnelle de la protéine NEMO induite par une mutation donnant la pathologie EDA-ID
E. Vinolo, F. Agou et M. Véron

■ Des leurres peptidiques comme solution potentielle au problème des inhibiteurs chez les hémophiles A
S. Villard, S. Lacroix-Desmazes, D. Piquer, S. Grailly, J.M. Saint-Remy et C. Granier

■ Identification of new mitotic arrest inhibitors targeting human mitotic motors
S. De Bonis, D. Skoufias, L. Lebeau, R. H. Wade et F. Kozielski

■ Etude des enzymes impliquées dans la biosynthèse des phéromones chez la Drosophile
C. Wicker-Thomas, T. Chertemps, R. Dallerac, C. Labeur et J.-M. Jallon

X-Sender: fagou@mail.pasteur.fr
Date: Wed, 24 Sep 2003 14:14:51 +0200
To: mgfabry@pasteur.fr
From: Fabrice Ag u <fagou@pasteur.fr>
Subject: Fwd: Infos pratiques : Congres annuel de la SFBBM

Pour information

X-Sender: gaburjon@mail.ibcp.fr
Date: Wed, 24 Sep 2003 12:26:06 +0200
To: (Recipient list suppressed)
From: Christophe Geourjon <c.geourjon@ibcp.fr>
Subject: Infos pratiques : Congres annuel de la SFBBM
X-Spam-Status: No, hits=2.9 tagged_above=-999.0 required=5.0 tests=HTML_40_50, HTML_MESSAGE, MIME_HTML_ONLY, MIME_LONG_LINE_QP, TO_MALFORMED
X-Spam-Level: **

Bonjour,

Nous sommes maintenant à un peu plus d'un mois du prochain congrès annuel de la SFBBM. Il est donc temps de penser aux aspects d'intendance.

Ce mail vous confirme que votre inscription a bien été enregistrée pour le congrès : **"Post-génomique : de la protéine aux molécules bio-actives"** les 4 et 5 novembre 2003 sur le **BioPôle de Lyon-Gerland.**
Nous vous rappelons qu'une liste d'hôtels est disponible sur le site du congrès (http://www.ibcp.fr/SFBBM/html/infos.html). Ne tarder pas trop à effectuer vos réservations, les hôtels se situant aux alentours du centre étant déjà presque complets.

Lieu du congrès : Amphithéâtre Charles Merieux (Grand Amphithéâtre de l'ENS Science), Allée d'Italie, 69 007 Lyon. Le BioPôle de Lyon-Gerland se situe au sud de la Ville de Lyon, près du stade de Gerland. Un plan de situation général est disponible à l'adresse : http://www.ibcp.fr/SFBBM/pict/Plan_Lyon.pdf, un plan d'accès du quartier est disponible a l'adresse : http://www.ibcp.fr/SFBBM/pict/Plan_Quartier.pdf

Durant le congres, il est possible de laisser un message a votre intention au secretariat du congres : 04 72 72 80 84

Posters : Les dimensions maximales sont de 95 cm en largeur et 190 cm en hauteur.

Pour ceux qui le désirent, des fiches congrès SNCF (-20%) sont disponibles ; nous les demander par mail.
Le programme est disponible sur le site du congrès (http://www.ibcp.fr/SFBBM/html/programme.html). Le congrès débute le mardi 4 novembre à 9 heures pour s'achever le mercredi 5 novembre à 18 heures.

Nous sommes **340 participants.** Il est encore possible de s'inscrire jusqu'au 30 septembre sur le site Internet du congrès : http://www.ibcp.fr/SFBBM. Vous trouverez sur ce même site les **150 résumés des communications qui seront présentées.**

Dans l'attente de votre venue à Lyon,

Cordialement

Michel Desmadril et Christophe Geourjon

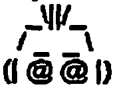

Dr. Christophe Geourjon, PhD | Tél : (33) (0)4 72 72 26 47
Pole BI Informatique Lyonnais | Fax : (33) (0)4 72 72 26 04
IBCP - CNRS UMR 5086 | e-mail : c.geourjon@ibcp.fr
7, Passage du Vercors | http://www.ibcp.fr
69 367 Lyon cedex 07, France | http://pbil.ibcp.fr

Dr. Fabrice AGOU
Unité de Régulation Enzymatique
des Activités Cellulaires
Département de Biologie Structurale et Chimie
INSTITUT PASTEUR
25 rue du Docteur Roux
75724 Paris Cedex 15

Tel: 331.45.68.83.80
Fax: 331.45.68.83.99
e mail: fagou@pasteur.fr
http://www.pasteur.fr/recherche/unites.html

INSTITUT PASTEUR

Direction de la Valorisation et des Partenariats Industriels

Service des Brevets et Inventions

N° de concertation [1] : BS-15 Date 25.11.02 Signature	DECLARATION D'INVENTION N° [2] : 2003_29 Date 6 Mars 2003 Signature Danielle BERNEMAN Chef du Service des Brevets & Inventions

1 *A remplir obligatoirement par le Relais de Valorisation (doc A)*
2 *A remplir obligatoirement par le Service des Brevets et Inventions*

1-DOSSIER ADMINISTRATIF

1-1 Titre de l'invention :

Nouvelle classe d'inhibiteurs spécifiques de la voie NF-kB agissant sur la protéine NEMO.

1-2 Inventeurs :
Indiquer les noms dans l'ordre devant figurer sur le texte de la demande de brevet.

Inventeur:	Nom :	Prénoms :	Nationalité :
	AGOU	Fabrice	Française

Domicile : 21 avenue du Bel-Air 75012 PARIS

Organisme employeur : INSTITUT PASTEUR

Date du contrat de travail ou du contrat de stage à l'IP : 01/08/1998

Fonctions exercées : Chargé de Recherche I.P.

Adresse professionnelle :

[1] campus Pasteur, nom du laboratoire et préciser si unité associée

Unité Régulation Enzymatique des Activités Cellulaires, Dpt. Biologie Structurale et Chimie, Institut Pasteur, 25 rue du Dr. Roux 75724 Paris cedex 15

1-2 Inventeurs :
Indiquer les noms dans l'ordre devant figurer sur le texte de la demande de brevet.

Inventeur:	Nom :	Prénoms :	Nationalité :
	COURTOIS	Gilles	Française

Domicile : 157 rue de Ménilmontant - 75020 PARIS

Organisme employeur : I.N.S.E.R.M

Fonctions exercées : D.R.2

Date du contrat de travail : ou du contrat de stage à l'IP 01/09/92

Adresse professionnelle :

1 campus Pasteur, nom du laboratoire et préciser si unité associée

Unité de Biologie Moléculaire de l'expression génique, Dpt Biologie Cellulaire et Infection, 25 rue du Docteur Roux, 75724 Paris cedex 15

1-2 Inventeurs :
Indiquer les noms dans l'ordre devant figurer sur le texte de la demande de brevet.

Inventeur:	Nom :	Prénoms :	Nationalité :
	ISRAEL	Alain	Française

Domicile : 20 rue Daguerre - 75014 PARIS

Organisme employeur : INSTITUT PASTEUR

Fonctions exercées : Directeur de l'évaluation scientifique, Chef d'unité

Date du contrat de travail : ou du contrat de stage à l'IP 01/01/83

Adresse professionnelle :

1 campus Pasteur, nom du laboratoire et préciser si unité associée

Unité de Biologie Moléculaire de l'Expression Génique, Dpt Biologie Cellulaire et Infection, 25 rue du Docteur Roux, 75724 Paris cedex 15

1-2 Inventeurs :
Indiquer les noms dans l'ordre devant figurer sur le texte de la demande de brevet.

Inventeur:	Nom :	Prénoms :	Nationalité :
	VERON	Michel	Française

Domicile : 16 rue de Fourcy 75004 Paris

Organisme employeur : INSTITUT PASTEUR (C.N.R.S, URA)

Fonctions exercées : Chef du Département B.S.C., Chef d'unité

Date du contrat de travail : ou du contrat de stage à l'IP 1/01/77

Adresse professionnelle :

1 campus Pasteur, nom du laboratoire et préciser si unité associée

Unité Régulation Enzymatique des Activités Cellulaires, Dpt. Biologie Structurale et Chimie, Institut Pasteur, 25 rue du Docteur Roux, 75724 Paris cedex 15

1-2 Inventeurs :
Indiquer les noms dans l'ordre devant figurer sur le texte de la demande de brevet.

Inventeur:	**Nom :**	**Prénoms :**	**Nationalité :**
	Yamaoka	**Shoji**	**Japonaise**

Domicile :

Organisme employeur : **Tokyo Medical and Dental University** **Date du contrat de travail : 03/96 au**
ou du contrat de stage à l'IP 03/99

Fonctions exercées : **Associate Professor**

Adresse professionnelle :

Institut Pasteur, nom du laboratoire et préciser si unité associée

Si d'autres inventeurs sont associés, ajouter les informations les concernant sur une feuille séparée.

1-3 Contribution de chaque inventeur :

1-3-1 Indiquer succinctement la nature de la contribution à l'invention de chaque inventeur :

- Fabrice AGOU: Conception des inhibiteurs spécifiques de la voie NF-kB. Mise au point des tests expérimentaux et évaluation de l'efficacité des drogues.

- Gilles Courtois et S. Yamaoka: Identification de la proteine NEMO et des sous-domaines fonctionnelles.

- Michel Véron: Mise en place logistique de l'invention

- Alain Israël: Identification de la proteine NEMO et du facteur de transcription NF-kB impliqué dans la réponse inflammatoire, immunitaire et anti-apoptotic.

1-3-2 Pourcentage de participation à l'invention pour chaque inventeur :

Inventeur :	**% Participation :**
Fabrice Agou	**24.5 %**
Gilles C urtois	**17 %**

Alain Israël	17 %
Michel Véron	24.5 %
Yamaoka Shoji	17 %

1-4 Financement :

Origine et montant du (des) financement(s) ayant mené à l'invention et date et référence du financement (Institut Pasteur, Appels d'offres, PTR, GPH,OMS, CE, MESR INRA , partenaires industriels, etc.).

1-4-1 Pour un laboratoire IP

Origine : Montant : 6000 ☒ Euro

PTR Pasteur-Necker n°74

Institut Pasteur

C.N.R.S.

1-4-2 Pour un laboratoire extérieur

Origine : Montant : ☐ Euro

1-5 Divulgation de l'invention

Il est rappelé que la protection d'une invention ayant divulgation est toujours la situation la plus efficace en terme de valorisation

1-5-1 L 'invention a-t-elle déjà fait l'objet d'une divulgation orale ou écrite par votre laboratoire ou une autre équipe ? Si oui, préciser les références et la date.

☐ Oui ☒ Non Références : Date :

1-5-2 L'invention doit-elle faire l'objet par votre laboratoire d'une publication,d'une communication orale, d'une soutenance de diplôme* ou d'une affiche.

**Possibilité de demander une soutenance à huis clos (attestation à faire valider par l'université, document pré-établi au SBI).*

1ère soumission	☐ Oui	☒ Non	Si oui Date :
Soumission après corrections	☐ Oui	☒ Non	Si oui Date :
Bon à tirer	☐ Oui	☒ Non	Si oui Date :
Prévision de divulgation y compris résumé congrès/séminaire:			
- Publication en ligne	☐ Oui	☒ Non	Si oui Date :
- Publication journal	☐ Oui	☒ Non	Si oui Date :

1-6 Renseignements complémentaires *(si nécessaire)* :

L'ensemble des résultats fera l'objet d'une publication scientifique

Date et signature : 02/12/2002

DI N°

2-SCIENTIFIC FILE (CONFIDENTIAL NOTICE)

2-1-2 Abstract In response to a wide variety of stimulus like the pro-inflammatory cytokines (TNF-alpha, IL-1), endotoxines (LPS etc....), most cells activate a series of genes involved in the inflammatory and immune responses as well as in oncogenesis and apoptosis. The majority of these genes are under the control of NF-kB transcription factor whose activation is controled by a high molecular weight protein complex called IKK complex. This "signalosome" is composed of at least three components. Two of them IKK-alpha and IKK-beta have protein kinase activity whereas the third one, NEMO (also called IKK-gamma) is a regulatory protein which takes part in their activation. The presence of NEMO is crucial since fibroblast and B-lymphocytes cells deleted for the NEMO gene are unable to activate NF-KappaB after LPS or cytokine stimulation. Finding new molecules specifically inhibiting the NF-kB pathway is of great interest because it would lead to the emergence of new drugs acting as anti-inflammatory drugs and also as chemotherapeutic drugs in cancer models. NEMO constitutes a strategic protein target because it acts upstream of the NF-kB pathway and coordinates several molecular signals coming from stimulated receptors. For better understanding the molecular mechanism by which NEMO activates the IKK-alpha and -beta protein kinases, we developed a functional complementation assay in vivo and we studied the biochemical properties of wild type and mutant proteins after expression and purification in E. coli. NEMO is organized in three domains, each one composed of coiled coil motifs. The N-terminal domain is the IKK kinase-binding domain. The C-terminal domain can be divided into two sub-domains: the first one called "CC2", is responsible for the oligomerization of the protein while the second, which is made up of a leucine zipper motif and of a zinc finger motif, constitutes a functional unit necessary to the specific interaction with a not yet identified protein effector. We have synthesized peptides which mimic either the domain of oligomerization (motif CC2 = 38 residues) or the LZ domain (LZ motif = 40 residues) involved in the hetero-association with a protein effector. These peptides could interfere either with the oligomerization of NEMO, or with its binding to the protein effector. In both cases, peptides were identified as strong inhibitors of the NF-kB pathway. The peptides were chemically linked to a permeant peptide known as penetratin/antennapedia. They were also coupled with a fluorescent marker in order to follow their internalization in _-lymphocytes by F.A.C.S. The anti-inflammatory effects of these peptides were tested directly on lines of _-lymphocytes stably transfected by a reporter plasmid which bears the _-galactosidase gene and several NF-_B sites upstream of its promoter. Inhibitor effects of these peptides were measured using these suspension-cultured lymphocytes B in 96-well plates after LPS stimulation. Our results show that the presence of the "CC2" at 20 µM reduces the inflammatory response of 70% as compared to a mutant peptide control. At the same concentration, the "leucine zipper" peptide is more significant since its presence totally abolish the inflammatory response of cells.

Date et signature : 02 décembre 2002

2-2 Documents à joindre :

Pour chaque document joint, veuillez reporter le n° de concertation donné à votre DI

2-2-1 Données expérimentales, les résumés et/ou les articles en préparation.

2-2-2 Articles les plus pertinents ayant un rapport avec le projet.

2-2-3 Esquisses, dessins, photographies ou tout autres documents qui pourront aider à la description de l'invention.

(Les données brutes, les feuilles volantes, les dessins au crayon ou les photos Polaroïds sont acceptables si elle forment un ensemble cohérent et compréhensif).

2-2-4 L'appareil, le produit ou le procédé a-t-il été créé ou testé. Dans l'affirmative, en existe-t-il un échantillon ou une maquette? Une démonstration peut-elle être réalisée ?

2-3 Description simplifiée :

L'invention est-elle une nouvelle technique, formulation, outil ou produit (s), est-elle une nouvelle utilisation ou une amélioration d'un produit ou d'une technique existante ?

L'invention est un nouveau produit qui inhibe la voie NF-kB. Ce produit ou les dérivés peptidomimétiques qui en découleront peuvent être d'un intérêt majeur pour un usage thérapeutique et/ou en biotechnologies.

2-4 Mots clés

En vous référant aux tableaux des mots clés et aux domaines des pathologies des pages suivantes choisissez les mots clés et les pathologies les mieux appropriés pour définir les principales caractéristiques de votre invention.

4-1 Technologies utilisées : cochez le mot clé qui décrit le domaine de votre invention (1 à 6 mots clés)

Application	Chemistry	Diagnostics	Genomics	Therapeutic	Technology	Screening	Vaccine
Additives ☐	Additives ☐	Antibody ☐	allele ☐	analgesic ☐	antibiotic resistance ☐	biochip ☐	adjuvant ☐
Aquaculture ☐	alternative energy ☐	assay ☐	bioinformatic ☐	anaesthetic ☐	antibody ☐	cellular assay ☒	anatoxin ☐
Bacterial selection ☐	Antioxidants ☐	bacterial ☐	cDNA ☐	angiogenesis ☐	bacterial identification ☐	combinatorial biology ☐	anticancer ☐
Bacterial contamination ☐	Catalyst ☐	biochip ☐	database ☐	antibiotic/ antibacterial ☐	biological material ☐	genetic diseases ☐	attenuated live ☐
Biopesticides ☐	Coatings ☐	contrast agent ☐	epidemiology ☐	antibody ☐	cell line ☒	high throughput screening ☐	carbohydrate (polysaccharide) ☐
Bioremediation ☐	effluent treatment ☐	detection ☐	EST ☐	anticancer ☒	chromatography ☐	phage display ☐	conjugate ☐
Breeding ☐	exhaust treatment ☐	DNA probe ☐	gene ☐	antifungal ☐	culture ☐	screen ☐	dead entire ☐
Fermentation ☐	Foams ☐	Kits ☐	homologue ☐	anti-inflammatory ☒	directed evolution ☐	target ☒	delivery system (plasmid..) ☐
Fertilizer ☐	food chemistry ☐	fungal ☐	interactome ☐	antisense ☐	DNA/RNA sequencing ☐		human use ☐
Food ☐	Gels ☐	imaging ☐	isogene ☐	antiviral ☐	DNA/RNA synthesis ☐		hybrid ☐
Forestry ☐	Monomers ☐	immunoassay ☐	library ☐	apoptosis ☒	electrophoresis ☐		injectable administration ☐
Growth ☐	Oxidation ☐	in situ ☐	pharmacogenomics ☐	cell signalling ☒	enzyme ☐		live recombinant V. (LRV) ☐
Nitrogen fixation ☐	Remediation ☐	marker ☐	polymorphism ☐	disease model ☐	equipment ☐		mucosal administration ☐
Ornamental ☐	Solvents ☐	MRI ☐	positional cloning ☐	drug delivery ☐	expression system ☐		naked DNA ☐
Pesticides ☐		parasitic ☐	proteomics ☐	drug design ☒	fermentation ☐		peptide ☐
Plant ☐		point of use ☐	receptor ☐	fertility ☐	GFP ☐		polyvalent ☐
Remittance ☐		radioisotope ☐	RNA ☐	gene therapy ☐	hybridization ☐		prophylactic ☐
Seeds ☐		transgenic ☐	target validation ☐	hormone ☐	mutagenesis ☐		protected (encapsulation) ☐
tissue culture ☐		ultrasound ☐	screening ☐	immunotherapy ☐	oligonucleotide synthesis ☐		screening method ☐
Transgenic ☐		viral ☐		natural product ☐	PCR ☐		Sub-unit (molecular) ☐
Vegetable ☐				peptides ☒	protein sequencing ☐		sugar peptide mimic ☐
Veterinary ☐				pro-drug ☐	protein synthesis ☐		therapeutic ☐
				proteins ☐	reagent ☐		veterinary use ☐
				small molecule ☐	software ☐		
				vaccine ☐	(mass) spectroscopy ☐		
				wound healing ☐	transgenesis ☐		
				☐	vector ☐		

2-4-2 Domaines de pathologies

Veuillez cocher une à trois (1-3) cases correspondant aux mots clés pouvant caractériser les domaines pathologiques concernés par votre invention.

Infections bactériennes

Charbon bactérien/*Anthrax*		Leptospirose	
Arthrite infectieuse (*M. xenopi*)	☐	Listériose	☐
Botulisme (Clostridium)		Maladie de Lyme (*B. burgdorferi*)	☐
Bronchite (*S. pneumoniae, H. influenzae*)	☐	Méningite (*H. influenzae*, Méningocoque)	☐
Brucellose/fièvre maltе	☐	Otite	☐
Chlamydiose (infection urétro-cervicale)	☐	Peste (*Yersinia*)	☐
Choléra (*Vibrio cholerae*)	☐	Pneumonie (Pneumocoque, Staphylocoque)	☐
Coqueluche (*Bordetella pertussis*)	☐	Rhumatisme articulaire aigu (Streptocoque)	☐
Diphtérie (*Corynebacterium*)	☐	Rickettsiose	☐
Dysenterie bacillaire (Shigellose)	☐	Rougeole/ *Measles*	☐
Fièvre typhoïde (*Salmonella typhi*)	☐	Syphilis (*Treponema*)	☐
Infection cutanée (*Staphylo,Streptocoque*)	☐	Tétanos	☐
Infection à *E. coli*	☐	Tuberculose (*Mycobacterium tuberculosis*)	☒
Légionellose	☐	Ulcère et adénocarcinome dus à *H. pylori*	☒
Lèpre (*Mycobacterium leprae*)	☐	Autre	☐

Infections virales

Cancer dû au Papillomavirus humain HPV	☐	Méningite virale	☐
Diarrhée infantile due au Rotavirus	☐	Mononucléose infectieuse (EBV)	☐
Encéphalite virale	☐	Oreillons	☐
Fièvre aphteuse (Picornavirus)	☐	Poliomyélite à Entérovirus	☐
Fièvre hémorragique (Dengue, Ebola, Lassa)	☐	Rage (Rhabdoviridae)	☐
Fièvre jaune (Flavivirus)	☐	Rhume	☐
Grippe (Orthomyxovirus)/ Flu	☐	Rougeole (Virus morbilleux)	☐
Herpès génital (Herpesvirus)	☐	Rubéole (Rétrovirus)	☐
Hépatites A, B, C, D, E	☐	SIDA (HIV1/2)	☐
Immunodépression à Cytomégalovirus	☐	Varicelle (Herpesvirus)	☐
Infection respiratoire (Paramyxovirus)	☐	Variole (Poxvirus)	☐
Lentivirus SIDA	☐	Zona (Herpesvirus)	☐
Leucémie et paralysie dues au HLV-1	☐	Autre	☐

Infections parasitaires

Amibiase	☐	Maladie de Chagas	☐
Bilharziose	☐	Maladie du sommeil	☐
Cysticercose	☐	Malaria	☐
Distomatose	☐	Onchocercose	☐
Elephantiasis filarien	☐	Pneumocystose	☐
Echinococcose	☐	Schistosomiase	☐
Filariose	☐	Toxoplasmose	☐
Gale	☐	Trichinellose	☐
Leishmaniose	☐	Trypanosomose	☐
		Autre	☒

Mycoses

Aspergillose	☐
Candidose	☐
Cryptococcose	☐
Histoplasmose	☐
Nocardia	☐
Pneumocystose	☐
Autre	☐

Autres domaines de pathologies

Cancérologie	☒
Cardio-vasculaire	☐
Dermatologie	☒
Embryologie	☐
Endocrinologie	☐
Gastro-intestinal	☒
Gynéco-obstétrique	☐
Hématologie	☒
Hépatique	☐
Immunitaire	☒
Métabolique	☐
Musculaire	☐
Neurologie	☐
Ophtalmologie	☐
Oto-Rhino-Laryngologie	☐
Psychiatrie	☐
Respiratoire	☐
Urogénital	☐
Autres	☐
	☐

2-4-3 Les Maladies.

Ecrivez de 1 à 5 mots clés pour identifier d'autres maladies plus spécifiques (exemple : le diabète)

Ostéoarthrite Arthrite rhumatoïde

2-4-4 Définition libre.

Pour décrire votre invention plus précisément, vous pouvez indiquer 5 mots clés non inclus dans les précédentes catégories.

drogue peptidique inhibiteurs de la voie NF-kB anti-inflammatoire anticancéreux chimie thérapeutique

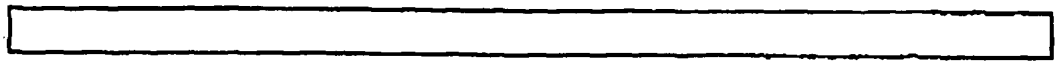

2-5 Nouveauté de l'invention

A partir de la description, mettez l'accent sur les nouveautés et le caractère original de l'invention.

Ces nouvelles molécules représentent une nouvelle classe d'inhibiteur de la voie NF-kB (i) car elles interviennent très tôt dans la processus d'activation du facteur de transcription NF-kB (ii) leurs actions inhibitrices qui reposent sur une interaction spécifique avec la protéine cible NEMO, ne s'exercent qu'après stimulation par les cytokines pro-inflammatoires; contrairement à la plupart des inhibiteurs enzymatiques de la kinase IKK-b recherchés actuellement par des grands groupes pharmaceutiques.

En quoi l'invention diffère-t-elle de technologies déjà existante ?

Sans objet

Quel problème permet-elle de résoudre, et avec quels avantages ?

Sans objet

2-6 Applications industrielles de l'invention

Si cela n'a pas été indiqué précédemment, quelles sont les principales applications de l'invention ? En plus des débouchés immédiats, d'autres applications pourraient-elles être envisagées éventuellement ?

-Sur le marché des biotechnologies, il n'existe qu'un seul inhibteur spécifique de la voie NF-kB dont la concentration effective est très élevée. Nos produits plus spécifiques présentent donc un atout majeur pour toutes les entreprises intéressées par des inhibiteurs spécifiques de la voie NF-kB.

- Sur le marché des entreprises pharmaceutiques, notre invention ou les produits qui peuvent en dériver peuvent donner lieu à un usage thérapeutique comme anti-inflammatoire et comme anti-cancéreux.

2-7 Limites de l'invention

L'invention présente-t-elle des inconvénients ou des limitations ? Peuvent-ils être surmontés ? De quelle manière ?

Le coût de la synthèse chimique des peptides par les biotechnologies peut présenter un handicap.

En outre, ceux sont des drogues peptidiques. Par conséquent, l'invention à usage thérapeutique est soumise aux mêmes contraintes relevant de traitements thérapeutiques par des peptides.

2-8 Autres informations

2-8-1 Existe-il un élément de l'invention (Biologique ou autre) vous ayant été fourni par une autre institution ou entreprise et ayant fait l'objet d'un accord signé de Transfert de Matériel (MTA) ? Dans l'affirmative, précisez la nature de cet élément, sa date de réception et les coordonnées du fournisseur.

Nature:	Date de réception :	Coordonnées du fournisseur :

2-8-2 Existe-il, à la connaissance de l'inventeur, d'autres brevets ou publications concernant l'invention ?

(Une recherche parmi les brevets existants a-t-elle été effectuée ? Dans l'affirmative, avec quels résultats ?)

☐ Oui ☒ Non

2-8-3 L'invention présente-t-elle un intérêt commercial immédiat ? Précisez le nom des compagnies ou des personnes si possible.

Toutes entreprises de biotechnologies intéressées dans la transduction du signal et dans les inhibiteurs spécifiques de la voie NF-kB.

Toutes les entreprises pharmaceutiques intéressées par des nouvelles molécules agissant comme anti-inflammatoires et comme anti-cancéreux.

Donnez la liste d'autres entreprises potentiellement intéressées :

Utilisez cet espace pour développer et fournir des données complémentaires sur l'invention

2-8-4 Les cahiers de laboratoire et autres données concernant l'invention sont-ils disponibles ? Indiquez leur référence et leur emplacement, sans les joindre.

Référence :	Emplacement :
Nº012766, 012768, 009319	Batiment Monod, unité REAC, pièce 07

Compléments d'informations techniques

I. Lignée cellulaire et plasmide

Les cellules "C3" sont issues d'une lignée murine de lymphocyte pré-B appelée, 70Z/3. $4x10^6$ cellules dans 400 µl de milieu complet (RPMI 1640 with Glutamax-1 contenant 100 µg/ml de pénicilline, 100 µg/ml de streptomycine et 10% de sérum (FCS)) ont été transfectées par électoporation (260V 1500 µF, résistance infinie) par 8 µg d'un plasmide portant le gène rapporteur de la bêta galactosidase (Lac-Z) sous le contrôle d'un promoteur minimal de l'IL-2 et de 3 sites NF-κB (Fiering et al., 1990). Le plasmide porte également un gène de résistance à l'hygromycin B comme marqueur de sélection des eucaryotes et d'un gène de résistance à l'ampicilline. Les clones positifs ont été sélectionnés en présence d'hygromycin B puis dilution infinie. Les clones isolés et résistants à l'hygromycin B ont été testés pour leur capacité à exprimer la bêta-galactosidase. Le clone "C3" qui présentait un bon niveau d'expression de la bêta-galactosidase a été retenu.

II. Internalisation des drogues

La vectorisation des drogues a été suivie à l'aide d'un FACS calibur (BD Biosciences) en mesurant l'intensité de fluorescence relative du Bodipy®-FL (Molecular Probes). L'internalisation a été effectuée en fusionnant par synthèse chimique nos séquences peptidiques d'intérêt à celles d'antennapedia/penetratin (Derossi et al., 1996). D'autres séquences de vectorisation peptidique auraient pu être utilisées et sont indiquées dans le Tableau 1.

Tableau 1: Séquences de vectorisation peptidiques permettant d'internaliser des macromolécules.

Nom	Source	Séquence en acide aminé	Référence
Tat	HIV-1 Tat (47-57)	YGRKKRRQRRR	Vives et al., 1997
Polyargimine	Synthèse chimique	RRRRRRRR	Suzuki et al., 2002
Kaposi FGF	Kaposi FGF	AAVALLPAVLLAL LAP	Lin et al., 1995
Grb2	Grb2 (SH2 domain)	AAVLLPVLLAAP	Rojas et al., 1998

III. Les inhibiteurs peptidiques : séquence, purification et synthèse.

Les peptides ont été synthétisés par F. Baleux de l'unité de Chimie Organique de l'Institut Pasteur dirigée par Dinh Tam Huynh comme décrit dans Mousson et al. Ils ont été synthétisés en phase solide selon la méthode de Merrifield à l'aide d'un synthétiseur automatique peptidique (Pioneer, Applied Biosystems, Inc., Foster, CA; Valenzuela-Fernandez et al., 2002). Afin de favoriser leur stabilité *in vivo*, chaque résidu amino-terminal a été acétylé sur son groupement α-NH_2 et chaque résidu carboxy-terminal a été modifié par amidation comme décrit dans Mousson et al. Certaines fractions des peptides synthétisés ont été couplées au Fluorophore Bodipy®FL N-(2-aminoethyl)maleimide de chez Molecular Probes (B-10250) afin de suivre leur internalisation par FACS comme mentionné ci-dessus. Les séquences biologiquement actives miment les séquences de la protéine NEMO murine (Accession number of the NIH genetic sequence database (Gene®bank), NP_034677). Elles correspondent soit au motif "CC2" (résidus 248-287), soit au "motif leucine zipper" (résidus 294-336). Les séquences de NEMO murines ou humaines sont indiquées ci-dessous (Figure 1).

"CC2 WT" de souris : SKGMQLEDLRQQLQQAREALVAKQELIDKLKEEAEQHKIV

"LZ" de souris : LKAQADIYKADFQAERHAREKLVEKKEYSQEQLEQSQREFNKL

"CC2 humaine": KRGMQLEDLKQQLQQAEEALVAKQEVIDKLKEEAEQHKIV

"LZ" humaine : LKAQADIYKADFQAERQAREKLAEKKELLQEQLEQLQREVSKL

Figure 1: Séquences humaine et murines biologiquement actives dans l'inhibition de la voie NF-κB. Les résidus qui diffèrent dans la séquence humaine ou murine sont soulignés

Afin de rendre les peptides perméables à la membrane cellulaire, une séquence peptidique de 16 résidus appelée antennapedia/penetratin et découverte par A. Prochiantz (Derossi et al., 1996) a été fusionnée aux différentes séquences de la protéine NEMO par synthèse chimique comme décrit ci-dessus. Tous les peptides possèdent en outre un résidu cystéine à l'extrémité N-terminale pour greffer spécifiquement le fluorophore. D'autres résidus naturels ou non naturels auraient pu être synthétisés à la place de la cystéine pour greffer le fluorophore. En outre, l'usage du fluorophore Bodipy®FL de chez Molecular Probes n'est pas exclusif et d'autres fluorophores auraient pu être utilisés. L'ensemble de ces peptides a été vérifié par spectrométrie de masse. Leur composition ainsi que leur titration ont été déterminées après hydrolyse acide (6N HCl, 20 h) et analyse des acides aminés à l'aide d'un analyseur Beckman 6300 comme décrit dans Mousson et al..

IV. Test d'inhibition de la voie de signalisation NF-κB

Dans un premier protocole 2.2 $x10^5$ cellules (clone C3) dans 220 μl de milieu complet (10^6 cellules/ml) ont été déposées dans un puit d'une plaque à 96 puits (TPP, référence T9297) puis incubées avec des concentrations variables de peptide (0.2 à 20 μM) à 37°C dans un incubateur à 5% CO_2. Après 2 h d'incubation, chaque lot de cellules est réparti dans deux

nouveaux puits contenant chacun 100 µl de cellules (10^5 cellules). Chaque lot de cellules est ensuite soit stimulé 5 h par 3 µl de lipolysaccharide bactérien (référence L6636, Sigma) à une concentration de 0.5 µg/µl, soit non stimulé par addition de 3 µl de PBS (Phosphate buffer saline, contrôle). Après stimulation, les cellules sont lavées trois fois par centrifugation à 400 x g et resuspendues dans 250 µl de tampon PBS froid. À la dernière centrifugation, les cellules sont reprises dans 100 µl d'un tampon de lyse cellulaire (25 mM Tris-phosphate pH 7.8 contenant 8 mM chlorure de magnésium, 1 mM dithioerythreitol, 1 % Triton x 100 et 15 % glycérol). Le matériel biologique insoluble est alors précipité par centrifugation à 3000 x g 20 min à 4°C et le surnageant correspondant à l'extrait brut, est récupéré. L'activité de la β-galactosidase a été mesurée en prélevant 30 µl d'extrait brut et en incubant 1 heure 200 µl d'un mélange de tampons fournis par "le kit de détection luminescente de la β-galactosidase" (BD Biosciences, référence K2048-1). Ce test enzymatique utilise le substrat "Galacton-star" qui devient luminescent après clivage spécifique par la β-galactosidase (Bronstein et al., 1989). La réaction enzymatique de la β-galactosidase a ainsi pu être suivie à l'aide d'un luminomètre (Berthold).

Un second protocole très similaire à celui décrit plus haut a été mis au point afin de tester la stabilité des inhibiteurs peptidiques *in vivo*. Dans ce dernier protocole, les cellules (2.2×10^5 cellules dans 220 µl de milieu) sont lavées 3 x par du tampon PBS après une inbubation de 2 heures avec les peptides inhibiteurs. Les cellules sont ensuite diluées dans un rapport 1:3 avec du sérum complet (70 µl de cellules dans 140 µl de milieu) et sont disposées 20 heures dans l'incubateur à 5% de CO_2 pour favoriser leur division cellulaire. Les étapes qui suivent sont identiques à celles décrites plus haut.

RÉFÉRENCES BIBLIOGRAPHIQUES

Bronstein, I., Edwards, B. and Voyta, J.C. (1989). "1, 2-dioxetanes:novel chemiluminescent enzyme substatres: applications to immunoassays". J. Chemilumi. Biolum. 4: 99-111

Derossi, D., Calvet, S., Trembleau, A., Brunissen, A., Chassaing, G. and Prochiantz, A. (1996). "Cell internalization of the third helix of the Antennapedia homeodomain is receptor-independent". Journal of Biological Chemistry 271: 18188-93.

Fiering, S., Northrop, J.P., Nolan, G.P., Mattila, P.S., Crabtree, G.R. and Herzenberg, L.A. (1990). "Single cell assay of a transcription factor reveals a threshold in transcription activated by signals emanating from the T-cell antigen receptor". Genes & Development 4: 1823-34.

Futaki, S., Suzuki, T., Ohashi, W., Yagami, T., Tanaka, S., Ueda, K. and Sugiura, Y. (2001). "Arginine-rich peptides. An abundant source of membrane-permeable peptides having potential as carriers for intracellular protein delivery". Journal of Biological Chemistry 276: 5836-5840.

Mousson, F., Coic, Y.M., Baleux, F., Beswick, V., Sanson, A. and Neumann, J.M. (2002). "Deciphering the role of individual acyl chains in the interaction network between phosphatidylserines and a single-spanning membrane protein". Biochemistry 41: 13611-6.

Lin, Y.Z., Yao, S.Y. and Hawiger, J. (1996). "Role of the nuclear localization sequence in fibroblast growth factor-1-stimulated mitogenic pathways". Journal of Biological Chemistry 271: 5305-5308.

Rojas, M., Donahue, J.P., Tan, Z. and Lin, Y.Z. (1998). "Genetic engineering of proteins with cell membrane permeability". Nature Biotechnology 16: 370-375.

Valenzuela-Fernandez, A., Planchenault, T., Baleux, F., Staropoli, I., Le-Barillec, K., Leduc, D., Delaunay, T., Lazarini, F., Virelizier, J.L., Chignard, M., Pidard, D. and Arenzana-Seisdedos, F. (2002). "Leukocyte elastase negatively regulates Stromal cell-derived factor-1

(SDF-1)/CXCR4 binding and functions by amino-terminal processing of SDF-1 and CXCR4". Journal of Biological Chemistry 277: 15677-89.

Vives, E., Brodin, P. and Lebleu, B. (1997). "A truncated HIV-1 Tat protein basic domain rapidly translocates through the plasma membrane and accumulates in the cell nucleus". Journal of Biological Chemistry 272: 16010-16017.

DL 2003-29 20/03/03

SPS
DL
CNRS
INSERM

NEMO : rendements de synthèse et masses expérimentales

		Nombre de résidus	M.W.	Rendement Synth+purif couplage	Masse expérimentale
CC2 w.t.	Fragment court	35	4155,75	25	4155,86+/-0,53
	Cys-antenna-linker	57	7019,30	7	7019,08+/-0,68
	bodipy	57	7433,51	62	7433,33+/-0,46
	acétamide	57	7076,36	32	7076,42+/-0,06
	biotine	57	7544,91	53	7545,25+/-0,09
NNN-LZ w.t.	Fragment court	43	5318,08	20	5318,21+/-0,50
	Cys-antenna	60	7649,99	4	7650,33+/-0,47
	bodipy	60	8064,20	40	8063,90+/-0,48
	acetamide	60	7706,05	37	7707,13+/-0,16
	biotine	60	8175,61	56	8176,08+/-0,21
CC2 contrôle = M	Fragment court	35	3987,43	25	3987,11+/-0,55
	Cys-antenna-linker	57	6850,97	9	6851,01+/-0,43
	bodipy	57	7265,18	70	7265,04+/-0,35
	acetamide	57	6907,02	36	6908,04+/-0,08
	biotine	57	7376,58	54	7376,86+/-0,16
NLP-LZ contrôle	Fragment court	43	5265,92	14	5265,82+/-0,18
	Cys-antenna	60	7597,83	9	7597,78+/-0,28
	bodipy	60	8012,04	77	8011,98+/-0,26
	acetamide	60	7654,89	36	7655,14+/-0,22
	biotine	60	8123,44	65	8123,73+/-0,16
NLP w.t.	Cys-antenna	38	4861,77	12	4861,67+/-0,35
	bodipy	38	5275,98	77	5275,66+/-0,28
NLP contrôle	Cys-antenna	38	4902,87	20	4902,55+/-0,48
	bodipy	38	5317,08	50	5316,38+/-0,26
GCN4	Cys-antenna-linker	55	6901,27	3	6901,01+/-0,41
	bodipy	55	7315,48	50	7314,76+/-0,40
Antennapedia	penetratin	16	2287,82	13	2287,52+/-0,08
	Cys-penetratin	17	2390,97	18	2390,43+/-0,02
	bodipy	17	2805,19	73	2805,06+/-0,52

NLP = NLM

Couplages :

- **bodipy** : 1 eq. Bodipy-maleïmide (*molecular probes B-10250*) dans CH_3CN, additionné au peptide réduit en solution dans eau + NH_4OH pH6 ou acétate d'ammonium 50 mM pH6 (1/2 heure sous agitation à t° ambiante, dans l'obscurité).

- **acetamide** : 15 eq. Iodoacetamide additionnés au peptide en solution dans TRIS/acetate 0,1M pH 8,6 (1/2 heure sous agitation à t° ambiante).

- **biotine** : 1,2 eq. Biotine PEO-maleïmide (*pierce 21901*) additionné au peptide en solution dans eau + NH_4OH pH6,5 (1/2 heure sous agitation à t° ambiante).

NEMO : protocoles de purification

		greffage	Gradient analytique (20 mn)	Gradient semi-prep (20 mn)	Gradient MPLC (60 mn)
CC2 w.t.	Fragment court	C18	20-60		25-75
	Cys-antenna-linker	C18	32-42		15-60
	bodipy	C4	30-40		20-70
	acétamide	C18	27-37	20-45	
	biotine	C18	27-37	20-45	
NNN-LZ w.t.	Fragment court	C18	30-40		15-60
	Cys-antenna	C18	30-40		15-60
	bodipy	C4	30-40		20-70
	acetamide	C18	27-37	25-45	
	biotine	C18	27-37	20-45	
CC2 contrôle	Fragment court	C18	25-35		25-60
	Cys-antenna-linker	C18	27-37		10-60
	bodipy	C18	27-37		20-70
	acetamide	C18	27-37	15-40	
	biotine	C18	27-37	20-45	
NLP -LZ contrôle	Fragment court	C18	25-35		15-60
	Cys-antenna	C18	27-37		15-60
	bodipy	C18	27-47		25-70
	acetamide	C18	27-37	25-45	
	biotine	C18	27-37	20-45	
NLP w.t.	Cys-antenna	C18	25-50		20-70
	bodipy	C18	25-50		20-70
NLP contrôle	Cys-antenna	C18	25-50		20-70
	bodipy	C18	25-50		20-70
GCN4	Cys-antenna-linker	C18	33-43		25-70
	bodipy	C18	33-43		20-70
Antennapedia	penetratin	C18	20-40		15-50
	Cys-penetratin	C18	20-40		15-50
	bodipy	C18	25-40		15-60

Analytique : 300-5C18 25%-35% CH3CN dans TFA 0,08%%

Purification :

- fragments courts, peptides SH et Bodipy : MPLC C18, 20%-70% CH3CN dans tampon TFA
- peptides acetamide et biotine : semi-prep C18, 20%-45% CH3CN dans tampon TFA

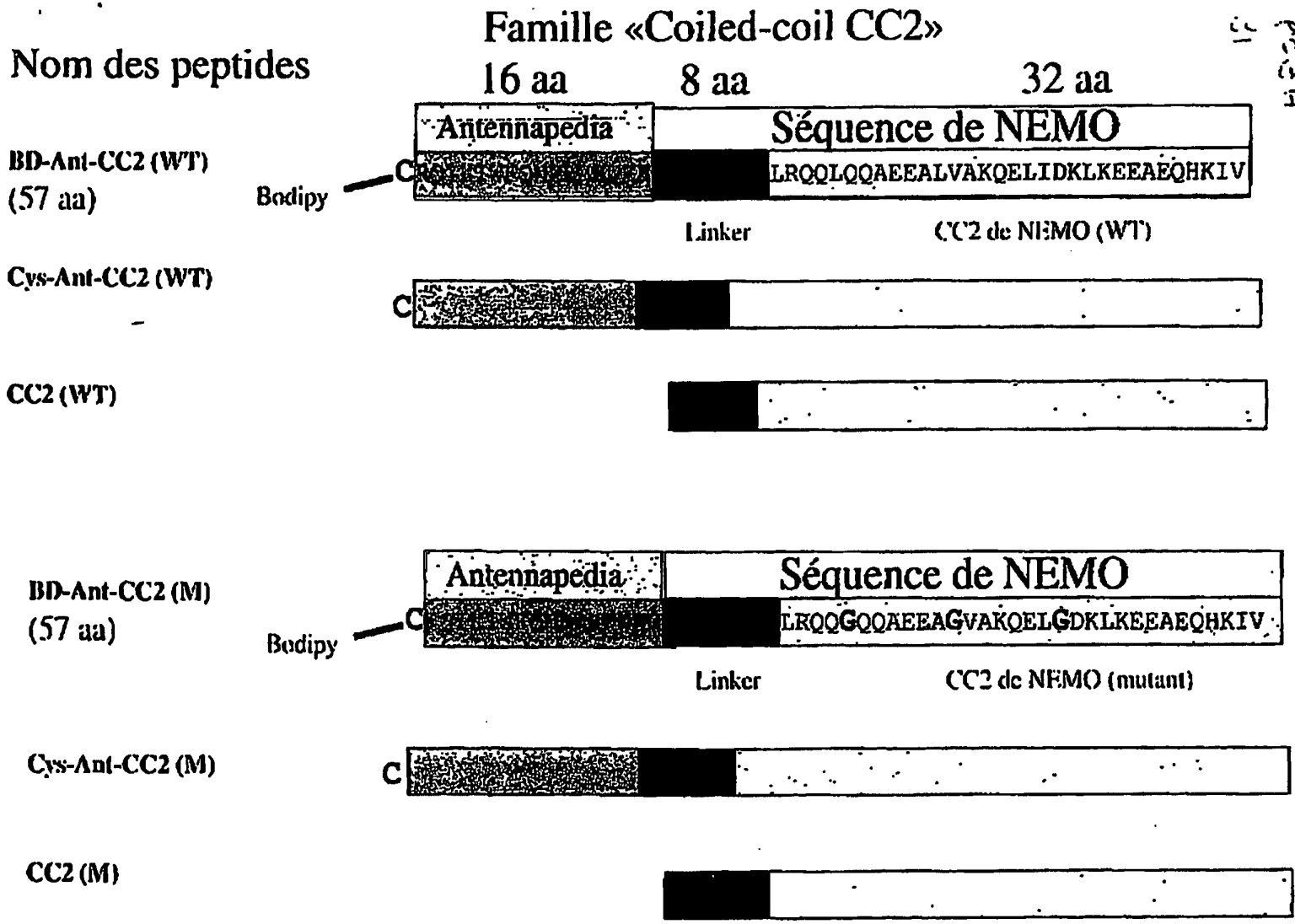

Famille « Leucine Zipper »

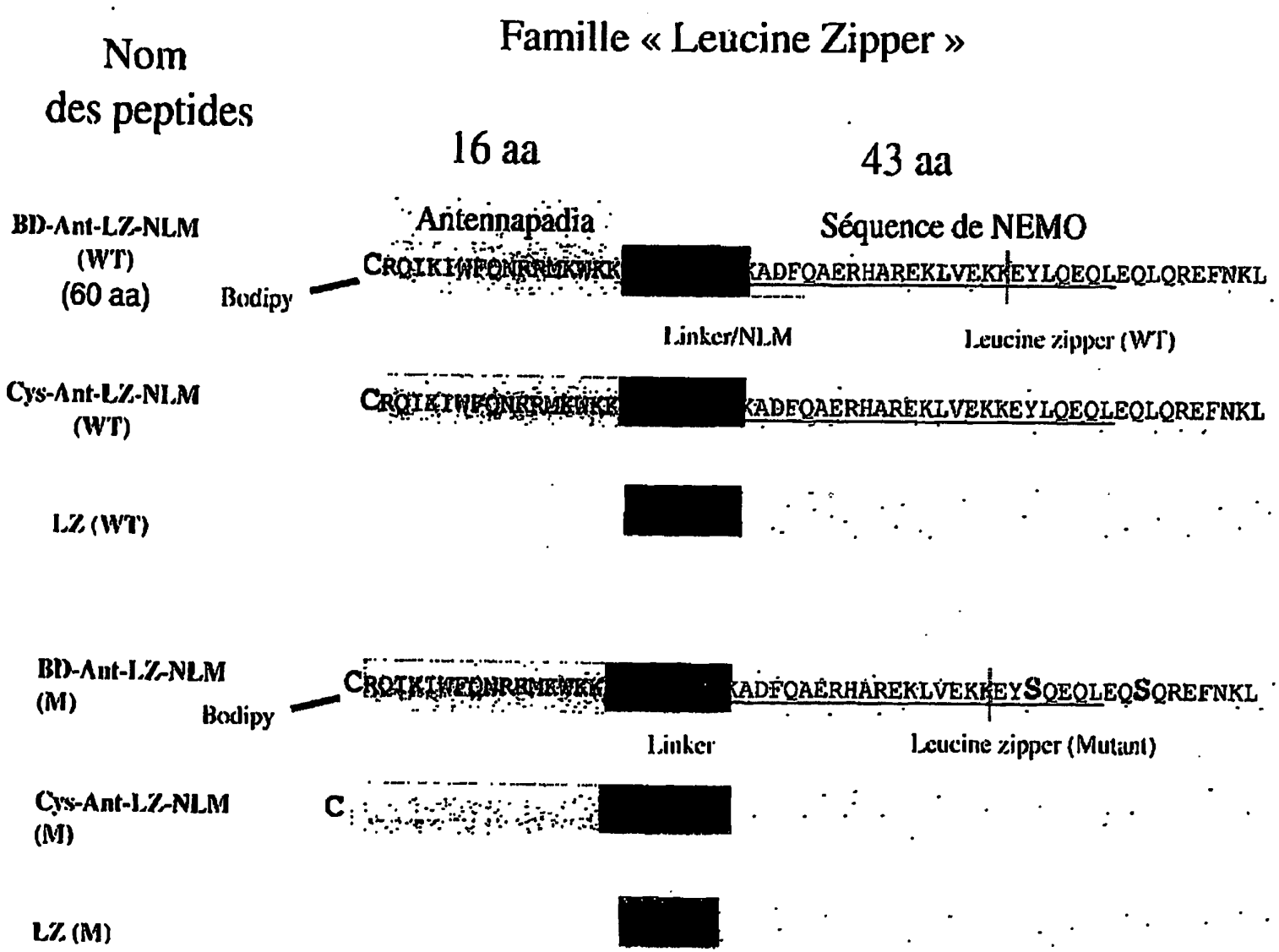

Famille « motif Nemo Like Protein »

Nom des peptides

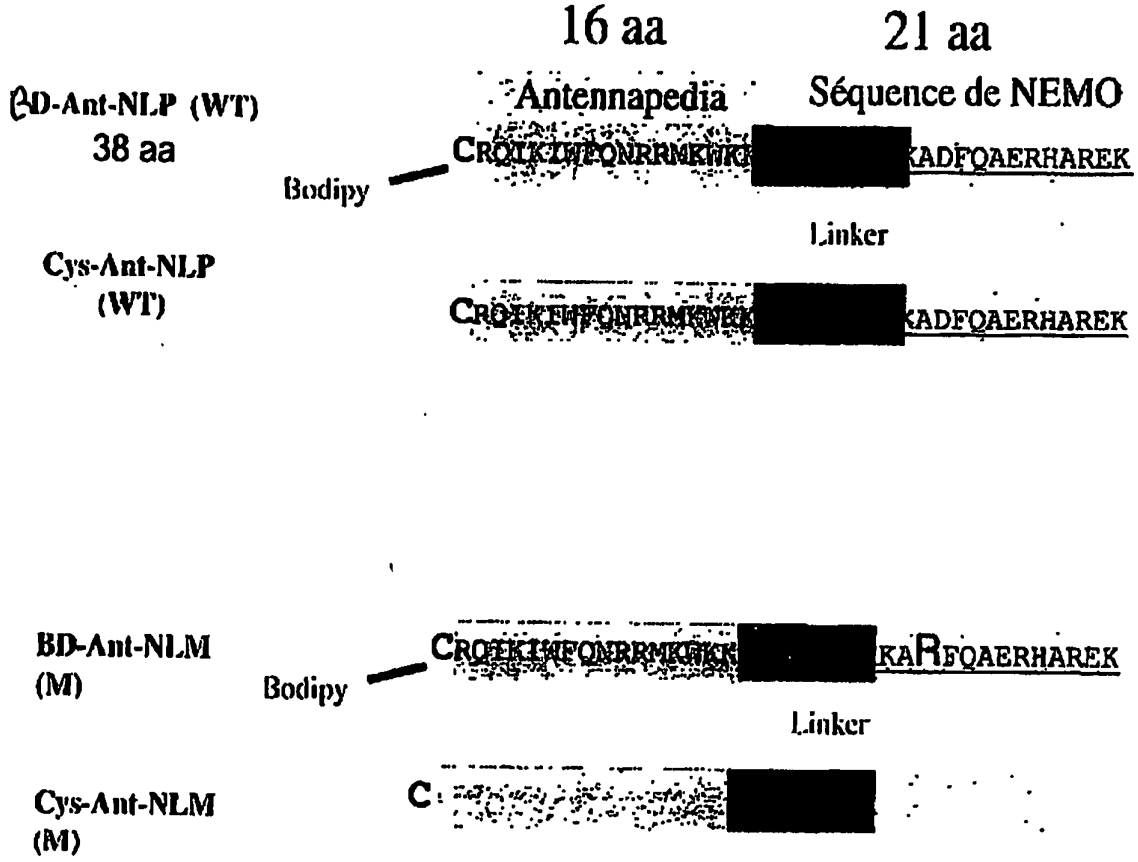

Peptide GCN4

BD-Ant-GCN4
(55 aa)

Antennapedia NEMO GCN4

CRQIKIWFQNRRMKWKK[redacted]RMKQLEDKVEELLSKNYHLENEVARLKKLVGER

Bodipy

Linker

CC2/GCN4

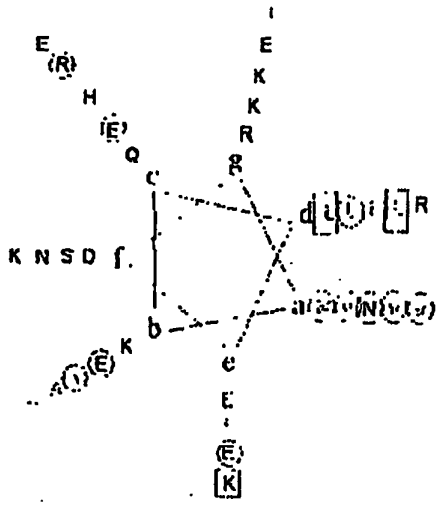

Structure GCN4

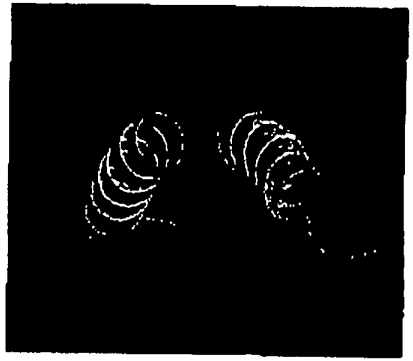

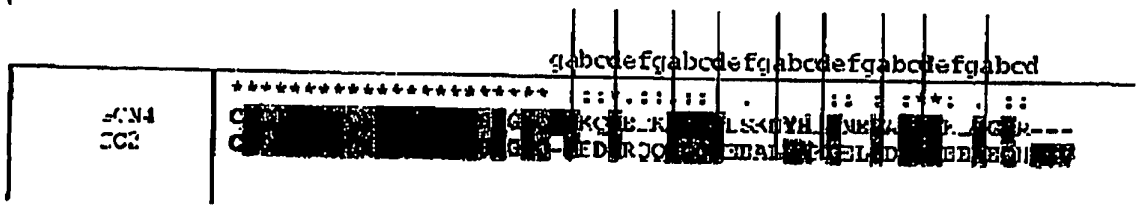

INSTITUT PASTEUR

Direction de la Valorisation et des Partenariats Industriels

Service des Brevets et Inventions

N° de concertation [1] : Date Signature	**DECLARATION D'INVENTION N° [2] :** 2003-88 [liée à DI 03-29] Date 17 juillet 2003 Signature Danielle BERNEMAN Chef du Service des Brevets & Inventions

1 *A remplir obligatoirement par le Relais de Valorisation (doc A)*
2 *A remplir obligatoirement par le Service des Brevets et Inventions*

1-DOSSIER ADMINISTRATIF

1-1 Titre de l'invention :

Caractérisation fonctionnelle du domaine minimal de NEMO nécessaire à son oligomérisation

1-2 Inventeurs :
Indiquer les noms dans l'ordre devant figurer sur le texte de la demande de brevet.

Inventeur:	Nom :	Prénoms :	Nationalité :
	AGOU	Fabrice	Française

Domicile : 21 avenue du Bel-Air - 75012 PARIS

Organisme employeur : INSTITUT PASTEUR — Date du contrat de travail : ou du contrat de stage à l'IP 01/08/98

Fonctions exercées : Chargé de Recherche I.P.

Adresse professionnelle :

1 campus Pasteur, nom du laboratoire et préciser si unité associée

Unité Régulation Enzymatique des Activités Cellulaires, Dpt. Biologie Structurale et Chimie, Institut Pasteur, 25 rue du Docteur Roux, 75724 Paris cedex 15

1-2 Inventeurs :
Indiquer les noms dans l'ordre devant figurer sur le texte de la demande de brevet.

Inventeur:	Nom :	Prénoms :	Nationalité :
	COURTOIS	Gilles	Française

Domicile : 157 rue de Ménilmontant - 75020 PARIS

Organisme employeur : I.N.S.E.R.M

Date du contrat de travail : ou du contrat de stage à l'IP 01/09/92

Fonctions exercées : D.R.2

Adresse professionnelle :

Ł campus Pasteur, nom du laboratoire et préciser si unité associée

Unité de Biologie Moléculaire de l'expression génique, Dpt Biologie Cellulaire et Infection,
25 rue du Docteur Roux, 75724 Paris cedex 15

1-2 Inventeurs :
Indiquer les noms dans l'ordre devant figurer sur le texte de la demande de brevet.

Inventeur:	Nom :	Prénoms :	Nationalité :
	ISRAEL	Alain	Française

Domicile : 20 rue Daguerre - 75014 PARIS

Organisme employeur : INSTITUT PASTEUR

Date du contrat de travail : ou du contrat de stage à l'IP 01/01/83

Fonctions exercées : Directeur de l'évaluation scientifique, Chef d'unité

Adresse professionnelle :

Ł campus Pasteur, nom du laboratoire et préciser si unité associée

Unité de Biologie Moléculaire de l'Expression Génique, Dpt Biologie Cellulaire et Infection,
25 rue du Docteur Roux, 75724 Paris cedex 15

1-2 Inventeurs :
Indiquer les noms dans l'ordre devant figurer sur le texte de la demande de brevet.

Inventeur:	Nom :	Prénoms :	Nationalité :
	VERON	Michel	Française

Domicile : 16 rue de Fourcy 75004 Paris

Organisme employeur : INSTITUT PASTEUR (C.N.R.S, URA)

Date du contrat de travail : ou du contrat de stage à l'IP 1/01/77

Fonctions exercées : Chef du Département B.S.C., Chef d'unité

Adresse professionnelle :

Ł campus Pasteur, nom du laboratoire et préciser si unité associée

Unité Régulation Enzymatique des Activités Cellulaires, Dpt. Biologie Structurale et Chimie, Institut Pasteur,
25 rue du Docteur Roux, 75724 Paris cedex 15

1-2 Inventeurs :
Indiquer les noms dans l'ordre devant figurer sur le texte de la demande de brevet.

Inventeur:	**Nom :**	**Prénoms :**	**Nationalité :**
	Traincard	**Francois**	**Française**

Domicile : 21 rue Jules Guesdes 92130 Issy les Moulineaux

Organisme employeur : Institut Pasteur — **Date du contrat de travail : ou du contrat de stage à l'IP** 01/05/1998

Fonctions exercées : Ingénieur Institut Pasteur

Adresse professionnelle :

t campus Pasteur, nom du laboratoire et préciser si unité associée

Si d'autres inventeurs sont associés, ajouter les informations les concernant sur une feuille séparée.

1-3 Contribution de chaque inventeur :

1-3-1 Indiquer succinctement la nature de la contribution à l'invention de chaque inventeur :

- Fabrice AGOU: Caractérisation des sous-domaines de NEMO CC2 et LZ qui forment le domaine minimal d'oligomérisation de la protéine NEMO

- Gilles Courtois : Identification de la proteine NEMO et des sous-domaines fonctionnels.

- Michel Véron: Mise en place logistique de l'invention

- Alain Israël: Identification de la proteine NEMO et du facteur de transcription NF-kB impliqué dans la réponse inflammatoire, immunitaire et anti-apoptotic.

- François Traincard: Étude des sous-domaines de NEMO par polarisation de fluorescence

1-3-2 Pourcentage de participation à l'invention pour chaque inventeur :

Inventeur :	**% Participati n :**
Fabrice Agou	24 %

Gilles Courtois	20 %
Alain Israël	20 %
Michel Véron	24 %
François Traincard	12 %

1-4 Financement :

Origine et montant du (des) financement(s) ayant mené à l'invention et date et référence du financement

(Institut Pasteur, Appels d'offres, PTR, GPH,OMS, CE, MESR INRA , partenaires industriels, etc.).

1-4-1 Pour un laboratoire IP

Origine : **Montant : 6000** ☒ **Euro**

PTR Pasteur-Necker n°74

Institut Pasteur

C.N.R.S.

1-4-2 Pour un laboratoire extérieur

Origine : **Montant :** ☐ **Euro**

1-5 Divulgation de l'invention

Il est rappelé que la protection d'une invention avant divulgation est toujours la situation la plus efficace en terme de valorisation

1-5-1 L 'invention a-t-elle déjà fait l'objet d'une divulgation orale ou écrite par votre laboratoire ou une autre équipe ? Si oui, préciser les références et la date.

☐ **Oui** ☒ **Non** **Références :** **Date :**

1-5-2 L'invention doit-elle faire l'objet par votre laboratoire d'une publication,d'une communication orale, d'une soutenance de diplôme* ou d'une affiche.

**Possibilité de demander une soutenance à huis clos (attestation à faire valider par l'université, document pré-établi au SBI).*

1ère soumission	☐ Oui	☒ Non	Si oui Date :
Soumission après corrections	☐ Oui	☒ Non	Si oui Date :
Bon à tirer	☐ Oui	☒ Non	Si oui Date :
Prévision de divulgation y compris résumé congrès/séminaire:			
- Publication en ligne	☐ Oui	☒ Non	Si oui Date :
- Publication journal	☐ Oui	☒ Non	Si oui Date :

1-6 Renseignements complémentaires *(si nécessaire)* **:**

L'ensemble des résultats fera l'objet d'une publication scientifique

1-7 ATTESTATION

Les inventeurs certifient qu'à leur connaissance aucune autre personne n'a contribué significativement à la conception et à la réalisation de l'invention.

Date : 15/07/2003

Les inventeurs ci-dessous signataires désignent comme correspondant administratif:

Nom : AGOU **Prénom :** Fabrice

Adresse professionnelle : Unité R.E.A.C. Dpt Biologie Structurale et Chimie, Institut Pasteur, 25 rue du Dr. Roux 750724 Paris cedex 15

Téléphone : 01.45.68.83.80. **e-mail :** fagou@pasteur.fr

Il a pour rôle d'assurer le contact et la correspondance avec les différents acteurs de la DVPI/DJ de l'Institut Pasteur (DVPI:coordination scientifique, service des brevets et inventions, service de transfert de technologie, service des accords industriels /Direction Juridique). Cette DI sera référencée ultérieurement sous son n° et le nom du correspondant. Celui-ci ne saurait engager ni l'Institut Pasteur, ni les inventeurs pris collectivement ou individuellement.

Signature des Inventeurs.

Nom :	Agou Fabrice	Signatures
Nom :	Courtois Gilles	
Nom :	Israël Alain	
Nom :	Véron Michel	
Nom :	Francois Traincard	

NOTE – REMARQUES IMPORTANTES

1. À la réception du présent document enregistré par le Service Brevets et Inventions de l'Institut Pasteur, les inventeurs non salariés de l'Institut Pasteur doivent prévenir leur organisme employeur.

2. L'ensemble des informations figurant dans ce questionnaire fait l'objet d'un traitement informatisé à l'usage de l'Institut Pasteur et, le cas échéant, des différents cabinets et offices de brevets auxquels il est amené à s'adresser.
Conformément à l'Art. 27 de la loi n° 78-17 " Information et Liberté " du 6 janvier 1978, les personnes directement concernées par ces informations ont un droit d'accès à celles-ci ainsi qu'un droit de rectification des éventuelles erreurs ou omissions contenues dans ce questionnaire. Si tel est le cas, il conviendra de vous adresser au Service des Brevets et Inventions de l'Institut Pasteur.
Par ailleurs, les réponses aux questions posées ont un caractère obligatoire si vous souhaitez être officiellement mentionné comme inventeur ou co-inventeur du ou des brevets objet de la présente déclaration.

3. Tous changements de situation personnelle ou professionnelle doivent être signifiés au Service des Brevets et Inventions qui a en charge votre dossier et est tenu de les transmettre aux offices de brevets concernés sous peine de déchéance des droits.

DI N° 2003-88 [liée à 03-29]

2-DOSSIER SCIENTIFIQUE (INFORMATIONS CONFIDENTIELLES)

2-1-1 Résumé La protéine NEMO (NF-kappaB essentiel modulator) qui joue un rôle crucial dans l'activation de la voie NF-kappaB (1), est associée aux protéines kinases IKK-alpha et -beta pour former le complexe multiprotéique IKK. Bien que le mode d'activation d'IKK reste encore peu compris, l'activation des kinases implique probablement une phosphorylation en trans des deux kinases induite par l'oligomérisation de NEMO. Nous avons montré que le domaine C-terminal (résidus 241-388) est le domaine de trimérisation de NEMO (2). L'examen de la séquence polypeptidique indique que ce domaine est composé de deux motifs coiled-coils en tandem (CC2 et LZ), d'un motif riche en proline et d'un motif en doigt de zinc (ZF) situé à l'extrémité C-terminale de la chaine polypeptidique.

Nous avons produit chez E. coli, et purifié à homogénéité, des formes tronquées de NEMO contenant des combinaisons de ces motifs et nous avons comparé leurs propriétés d'assemblage par des expériences de filtration sur gel et de sédimentation à l'équilibre. Les résultats indiquent que le motif riche en proline et le motif ZF ne participent pas à l'oligomérisation de NEMO puisque le segment "CC2-LZ", délété de ces deux éléments, présente une constante d'association trimérique identique à celle de la protéine sauvage. Nous avons alors recherché lequel des motifs "coiled-coil" gouverne l'homo-association en utilisant des peptides de synthèse mimant les motifs CC2 ou LZ. Le peptide CC2 forme un homotrimère de 12,5 kDa, alors que le peptide LZ s'associe en homodimère de 10 kDa. Leurs constantes d'association sont cependant très fortement diminuées par rapport à celle du segment CC2-LZ (100 fois pour CC2 et 40 fois pour LZ), suggérant que le motif LZ participe à la formation du trimère CC2-LZ. Lorsque que les deux peptides CC2 et LZ sont combinés, ils forment un hétérohexamère stable. Leur interaction a été confirmée par polarisation de fluorescence au moyen de peptides couplés au Bodipy.

L'ensemble de ces résultats indique que le domaine de trimérisation de NEMO est un hétérohexamère résultant d'interactions homo- et hétérotypiques des coiled-coils LZ et CC2.

23/07/2003

Date et signature : 15 juillet 2003

DI N° 2003_88 [liée à 03_29]

2-SCIENTIFIC FILE (CONFIDENTIAL NOTICE)

2-1-2 Abstract The protein NEMO (NF-kappaB essential modulator) plays an essential role in the NF-kappaB signaling pathway by interacting with the IKK-alpha and IKK-beta kinases to form the IKK complex. Although the mode of activation of IKK is not well understood, the kinase activation most likely involves the trans-phosphorylation of both kinases, triggered by NEMO oligomerization. We showed that the C-terminal domain (residues 241-388) is the trimerization domain of NEMO. The analysis of the polypeptide sequence indicates that the domain is composed of several structural motifs including two coiled-coils motifs in tandem (CC2, LZ), a proline rich motif and a zinc finger motif situated at the extremity of the C-terminus. We highly purified truncated forms of NEMO containing a combination of these motifs and we compared their assembly properties by gel filtration and equilibrium sedimentation methods. Results indicate that the proline rich motif and the zinc finger motif are not required for NEMO oligomerization. The CC2-LZ polypeptide, which does not contain these two motifs, displays the same trimeric association constant as that of the wild type. We then examined whether CC2 or LZ individually govern the homo-association by using chemical peptides designed to mimic their sequences. We found that the CC2 peptide forms a 12.5 kDa homo-trimer and that the LZ peptide forms a 10 kDa homo-dimer. However their repective dissociation constants were low as compared to that of the CC2-LZ polypeptide (100 x and 40 x for CC2 and LZ respectively), suggesting that the LZ motif contributes to the formation of the trimer. When we combined both peptides, they formed a stable hetero-hexamer. This specific interaction was confirmed by fluorescence polarization using peptides conjugated with bodipy dye.

Taken together, these results indicate that the trimerization domain of NEMO is a heterohexamer formed by a specific combination of homo- and heterotypic interactions with LZ and CC2 coiled-coils.

19/09/2003

Date et signature : 15 juillet 2003

2-2 Documents à joindre :

Pour chaque document joint, veuillez reporter le n° de concertation donné à votre DI

2-2-1 Données expérimentales, les résumés et/ou les articles en préparation.

2-2-2 Articles les plus pertinents ayant un rapport avec le projet.

2-2-3 Esquisses, dessins, photographies ou tout autres documents qui pourront aider à la description de l'invention.

(Les données brutes, les feuilles volantes, les dessins au crayon ou les photos Polaroïds sont acceptables si elle forment un ensemble cohérent et compréhensif).

2-2-4 L'appareil, le produit ou le procédé a-t-il été créé ou testé. Dans l'affirmative, en existe-t-il un échantillon ou une maquette? Une démonstration peut-elle être réalisée ?

2-3 Description simplifiée :

L'invention est-elle une nouvelle technique, formulation, outil ou produit (s), est-elle une nouvelle utilisation ou une amélioration d'un produit ou d'une technique existante ?

L'invention est un nouveau produit qui peut s'apparenter à un récepteur cible pour la recherche de nouvelles molécules qui ,par leur interaction, pourront agir comme des inhibiteurs de la voie NF-kB.

2-4 Mots clés

En vous référant aux tableaux des mots clés et aux domaines des pathologies des pages suivantes choisissez les mots clés et les pathologies les mieux appropriés pour définir les principales caractéristiques de votre invention.

3-4-1 Technologies utilisées : cochez le mot clé qui décrit le domaine de votre invention (1 à 6 mots clés)

Agricultural	chemical	Diagnostic	genomics	therapeutic	research tool	screening	vaccine
Additives ☐	Additives ☐	Antibody ☐	allele ☐	analgesic ☐	antibiotic resistance ☐	biochip ☐	adjuvant ☐
Aquaculture ☐	alternative energy ☐	assay ☐	bioinformatic ☐	anaesthetic ☐	antibody ☐	cellular assay ☒	anatoxin ☐
Bacterial selection ☐	Antioxidants ☐	bacterial ☐	cDNA ☐	angiogenesis ☐	bacterial identification ☐	combinatorial biology ☐	anticancer ☐
Bacterial contamination ☐	Catalyst ☐	biochip ☐	database ☐	antibiotic/ antibacterial ☐	biological material ☐	genetic diseases ☐	attenuated live ☐
Biopesticides ☐	Coatings ☐	contrast agent ☐	epidemiology ☐	antibody ☐	cell line ☒	high throughput screening ☐	carbohydrate (polysaccharide) ☐
Bioremediation ☐	effluent treatment ☐	detection ☐	EST ☐	anticancer ☒	chromatography ☐	phage display ☐	conjugate ☐
Breeding ☐	exhaust treatment ☐	DNA probe ☐	gene ☐	antifungal ☐	culture ☐	screen ☐	dead entire ☐
Fermentation ☐	Foams ☐	Elisa ☐	homologue ☐	anti-inflammatory ☒	directed evolution ☐	target ☒	delivery system (plasmid...) ☐
Fertilizer ☐	food chemistry ☐	fungal ☐	interactome ☐	antisense ☐	DNA/RNA sequencing ☐		human use ☐
Food ☐	Gels ☐	imaging ☐	isogene ☐	antiviral ☐	DNA/RNA synthesis ☐		hybrid ☐
Forestry ☐	Monomers ☐	immunoassay ☐	library ☐	apoptosis ☒	electrophoresis ☐		injectable administration ☐
Growth ☐	Oxidation ☐	in situ ☐	pharmacogenomics ☐	cell signalling ☒	enzyme ☐		live recombinant V. (LRV) ☐
Nitrogen fixation ☐	Remediation ☐	marker ☐	polymorphism ☐	disease model ☐	equipment ☐		mucosal administration ☐
Ornamental ☐	Solvents ☐	MRI ☐	positional cloning ☐	drug delivery ☐	expression system ☐		naked DNA ☐
Pesticides ☐		parasitic ☐	proteomics ☐	drug design ☒	fermentation ☐		peptide ☐
Plant ☐		point of use ☐	receptor ☐	fertility ☐	GFP ☐		polyvalent ☐
Resistance ☐		radioisotope ☐	RNA ☐	gene therapy ☐	hybridization ☐		prophylactic ☐
Seeds ☐		transgenic ☐	target validation ☐	hormone ☐	mutagenesis ☐		protected (microencapsulation) ☐
tissue culture ☐		ultrasound ☐	screening ☐	immunotherapy ☐	oligonucleotide synthesis ☐		screening method ☐
Transgenic ☐		viral ☐		natural product ☐	PCR ☐		Sub-unit (molecular) ☐
Vegetable ☐				peptides ☒	protein sequencing ☐		sugar peptidic mimic ☐
Veterinary ☐				pro-drug ☐	protein synthesis ☐		therapeutic ☐
				proteins ☐	reagent ☐		veterinary use ☐
				small molecule ☐	software ☐		
				vaccine ☐	(mass) spectroscopy ☐		
				wound healing ☐	transgenesis ☐		
				☐	vector ☐		

2-4-2 Domaines de pathol gies

Veuillez cocher une à trois (1-3) cases correspondant aux mots clés pouvant caractériser les domaines pathologiques concernés par votre invention.

Infections bactériennes

Charbon bactérien/*Anthrax*	☐	Leptospirose	☐
Arthrite infectieuse (*K. xerosis*)	☐	Listériose	☐
Botulisme (Clostridium)	☐	Maladie de Lyme (*B. burgdorferi*)	☐
Bronchite (*S. pneumoniae, H. influenzae*)	☐	Méningite (*H. influenzae*, Méningocoque)	☐
Brucellose/fièvre maltc	☐	Otite	☐
Chlamydiose (infection urétro-cervicale)	☐	Peste (Yersinia)	☐
Choléra (Vibrio cholerae)	☐	Pneumonie (Pneumocoque, Staphylocoque)	☐
Coqueluche (Bortedella pertussis)	☐	Rhumatisme articulaire aigu (Streptocoque)	☐
Diphtérie (Corynebacterium)	☐	Rickettsiose	☐
Dysenterie bacillaire (Shigellose)	☐	Rougeole/ *Measles*	☐
Fièvre typhoïde (Salmonella typhi)	☐	Syphilis (Treponema)	☐
Infection cutanée (Staphylo.Streptocoque)	☐	Tétanos	☐
Infection à E. coli	☐	Tuberculose (Mycobacterium tuberculosis)	☒
Légionellose	☐	Ulcère et adénocarcinome dus à *H. pylori*	☒
Lèpre (Mycobacterium leprae)	☐	Autre	☐

Infections virales

Cancer dû au Papillomavirus humain HPV	☐	Méningite virale	☐
Diarrhée infantile due au Rotavirus	☐	Mononucléose infectieuse (EBV)	☐
Encéphalite virale	☐	Oreillons	☐
Fièvre aphteuse (Picornavirus)	☐	Poliomyélite à Entérovirus	☐
Fièvre hémorragique (Dengue, Ebola, Lassa)	☐	Rage (Rhabdoviridae)	☐
Fièvre jaune (Flavivirus)	☐	Rhume	☐
Grippe (Orthomyxovirus)/*Flu*	☐	Rougeole (Virus morbilleux)	☐
Herpès génital (Herpesvirus)	☐	Rubéole (Rubivirus)	☐
Hépatites A, B, C, D, E	☐	SIDA (HIV1/2)	☐
Immunodépression à Cytomégalovirus	☐	Varicelle (Herpesvirus)	☐
Infection respiratoire (Paramyxovirus)	☐	Variole (Poxvirus)	☐
Lentivirus SIDA	☐	Zona (Herpesvirus)	☐
Leucémie et paralysie dues au HLV-1	☐	Autre	☐

Infections parasitaires

Amibiase	☐	Maladie de Chagas	☐
Bilharziose	☐	Maladie du sommeil	☐
Cysticercose	☐	Malaria	☐
Distomatose	☐	Onchocercose	☐
Elephantiasis filarien	☐	Pneumocystose	☐
Echinococcose	☐	Schistosomiase	☐
Filariose	☐	Toxoplasmose	☐
Gale	☐	Trichinellose	☐
Leishmaniose	☐	Trypanosomose	☐
		Autre	☒

Mycoses

Aspergillose	☐
Candidose	☐
Cryptococcose	☐
Histoplasmose	☐
Nocardia	☐
Pneumocystose	☐
Autre	☐

Autres domaines de pathologies

Cancérologie	☒
Cardio-vasculaire	☐
Dermatologie	☒
Embryologie	☐
Endocrinologie	☐
Gastro-intestinal	☒
Gynéco-obstétrique	☐
Hématologie	☒
Hépatique	☐
Immunitaire	☒
Métabolique	☐
Musculaire	☐
Neurologie	☐
Ophtalmologie	☐
Oto-Rhino-Laryngologie	☐
Psychiatrie	☐
Respiratoire	☐
Urogénital	☐
Autres	☐
	☐

2-4-3 Les Maladies.

Ecrivez de 1 à 5 mots clés pour identifier d'autres maladies plus spécifiques (exemple : le diabète)

Ostéoarthrite Arthrite rhumatoïde

2-4-4 Définition libre.

Pour décrire votre invention plus précisément, vous pouvez indiquer 5 mots clés non inclus dans les précédentes catégories.

Site d'oligomérisation | inhibiteurs de la voie NF-kB | anti-inflammatoire | anticancéreux | chimie thérapeutique

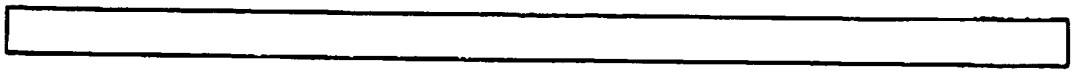

2-5 Nouveauté de l'invention

A partir de la description, mettez l'accent sur les nouveautés et le caractère original de l'invention.

La caractérisation du domaine minimal d'oligomérisation de la protéine NEMO permet d'entrevoir de nouvelles molécules qui peuvent potentiellement représenter une nouvelle classe d'inhibiteur de la voie NF-kB. L'intérêt de cibler la protéine NEMO est décrit dans la D.I. 03-29.

En quoi l'invention diffère-t-elle de technologies déjà existante ?

Sans objet

Quel problème permet-elle de résoudre, et avec quels avantages ?

Sans objet

2-6 Applications industrielles de l'invention

Si cela n'a pas été indiqué précédemment, quelles sont les principales applications de l'invention ? En plus des débouchés immédiats, d'autres applications pourraient-elles être envisagées éventuellement ?

-Sur le marché des biotechnologies, il n'existe qu'un seul inhibteur spécifique de la voie NF-kB dont la concentration effective est très élevée. Nos produits plus spécifiques présentent donc un atout majeur pour toutes les entreprises intéressées par des inhibiteurs spécifiques de la voie NF-kB.

- Sur le marché des entreprises pharmaceutiques, notre invention ou les produits qui peuvent en dériver peuvent donner lieu à un usage thérapeutique comme anti-inflammatoire et comme anti-cancéreux.

2-7 Limites de l'invention

L'invention présente-t-elle des inconvénients ou des limitations ? Peuvent-ils être surmontés ? De quelle manière ?

L'invention constitue une cible moléculaire thérapeutique pour cribler tout un ensemble de petites molécules qui peuvent potentiellement altérer le site d'oligomérisation de la protéine NEMO. Elle peut donc représenter une limitation car la rupture des interactions protéine par des petites molécules organiques n'est pas aisée.

2-8 Autres informations

2-8-1 Existe-il un élément de l'invention (Biologique ou autre) vous ayant été fourni par une autre institution ou entreprise et ayant fait l'objet d'un accord signé de Transfert de Matériel (MTA) ? Dans l'affirmative, précisez la nature de cet élément, sa date de réception et les coordonnées du fournisseur.

Nature: Date de réception : Coordonnées du fournisseur :

2-8-2 Existe-il, à la connaissance de l'inventeur, d'autres brevets ou publications concernant l'invention ?

(Une recherche parmi les brevets existants a-t-elle été effectuée ? Dans l'affirmative, avec quels résultats ?)

☐ Oui ☒ Non

2-8-3 L'invention présente-t-elle un intérêt commercial immédiat ? Précisez le nom des compagnies ou des personnes si possible.

Toutes entreprises de biotechnologies intéressées dans la transduction du signal et dans les inhibiteurs spécifiques de la voie NF-kB.

Toutes les entreprises pharmaceutiques intéressées par des nouvelles molécules agissant comme anti-inflammatoires et comme anti-cancéreux.

Donnez la liste d'autres entreprises potentiellement intéressées :

Utilisez cet espace pour développer et fournir des données complémentaires sur l'invention

2-8-4 Les cahiers de laboratoire et autres données concernant l'invention sont-ils disponibles ? Indiquez leur référence et leur emplacement, sans les joindre.

Référence : Emplacement :

Nº006644 Batiment Monod, unité RBAC, pièce 07

FORMULAIRE DE DEPOT
APPLICATION FORM

TRAITE DE BUDAPEST SUR LA RECONNAISSANCE INTERNATIONALE DU DEPOT DES MICROORGANISMES AUX FINS DE LA PROCEDURE EN MATIERE DE BREVETS
BUDAPEST TREATY ON THE INTERNATIONAL RECOGNITION OF THE DEPOSIT OF MICROORGANISMS FOR THE PURPOSES OF PATENT PROCEDURE

CNCM
Collection Nationale de Cultures de Microorganismes
INSTITUT PASTEUR
25, Rue de Docteur Roux
F-75724 PARIS CEDEX 15

Yvonne CERISIER
Directeur Administratif

AUTORITE DE DEPOT INTERNATIONALE
INTERNATIONAL DEPOSITARY AUTHORITY

CELL LINE

* **DECLARATION**
Statement

EN VUE D'UN DEPOT INITIAL CONFORMEMENT A LA REGLE 6.1 ☒
in the case of an original deposit pursuant to Rule 6.1

EN VUE D'UNE CONVERSION CONFORMEMENT A LA REGLE 6.4.d ☐
in the case of a conversion pursuant to Rule 6.4.d

EN VUE D'UN CONTRAT ASSOCIE (SOUCHE-HOTE OU COMPOSANT) ☐
in the case of an associated contract (host strain or component)

* **TYPE DE MICROORGANISME**
Type of microorganism
CULTURE CELLULAIRE
Cell culture

* **MICROORGANISME ISOLE**
Single microorganism ☐

MELANGE DE MICROORGANISMES
Mixture of microorganisms
ou cellules infectées, contaminées, –
or infected cells, contaminated cells, etc ☐

INDIQUER LE CAS ECHEANT LE NOMBRE DE MICROORGANISMES ET LEURS TYPES
GIVE THE NUMBER OF MICROORGANISMS AND THEIR KINDS WHERE APPLICABLE

LE SOUSSIGNE DEPOSE LE MATERIEL IDENTIFIE CI-APRES ET S'ENGAGE A NE PAS RETIRER LE DEPOT PENDANT LA PERIODE PRECISEE A LA REGLE 9.1.
The undersigned hereby deposits the material identified hereunder and undertakes not to withdraw the deposit for the period specified in rule 9.1.

1. **REFERENCE D'IDENTIFICATION**
Identification reference
NUMERO OU SYMBOLES, PAR EXEMPLE, DONNES PAR LE DEPOSANT AU MATERIEL
NUMBER, SYMBOLS, etc. GIVEN TO THE MATERIAL BY THE DEPOSITOR

70 E/3 – C3

2. **DEPOSANT(S)**
Nom(s) et adresse(s)
Depositor(s)
Name(s) and address(es)

SERVICE DES BREVETS
ET INVENTIONS

INSTITUT PASTEUR

25-28, rue du Docteur Roux
75724 Paris Cedex 15

CETTE FORMULE DOIT ETRE REMPLIE SANS RATURES NI SURCHARGES
THIS FORM SHOULD BE DULY COMPLETED WITHOUT DELETIONS OR ALTERATIONS

REFERENCE D'IDENTIFICATION _____ **Date** _____
Identification reference

3. DESCRIPTION SCIENTIFIQUE ☐
Scientific description

COCHER SI DES INFORMATIONS COMPLEMENTAIRES SONT FOURNIES SUR UNE FEUILLE JOINTE
MARK WITH A CROSS IF ADDITIONAL INFORMATION IS GIVEN ON AN ATTACHED SHEET

Type et origine (organe/tissu, espèce animale, ...)
Type and origin (organ/tissue, animal species, etc) Souris

Caractéristiques et productions des cellules
Characteristics and products of the cells

COCHER LES CASES QUI CONVIENNENT ET DONNER DES INFORMATIONS COMPLEMENTAIRES
MARK WITH A CROSS WHERE APPLICABLE AND GIVE ADDITIONAL INFORMATION

☐ **Hybridome** *Hybridoma*
- **Myélome utilisé** *Myeloma designation* :
- **Spécificité antigénique** *Antigenic specificity* :
- **Classe Ig** *Antibody subclass* :
- **Stabilité de la sécrétion** *Stability of secretion* :

☐ **Lignée génétiquement modifiée** *Genetically modified cell line*
- ☐ **Vecteur(s)** *Vector(s)* _____
- ☐ **Acide nucléique(s) inséré(s)** *Nucleic acid insert(s)* _____
- ☐ _____

☐ **Cellules infectées (virus sauvage)** *Cells infected by a wild-type virus* _____

☒ **Lignée cellulaire nouvellement établie** *Newly established cell line* 70Z/3 - C3

☐ **Autres particularités** *Further or other particularities* _____

Description
Details

(70Z/3)
Lignée pré-B de souris transfectée stablement avec reporteur β galactosidase sous contrôle de site NF-KB. Isolement d'un clone par dilution limite (70Z/3-C3)

Références bibliographiques
Literature references

Lignée originale 70Z/3 : Page et al. J. Immunol. 121 : 641-647

L'INDICATION DE CES INFORMATIONS EST FACULTATIVE, MAIS VIVEMENT RECOMMANDEE AUX TERMES DE LA REGLE 6.1.b
THE SUPPLYING OF SUCH INFORMATION IS OPTIONAL, BUT STRONGLY RECOMMENDED IN ACCORDANCE WITH RULE 6.1.b

REFERENCE D'IDENTIFICATION _____ **Date** _____
Identification reference *Date*

4. PROPRIETES DANGEREUSES POUR LA SANTE OU L'ENVIRONNEMENT
Properties dangerous to health or environment

☐ **La culture ou le mélange identifié sous le chiffre 1 a les propriétés suivantes qui présentent ou peuvent présenter des dangers pour la santé ou/et l'environnement**
The culture or the mixture identified under 1 above has the following properties which are or may be dangerous to health orland the environment

☐

COCHER SI DES INFORMATIONS COMPLEMENTAIRES SONT FOURNIES SUR UNE FEUILLE JOINTE.
MARK WITH A CROSS IF ADDITIONAL INFORMATION IS GIVEN ON AN ATTACHED SHEET

☒ **Le soussigné n'a pas connaissance de telles propriétés.**
The undersigned is not aware of such properties.

COCHER LA CASE QUI CONVIENT
MARK WITH A CROSS THE APPLICABLE BOX

TOUTE ACTION DIRECTE OU INDIRECTE, CONNUE OU PREVISIBLE, SUR QUELQU'ORGANISME QUE CE SOIT (ANIMAL, VEGETAL OU AUTRE) DOIT ETRE SIGNALEE.
ANY DIRECT OR INDIRECT, KNOWN OR LIKELY TO BE EXPECTED EFFECT ON ANY ANIMAL, VEGETAL OR OTHER ORGANISM MUST BE INDICATED

5. CONDITIONS DE SECURITE POUR LA MANIPULATION DE LA CULTURE
Biosafety measures required to manipulate the culture

☐ L1 / P1 ☒ L2 / P2 ☐ L3 / P3 ☐ **Autres** *Others* _____

(EFB: Safe Biotechnology / FEDERAL REGISTER: Guidelines for Research Involving Recombinant DNA Molecules)

6a. CONDITIONS DE CULTURE - partie 1
Conditions for cultivation - Part 1

☐

COCHER SI DES INFORMATIONS COMPLEMENTAIRES SONT FOURNIES SUR UNE FEUILLE JOINTE
MARK WITH A CROSS IF ADDITIONAL INFORMATION IS GIVEN ON AN ATTACHED SHEET

Milieu de culture (avec les références précises des composants)
Culture medium *(give full details if special formulation)*

RPMI (endoxine ≤0.01 ng/ml)

Bicarbonate de sodium (mg/l)
Sodium bicarbonate

Sérum (type - %) 10%
Serum

pH
pH

Température optimale
Optimal temperature

Atmosphère
Gaseous phase (endoxine ≤0.01 ng/ml)

Précautions particulières à la décongélation
Precautions to be taken for thawing

Précautions particulières à l'incubation
Further details: shaking system, etc

Solutions dispersantes utilisées
Solutions used for cell dispersion

REFERENCE D'IDENTIFICATION _____ **Date** _____
Identification reference *Date*

6b. CONDITIONS DE CULTURE - partie 2 ☐
Conditions for cultivation - Part 2

COCHER SI DES INFORMATIONS COMPLEMENTAIRES SONT FOURNIES SUR UNE FEUILLE JOINTE
MARK WITH A CROSS IF ADDITIONAL INFORMATION IS GIVEN ON AN ATTACHED SHEET

Type de culture (cellules en suspension, cellules adhérentes, ...) et morphologie cellulaire attendue
Type of culture : suspension, monolayer, etc, and expected cell morphology

Suspension

Temps de doublement de population 3-4X/24h
Population doubling time

Temps optimal entre les passages
Optimal split ratio

Densité cellulaire attendue
Expected cell density

Durée de vie limitée
Limited lifespan

Détails pour le passage des cellules
Technique for routine sub-culture

Ne pas dépasser 1X10⁶ c/ml.

Remarques
Comments

!!! Utiliser un milieu + Serum pouvant un taux d'endotoxine faible !!! (NF-KB est activé par l'endotoxine)

7. ACTIVITES A VERIFIER POUR CONFIRMER LA VIABILITE DU DEPOT ☐
Activities to be checked confirming the viability of the deposit

COCHER SI DES INFORMATIONS COMPLEMENTAIRES SONT FOURNIES SUR UNE FEUILLE JOINTE
MARK WITH A CROSS IF ADDITIONAL INFORMATION IS GIVEN ON AN ATTACHED SHEET

Lorsque le dépôt porte sur un mélange de microorganismes, la déclaration doit contenir en outre la description des composants du mélange et d'au moins une des méthodes permettant de vérifier leur présence (Règle 6.1.a.iii).
Where a mixture of microorganisms is deposited, descriptions of the components of the mixture and at least one of the methods permitting the checking of their presence should be given in accordance with Rule 6.1.a.iii.

8. CONDITIONS DE CONSERVATION ☐
Conditions for storage

COCHER SI DES INFORMATIONS COMPLEMENTAIRES SONT FOURNIES SUR UNE FEUILLE JOINTE
MARK WITH A CROSS IF ADDITIONAL INFORMATION IS GIVEN ON AN ATTACHED SHEET

Milieu de suspension
Suspending fluid

Modalités de la récolte des cellules
Technique for cell harvesting

Modalités de la congélation
Technique for freezing

RPMI/Serum +10% DMSO

Autres informations
Further comments

REFERENCE D'IDENTIFICATION _____ **Date** _____
Identification reference *Date*

XX. INFORMATIONS SUR LA CULTURE TRANSMISE ☐
nécessaires à des fins d'importation et/ou d'exportation
Details on the transmitted culture required for export/import formalities

COCHER SI DES INFORMATIONS COMPLEMENTAIRES SONT FOURNIES SUR UNE FEUILLE JOINTE
MARK WITH A CROSS IF ADDITIONAL INFORMATION IS GIVEN ON AN ATTACHED SHEET

Références des substrats organiques (fournisseur, référence, lot, date, pays d'origine)
References of the organic substrates (supplier, reference, batch, date, country of origin)

9a. AUTRES INFORMATIONS SUR LA CULTURE TRANSMISE ☐
Further details on the transmitted culture

COCHER SI DES INFORMATIONS COMPLEMENTAIRES SONT FOURNIES SUR UNE FEUILLE JOINTE
MARK WITH A CROSS IF ADDITIONAL INFORMATION IS GIVEN ON AN ATTACHED SHEET

Niveau de passage de la culture transmise
Passage level of the transmitted culture

Date de préparation
Date of preparing

Concentration en cellules
Cell concentration

Date du dernier contrôle de viabilité
Last viability check (date)

Date du contrôle d'étanchéité des ampoules
Last airtightness check of the vials (date)

CONTROLES DE PURETE récents *Last PURITY CHECKS*	**Date / Passage** *Date / Passage level*	**Résultats** *Results*
Bacteria - Fungi		
Mycoplasma	17/3/2003	Négatif
Virus		

EN CAS DE CONTAMINATION, LE DEPOT DOIT ETRE DECLARE COMME 'MELANGE DE MICROORGANISMES' (VOIR LES INSTRUCTIONS DONNEES SOUS LE CHIFFRE 7)
WHERE A DEPOSIT IS CONTAMINATED, IT SHOULD BE DENOTED AS A 'MIXTURE OF MICROORGANISMS' (SEE INSTRUCTIONS GIVEN UNDER 7 ABOVE)

Autres informations
Further comments

CES INFORMATIONS NE SONT LIEES, NI AUX DISPOSITIONS DES REGLES 6.1.b, 6.2.a.iii, 7.6 ET 8, NI AUX DISPOSITIONS DES REGLES 6.1.a.iii, ET 11.4.f. LEUR INDICATION EST FACULTATIVE
SUCH INFORMATION IS NEITHER LINKED TO THE PROVISIONS OF RULE 6.1.b, RULE 6.2.a.iii, RULE 7.6 AND RULE 8, NOR TO THE PROVISIONS OF RULE 6.1.a.iii AND RULE 11.4.f. ITS FURNISHING IS OPTIONAL.

REFERENCE D'IDENTIFICATION _____ **Date** _____
Identification reference

9b. INFORMATIONS SUPPLEMENTAIRES
Additional information

☐

COCHER SI DES INFORMATIONS COMPLEMENTAIRES SONT FOURNIES SUR UNE FEUILLE JOINTE
MARK WITH A CROSS IF ADDITIONAL INFORMATION IS GIVEN ON AN ATTACHED SHEET

Origine de la culture cellulaire ou du mélange (= complément éventuel aux indications données sous le chiffre 3)
Source of the cell culture or the mixture (as far as not given under 3 above)

Lignée établie par G. COURTOIS **le**
Cell line established by *(date)*

Cellule clonée par G. COURTOIS **le**
Cell cloned by *(date)*

Enregistrement dans d'autres institutions de dépôt (Noms, dates, numéros attribués, ...)
Registration in any other depositary institution (Names, dates, references, etc)

Autres informations
Further comments

CES INFORMATIONS NE SONT LIÉES, NI AUX DISPOSITIONS DES REGLES 6.1.b, 6.2.a.iii, 7.8 ET 8, NI AUX DISPOSITIONS DES REGLES 6.1.a.iii, ET 11.4.f. LEUR INDICATION EST FACULTATIVE
SUCH INFORMATION IS NEITHER LINKED TO THE PROVISIONS OF RULE 6.1.b, RULE 6.2.a.iii, RULE 7.8, AND RULE 8, NOR TO THE PROVISIONS OF RULE 6.1.a.iii, AND RULE 11.4.f. ITS FURNISHING IS OPTIONAL.

* **Nom, adresse et numéro de téléphone (ou/et de télécopieur) du scientifique reponsable de la culture transmise**
Name, address, phone and/or fax number of the scientist responsible for the culture transmitted

Gilles COURTOIS, Unité OMEG, Institut Pasteur
Tel : 01-45-68-84-38 e-mail : gmcourt@pasteur.fr
Fax : 01-40-61-30-40

* **En vue du dépôt la culture cellulaire sera transmise, conditionnée en carboglace** ☐ **ou en azote liquide** ☐
The cell culture released for the purpose of deposition will be transmitted in dry ice *or in liquid nitrogen*
sous forme de 12 échantillons, d'un même lot, en tubes étanches, marqués conformément aux exigences indiquées.
as 12 samples from the same batch, in airtight vials, marked as requested.

* **DATE** *Date* 20 Nov 2003

SIGNATURE(S) *Signature(s)*
Danielle BERNEMAN
Chef du Service des Brevets & Inventions.

SIGNATURE(S) du(des) SCIENTIFIQUE(S) RESPONSABLE(S)

LES NOMS DACTYLOGRAPHIES DES PERSONNES PHYSIQUES QUI SIGNENT AU NOM DE LA PERSONNE MORALE DOIVENT ACCOMPAGNER LES SIGNATURES.
THE TYPEWRITTEN NAMES OF THE NATURAL PERSONS SIGNING ON BEHALF OF THE LEGAL ENTITY SHOULD ACCOMPANY THE SIGNATURES.

CETTE FORMULE DOIT ETRE REMPLIE SANS RATURES NI SURCHARGES
THIS FORM SHOULD BE DULY COMPLETED WITHOUT DELETIONS OR ALTERATIONS

ACCORD DU 25 AOUT 1978 ENTRE L'ORGANISATION EUROPEENNE DES BREVETS ET LA COLLECTION NATIONALE DE CULTURES DE MICROORGANISMES, INSTITUT PASTEUR, PARIS, MODIFIE LE 4 OCTOBRE 1982 CONCERNANT LE DEPOT DE MICROORGANISMES EN APPLICATION DES REGLES 28 ET 28bis DE LA CONVENTION SUR LE BREVET EUROPEEN / TRAITE DE BUDAPEST SUR LA RECONNAISSANCE INTERNATIONALE DU DEPOT DES MICROORGANISMES AUX FINS DE LA PROCEDURE EN MATIERE DE BREVETS

AGREEMENT OF 25 AUGUST 1978, AS AMENDED ON 4 OCTOBER 1982, BETWEEN THE EUROPEAN PATENT ORGANISATION AND THE COLLECTION NATIONALE DE CULTURES DE MICROORGANISMES, INSTITUT PASTEUR, PARIS, CONCERNING THE DEPOSIT OF MICROORGANISMS FOR THE PURPOSES OF PATENT PROCEDURE UNDER RULES 28 AND 28a OF THE EUROPEAN PATENT CONVENTION / BUDAPEST TREATY ON THE INTERNATIONAL RECOGNITION OF THE DEPOSIT OF MICROORGANISMS

DIRECTIVE 93/88/CEE RELATIVE A LA PROTECTION DES TRAVAILLEURS CONTRE LES RISQUES LIES A UNE EXPOSITION A DES AGENTS BIOLOGIQUES AU TRAVAIL - DIRECTIVE 90/219/CEE RELATIVE A L'UTILISATION CONFINEE DE MICROORGANISMES GENETIQUEMENT MODIFIES - DIRECTIVE 90/220/CEE RELATIVE A LA DISSEMINATION VOLONTAIRE D'ORGANISMES GENETIQUEMENT MODIFIES DANS L'ENVIRONNEMENT

DECRET n° 94-352 DU 4 MAI 1994 RELATIF A LA PROTECTION DES TRAVAILLEURS CONTRE LES RISQUES RESULTANT DE LEUR EXPOSITION A DES AGENTS BIOLOGIQUES - LOI n° 92-654 DU 13 JUILLET 1992 RELATIVE AU CONTROLE DE L'UTILISATION ET DE LA DISSEMINATION DES ORGANISMES GENETIQUEMENT MODIFIES

CNCM

Collection Nationale de Cultures de Microorganismes
INSTITUT PASTEUR
25, Rue du Docteur Roux
75724 PARIS CEDEX 15
Tél (33-1) 45 68 82 60
Fax (33-1) 45 68 82 39

ADDENDUM AU FORMULAIRE DE DEPOT
ADDENDUM TO THE APPLICATION FORM

obligatoire à partir du 4 février 1994
Required from February 4th, 1994

REFERENCE D'IDENTIFICATION
Identification reference

NUMERO OU SYMBOLES, PAR EXEMPLE, DONNES PAR LE DEPOSANT AU MATERIEL
NUMBER, SYMBOLS, etc, GIVEN TO THE MATERIAL BY THE DEPOSITOR

ORGANISME GENETIQUEMENT MODIFIE *Genetically modified organism* — OUI *yes* ☐ non *no* ☐

CLASSE DE RISQUE *Hazard group* — 1 ☐ 2 ☐ 3 ☐ E (*) ☐

EUROPEAN FEDERATION OF BIOTECHNOLOGIES : Safe Biotechnology / BF X 42-070
FEDERAL REGISTER: Guidelines for Research involving Recombinant DNA Molecules

(*) RISQUE POUR L'ENVIRONNEMENT
ENVIRONMENTAL RISK

Le soussigné déclare avoir procédé à toutes les notifications requises par les réglementations nationales en vigueur le concernant quant à l'utilisation et à la dissémination du micro-organisme cité ci-dessus et de toutes les composantes associées et avoir reçu des autorités compétentes les autorisations s'y rapportant.

The undersigned declares that he has proceeded to the notifications required by his own national regulations in force concerning the use and the release of the above-mentioned microorganism and all the associated components, and that he has got from the competent authorities the relevant permits.

Le(s) déposant(s)
The Depositor(s)
SERVICES DES BREVETS
ET INVENTIONS
INSTITUT PASTEUR
25-28, rue du Docteur Roux
75724 Paris Cedex 15

Date 20 Mars 2003

Signature(s) Danielle BERNEMAN
Chef du Service des Brevets & Inventions

Le(s) scientifique(s) responsable(s) des matériels biologiques transmis
The scientist(s) responsible for the biological materials transmitted

G. COURTOIS
F. AGOU

Date 15/7/2003

Signature(s)

DOCUMENT SUSCEPTIBLE D'ETRE REMIS A TOUTE PARTIE REQUERANTE, CERTIFIEE OU AUTORISEE ET A TOUTE AUTORITE PUBLIQUE COMPETENTE
DOCUMENT LIKELY TO BE COMMUNICATED TO ANY REQUESTING, CERTIFIED OR AUTHORIZED PARTY AND TO ANY COMPETENT PUBLIC AUTHORITY

Received at: 11:47AM, 9/24/2003

24. SEP. 2003 16:10 BUREAU DES BREVETS Nº1143 P. 67

TRAITE DE BUDAPEST SUR LA RECONNAISSANCE INTERNATIONALE DU DEPOT DES MICROORGANISMES AUX FINS DE LA PROCEDURE EN MATIERE DE BREVETS / ACCORD DU 25 AOUT 1978 ENTRE L'ORGANISATION EUROPEENNE DES BREVETS ET LA CNCM, INSTITUT PASTEUR, PARIS, MODIFIE LE 4 OCTOBRE 1982 CONCERNANT LE DEPOT DE MICROORGANISMES EN APPLICATION DES REGLES 28 ET 28bis DE LA CONVENTION SUR LE BREVET EUROPEEN

CONTRAT établi aux termes

- [x] de la règle 6.3.a.(v) du Traité de Budapest
- [ ] du point 13.a.(v) de l'Accord bilatéral en application des règles 28 et 28bis de la Convention sur le brevet européen

entre les parties désignées ci-dessous

AUTORITE DE DEPOT	DEPOSANT(S) Nom(s) et adresse(s)
CNCM Collection Nationale de Cultures de Microorganismes INSTITUT PASTEUR 25, Rue du Docteur Roux F-75724 PARIS CEDEX 15 Téléphone: (33-1) 45 68 82 60 Télécopie: (33-1) 45 68 82 36 *Yvonne CERISIER* *Directeur Administratif*	SERVICE DES BREVETS ET INVENTIONS INSTITUT PASTEUR *25-28, rue du Docteur Roux* *75724 Paris Cedex 15*

relatif au microorganisme (*) désigné ci-après

20 Z/3_C3

REFERENCE D'IDENTIFICATION — NUMERO OU SYMBOLES, PAR EXEMPLE, DONNES PAR LE DEPOSANT AU MICROORGANISME

1.- Le déposant reconnait avoir connaissance des exigences et des recommandations relatives au dépôt de microorganismes aux termes du Traité de Budapest ou aux termes de l'Accord bilatéral en application des règles 28 et 28 bis de la Convention sur le brevet européen.

2.- La CNCM accepte le microorganisme identifié ci-dessus, une fois que sont assurées

toutes les conditions de validité du dépôt en vertu de la règle 6.1.(a) ou 6.2.(a) et de la règle 6.3.(a) du Traité de Budapest ou du point 12.(a) ou 12.(b) et du point 13.(a) de l'Accord bilatéral, nécessitant, entre autre,

la réception par la CNCM de douze échantillons du microorganisme identifié ci-dessus, préparés à partir d'une même subculture, en vue d'une longue conservation, conformément aux indications fournies (#), portant de façon lisible et indélébile la référence d'identification et la date de préparation, et

l'examen préliminaire d'un des échantillons reçus par la CNCM en vue de la constatation de la validité des renseignements fournis en vertu de la règle 6.1.a.(iii) du Traité de Budapest ou du point 12.a.(iii) de l'Accord bilatéral et en vue de la constatation de l'acceptabilité du matériel transmis pour dépôt en vertu de la règle 6.4.(a) du Traité de Budapest ou du point 14.(a) de l'Accord bilatéral.

(*) On entend par 'MICROORGANISME' tout matériel biologique que la CNCM est susceptible d'accepter en vue d'un dépôt aux termes du Traité de Budapest ou de l'Accord bilatéral.

(#) Les ampoules doivent être compatibles avec les dispositifs de conservation de la CNCM, étanches et sans risque de fissuration, de rupture ou d'explosion pendant la période de conservation prévue à la règle 9.1. du Traité de Budapest ou au point 11. de l'Accord bilatéral.

3.- Un numéro d'enregistrement p ut être communiqué au déposant dès réception du microorganisme. La réception et l'enregistrement d'un microorganisme n'implique pas son acceptation.

4.- Un refus d'acceptation du microorganisme peut être notifié dans les conditions prévues à la règle 6.4.(a) du Traité de Budapest ou au point 14.(a) de l'Accord bilatéral.

5.- Si les conditions de validité du dépôt ne sont pas toutes remplies, une procédure de report d'acceptation est appliquée: La CNCM en notifie les raisons et fixe le délai de un mois au déposant pour qu'il satisfasse à toutes les exigences. Si le déposant ne satisfait pas aux exigences dans le délai fixé, la CNCM procède à l'annulation de la demande de dépôt et à la destruction du matériel biologique transmis.

Cette procédure implique un dépôt de remplacement ($) si une irrégularité de forme, de quantité ou de présentation est constatée par la CNCM sur le matériel biologique transmis par le déposant en vue d'un dépôt initial ou d'un nouveau dépôt. Un dépôt de remplacement est considéré comme un autre dépôt initial tant que la viabilité du dépôt en attente d'acceptation n'est pas établie.

6.- Chaque fois que du matériel biologique est transmis par le déposant à la CNCM, la CNCM perçoit la taxe de conservation prévue à la règle 12.1.a.(i) du Traité de Budapest ou au point 26.a.(i) de l'Accord bilatéral.

7.- Si le dépôt est accepté, le numéro d'ordre attribué au dépôt par la CNCM est identique au numéro d'enregistrement, et la date de dépôt est la date de réception par la CNCM du microorganisme identifié ci-dessus.

8.- La notification de l'acceptation, du refus ou de l'annulation de la demande de dépôt est établie dans un délai de six mois après réception du microorganisme. L'acceptation est attestée par le récépissé.

9.- La CNCM ne procède au premier contrôle de viabilité qu'une fois assurée que le déposant a satisfait à toutes les exigences en matière de dépôt.

10.- La première déclaration sur la viabilité atteste la validation ou l'annulation du dépôt : le dépôt est validé si le microorganisme est viable, il est annulé si le microorganisme n'est pas viable.

11.- En cas de refus, d'annulation de demande de dépôt ou d'annulation de dépôt, les échantillons de matériel biologique transmis sont détruits ; en cas de désaccord sur les motifs du refus ou de l'annulation, ils peuvent être conservés à la CNCM ; ils ne sont pas restitués au déposant, sauf accord particulier intervenu après réception de la notification du refus ou de l'annulation par le déposant; en aucun cas, les échantillons ne peuvent donner lieu à un dépôt à la CNCM à d'autres fins.

12.- La taxe de conservation prévue à la règle 12.1.a.(i) du Traité de Budapest ou au point 26.a.(i) de l'Accord bilatéral est due dans tous les cas, que le dépôt soit accepté, refusé ou annulé.

13.- Le déposant s'engage à déposer sous contrat associé tout matériel vivant, non ou difficilement accessible, nécessaire aux contrôles et/ou à la conservation du microorganisme identifié ci-dessus.

14.- Le déposant s'engage à fournir tous les substrats non ou difficilement accessibles, nécessaires aux contrôles et/ou à la conservation du microorganisme identifié ci-dessus, en quantité suffisante pour douze épreuves ou passages.

15.- Le déposant certifie avoir fourni toute indication dont il a connaissance sur les propriétés du microorganisme identifié ci-dessus qui présentent ou peuvent présenter une action directe ou indirecte, connue ou prévisible, sur l'homme ou sur quelqu'organisme que ce soit, animal, végétal ou autre.

Il s'engage à porter immédiatement à la connaissance de la CNCM toute nouvelle information y relative.

16.- Après acceptation du microorganisme, la CNCM le conserve, assure les contrôles de viablité, établit les déclarations, attestations et notifications, remet les échantillons aux parties autorisées, certifiées, ou requérantes, conformément à la réglementation applicable.

($) On entend par "DEPOT DE REMPLACEMENT" une série complémentaire d'échantillons du microorganisme ayant fait l'objet d'un dépôt initial ou d'un nouveau dépôt en attente d'acceptation, préparés conformément aux exigences de la CNCM et transmis en une seule fois par le déposant à la demande et à l'adresse de la CNCM dans le délai fixé au point 6 du présent contrat, accompagnés d'une déclaration semblable à celle définie à la règle 6.2.(a) du Traité de Budapest.

17.- Chaque fois que la CNCM juge opportun d'adresser au déposant (**) un échantillon d'une subculture du microorganisme identifié ci-dessus en vue d'un contrôle de conformité, le déposant (**) vérifie l'expression des propriétés dudit microorganisme dans la dite subculture et renvoit à la CNCM, dans le délai de trois mois après réception de l'échantillon, la formule jointe à l'envoi après l'avoir dûment remplie et signée.

Le déposant (**) reconnait qu'en cas de non-réponse à une demande d'accord de conformité telle qu'elle est présentée ci-dessus, les propriétés de la subculture en question sont à considérer identiques aux propriétés de la subculture transmise à la CNCM à la date du dépôt.

18.- Le déposant ne peut pas retirer, annuler ou modifier le dépôt pendant la période de conservation prévue à la règle 9.1 du Traité de Budapest ou au point 11 de l'Accord bilatéral.

Cette période de conservation est de trente-cinq ans dans tous les cas à la CNCM.

19.- A l'expiration de la période de conservation, tout le matériel biologique conservé est détruit, sauf dans le cas d'une demande particulière formulée par le déposant au courant de la trente-cinquième année de conservation.

20.- Lorsque, pour quelque raison que ce soit, la CNCM ne peut pas remettre d'échantillons du microorganisme identifié ci-dessus, une fois accepté et déclaré viable, le déposant procède conformément aux dispositions de la réglementation applicable à un nouveau dépôt dudit microorganisme dans un délai de trois mois à compter de la date de réception de la notification correspondante.

La définition des raisons de bon usage en matière d'autorité de dépôt, interdisant la remise d'échantillons, est soumise à la seule appréciation de la CNCM.

21.- La CNCM est dégagée de toute responsabilité en cas de variation de caractères du matériel biologique déposé. Il en est de même si une perte de viabilité, une contamination ou une destruction accidentelle était constatée malgré l'application des précautions prévues pour sa conservation.

22.- Si, par la faute ou la négligence du déposant, un fait dommageable à la CNCM survient à la réception, à la manipulation ou pendant la durée de conservation du dépôt, le déposant indemnise la CNCM du préjudice subi.

23.- A moins que le fait dommageable ne soit imputable à la faute ou à la négligence de la CNCM, le déposant garantit celle-ci contre toute action à son encontre en réparation d'un préjudice lié à la remise d'un échantillon du microorganisme identifié ci-dessus.

24.- En cas de contestation la loi française est applicable et le tribunal compétent est celui de Paris.

LE(S) DEPOSANT(S) (***)

SERVICE DES BREVETS
ET INVENTIONS
INSTITUT PASTEUR

25-28, rue du Docteur Roux
75724 Paris Cedex 15

Date et signature(s) 20 Mars 2003

Danielle BERNEMAN
Chef du Service des Brevets
& Inventions

LE(S) SCIENTIFIQUE(S) RESPONSABLE(S)

Date et signature(s) 20-03-2003

Dr Gilles COURTOIS

(**) Les engagements indiqués au point 17 peuvent être assurés indifféremment par le déposant ou le responsable scientifique indiqué par le déposant.

(***) Les noms dactylographiés des personnes physiques qui signent au nom d'une personne morale doivent accompagner les signatures. Lorsqu'une demande de dépôt est présentée par plusieurs personnes, le formulaire et le contrat correspondants doivent porter la signature de chacun des déposants. Dans ce cas, une des personnes doit être désignée REPRESENTANT UNIQUE, habilitée à recevoir, les documents originaux émis par la CNCM pendant la période de conservation prévus dans la réglementation applicable.

CLONE 702/3 (C3)

Plasmids Cells 05/07/01

CRABTREE LAB DNA DATABASE

Plasmid name: cx12lacZ-kB (14kBZH)
Prokaryotic selection: Ampicillin
Eukaryotic selection: Hygromycin

Description: This plasmid was derived by Petri from cx12lacZ by cloning 3 tandem copies of the NF-kB oligonucleotide derived from the Igk sequence (TCAGAGGGGACTTTCCGAG) into the XhoI site in the minimal IL-2 promoter. The tandem oligos had blunt Bam ends which destroyed the Xho sites upon ligation. The IL-2 enhancer has been deleted in the minimal promoter from -294 to -72, leaving only the TATA box.

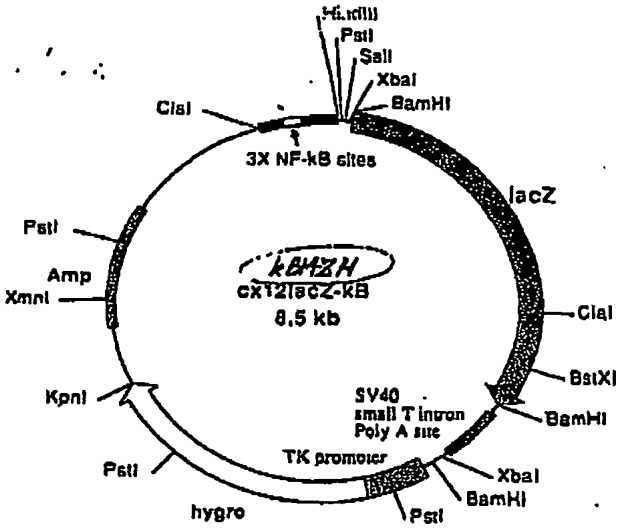

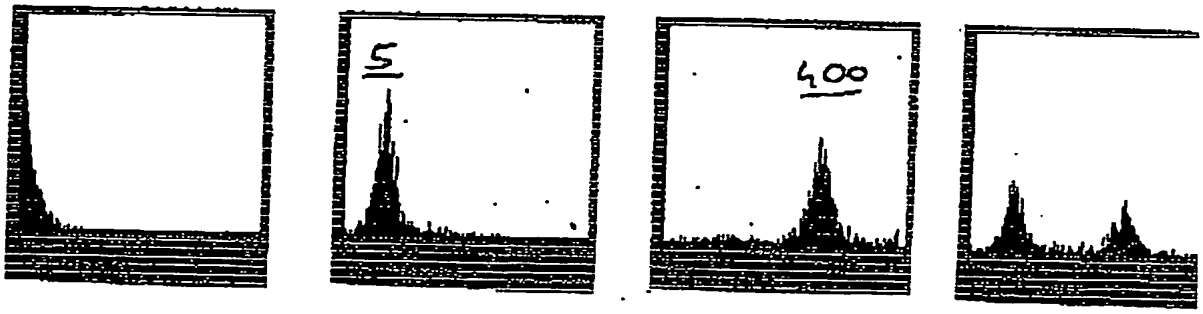

⊖FDG ⊕FDG ⊖LPS ⊕FDG ⊕LPS ⊕FDG ⊖LPS/⊕LPS

Analysis of the oligomerization domain of the NF-κB Essential Modulator NEMO protein

François Traincard[1], Emilie Vinolo[1], Gilles Courtois[2], Alain Israël[2], Michel Véron[1] et Fabrice Agou[1]

[1] Unité de Régulation Enzymatique des Activités Cellulaires, [2] Unité de Biologie Moléculaire de l'Expression Génique, Institut Pasteur, 25 rue du Dr Roux, 75724 Paris Cedex 15, France

ABSTRACT

The murine NEMO protein (*NF-κB essentiel modulator*) which plays a keyrole in the NF-κB pathway activation, is associated with the IKKα and IKKβ protein kinases in a high molecular weight complex called the IKK complex. The IKK kinases are activated by phosphorylation upon a still unknown mechanism which has been hypothesized to occur upon NEMO oligomerization. We have shown that the C-terminal domain (AA 241-338) of NEMO is responsible for the trimerization of the protein (Agou, JBC, 02). This domain contains two putative coiled-coil motives, the CC2 motif and the leucine zipper LZ motif, a proline rich region and a putative Zinc-finger domain at the far C-terminus of the polypeptide. We have expressed in *E. coli* and purified various truncation mutants of the C-terminal domain of NEMO. By gel filtration and equilibrium sedimentation of deleted recombinant proteins we have show that the proline rich region and the Zinc-finger domain are dispensable for NEMO oligomerization. We have shown that the CC2-LZ recombinant polypeptide self-associates in trimer with an association constant close to the one of the wild type protein while CC2 and LZ synthetic peptides self-associate respectively in trimers and dimers with a 100 times and 40 times weaker association constant than CC2-LZ. By functional complementation we have shown that the CC2 and the LZ domains are nevertheless crucial for the activation of the NF-κB pathway by LPS. When the CC2 and the LZ synthetic peptides are mixed together in an equimolecular ratio they form a unique and stable molecular species with a MW corresponding to a heterohexamer. The physical association of CC2 to LZ was established by fluorescence anisotropy using a bodipy labelled LZ synthetic peptide. These results indicate that the trimerization domain of NEMO contains the CC2 and the LZ motif (AA 251-337) which associate in a stable heterohexamer. A model of the trimeric structure of

NEMO is given in relationship with its putative activation mechanism. The structural relationship with the six helix bundle of the ectodomains of the HIV-1 gp41 transmembrane glycoprotein is discussed.

INTRODUCTION

The NF-κB signaling pathway is implicated in the regulation of eukaryote gene expression in response to proinflammatory signals, to viral proteins, to antigens, and to cell growth and morphogenesis regulators (revues récentes). These extracellular stimuli promote NF-κB activation by phosphorylation of the IκB kinases IKKα and IKKß. Activated IKKs phosphorylate in turn the Inhibitor of κB (IκB) molecules which sequester the NF-κB transcription factors in the cytoplasm. This phosphorylation followed by ubiquitination results in the degradation of IκB by the proteasome, allowing the NF-κB transcription factors to enter the nucleus (Karin, 00, Annu Rev Immunol). The IKK kinases have been found associated to the NEMO (NF-κB Essential Modulator) protein in a high molecular complex, the IKK complex (Yamaoka,98,Cell; Mercurio, 99, Mol Cell Biol, Rothwarf, 98, Nature). NEMO (alias IKKγ, FIP-3, IKKAP-1 in human), while devoid of kinase activity, behave as the key regulator of the NF-κB pathway as its genetic inactivation (Yamaoka, 98,Cell; Makris, 00, Mol Cell; Rudolf, 00, Genes Dev) or its biochemical inactivation (May,00, Science) leads to the inhibition of the pathway. The presence of the C-terminal domain of NEMO is crucial for IKKα and IKKß phosphorylation and more generally for activation of the NF-κB pathway (Ye, 00, JBC; Tegethoff, 03, Mol Cell Biol). This activation mechanism is still unclear today. The enforced oligomerization of the N-terminus of NEMO through fusion with the FKBP12 polypeptide was sufficient to activate the NF-κB cascade (Poyet, 00, JBC). Huang (02, FEBS) demonstrated that the binding of the well known NF-κB activator Tax to IKKγ promotes its oligomerization. NEMO oligomerization has thus been hypothesized as the molecular activation

mechanism of the IKK complex (Inohara, 00, JBC; Poyet, 00, JBC; Poyet, 01, JBC; Agou, 02; Huang, 02, FEBS; Tegethoff, 03, Mol cell biol). Huang (02, FEBS) established, using the bis(sulfoccinimidyl)suberate crosslinker and in vitro crosslinking of purified IKKγ protein, that IKKγ auto-associates in dimers and trimers. Rothwarf et al. (98, Nature) using the EGS (ethyleneglycol-bis-succinimidylsuccinate) crosslinker and recombinant protein found also dimeric and trimeric forms of IKKγ but a recent publication using the same broad spectrum crosslinking agent in crude HeLa cell extracts emphazised that IKKγ associates in tetramers (Tegethoff, 03, Mol cell biol). We have demonstrated using the cell permeant cystein-specific crosslinker BMOE (bis(maleimido)ethane) and HeLa cells that NEMO associates *in vivo* in dimer and trimer (Agou et al. 02, JBC). We have also shown that the purified C-terminal domain of NEMO self trimerizes (AA 242-388) (Agou, 02, JBC). Tegethoff et al. (03, Mol Cell Biol) have genetically restricted the minimal oligomerization domain (MOD) of IKKγ to its 246-365 region. The C-terminal domain of NEMO contains three predicted structural motives: the CC2 coil-coiled motif (AA 246-286 in mouse), a Leucine-Zipper (LZ) (AA 303-337) and a Zinc-Finger (ZF) motif at the far C-terminus of the protein (AA 390-412). Mutations or deletions in CC2, in LZ, in ZF and in the linker region between CC2 and LZ result in impaired NF-κB functionning and in severe human diseases (Döffinger, 01, Nat gen; Makris, 02, Mol Cell Biol; Huang, 02, Mol Cell Biol)). Mutations in the AHD2 region of the ABIN-1 NF-κB inhibiting protein, a counterpart of the CC2-LZ linker region of IKKγ, abolishes the inhibition of the pathway by ABIN-1 (Heyninck, 03,FEBS).] A role of each of these motives in NEMO oligomerization could be hypothezised.

By functional complementation of 1.3E2 cells we demonstrated that CC2 and LZ are not dispensable for the rescue of the NF-κB pathway activation. Using purified recombinant and synthetic sub-domains, we quantitatively analyzed the roles of the

CC2, LZ and ZF domains in NEMO oligomerization. We showed that the ZF motif is dispensable for oligomerization. We demonstrated that the CC2 motif displayed trimeric self association properties and that the LZ motif strongly contributes to the oligomerization process. We propose a structural model of the trimerized C-ter domain of NEMO and discuss it in relationship to the structure of ectodomains from coiled-coil and LZ containing proteins like the gp41 of HIV.

EXPERIMENTAL PROCEDURES

Reagents

Functional complementation of L3E2 cells

Transient transfection

Stable transfection

Peptides and recombinant NEMO sub-domains obtaining

The following peptides were synthetized by F. Baleux (Unité de Chimie Organique, Institut Pasteur): CC2 ($_{253}$LEDLRQQLQQAEEALVAKQELIDKLKEEAEQHKIV$_{287}$-NH_2), mutated CC2 named $CC2_{Mut}$ (LEDLRQQGQQAEEAGVAKQELGDKLKEEAEQHKIV-NH_2) in which mutations are underlined, LZ in which the putative leucine zipper begins at L_{395} ($_{194}$LKAQADIYKADFQAERHAREKLVEKKEYLQEQLEQLQREFNKL$_{236}$-NH_2) ,
N-terminal Cys Bodipy (B) labelled LZ (Ac-Cys-p-LZ) called Bp-LZ in which p corresponds to penetratin (RQIKIWFQNRRMKWKK).

Gel filtration analysis

Sedimentation equilibrium

- Peptides LZ and CC2 (200μM each) were pre-mixed (xxx min) in 4M guanidine, 150 mM KCl and 1 mM DDM containing 20mM Tris-HCl (pH 8.0) buffer. The column

was preequilibrated in 200 mM NaCl containing 50mM Tris-HCl (pH 8.0) buffer prior to loading with the peptide mixture.

Fluorescence anisotropy

Bp-LZ - CC2 hetero-association experiments were performed in 150 mM KCl containing 50mM Tris-HCl buffer (pH 8.0). Bp-LZ was used at a 100 nM concentration, and CC2 and $CC2_{Mut}$ at various concentrations (see legend Fig. 4A). Anisotropy measures were performed with a PTI fluorometer (excitation at 495 nM and emission at 520 nM) after a 3 hours preincubation of the samples at 22°C. Measures were at least performed in duplicates.

RESULTS

Deletion of the CC2 or of the LZ motives or L to S mutations in the LZ motif cancel functional complementation of 1.3E2 cells by NEMO.

We have already described the 1.3E2 70Z/3 murine pre-B cell mutant (Courtois, 97,Mol Cell Biol) and we have demonstrated that the mutant do not express NEMO and is non-responsive to LPS activation (Yamaoka, 98, Cell; Fig 1B). 1.3E2 cells were transiently co-transfected with the reporter plasmid Igκ-luciferase and with a plasmid bearing a *Nemo* wt or mutant gene (Fig. 1A). When transfected with a control plasmid and with the reporter plasmid, cells were non-responsive while they recover LPS response when transfected with the wt *Nemo* gene. When transfected with a *Nemo* gene deleted from the region coding for the CC2 domain (ΔCC2) or for the LZ motif (ΔLZ), no luciferase activity increase resulted from LPS stimulation (Fig. 1A). Stable transfection of 1.3E2 cells were performed with variants of the *Nemo* gene (Fig. 1B). Stable transfection with a gene coding for wild type His-tagged NEMO resulted in a rescue of the Igκ oligonucleotide binding activity of nuclear extracts from LPS activated cells. When transfection was performed with a plasmid coding

for a LZ motif L_{322}->S and L_{329}->S mutant His-tagged NEMO protein, no target DNA retardation activity could be detected in cell nuclear extracts while the expression level of the endogeneous NEMO protein and of the wild type and mutant His-tagged NEMO proteins are comparable in the parental 70Z/3 cells and in transfected 1.3E2 cells.

Obtaining and purification of recombinant NEMO sub-domains

The His-tag labelled recombinant NEMO C-terminus proteins and the synthetic peptides (LZ, CC2) used in this work are diagrammed in Fig. 2A. SDS-PAGE analysis of the purified proteins is shown in Fig.2B. Three of the four proteins were purified to homogeneity and the fourth one (HisCter-ΔZF) migrated as a doublet whose minor component is a proteolysed, His-tag deleted polypeptide whose nature was checked by WB (anti-His tag and anti-NEMO C-terminus antibodies) and mass spectrometry (not shown). The apparent molcular weights of the four proteins were in agreement with their calculated molecular weights.

Dnak??

The C-terminal ZF motif is dispensable for NEMO oligomerization

We have already demonstrated by sedimentation equilibrium that the His-tag labelled ZF truncated C-terminal domain of NEMO (AA 241-388) auto-associates in dimers and trimers (Agou, JBC, 02). We have performed size exclusion chromatography to compare the apparent Stoke's radius of the His-Cter wt and of the His-Cter ΔZF recombinant sub-domain of NEMO. The 280 nm absorbance distribution diagrams of the His-C-ter wt and of the His-C-ter ΔZF polypeptides are shown in relation to their elution volume (Fig 3). The two proteins elute at very close volume (xml for wt, yml for ΔZF), measured at the tipping of the peaks. The Kav of

the wt and of the ΔZF proteins were respectively (xx and xx) estimated by comparison to the Rs (Å) of standard proteins (Inset Fig. 3). The Kav of the His-C-ter wt and of the His-C-ter ΔZF proteins are those of trimeric proteins. The broadnesses of the peaks suggest that trimers are in association with lower MW compounds. The chromatography was performed at different initial protein concentrations ranging from xxmM to yymM and the relative concentration of monomer/trimer (M/T) allowed to calculate the apparent K_A of the association (Table 1). The K_A(M/T) of C-ter wt ($10^6 M^{-2}$) was almost identical to the K_A(M/T) of C-ter ΔZF ($9.9x10^5 M^{-2}$).

The minimal oligomerization domain of NEMO is CC2-LZ

Having established (see above; Agou, 02, JBC) that the ZF motif is dispensable for NEMO oligomerization we next deleted the proline riche PPP region joining LZ to ZF (AA 337-390, Fig. 2). Gel filtration experiments with the ZF deleted His-CC2-LZ recombinant protein (Fig. 2) were performed at 0.5, 3 and 15 μM loading protein concentrations (Fig. 4A). His-CC2-LZ elution profile is concentration independent and monomodal even at a 0.5 μM concentration. A slight concentration dependent difference in the elution volume of the protein is observed suggesting that, at low concentration, the protein is xxxxxx. The Stoke's radius of His-CC2-LZ was measured at xx Å in reference to a calibration curve for globular markers eluted in the same experimental conditions (inset Fig. 4A). It corresponds to the one of a globular protein whose MW (xxxkD) is that of a trimer of His-CC2-LZ (theoretical MW: xxxkD). Its monomer/trimer K_A was estimated as above and was $10^6 M^{-2}$ (Table 1).

CC2 self associates in trimers

We then used synthetic CC2 peptide to analyse self-association properties of this CC2-LZ sub-domain. Various concentrations of CC2 were loaded on a xx column and

conditions CC2 and LZ again auto-associate respectively in trimer and dimer when alone (Fig 5). The Kav of the LZ peptide is shifted to a higher MW compound when premixed with CC2 suggesting an association of CC2 to LZ. The Kav of this complex correspond to the one of chymotrypsin whose MW (25 kDa) is close to the theoretical MW of an oligomer composed of three CC2 peptides associated to three LZ peptides (theoretical MW: 28.2 kDa). Note that the band is monomodal suggesting that most of the LZ peptide has been associated to CC2 in a more stable form than the LZ dimer. (Moreover, no peak was monitored at 247 nm located at the position of the CC2 trimer (not shown))

CC2 interaction with LZ was analysed by fluorecence anisotropy using Bp-LZ peptide as probe. Titration of Bd-LZ by increasing concentrations of CC2 resulted in a progressive increase of anisotropy which reached seven times the basal value at a 100μM CC2 concentration without reaching saturation (Fig 5). We then replaced peptide CC2 by peptide $CC2_{Mut}$. The CC2 mutated $CC2_{Mut}$ peptide bound Bd-LZ very differently (higher Ka, plateau at a lower concentration) (Fig. 5) indicating that the CC2 part of the peptide is implicated in Bd-LZ binding. Indeed, the $CC2_{Mut}$ peptide behave as a monomer in gel filtration experiments (not shown).

DISCUSSION

Using functional complementation we have first questionned the importance of the CC2 and of the LZ domain of NEMO in the activation of the NF-κB pathway by LPS. Transient transfection of 1.3E2 cells by a *Nemo* gene deleted from its CC2 or from its LZ coding region cancel the NF-κB activity rescue upon activation of the cells by LPS (Fig 1A). In a stable transfection experiment we also demonstrated that the rescue of the NF-κB pathway requires an intact LZ domain since an inner doublet of point mutations (L_{327}->S and L_{329}->S) abolish phenotypic rescue (Fig 1B). It should be noted

that no significant difference in NEMO expression is observed between the wt parental strain, the wt *Nemo* transfected clone and in the mutant transfected clone, ruling out the hypothesis of a pathway inhibition by overexpression of mutant NEMO in transfected 1.3E2 cells. Our experiments pointed out the importance of both the CC2 and of the LZ domain of NEMO in NF-κB pathway activation by LPS. Makris et al. (02, Mol Cell Biol), but using MEF cells complemented with a *Nemo* gene carrying a single L_{321}> P mutation in LZ and TNFα or IL1 activators, observed a similar absence of phenotypic rescue upon complementation with this mutant gene. The L ->P point mutations in LZ very likely alter the helix structure of the coil-coiled LZ motif while we hypothesized that L->S mutations were more likely promoting an alteration of the oligomerization property of LZ (insertion of a charged residue into the hydrophobic surface of the amphipatic LZ helix) than changing the helical structure of the motif. Indeed a LZ peptide bearing the two L->S mutations is 50% dimeric while at the same concentration (10 μM) the wild type peptide is 100% dimeric in gel filtration (not shown).

Using *in vivo* crosslinking (BMOE) in HeLa cells, we have shown that endogeneous NEMO is found as trimers and dimers and crosslinked to IKK in a 350 kD complex, very likely corresponding to the IKK complex (Agou, 02, JBC). We have also shown that recombinant wt NEMO as well as a C-terminal truncated form of NEMO associate in dimers and trimers (Agou, 02, JBC). We hace therefore investigated the role of the CC2, LZ, PPP and ZF predicted domains of NEMO (Fig. 2) in its oligomerization.

We first demonstrated that the ZF domain is not required for NEMO oligomerization as a deletion of this domain (AA388-412) resulted in a mutant protein (His-CterΔF) with a Stoke's radius (ou Ka?M/T) almost identical to the one of the His-Cter wt protein which is trimeric in the same conditions (Fig 3) and which we have

previously determined to associate in dimers and trimers in sedimentation equilibrium experiments (Agou, 02, JBC). The homoassociation constants (Ka, ΔG^o) of the mutant are very close to those of the His-CterWT protein (Tab I). These results are in agreement with the Tegethoff (03, Mol Cell Biol) conclusion that the MOD of NEMO can be restricted to the 246-365 region of the protein and with our previous conclusions (Agou, 02, JBC). These results also strongly suggest that the ZF motif which is not implicated in NEMO oligomerization serves as an upstream activator anchoring motif as already suggested by several authors (ref; Huang, 02, Mol Cell Biol; Makris, 02, Mol Cell Biol). We next investigated by gel filtration the oligomerization status of the recombinant His-CC2-LZ polypeptide devoid of the PPP region (see Fig. 2). His-CC2-LZ eluted as a monomolecular trimer (MWxx) even at a 0.2 μM loading concentration (Fig 4A). The monomer-trimer association constant of His-CC2-LZ was measured by sedimentation equilibrium at $0.8 \pm 0.4 \times 10^9\ M^{-2}$ i.e. very close to the one's displayed by His-CC2-LZ ($0.5 \pm 0.2 \times 10^9\ M^{-2}$) and by His-CterWT ($1.5 \pm 0.7 \times 10^9\ M^{-2}$) (Tab 1). Presence of the CC2-LZ joining peptide is thus dispensable for NEMO oligomerization and the MOD domain of the protein could be restricted to the 251-337 region which contains the CC2 and the LZ domains. We then analysed the oligomerization properties of these two sub-domains using synthetic CC2 peptide, recombinant His-LZ protein and a synthetic LZ peptide (Fig 2).

The synthetic CC2 peptide was submitted it to gel filtration analysis and to equilibrium sedimentation. In these experiments the CC2 peptide splitted between molecular species with Stoke's radii corresponding again to monomers and trimers and the ration trimer/monomer increases with peptide concentration. No peak corresponding to the MW of a tetramer was observed in this experiment. In order to circumvent the potential odd behaviour of short peptides in gel filtration we performed equilibrium sedimentation experiments (concentrations?). The better radial distribution fit is achieved with a two species model composed of monomers

and trimers (Fig 4B). It is noteworthy that a monomer/tetramer equilibrium hypothesis is not supported by the analysis of the equilibrium distribution of the CC2 peptide (Fig 4B?) (commentaire sur une distribution trimoléculaire/ Tegethoff). The Ka of this association equilibrium was $3.3 \pm 0.5 \times 10^7 M^{-2}$ while the Ka for the C-ter wt protein was around 100 times higher (Tab 1). We can thus conclude that CC2 display self-trimerization properties but with a weaker association constant than the full length C-ter wt protein or the His-CC2-LZ polypeptide. Similar gel filtration and equilibrium sedimentation experiments demonstrated that the recombinant LZ polypeptide (His-LZ) and the LZ synthetic peptide (LZ) self associate in dimers with respective association constants (M/D) of $9 \pm 5\ 10^4 M^{-1}$ and of $6 \pm 5\ 10^4 M^{-1}$ (not shown, Tab 1). The strenght of the LZ autoassociation (ΔG° of $-6.6 \pm 0.$ kcal.mol^{-1}) is weak as compared to the one of CC2 (ΔG° of -10 ± 0.1 kcal.mol^{-1}) and the presence of both motives in theHis-CC2LZ polypeptide resulted in a trimeric structure with a very different ΔG° (-11.9 ± 0.3 kcal.mol^{-1}) (Tab 1). The fact that the LZ motif of NEMO associates in dimer but not in trimer like His-CC2LZ (see before) and according to the low association constant of this association we figured out that LZ could physically interact with CC2. To probe this hypothesis we mixed CC2 and LZ peptides and submitted the mixture to gel filtration analysis. Fig 5 shows that, at peptide concentrations where CC2 and LZ alone are trimers and dimers (xμM and xμM respectively), the mixture of the peptides generate higher stock radius components (between xx and xx Å) which suggest the presence of CC2-LZ complex (es). To further investigate this association we labelled the LZ peptide N-terminally with the bodipy fluorochrom (Bp-LZ, see material and methods) and followed by fluorescence the anisotropy change resulting from the association of CC2 with Bp-LZ. A CC2 concentration dependent Bp-LZ anisotropy increase resulted from the adding of increasing concentrations of CC2 to Bp-LZ. This association is very strong

as it can be observed in a buffer containing 1mM DDM (n-Dodecylmaltoside) and 1mM DTE (Dithioerythiol) (not shown). We mutated CC2 in three of the leucines (L->G) important for its self-trimerization (peptide $CC2_{Mut}$, see material and methods) and controlled by gel filtration that $CC2_{Mut}$ is a monomer (not shown). When using $CC2_{Mut}$ instead of CC2 in Bd-p-LZ titration experiments, a drastic change in the dose dependent anisotropy increase was observed (Fig. 5B) indicating that the mutated leucines in $CC2_{Mut}$ contribute to Bd-p-LZ binding. Indeed the monomeric $CC2_{Mut}$ peptide associate to Bd-p-LZ at lower concentrations than CC2 and the association reach a saturation plateau which is not observed with CC2. It should be nevertheless noted that the mutated leucines are modelized as contact AA between the CC2 helices and are thus supposed not to be exposed to the solvent and accessible to partnership proteins or peptides (ref). The contribution of LZ peptide subdomains to CC2 binding needs to be further precised as the peptide contains, upstream the predicted leucine-zipper, a stretch of 21 AA which could be implicated in CC2 binding as it is predicted to form itself an α-helix (program?). Heyninck et al. (FEBS, 2003) demonstrated that, in the ABIN-1 NF-κB pathway inhibitor protein, the AA 444-560 region bears the key-region for inhibition. This 116 AA long region carries a counterpart of the 21 AA stretch of IKKγ ($AA_{475-497}$ in ABIN-1, AHD2 region) which must be surrounded by N- and C-terminal sequences, to provide the ABIN-1 inhibitory function. ABIN-1 structure prediction (program) positionned the AHD2 motif in a coiled-coil environment like is the 21AA stretch of NEMO between the CC2 motif and the leucine zipper motif. Heyninck postulates that ABIN-1 competes with IKKγ for upstream activators but a direct inhibitory binding of ABIN-1 to IKKγ through its IKKγ like sequence and its neighbouring sequences cannot be ruled out. In this region a point mutation in this 21AA long sequence of human IKKγ (D_{311}->N) resulted in a fatal EDA-ID disease (Döffinger, 01, Nature gen) and mutants in the

fluorescence, verifying that our extensive washing protocol before FACS analysis was optimal to minimize any contribution of surface-bound peptide in measuring NEMO peptide internalization (see "Materials and methods"). Thus, these data suggest that the observed cellular fluorescence signaling mostly reflects the intracellular concentration of transduced NEMO peptide and not a non specific adsorption onto the membrane surface.

We next investigated the kinetic and concentration dependency of cellular uptake for the Ant-CC2 BODIPY peptide keeping in mind that the transduction of other NEMO peptides should occur in a similar fashion (Fig. 2B and 2C). FACS analysis 5 h after addition of 70Z3-C3 cell treated with 0.2, 2 or 20 μM BODIPY-Ant-CC2 peptide at 37°C demonstrate the linear dependancy of the intracellular concentration as a function of the incubated concentration of the antennapedia fusion peptide as widely reported in litterature (ref). Notably, the cells treated with the Ant-CC2 at 20 μM and at 37°C already reach maximum intracellular concentration in 30 min and remain unchanged for up to 5 h. Since the time to induce a strong NF-kB activation in response to LPS requires 3-5 hours of cell treatment, these results indicate that the intracellular concentration of each peptide remains constant during the LPS stimulation.

Specific inhibition of LPS-induced NF-κB activation by cell permeable CC2 and LZ

To analyze the inhibition potential of LPS-induced NF-κB activation by cell permeable BODIPY-Ant-CC2 and BODIPY-Ant-LZ peptides, we stably transfected the murine pre-B 70Z3 cell line with p12XlacZ-kB, which bears the β-galactosidase reporter gene

as the ratio of the luciferase activity in cell extracts from the corresponding cell line in presence and in absence of LPS activation.

B/ Permanent transfection: Western blot (WB) expression of NEMO in in cell extracts from 1.3E2 cells (E), from the parental 70Z3 wt cells (Z), from 1.3E2 cells permanently transfected with a wt *Nemo* gene (WT) and from 1.3E2 cells permanently transfected with a *Nemo* gene whose L342 and L349 of the LZ motif were mutated (L342S-L349S). HA-NEMO, His-tagged NEMO; mNEMO, endogeneous NEMO. Gel retardation analysis (EMSA) of nuclear extracts from resting cells (-) and from cells activated by LPS (+) of the indicated cell lines.

Figure 2: **Recombinant proteins and synthetic peptides**

A/ Diagram representation of the wild type NEMO protein (WT-NEMO), of the His-tagged (His) (black box) recombinant proteins His-CterWT, His-CterΔZF, His-CC2LZ and His-LZ, and of the synthetic peptides LZ and CC2 used in the experiments with box representation of the predicted coiled-coil (CC), leucine zipper (LZ) anf Zinc-finger (ZF) motives. Amino acid numbering correspond to the mouse NEMO protein.

B/ Coomassie staining of the indicated purified recombinant proteins. The MW ladder for the His-CterWT protein is on the left of the panel, while the ladder for the other recombinant proteins is on the right of the panel. MW are expressed in kilo daltons (kDa).

Figure 3: **Analysis of the ZF deleted recombinant NEMO protein by exclusion chromatography**

Distribution profile of the His-CterWT and of the (His-CterΔZF) recomi proteins in a gel filtration experiment. The gel filtration was performed as described under "Experimental procedures". Proteins were followed by absorbance at 220 nm

and optical density was plotted against the elution volume (Ve) in mL Distribution profile of the bovine serum albumine (*BSA*) and ovalbumine (*OVA*) molecular weight standards are shown in dotted lines. *Inset*: calibration curve for globular proteins measured under the same experimental conditions. *Chymo.*, chymotrypsin; *Ribo. A*, Ribonuclease A; *Cyt. C*, Cytochrom C; *Aprot.*, Aprotinin. The K_{av} of the His-CterWT and of the His-CterΔZF recombinant proteins are indicated by arrows.

Figure 4: Analysis of the oligomerization state of the His-CC2LZ protein and of the CC2 synthetic peptide

A/ Exclusion chromatography

Distribution profile of the His-CC2LZ recombinant protein and of the CC2 peptide in a gel filtration experiment. The gel filtration was performed as described under "Experimental procedures". The μmolar concentration of the injected product is indicated at the top of each corresponding diagram. The His-CC2LZ protein was detected using 220 nm (low protein concentrations) and 280 nm (high protein concentration) wavelenghth absorbance while the synthetic peptide was detected using 220 nm absorbance. Absorbance is plotted against the elution volume in ml. The elution profile of several globular protein used as standards are shown as dotted lines. *OVA*, Ovalbumin; *Chymo.*, chymotrypsin; *Ribo.*, Ribonuclease ; *Cyt. C*, Cytochrom C. *Insets*: calibration curve for globular proteins measured under the same experimental conditions. The log of their MW (Da) is ploted against their K_{av}. *BSA*, bovine serum albumine; *Aprot.*, Aprotinin. The K_{av} of His-CC2LZ and of CC2 are indicated by a black square and by a black dot with the theoretical position of a tetramer (Tetra), of a trimer (Tri) and of a dimer (D) of each of the polypeptide.

B/Equilibrium sedimentation

Analysis of the CC2 peptide by sedimentation velocity. The experiment was performed as described under "Experimental procedures". Sedimentation profile of

CC2 was recorded at 230 nm as a function of the radius of migration.(top pannel). The sedimentation data were fitted using mono-species models (monomer) and a two-species model (dimer or trimer) as indicated at the top of the 3 corresponding bottom pannels in which the residuals are plotted against the radial distance. *Inset*: Percent of monomer (circle) and trimer (black squares) species as a function of the µmolar concentration of the CC2 peptide.

Figure 5: Analysis of the interaction of the CC2 peptide with the LZ peptide

A/ Exclusion chromatography

Distribution profile of the LZ peptide, of the CC2 peptide and of a mixture of the CC2 and the LZ peptide (CC2+LZ) in a gel filtration experiment. Aborbance was plotted against elution volume in ml. The CC2 peptide was detected at 247 nm while the LZ peptide was specifically detected at 280 nm.. The elution volume of markers is indicated (arrows), with their MW in kDa, at the top of the panel: *Chymo.*, chymotrypsin; *Cyt. C*, Cytochrom C; *Aprot.*, Aprotinin. The gel filtration was performed as described under "Experimental procedures".

B/ Fluorescence anisotropy

Figure 6: Model for the trimeric structure of NEMO

Initial peptide concentration	Speed	Single species	χ^2	Monomer-trimer equilibrium	χ^2
μM	rpm	Da		M^{-2} (x 10^7)	
35	25000	6600 ± 300	20	2 ± 1	18
35	35000	6550 ± 200	54	1.3 ± 0.2	40
35	55000	6250 ± 200	263	1.3 ± 0.1	90
15	40000	5800 ± 200	62	3.5 ± 0.7	50
15	55000	5300 ± 150	60	5 ± 2	35

Table I : Sedimentation Equilibrium Results with the CC2 peptide

His-tagged protein or peptide	Oligomeric state	Monomer-Trimer Association K_A (M^{-2})	Monomer-Dimer Association K_A (M^{-1})	Homoassociation energy ΔG° (kcal.mol^{-1}) at 293.15 K
His-CterWT	Trimer [a]	1.5 ± 0.7 x 10^9		- 12.3 ± 0.3
His-CterΔZF	Trimer [a]	0.5 ± 0.2 x 10^9		-11.7 ± 0.2
His-CC2LZ	Trimer	0.8 ± 0.4 x 10^9		-11.9 ± 0.3
His-LZ	Dimer [b]		9 ± 5 x 10^4	-6.6 ± 0.3
LZ	Dimer [b]		6 ± 4 x 10^4	-6.4 ± 0.4
CC2	Trimer	3.3 ± 0.5 x 10^7		-10.0 ± 0.1

Table II: Table summarizing the oligomerization state of NEMO recombinant proteins and of NEMO synthetic peptides

The oligomeric state of NEMO His-tagged (His) recombinant proteins and of LZ and CC2 synthetic peptides (first column) is given in the second column. The association

constant (K_A) of the Monomer/Trimer (M^{-2}), of the Monomer/Dimer (M^{-1}) equilibria as well as the $\Delta G°$ (kcal.mol-1) of the reaction are given for each of the polypeptides. (a) Data are taken from Agou et al., JBC, 02.: (b) values calculated from gel filtration experiments while others are from equilibrium sedimentation.

REFERENCES

Agou, 02, JBC

Heyninck et al., FEBS, 2003

Döffinger, 01, Nature gen

Tegethoff, 03, Mol Cell Biol

Huang, 02, Mol Cell Biol;

Makris, 02, Mol Cell Biol

Makris, 00, Mol Cell

Rothwarf, 98, Nature

Mercurio, 99, Mol Cell Biol

Huang, 02, FEBS

Inohara, 00, JBC

Poyet, 00, JBC

Poyet, 01, JBC

Ye, 00, JBC

Yamaoka, 98,Cell

Rudolf, 00, Genes Dev

May,00, Science

Karin, 00, Annu Rev Immunol

Revue générale récente

SELECTIVE INHIBITION OF NF-κB ACTIVATION BY PEPTIDES DESIGNED TO DISRUPT NEMO OLIGOMERIZATION

Fabrice Agou *‡, Gilles Courtois ‡, Francoise Baleux ¶, Yves-Maris Coic ¶, Francois Traincard ‡, Alain Israël † and Michel Véron ‡

‡Unité de Régulation Enzymatique des Activités Cellulaires CNRS URA 2185, †Unité de Biologie Moléculaire Expression Génique CNRS URA 2582 and ¶ Unité de Chimie Organique CNRS URA 487, Institut Pasteur, 25/28 rue du Dr. Roux 75724 Paris cedex 15

*: To whom correspondence should be addressed

Corresponding Author:

Fabrice AGOU
Unité de Régulation Enzymatique des Activités Cellulaires
Institut Pasteur
25 rue du Docteur Roux
75724, Paris cedex 15, France

Tel: (33-1) 45 68 83 80
Fax: (33-1) 45 68 83 99
email: fagou@pasteur.fr

Running title: Inhibition of the IKK complex by peptide interactions with NEMO

SUMMARY

NEMO/IKK-γ plays a key role in the activation of the NF-κB pathway in response to proinflammatory stimuli and the mechanism leading to signal dependent activation of the IκB kinases (IKK) involves NEMO oligomerization. Previous studies have demonstrated that NEMO trimerizes through its C-terminal CC2-LZ coiled-coil subdomain. This minimal oligomerization domain likely folds as a trimer of heterodimers that is reminiscent of the trimeric structure of the gp41 ectodomain from HIV-1 (Traincard et al.). On the basis of a structural model, we rationally designed cell-permeable peptides corresponding to optimal portions of CC2 or LZ subdomains that mimic the contact area between NEMO subunits. These peptides were delivered to cells to block the NF-κB pathway by disrupting NEMO oligomerization. Peptide transduction was monitored by FACS and their effect on LPS-induced NF-κB activation was quantified using a NF-κB dependent β-galactosidase assay in stably transfected pre-B 70Z/3 lymphocytes. Our results show that the LZ peptide and, to a lesser extent the CC2 peptide, inhibit NF-κB activation with IC_{50} values in the μM range. Control peptides including mutated CC2 and LZ peptides as well as heterologous coiled-coil peptides had no inhibitory effect on NF-κB activation. Moreover we also demonstrated that these NF-κB peptidic inhibitors induced the cell death in the human retinoblastoma cell lines Y79 that exhibit constitutive NF-κB activity. Taken together, our results provide "proof of concept" for a new and promising strategy to inhibit the NF-κB pathway by targeting NEMO's oligomerization site.

INTRODUCTION

Nuclear factor-κB (NF-κB) signaling is an essential signal transduction pathway involved in inflammatory responses, oncogenesis, viral infection, the regulation of cell proliferation and apoptosis and in the case of B and T lymphocytes in antigenic stimulation (Amici, Karin, ghosh and karin and israel). In mammalian cells, there are five NF-kB family members that dimerize: RelA, RelB, c-Rel, NF-kB2/p100/p52 and NF-kB1/p105/p50. NF-kB whose predominant form is a heterodimeric transcription factor composed of p50 and RelA subunits, remains sequestered in the cytoplasme through association with members of an inhibitory family of proteins known as IκB. Upon stimulation by the cytokines TNF-α and interleukin-1, endotoxin (LPS), microbial and viral infections, pro-inflammatory signals converge on the canonical IkB kinase complex (IKK), a protein complex that is composed of two kinases subunits, IKK-a/IKK-1 and IKK-b/IKK-2 and a structural/regulatory subunit NEMO/IKK-γ. Once activated IKK complex phosphorylates IkB proteins, triggering their ubiquitination and subsequent degradation by proteasome. Free NF-kB can then move into nucleus to initiate or upregulate gene expression. Although IKK-α and IKK-β exhibit striking structural similarity (52%), exquisite genetic studies have shown that they are involved in two pathways for the activation of NF-kB (review baltimore). IKK-β is the pro-inflammatory kinase that is responsible of activation of classical NF-κB complexes whereas IKK-α in association with NF-kB inducing kinase (NIK) play essential roles in the non-canonical NF-kB signaling pathway (J. Exp Med, Senftleben/Karin science). IKK-a plays also a role in keratinocyte

differentiation but this process is independent of its kinase activity (Karin Nature). The presence of the NEMO protein underlies IKK activation since NEMO-deficient cells are unable to activate NF-kB in response to many stimuli. NEMO is composed of a N-terminal IKK-binding domain including a large coiled-coil (CC1). The C-terminal domain functions as the regulatory part of the protein that has often been reported as binding template to link many upstream signaling molecules or viral proteins (ref, ref, ref). Interestingly, mutations responsable for IP and EDA-ID pathologies were mainly found in this part of the molecules (ref, ref). The C-terminal domain is composed of the minimal oligomerization domain including two sucessives coiled-coil motifs, CC2 (residues 246-286) and LZ (residues 390-412) (our ref, and sheideireit ref), and a zinc finger motif at the extremity of the C-terminus.

The biochemical mechanisms triggering the activation of IKK in response to pro-inflammatory stimuli remain unclear. It has been demonstrated that phosphorylation on two serine residues in the activation T-loop induces activation of the IKK-b. However, the mechanism that leads to this phosphorylation event is still unknown. One possible mechanism consists of the conformation change of the kinase induced by NEMO oligomerization (our ref). This change of the oligomeric state may induce the T-loop activation by a mechanism of trans-autophosphorylation (Zandi et al. Cell 1997; Tang et al., J. Biol. Chem 2003). Consistent with the role of NEMO oligomerisation in IKK activation, mutations in the minimal oligomerization domain failed to rescue NF-KB by genetical complementation in NEMO-deficient cells activation in responses to many stimuli. Moreover, enforced oligomerization de NEMO lead to full activation of IKK complex. (ref, ref). Recently, the

phosphorylation and the ubiquitination of NEMO in response to TNF-α have been reported, (ref, ref). However, these NEMO modifications have not been demonstrated yet as a crucial step to activate IKK complex in response to several pro-inflammatory stimuli.

Inhibition of NF-kB activation constitutes a priviliged target for development of new anti-inflammatory and anti-cancer drugs (ref, ref, ref, ref). Among many protein actors in NF-kB signaling pathway, IKK complex represents one of the most promising molecular target for discoveries of the new specific NF-kB inhibitors (ref). To minimize the potential toxicity effects *in vivo*, therapeutical success will greatly depend on the abilities of the NF-κB inhibitors to block activating signals without modifying the basal level of NF-kB activity. May et al. described a cell-permeable peptidic inhibitor that block specifically the pro-inflammatory NF-kB activation by disrupting the constitutive NEMO interaction with IKK kinases (ref, ref). Modulating protein-protein interactions by the rational design of peptide that alter protein's function provides an important tool for both basic research and development of new classes of therapeutic drugs (Nat Biotech, 1998; Mochly-Rosen), especelly with signaling proteins that exhibit flexible and dynamic binding properties (Nash; science avril 2003). Numerous studies of peptide modulators have been described in the litterature where peptides mediate protein's function by interfering with localisation (translocation) (ref), recrutment to receptor (ref), intramolecular interactions (ref) and oligomerization (ref). In the latter, inhibition of HIV-1 gp41 fusion protein with various peptides provides a clear proof-of concept (review Kim; Cell 93 1998 p 681-684; and Eckert DM Ann Rev Biochem 70, 777-810 (2001).

In this report we studied the potential inhibition of NF-κB activation by peptides designed to disrupt NEMO oligomerization. We have previously shown that the minimal trimerization domain comprises the CC2-LZ coiled-coil subdomain and that the isolated CC2 and LZ domains bind to each other to form a stable trimer of heterodimers. This structural model is reminiscent of the fold of the gp41 ectodomain from HIV-1 (our ref, traincard). It consist of a central three-stranded coiled coil (formed by the CC2 coiled coil motif of NEMO) which is surrounded by the LZ helical motif derived from the C-terminal end of NEMO, packed in an antiparallel manner around the outside of the CC2 coiled-coil. On the basis of this model, we rationally designed two cell-permeable peptides corresponding to optimal portions of CC2 or LZ subdomains that mimic the contact area between NEMO subunits. Peptide transduction was monitored by FACS and their effect on LPS-induced NF-κB activation was quantified using a NF-κB dependent β-galactosidase assay in stably transfected pre-B 70Z/3 lymphocytes. We demonstrate that the LZ peptide and, to a lesser extent the CC2 peptide, inhibit specifically NF-κB activation with IC_{50} values in the μM range. The effects were specific because control peptides including mutated CC2 and LZ peptides as well as heterologous coiled-coil peptides (GCN4), had no inhibitory effect on NF-κB activation. Furthermore, we also showed that these NF-κB peptidic inhibitors induced the cell death in the human retinoblastoma cell lines Y79 that exhibit constitutive NF-κB activity. Collectively, our findings provide "proof of concept" for a new and promising strategy to inhibit the NF-κB pathway by targeting NEMO's oligomerization.

Materials and methods

Cell culture, stable transfections and cell lines

The grow conditions of the murine pre-B 70Z/3 were as described in Courtois et al., 1997 Mol. cell. Biol). 70Z3-C3 stable cell lines were prepared by electroporation as described in Courtois et al. with the plasmid cx12lacZ-kB (a kind gift from G.R. Crabtree), bearing three tandem copies of NF-kB sites in the IL-2 promoter (Fiering et al., 1990), The human retinoblastoma cell lines Y79 were purchased from the American Type Culture Collection (Manassas, VA) and grown in RPMI 1640 medium supplemented with 100 U/ml penicillin, 100 µg/ml streptomycin, and 10 % fetal calf serum (FCS).

FACS analysis

0.5 x 10^5 70Z/3-C3 cells in 0.5 ml were incubated at 37°C for different times and with various concentrations of peptides as indicated in the Figure legends. The cell suspension was centrifugated at 1,000 x g at room temperature and the cell pellet was then washed three times with PBS buffer (1 ml), and finally was resuspended with 500 µl of PBS buffer containing 0.1 % sodium azide. Fluorescence analysis was performed with a FACSCalibur (BD Biosciences) and a minimum of 15,000 events per sample was selected. All experiments were performed in duplicates.

Peptide synthesis and purification

Peptides were synthesised as described in Mousson et al. 2002 (Biochemistry,41 p13611- p13616), by using continuous-flow Fmoc/tBu chemistry (Chan, WC, and White, P.D. (2000); Fmoc Solid Phase Peptide Synthesis. A pratical approach) on an Applied

Biosystems (Foster City, CA) Pioneer peptide synthesiser. All chemical reagents were purchased from Applied Biosystems. All peptides were blocked at the N-terminus with an acetyl group and at the C-terminus with an amide. A single extra-cystein residue was incorporated at the N-terminus of the peptides for subsequent specific labelling (see Table 1). Crude peptides were directly purified by reverse-phase medium-pressure liquid chromatography (MPLC) on a Nucleoprep 20 µM C18 100 Å preparative column, using a linear gradient of acetonitrile (1%/min) in 0.08 % aqueous trifluoroacetic acid (TFA) (pH 2) for 60 min at a 18 ml/min flow rate. The purity of the peptides was verified on a nucleosil 5 µM C18 300 Å analytical column, using a linear gradient of acetonitrile (0.5 %/min) in 0.08 % aqueous TFA (pH2) for 20 min at a 1 ml/min flow rate. Conjugation of the fluorophore bodipy®FL N-(2 aminoethyl)maleimide (Molecular Probes) to the sulfhydryl group was under equimolar conditions at pH 6 in 50 mM ammonium acetate buffer for 30 min in the dark. The mixture was then loaded on a Nucleoprep 20 µM C18 100 Å preparative column to purify the BODIPYconjugated peptide. In cell death experiments, all peptides devoid of BODIPY-labeling were subjected to treatment with iodoacetamide to prevent any oxidation of cysteine residue. All purified peptides were then quantified by amino acid analysis and finally characterised by using positive ion electrospray ionisation mass spectrometry (ES+). Once integrity of the peptides and coupling efficiency were verified by mass spectrometry, the extinction coefficients of the peptides were measured at 505 nm or at 280 nm when peptides contained aromatic residues (see Table 1). Stability of the labeling was monitored periodically

by measuring the absorbances of peptides at 280 nm and at 505 nm and by calculating the absorbance ratio. All peptides were dissolved in water to stocks of 2 mM.

NF-κB inhibition assays

In a first procedure 2.2 x 10^5 70Z3-C3 cells in 220 µl of RPMI 1640 supplemented with 10% fetal calf serum (FCS) and 50 µM b-mercaptoethanol were placed in a 96-well plate and incubated with various concentrations of peptide (0 to 20 µM) at 37°C in 5% CO_2 incubator. After two hours an equal portion (100 µl) of each cell sample transferred in two wells containing each 10^5 cells. One aliquot of cells was then treated for 5 hours with lipopolysaccharides from *Salmonella abortus* (Sigma) at 0.5 µg/ml final concentration, and the other one left-treated. After 5 hours, cells were centrifuged at 400 x g for 5 min at room temperature and the cell pellets were washed three times with cold PBS (250 µl) by centrifugation. Cells were then lysed in the lysis buffer (25 mM tris-phosphate buffer at pH 7.8 containing 8 mM magnesium chloride, 1 mM dithioerythreitol, 1 % Triton X-100, 15 % glycerol and a protease inhibitor mixture (Roche)), and samples were centrifuged at 4°C for 20 min to clarify the lysate. The supernateant was then kept on ice, and 30 µl was then assayed to measure the β-galactosidase activity with a plate luminometer (Berthold) using the galacton-star as chemiluminescent substrate (BD Biosciences Clontech, Bronstein et al., 1989). Background of reaction was measured by mixing for 1 hour 30 µl of lysis buffer with the reaction buffer (196 µl) and the galacton-star substrate (4 µl) provided by BD Biosciences. In a second procedure and a more stringent assay, 70Z3-C3 cells (2.2 x 105 in 220 µl medium) were centriguged at 400 x g at room temperature after peptide internalization for 2

hours, and cell pellets were washed three times with 200 µl of PBS by centrifugation. Cells were then diluted three times with complete medium, and allowed to grow for at least 24 hours. The following steps are identical to the first procedure.

Cell death assays

The detection of cell death was performed using the MTS assay provided by Promega (CellTiter 96® AQ_{ueous} one solution cell proliferation assay). Briefly, 0.3 x 10^6 Y79 cells in 450 µl were treated with 50 µl of the wild type Ant-CC2 and Ant-LZ peptides (0.1 to 20 µM) or their mutants Ant-CC2 (Mu), Ant-LZ (Mu) or the Ant or left untreated in serum-free RPMI medium at 37°C. After an incubation of 1 or 14 hours, an aliquot of the cell suspension (200 µl, 0.12 x 10^6 cells), was then transfered in 96-well plates and mixed with the MTS solution (40 µl) containing the MTS compound and the phenazine ethosulfate. Two hours after, the quantity of formazan producted by viable cells was measured by the amount of 490 nm absorbance using an automated microplate reader (Bio-TeK Instruments, INC). Cell survival was observed under microscope and was estimated as a percentage of the value of untreated controls. The background of the reaction was determined by mixing the MTS solution with cell-free RPMI medium. To inscrease the sensivity of the cell death assay, we used peptides devoid of BODIPY-labeling because the absorption spectra of the fluorophor overlaps with that of the formazan product. All experiments were repeated twice and each experiment condition was repeated in duplicate wells in each experiment

Analytical Gel filtration experiments

The oligomeric states of peptides were determined by filtration as described in Traincard et al., 2003. In brief, 500 µl samples were loaded on a Superdex 75 HR 10/30 column equilibrated in 50 mM Tris-HCl pH 8.0 containing 200 mM NaCl and 0.1 mM DDM, at a constant flow rate of 0.4 ml/min. The presence of the DDM detergent was added in the equilibrium buffer to minimize the adsorption in the column and to increase the peptide recovery. The column was calibrated in the same equilibrium buffer with blue dextran 2000 (void volume), dithioerythritol (total volume), bovine serum albumine (67 kDa, Rs = 35.2 Å), ovalbumine (43 kDa, Rs = 27.5 Å), chymotrypsinogen A (25 kDa, Rs = 21.1 Å), ribonuclease A (13.7 kDa, Rs = 16.4 Å), cytochrome C (12.4 kDa, Rs = 17.7 Å) and aprotinin (6.5 KDa, Rs = 13.5 Å).

Fluorescence anisotropy measurements

Anisotropy measurements were performed with a PTI Quantamaster fluorometer equiped with polarizers for the excitation and emission beams. This instrument uses a PMT in the L-configuration. All experiments were carried out in a 1 cm path-length cuvette at 22°C with excitation and emission wavelengths at 495 nm and 520 nm, respectively. The bandpass of excitation and emission monochromators was set at 2 and 4 nm, respectively. Steady-state fluorescence anisotropy was expressed as millianisotropy (mA) and was calculated according to the equations: (1) $A = (I_{VV} - GI_{VH})/(I_{VV} + 2GI_{VH})$; (2) $G = I_{HV}/I_{HH}$; where A is anisotropy, G is a correction factor for wavelength-dependent distortion and I is the fluorescence intensity component (subscript referring to the vertival and horizontal positioning at the excitation and

emission polarizers, respectively). Experiments were at least performed twice and each data is the result of 20 records along a 2 min period. All measurements were carried out in 50 mM Tris-HCl buffer at pH 8 containing 150 mM KCl. We verified that at the BODIPY-Ant-CC2 and BODIPY-Ant LZ concentration used (1µM and 0.1 µM respectively), the filter effect was negligeable. The BODIPY-Ant-CC2 peptide was preincubated overnight at 22°C alone or with increasing concentrations (1-125 µM) of CC2 prior to anisotropy measurement. The BODIPY-Ant-LZ peptide (100 nM) was preincubated overnight at 22°C alone or with 10 µM and 100 µM concentrations of CC2 (see legend Fig. 7) prior to anisotropy measurement. The dissociation constant parameter was estimated by globally fitting the anisotropy data to binding isotherm equation as described in Agou et al. (J. Biol. Chem) using Kaleidagraph nonlinear regression software (Synergy Software, reading PA). The binding stoichiometry, n, was estimated from the intersection of lines (dashed lines in Figure 7) drawn through the descending and plateau region of the anisotropy data.

RESULTS

Rational design of NEMO derived peptides that block NF-κB activation

We previously showed that the minimally trimerization domain of NEMO comprised of the sequence 251 to 337 (Fig. 1A). This region likely contains two coiled-coil sequences of about 35 residues denoted CC2 (residue 253-285) and LZ (301-337) at the N- and C-terminus respectively. Although the structure of the minimal oligomerization domain has not yet been determined, several biochemical studies combined with the fluorescence polarization method prompted us to propose that the CC2/LZ trimer probably forms a six-stranded helical bundle composed of closely packed CC2 and LZ coiled-coils in an antiparallel orientation (our Ref). Furthermore PSI-BLAST searches reveal that this domain of NEMO contains a conserved motif of 20 residues called "NEMO like Motif" (NLM) which is shared with four other proteins including ABIN-1 (ref), ABIN-2/NAF (ref), ABIN-3/LMP1 and NRP/oviporine (ref) (Fig. 1B). Interestingly, most of these proteins including the conserved motif of ABIN-1 (ref), the C-terminal domain of NEMO (ref) and ABIN-2 (ref) or ABIN-3/LIND (ref) proteins have been shown to inhibit NF-κB activation in a dominant-negative manner when overexpressed in cells.

Since disrupting NEMO oligomerization represents a potential therapeutic strategy for inhibiting NF-κB activation, we designed NEMO-derived partner peptides that mimic either the CC2 or the LZ sequence (Table 1). It is interesting to note that, unlike the CC2 peptide, the LZ peptide also includes the NLM motif at the N-terminal extremity. To mediate all

peptide uptake into cells, we conjugated a functional anal gue at the peptide N-terminus comprised of the 16-amino acid sequence derived from the third helix of the Antennapedia/penetratin protein (Ant). This amphipatic helix acts as an internalization vector (ref Prochiantz et review). Most of antennapedia fusion peptides were labeled with the BODIPY fluorophore to analyze the transduction potential of each peptide into the cells. Specific labeling was performed by adding a single cystein residue at the extremity of the N-terminus and sequence integrity was verified by mass spectrometry (see "Materials and methods" and Table 1).

Cellular uptake of NEMO derived-peptides mediated by the antennapedia fusion peptide

The uptake of BODIPY labeled NEMO peptides into living cells was monitored by fluorescence activated cell sorting (FACS) which is a conventional tool used to quantify cellular internalization. Figure 2A shows FACS analyses of cells treated with Ant-CC2 (WT), Ant-CC2 (Mu), Ant-LZ (WT) or Ant-LZ (Mu) BODIPY-peptides for 2 h at 37°C, and were compared with those of the autofluorescence of untreated cells and control cells treated with an equal concentration of free BODIPY or with BODIPY-conjugated BSA. Consistent with the role of antennapedia peptide to transduce peptides and proteins into mammalian cells, 100% of 70Z3-C3 cell line were similarly transduced by the four different NEMO peptides, suggesting that all of the cells in the treated population have a near identical intracellular concentration of NEMO-derived BODIPY-peptides. Comparative analysis indicate that untreated cells and treated cells with BODIPY-BSA or free BODIPY exhibit a similar cell

fluorescence, verifying that our extensive washing protocol before FACS analysis was optimal to minimize any contribution of surface-bound peptide in measuring NEMO peptide internalization (see "Materials and methods"). Thus, these data suggest that the observed cellular fluorescence signaling mostly reflects the intracellular concentration of transduced NEMO peptide and not a non specific adsorption onto the membrane surface.

We next investigated the kinetic and concentration dependency of cellular uptake for the Ant-CC2 BODIPY peptide keeping in mind that the transduction of other NEMO peptides should occur in a similar fashion (Fig. 2B and 2C). FACS analysis 5 h after addition of 70Z3-C3 cell treated with 0.2, 2 or 20 μM BODIPY-Ant-CC2 peptide at 37°C demonstrate the linear dependancy of the intracellular concentration as a function of the incubated concentration of the antennapedia fusion peptide as widely reported in litterature (ref). Notably, the cells treated with the Ant-CC2 at 20 μM and at 37°C already reach maximum intracellular concentration in 30 min and remain unchanged for up to 5 h. Since the time to induce a strong NF-kB activation in response to LPS requires 3-5 hours of cell treatment, these results indicate that the intracellular concentration of each peptide remains constant during the LPS stimulation.

Specific inhibition of LPS-induced NF-κB activation by cell permeable CC2 and LZ

To analyze the inhibition potential of LPS-induced NF-κB activation by cell permeable BODIPY-Ant-CC2 and BODIPY-Ant-LZ peptides, we stably transfected the murine pre-B 70Z3 cell line with p12XlacZ-kB, which bears the β-galactosidase reporter gene

under the control of the NF-κB transcription factor. When the resulting cell line 70Z3-C3 was treated for 5 hours with LPS (3 µg/ml) a 100 fold-activation of the LacZ gene was observed, indicating that our cellular assay monitors NF-κB activation in response to LPS with extreme sensitivity (Figure 3A, control "no peptide). Interestingly the incubation of cells with 20 µM of both NEMO-derived peptides decreased significantly the NF-kB activation. This lowering was stronger in the presence of BODIPY-Ant-LZ as compared to BODIPY-Ant-CC2. The inhibition effect was essentially due to the NEMO sequence because the presence of the isolated antennapedia peptide containing or not containing a N-terminal BODIPY label (BODIPY-Ant or Ant) induces the same level of NF-kB activation as the control (Fig. 3A). Note that the basal NF-κB activity measured in the absence of LPS was very similar in all samples indicating that both CC2 and LZ peptides abolish the responsiveness to LPS without affecting the intrinsic basal NF-kB activity. This was essential to minimize the *in vivo* cytotoxity, resulting mainly from apoptosis induced by inhibition of NF-kB (ref).

To determine whether the BODIPY-Ant-LZ or the BODIPY-Ant-CC2 peptide is the most efficient inhibitor, we next measured the concentration dependent inhibition of each peptide. As shown in Figure 3B, both NEMO peptides exhibit NF-kB dose dependant inhibition of NF-kB in response to LPS. BODIPY-Ant-LZ inhibited NF-kB to a greater extend that BODIPY-Ant-CC2 did with IC_{50} values of 3 µM and 22 µM respectively (Fig. 3C). This striking difference could be explained by the NLM motif included in the LZ sequence. Consistent with the intracellular nature of the NEMO target, both LZ and CC2 peptides not fused to the antennapedia protein transduction domain (PTD) exhibited the same

level of activation as the control (Fig. 3 D), confirming that NEMO derived peptides must cross the cell membrane for inhibition of NF-κB. Taken together these results indicate that peptides that mimic the two coiled-coil sequences of the NEMO oligomerization domain are potent peptide inhibitors of NF-kB activation in response to LPS.

Mutations in the hydrophobic core of the LZ and CC2 coiled-coils disrupt their specific inhibition of the NF-kB signaling pathway

Theoretically, If BODIPY-Ant-LZ or BODIPY-Ant-CC2 peptide inhibit NF-κB activation through specific binding to the NEMO oligomerization domain, mutations that disrupt the coiled-coil association should therefore exhibit impaired abilities to inhibit NF-kB inhibition. α-helical coiled-coil interactions have been extensively studied and most of the rules governing their specific assembly have been well documented (ref, ref, ref). The coiled-coil interface which is represented by the first (a) and fourth position (d) of the heptad repeat is generally occupied by hydrophobic amino acids. Proline or glycine are largely excluded to preserve the helical architecture. Core polar residues are destabilizing relative to leucine substitutions, especially when changes occur at d positions. Considering these rules, we synthetized a variant of BODIPY-Ant-LZ containing two mutations L → S at the d positions (BODIPY-Ant-LZ (Mu) and a variant of BODIPY-Ant-CC2 containing two mutations L → G and one mutation I → G at the a positions (BODIPY-Ant-CC2 (Mu) (Fig. 4A and 4B, and Table 1). To test the effects of these mutations on the potential inhibition of NF-κB activation, we developped a more stringent cellular assay that consists of the internalization of the

peptides for 2 hours followed by an extensive washing of 70Z3-C3 cells to remove any remaining peptide in the extracellular media. Cells were allowed to grow for at least 24 hours before LPS-induced NF-kB activation. In this way, peptide interference with the receptor binding LPS was excluded. As with the cellular assay described above, the BODIPY-Ant-CC2 (WT) and the BODIDY-Ant-LZ (WT) also inhibited NF-κB activation with a 1.7 and 5.8 -fold reduction respectively (Fig. 4A and 4B) when used at a 10 μM concentration. This indicates that the peptides do not competively act on the receptor binding of LPS. As expected, the presence of the CC2 variant (BODIPY-Ant-CC2 (Mu)) did not affect the NF-κB activation since β-galactosidase activity was equivalent to that of the control (Fig. 4A, no peptide). In response to LPS, NF-kB is more strongly activated in the presence of the BODIPY-Ant LZ mutant than in the presence of wild type. However, unlike the BODIPY-Ant-CC2 (Mu), a slight inhibition of the LZ mutant was observed when compared to the control (15 %). When taken together, these data demonstrate that CC2 and LZ mutants are unable to inhibit the LPS-induced NF-kB activation as effectively the wild type did.

Inhibition of NF-κB activation is mediated by a specific coiled coil interaction of the LZ peptide.

Computational analyzes using the program MULTICOIL (ref) predicted that greater than 5 % of all putative ORFs found in sequenced genomes are predicted to contain coiled-coil motifs (ref) and that approximately 2-4 % of amino acids in proteins are estimated to adopt coiled-coil folds (ref). This abundance raises the question if the NEMO derived- LZ

peptide maintains its coiled-coil interaction partnering specificity *in vivo*. To adress this question, we synthetized another coiled-coil peptide that mimics the sequence of the GCN4 leucine zipper and tested its ability to inhibit NF-kB activation. BODIPY-Ant-GCN4 contained the antennapedia sequence at its N-terminus and a short SKGMQ linker identical to the CC2 sequence for convenience of peptide delivery (Table 1). It was also labeled at its N-terminus with BODIPY to monitor its cellular uptake by FACS (data not shown). The GCN4 peptide displays a low sequence similarity with the LZ sequence of NEMO (22 %) but identical residues are mostly represented by leucines at d positions (Figure 5). These residues contribute most of the energy to coiled-coil oligomerization stability (ref). Note that a positions which are important for coiled-coil specificity (ref) are composed of a set of different amino acids. While GCN4 is composed of hydrophobic residues and the typical asparagine residue, the LZ of NEMO contains two charged amino acids R and K (Figure 4B and Fig. 5A). Thus, these residues which are located at the coiled coil interface likely contributes to the selectivity of coiled coil interaction.

Figure 5B shows the effect of the BODIPY-Ant-GCN4 at a 10 µM concentration on the inhibition of NF-kB activation in response to LPS. To compare the effects of coiled coil sequences, we used the stringent cellular assay described above. BODIPY-Ant-GCN4, unlike BODIPY-Ant-LZ, has no ability to inhibit NF-kB activation since the level of NF-kB activation was near that of the control without peptide. Taken together, these results strongly support the hypothesis that the LZ peptide of NEMO inhibits NF-kB activation through selective coiled-coil interactions.

The antennapedia sequence induces monomerization of NF-kB peptidic inhibtors

The antennapedia sequence is a protein transduction domain (PTD) which adopts an alpha-helical amphiphatic structure (ref). When fused to the N terminus of a coiled-coil sequence like CC2 or LZ, the antennapedia could alter the coiled-coil association by covering the hydrophobic interface of the coiled-coil through intramolecular interactions. To examine the effect of N-fusion of the antennapedia peptide on the oligomerization properties of the CC2 and the LZ peptides, we analyzed peptides containing or not containing the antennapedia sequence at their N-terminus by gel filtration. As shown in Figure 6, all peptides containing an N-terminal fusion of antennapedia coelute with an elution volume corresponding to their monomeric forms as compared to globular protein markers. Note that we had to add a detergent in the buffer below its cmc to improve peptide recoveries. When injected at the same 10 μM concentration, CC2 wild type and LZ wild type without the antennapedia N-fusion oligomerize. CC2 (WT) forms a trimer whereas LZ (WT) forms a dimer as recently reported (Traincard et al). As expected, when a CC2 mutant was chemically obtained with three of its aliphatic residues at a positions replaced with glycine residues, it lost its ability to oligomerize (bottom panel, dashed line). The effect of the two L→S mutations at d positions was less strong with LZ (mutant). However, we still detected dimerization of the LZ mutant at a 10 μM concentration (dashed line) although its association was markedly reduced by mutations as compared to the wild type LZ (solid line). Taken together, these data indicate that the N-fusion of the antennapedia sequence to both CC2 and LZ peptides alter homotypic

coiled-coil interactions, facilitating the monomerization of the NEMO derived-peptides. Furthermore these results also show that residue changes at a and d position alter oligomerization of LZ and CC2 peptides. Thus, it is likely that the synthetic peptides form α-helical coiled-coil structures.

Homo- and heterotypic interactions of CC2 and LZ peptides with and without the N-fusion of antennapedia sequence.

Because the N-fusion of antennapedia modifies the oligomerization properties of the CC2 and LZ peptides, we next studied by fluorescence polarization whether the Ant-CC2 and the Ant-LZ monomers labelled with BODIPY could bind to the NEMO-derived peptides devoid of the antennapedia sequence. These peptides CC2 and LZ may be also considered as the *in vivo* binding target for both cell permeable BODIPY-Ant-CC2 and BODIPY-Ant-LZ NF-kB inhibitors. Figure 7 shows a typical binding isotherm for the interaction of various concentrations of the CC2 peptide with a fixed concentration of the BODIPY-Ant-CC2. The shape of the binding curve is not sigmoidal, indicating that CC2 binds to the BODIPY-Ant-CC2 peptide without cooperativity. The stoichiometry calculated from the intercept between the tangent of the initial part of the anisotropy and the asymptote is equal to 0.8. Taking into account this stoichiometry, the dissociation constant K_D is 15.2 μM. Similar results were obtained when a fixed concentration of the BODIPY-Ant-LZ was titrated with various concentrations of the CC2 peptide as we previously reported (Inset Figure 7, Traincard et al.).

Collectively, these data demonstrate that both Ant-CC2 and Ant-LZ monomers binds *in vitro* to the CC2 peptide composing the minimal oligomerization domain of NEMO.

Cell death in human Retinoblastoma cell is induced by NF-κB inhibitors Ant-CC2 and Ant-LZ, but not by their mutants Ant-CC2 (Mu) and Ant-LZ (Mu)

It has become clear that constitutively activated NF-κB transcription factors have been associated with several aspects of tumorigenesis (Karin review), including most of six essential alterations in cell physiology that dictate the conversion of normal human cells into cancer cells (Hanahan and Weinberg; cell 2000 for review). This led to a significant enthusiasm for the use of NF-kB inhibitors as a new anti-cancer therapy. Promising results have been reported recently using proteasome inhibitors or the SN50 peptide that blocks the nuclear translocation (ref baldwin). However, the specificity of these agents on NF-κB inhibition have been questioned. Poulaki et al. showed recently that the treatment of the human retinoblastoma (Rb) cell lines Y79 with SN50 peptide induced apoptosis of cancer cells (ref). Sequence alignement of murine and human NEMO proteins indicate that the minimal oligomerization domain of NEMO is strictly conserved, suggesting that similar effects of NF-kB inhibition could be observed in rodent as well as in human cells.

Given that specific NF-kB inhibition may trigger apoptosis of cancer cells, we examined the effects of both cell-permeable Ant-LZ and Ant-CC2 peptides on human retinoblastoma cell viability. In these experiments, we used NEMO-derived peptides without a N-terminal BODIPY labeling to prevent any interference with the MTS assay (see "Materials and

Methods"). As shown in Figure 7, we found a dose dependance f the Y79 cell viability when cells were treated for 3 hours with Ant-CC2 (Fig. 8A) or Ant-LZ (Fig 8B). The effect of the Ant-LZ peptide on cell death was stronger than that of the Ant-CC2. This induction of cell death was significant since Rb cell survival was 20% and 65 % with the Ant-LZ and the Ant-CC2 peptides respectively when cancer cells were treated for 3 hours at a 20 μM concentration. Remarquably, the same cell treatment with the Ant-CC2 (Mu) (Fig.8A) or with the Ant-CC2 (Mu) (Fig.8B) did not induce concentration cell death as did WT peptides. These effects on cell death were essentially du to the NEMO sequence because a longer treatement of Y79 cell lines with the antennapedia peptide did not affect cell survival (Fig. 8C). In contrast, 80 % and 55% of Y79 cell died in the presence of Ant-LZ and Ant-CC2 respectively at 5 μM concentration (Fig. 8C). Taken together, these results indicate that specific NF-κB inhibition by Ant-CC2 and Ant-LZ peptides induce cell death in Rb cell lines, validating the ths use of specific NF-kB inhibitors as anticancer chemotherapy.

DISCUSSION

1) LZ peptide stronger effect than CC2 peptide. [Discuss with the model and the time equilibrium required for exhange and the NNN motif.]

2) Peptide are coiled-coil [Peptides and coiled-coil.....Mutations and NOE indicate that its alpha helical coiled-coil]

3) What is the action mode of both peptides [How act the peptides inhibitors. CC2 by competitive exchange and LZ by blocking an open conformation (similarly to gp41)??].

4) Monomerization may be crucial because oligomerization should be the limiting step. [Other internalization peptide could not do that]

5) Coiled-coil specificity (discuss more in the context of recent publications with bzip, What does it give the specificity. The NNN motif did not give any effect. discuss)

In the absence of the pro-inflammatory signals, all peptides assayed have no detectable cytotoxicity for lymphocytes B tested at a concentration up to 30 μM according to the MTS assay, the direct observation under microscope, and the forward scatter-FSC and side scatter-SSC parameters deduced from FACS analyses. However, we could detect a slight cell death by FACS in a concentration-dependent manner when the pre-B lymphocytes were stimulated by LPS in the presence of NEMO-derived peptides. The cellular proportion of cell death was 9 % in the absence of stimuli at a 20 μM concentration of Ant-CC2 whereas it increased at 13 % after LPS stimulation (data not shown). This was in agreement with the role of the NF-κB pathway in protecting cells from apoptosis. The cell death was more pronounced and fast on the Rb cell lines Y79 in which constitutive NF-κB activity has been reported (Poulaki et al., 2002). We did not demonstrate here by the Annexin V labeling and the TUNEL method that the NEMO peptides-induced cell death is indeed apoptosis. Nevertheless considering the role of the NF-kB patway in the regulation of apoptosis, it is likely that the cell death induced by NEMO-derived peptides is apoptotic in nature.

Our results that provide molecular bases for developpement of new anti-inflammatory and anti-cancer drugs raises several questions. First, if the long LZ peptide shows this selective inhibition on the NF-kB pathway, could a smaller molecule with more desirable pharmacologic characteristics (oral bioavailability and centra nervous system penetration) be designed with similar inhibition activity ? Second, would it be possible to design LZ-derived peptides to improve inhibition activity with a IC_{50} value in the nM range ? Third are the kinases (IKK-α and IKK-β) (ref, ref), and to a lesser extent the NEMO/kinase interaction (ref, ref) more attractive targets to block the NF-κB pathway with small molecule ligands ? There are a few exemples in the literature of identification of small molecules that inhibit protein/protein interactions including oligomerization (ref Nature cell biology BH3 and Bcl-XL and review of Frank McCormick). Thus it is conceivable to get small molecules that block NF-κB activation by interfering with NEMO's oligomerization with the same specificity as the peptides. From another point of view coiled-coils are one of best-studied protein-protein interface (ref, ref). It is then reasonable to expect that future work will lead to the discovery of peptides of peptidomimetic compounds with an improved inhibition potential. Whatever the nature of the future NF-κB inhibitors (organic or peptidomimetic compounds), targeting NEMO's oligomerization will remain a more attactive and promising strategy as compared to those of IKK kinase activity and of NEMO-kinase association because this molecular event strictly depend on the pro-inflammatory signal. Therefore, such drugs would interfer less with the basal NF-κB activity in normal cells that is required for cell viability.

REFERENCES

Footnotes: Abbreviations used: Ant, Antennapedia; .PTD, protein transduction domain; DDM, dodecyl maltoside; cmc, critical micelle concentration; Rs, Stokes radius; PBS, phosphate buffer saline

FIGURE LEGENDS

Figure 1 : Functional domains of the NEMO protein.

(A) The murine NEMO protein contains 412 amino acids and multiple domains including the N-terminal IKK binding domain and the oligomerization domain, the proline rich motif (PPP) and the zinc finger motif (ZF) at the C-terminus. The coiled-coil predictions (open boxes) using the algorithm developed by XXX et al. (ref) and the NLM conserved motif (black bar) are shown. The sequence of $NEMO_{253-337}$ corresponding to the second coiled-coil (CC2) and leucine zipper (LZ) motifs, which contains all determinants required for NEMO oligomerization (Ref, nous), is indicated with the NLM conserved motif underlined and with the coiled-coil sequences showed as cylinders below the sequence. Letters immediately above the sequence indicate the heptad repeat 'a' and 'd' positions which is a key feature of coiled-coil sequences (ref, ref). **(B)** Multiple sequence alignement of NEMO proteins from *Mus musculus* (Mm), *Homo sapiens* (Hs), *Bos taurus* (Bt) and *Drosophila melanogaster* (Dm), showing the NEMO like motif (NLM) shared with NRP/optineurin, ABIN-1/Naf 1, ABIN-2 and ABIN-3/LIND of different species. The multiple sequence alignement was constructed by parsing PSI-BLAST-generated highest-scoring pairs of sequence segments and realigning them with CLUSTAL W (ref). Identical and similar amino acid residues (shaded) are indicated by (!) or (*), respectively

Figure 2: Flow cytometry analysis of NEMO peptide uptake

(A) Cellular delivery of NEMO peptides mediated by conjugation with the Antennapedia peptide. 70Z/3 cells were incubated for 2 h at 37°C in the absence (W/O) or in the presence of 2 µM BODIPY-tagged Ant-CC2 wild type (WT), or Ant-CC2 mutant (Mu), or Ant-LZ wild type (WT) or Ant-LZ mutant (Mu) peptide as indicated, or with controls corresponding to 2

μM BODIPY-conjugated BSA (BODIPY-BSA) or BODIPY-FL alone. B) Concentration dependance of antennapedia-mediated uptake of 0, 0.2, 2 and 20 μM Ant-CC2 at 37°C for 5 h in 70Z/3-C3 cells (left panel) and FACS kinetic analysis of BODIPY-conjugated Ant-CC2 at 0, 0.5, 1, 2 or 5 h after addition of 20 μM Ant-CC2 at 37°C.

Figure 3: Inhibition of LPS-induced NF-κB activation by cell-permeable Ant-CC2 and Ant-LZ peptide

(A) 70Z3 lymphocyte B were stably transfected with pIL1-β-galactosidase which bears the β-galactosidase gene under the control of the NF-κB (see "Materials and methods"). The resulting cell line, 70Z3-C3, was incubated for 2 hours in the absence or in the presence of 20 μM of antennapedia peptide (Ant), or BODIPY-labeled antennapedia peptide (BODIPY-Ant), or BODIPY-labeled antennapedia peptide coupled to CC2 (BODIPY-Ant-CC2) or LZ (BODIPY-Ant-LZ) peptides, After peptide internalization, cells were treated for 5 hours with LPS (3 μg/ml, (+) in left panel) or untreated (right panel and (-) in left panel) and the NF-kB activity was measured by β-galactosidase assay. Error bars represente the standard deviation of three separate experiments. (B) Concentration dependance of inhibition of LPS-induced NF-κB activation by BODIPY-Ant-CC2 peptide (left panel) or BODIPY-Ant-LZ peptide (right panel). Cells were treated as in (A) but with different concentration of peptide as indicated. The potential of each peptide to inhibit LPS-induced NF-κB activation was measured by determining the IC_{50} value which correspond to 50% inhibition of LPS-induced NF-kB activation as compared to the control (no peptide) (C). (D) Effect of the N-fusion

sequence of antennapedia on the inhibition of NF-κB activation. Control (no peptide) or CC2, or LZ peptides, with (BODIPY-ANT-CC2, BODIPY-ANT-LZ) or without the antennapedia sequence at the N-terminus (CC2, LZ) were incubated for 2 hours with 70Z3-C3 cells followed with (+) or without (-) the LPS-treatement for 3 hours. NF-kB activity was then measured by β-galactosidase assay.

Figure 4: Specific inhibition of NF-κB activation in response to LPS depends on a few mutations in the hydrophobic core of CC2 and LZ coiled-coils

Left panels show a helical wheel diagram of CC2 (A) and LZ (B) peptides. The view is from the top the molecule. The (a) through (g) positions, which is an essential feature of coiled coil sequence (ref) represent sequential positions in each peptidic sequence. The first (a) and fourth (d) positions which are generally occupied by hydrophobic amino acids constitute the hydrophobic core for parallel as well as antiparallel coiled coils. Mutations that were introduced in (a) positions of the CC2 variant (BODIPY-Ant-CC2 (Mu)) or in (d) positions of the LZ variant (BODIPY-Ant-(Mu) are shown. In the right panels, 70Z3-C3 cells were incubated for 2 hours in the absence (control) or in the presence of 10 μM of cell permeable wild type (BODIPY-Ant-CC2 (WT)) or mutant (BODIPY-Ant-CC2 (Mu)) CC2 peptides (A) or wild type (BODIPY-Ant-LZ (WT)) or mutant (BODIPY-Ant-(Mu)) LZ peptides (B). The cells were then extensively washed to remove the excess peptide which had not been internalized and the cells were then diluted three times and allowed to grow for for 24 hours before treatment for 5 hours with (+) or without LPS (-). NF-κB activity was measured using

the β-galactosidase assay. Error bars represente the standart deviation of two independant experiments.

Figure 5: Inhibition of NF-kB activation by the LZ peptide occurs through the formation of specific coiled-coil strands.

(A) Sequence alignement of the NEMO-derived LZ and the GCN4 peptides. Both coiled-coil motifs were aligned using clustalX. Identical and similar amino acid residues (shaded) are indicated by (!) or (★), respectively. **(B)** Overview and helical wheel diagram of the GCN4 coiled-coil (top view). The amino-acid sequence of GCN4 is shown with its corresponding [a – g] positions and residues that differ from the corresponding NEMO-derived LZ sequence are boxed according to their degree of conservation. Identical (open square) and similar residues (open triangle) are indicated. **(C)** Comparison of the cell permeable NEMO-derived LZ and GCN4 peptide on the inhibition of LPS-induced NF-κB activation. 70Z3-C3 cells were incubated for 2 hours in the absence (no peptide) or in the presence of 10 μM of the antennapedia fusion LZ (BODIPY-Ant-LZ) or GCN4 (BODIPY-Ant-GCN4) peptide. Cells were then extensively washed to remove any peptide excess which was not internalized, and diluted three times to facilitate 24 hours of growth before treatment for 5 hours with (+) or without LPS (-). NF-kB activity was measured using the b-galactosidase assay. Error bars represent the standard deviation of two independant experiments.

Figure 6: Oligomerization properties of NEMO-derived peptides with or without the antennapedia sequence

All peptides were loaded at a 10 µM concentration on a superdex 75 HR10/30 column equilibrated in a buffer containing 0.1 mM DDM to improve recovery (see "Materials and methods"). Chromatographic profiles of the CC2 mutant (dashed line) and the CC2 wild type (solid line) fused (BODIPY-Ant-CC2 (WT), BODIPY-Ant-CC2 (Mu), or not fused to the antennapedia sequence (CC2 (WT), CC2 (Mu)) are shown in left panels, and elution profiles of the LZ mutant (dashed line) and the wild type (solid line) fused (BODIPY-Ant-LZ (WT), BODIPY-Ant-LZ (Mu), or not fused to the antennapedia sequence (LZ (WT), LZ (Mu)) are represented in right panels. Elution volumes of globular protein markers are indicated by arrows : Oval, ovalbumin (43 kDa); Chym, chymotrypsinogene A (25 kDa); Ribo, Ribonuclease (13.4 kDa) and Apro, aprotinin (6.5 kDa).

Figure 7: : Association of Ant-CC2 and Ant-LZ peptides to the CC2 peptide

(A) Direct titration of BODIPY-Ant-CC2 (1 µM) with CC2 by fluorescence anitropy. The concentration of CC2 was determined by amino acid analysis. Anisotropy values of BODIPY-Ant-CC2 in millionits (mA) were plotted against an increasing concentration of the CC2 peptide. Data points were fitted (solid line) to the binding isotherm equation with a K_D of 15.2 µM (*Materials and Methods*). The two dashed lines represent a stoichiometric titration and intersect at an CC2 concentration of 16 µM. Given the 1 µM concentration of the BODIPY-Ant-CC2, this gives a complex stoechiometric of 0.8. (B) Direct titration of BODIPY-Ant-LZ (0.1 µM) with CC2 by fluorescence anitropy. The anisotropy values of the BODIPY-Ant-LZ alone (white bar) or in the presence of the CC2 peptide (30µM, grey bar; 100 µM, black bar) are given in *millionits* (mA).

Figure 8: Cell death induced in the retinoblastoma cell line Y79 by Ant-CC2 and Ant-LZ peptides

Rb cell line Y79 were treated with various concentration of the Ant-CC2 (WT) (filled squares) or Ant-CC2 (Mu) (open squares) (A), or Ant-LZ (WT) (filled circles), or Ant-LZ (Mu) (open circles) (B), or Ant peptide (open triangle) (C) for 3 hours (A, B) or 16 hours (C). Cell survival was then evaluated using the MTS assay as described in "Materials and methods"

Table 1

Sequence of NEMO derived peptides

Name	Sequence (a)	Theoritical mass	Experimental mass
BODIPY-Ant	CRQIKIWFQNRRMKWKR	2805.19	2805.06 ± 0.52
BODIPY-Ant-CC2 (WT)	CRQIKIWFQNRRMKWKKSKGMQLEDLRQQLQQAEEA LVAKQELIDKLKEEAEQHKIV	7433.51	7433.33 ± 0.46
CC2 (WT)	SKGMQLEDLRQQLQQAEEALVAKQELIDKLKEEAEQ HKIV	4155.75	4155.86 ± 0.53
BODIPY-ANT-CC2 (Mu)	CRQIKIWFQNRRMKWKKSKGMQLEDLRQQ**G**QQAEEA **G**VAKQEL**G**DKLKEEAEQHKIV	7265.18	7265.04 ± 0.35
CC2 (Mu)	SKGMQLEDLRQQ**G**QQAEEA**G**VAKQEL**G**DKLKEEAEQ HKIV	3987.43	3987.11 ± 0.55
BODIPY-ANT-LZ (WT)	CRQIKIWFQNRRMKWKKLKAQADIYKADFQAERHAR EKLVEKKEYLQEQLEQLQREFNKL	8064.2	8063.9 ± 0.48
LZ (WT)	LKAQADIYKADFQAERHAREKLVEKKEYLQEQLEQL QREFNKL	5318.08	5318.21 ± 0.5
BODIPY-ANT-LZ (Mu)	CRQIKIWFQNRRMKWKKLKAQADIYKADFQAERHAR EKLVEKKEY**S**QEQLEQ**S**QREFNKL	8012.04	8011.98 ± 0.26
LZ (Mu)	LKAQADIYKADFQAERHAREKLVEKKEY**S**QEQLEQ**S** QREFNKL	5265.92	5268.82 ± 0.18
BODIPY-ANT-GCN4	CRQIKIWFQNRRMKWKKSKGMQRMKQLEDKVEELLS KNYHLENEVARLKKLVGER	7315.48	7314.76± 0.40

(a) In all peptides the N-terminus contains a cystein residue for convenience of specific peptide coupling with the maleimide group as described in "Materials and Methods". The sequence of antennapedia fused to the NEMO sequence (plain text) is highlighted in bold caracters. Residues which may be involved in coiled-coil sequence are underlined and those which were replaced in the CC2 and LZ mutants are underlined in bold caracters.

figure 1

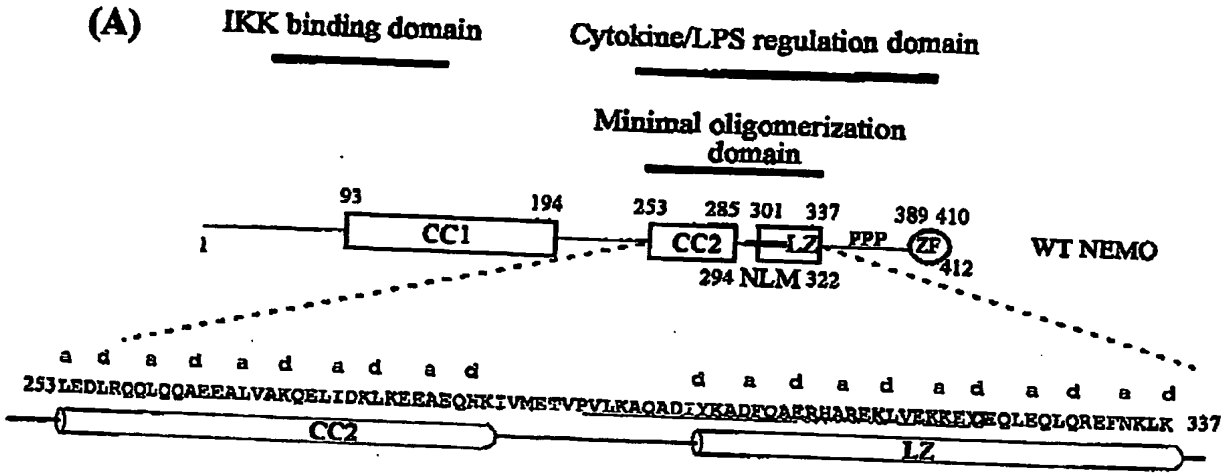
(A)
IKK binding domain
Cytokine/LPS regulation domain
Minimal oligomerization domain
93
194
253
285
301
337
389
410
412
1
CC1
CC2
LZ
FPP
ZF
WT NEMO
294 NLM 322
a d a d a d a d a d
253LEDLRQQLQQAEEALVAKQELIDKLKEEAEQHKIVMETVPVLKAQADIYKADFQAERHAREKLVEKKEYQEQLEQLQREFNKLK 337
d a d a d a d a d a d
CC2
LZ

(B)

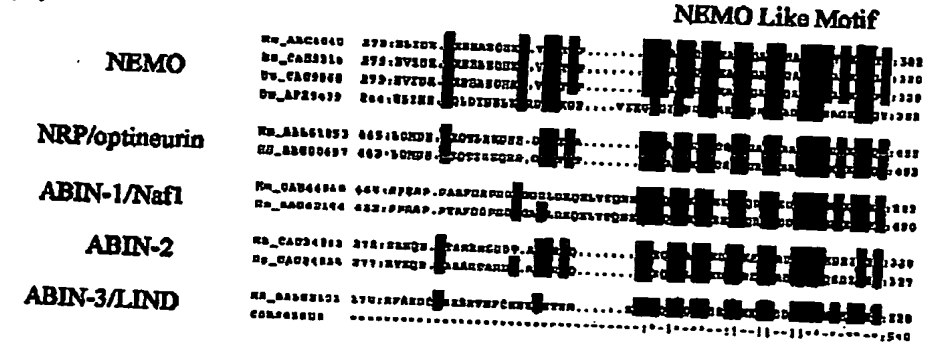
NEMO Like Motif
NEMO
NRP/optineurin
ABIN-1/Naf1
ABIN-2
ABIN-3/LIND

Figure 2

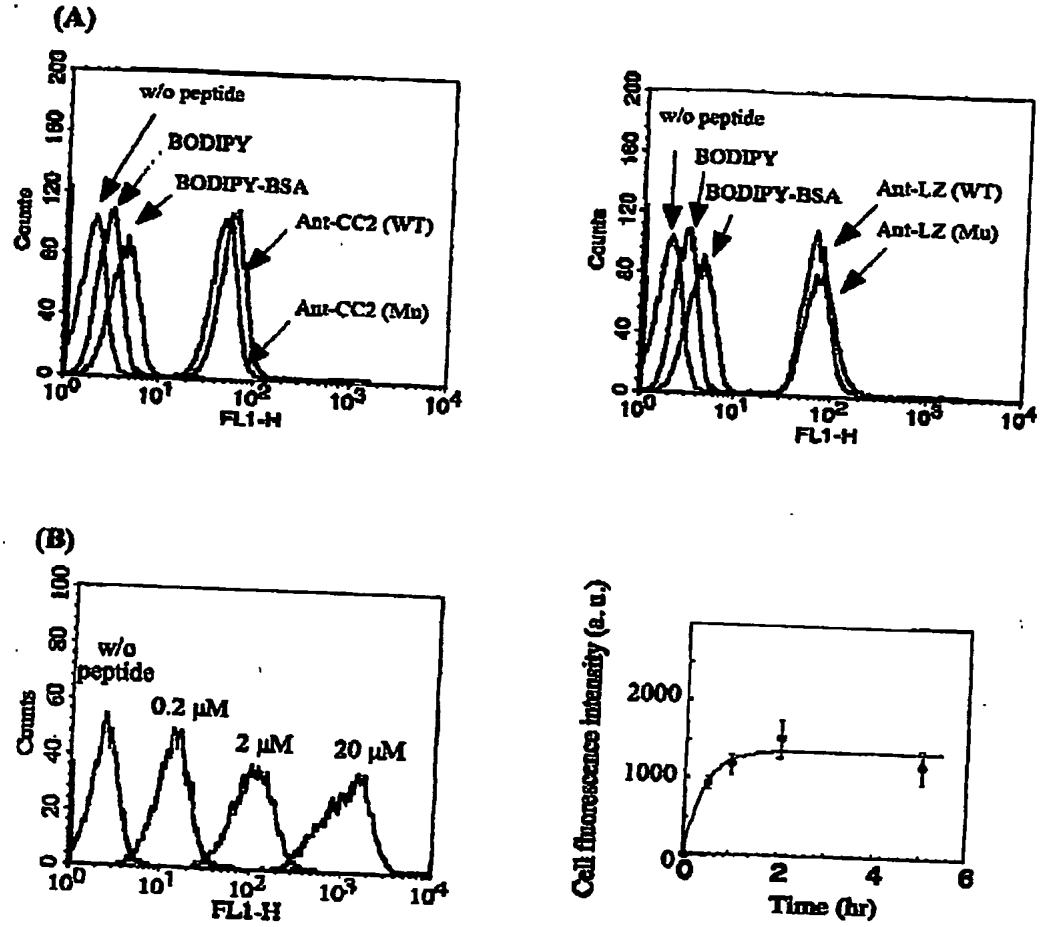
(A)
w/o peptide
BODIPY
BODIPY-BSA
Ant-CC2 (WT)
Ant-CC2 (Mu)
Counts
FL1-H
w/o peptide
BODIPY
BODIPY-BSA
Ant-LZ (WT)
Ant-LZ (Mu)
Counts
FL1-H
(B)
w/o peptide
0.2 μM
2 μM
20 μM
Counts
FL1-H
Cell fluorescence intensity (a. u.)
Time (hr)

Figure 3

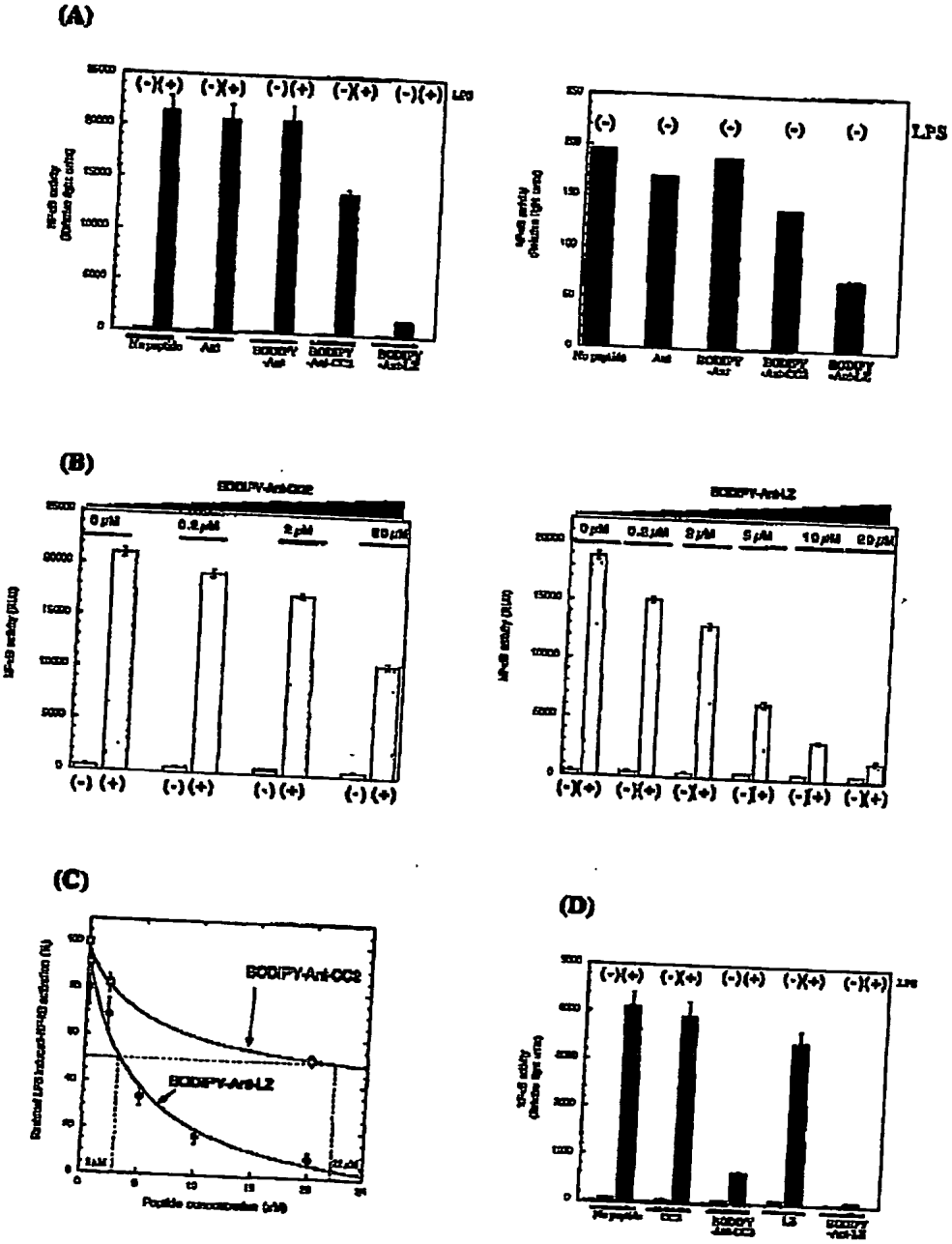
(A)
(-)(+)
(-)(+)
(-)(+)
(-)(+)
(-)(+)
LPS
(-)
(-)
(-)
(-)
(-)
LPS
(B)
BODIPY-Ant-CC2
0 μM
0.2 μM
2 μM
20 μM
(-) (+)
(-) (+)
(-) (+)
(-) (+)
BODIPY-Ant-L2
0 μM
0.2 μM
2 μM
5 μM
10 μM
20 μM
(-)(+)
(-)(+)
(-)(+)
(-)(+)
(-)(+)
(-)(+)
(C)
BODIPY-Ant-CC2
BODIPY-Ant-L2
(D)
(-)(+)
(-)(+)
(-)(+)
(-)(+)
(-)(+)
LPS

Figure 4

(A)

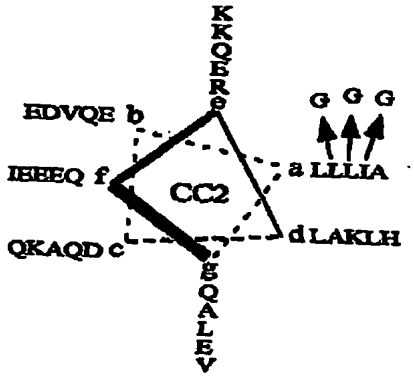
KKQERE
EDVQE b
G G G
IEEEQ f
a LLLIA
CC2
QKAQD c
d LAKLH
EQALEV

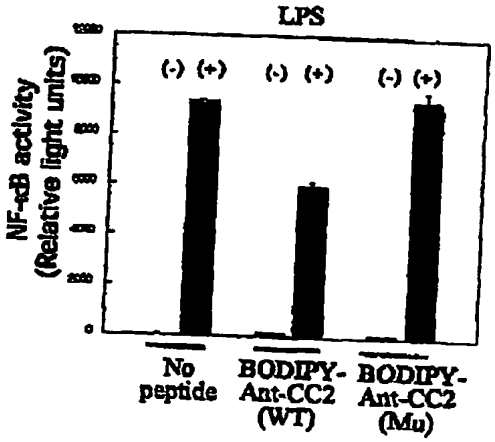
LPS
NF-κB activity
(Relative light units)
(-) (+) (-) (+) (-) (+)
No peptide
BODIPY-Ant-CC2 (WT)
BODIPY-Ant-CC2 (Mu)

(B)

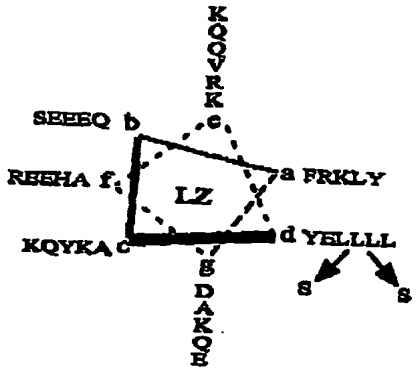
KQQVRK
SEEEQ b
REEHA f
a FRKLY
LZ
KQYKA c
d YELLLL
EDAKEQ
s s

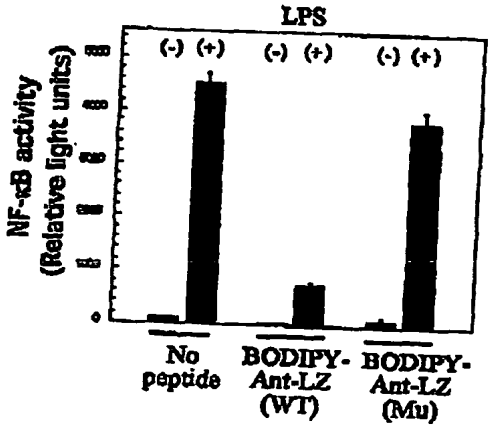
LPS
NF-κB activity
(Relative light units)
(-) (+) (-) (+) (-) (+)
No peptide
BODIPY-Ant-LZ (WT)
BODIPY-Ant-LZ (Mu)

Figure 5

(A)

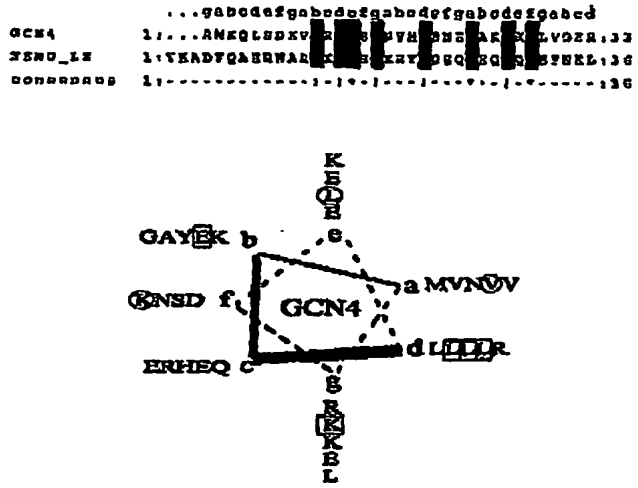
GCN4
MVNVV
ERHEQ
GAYEK
NSD

(B)

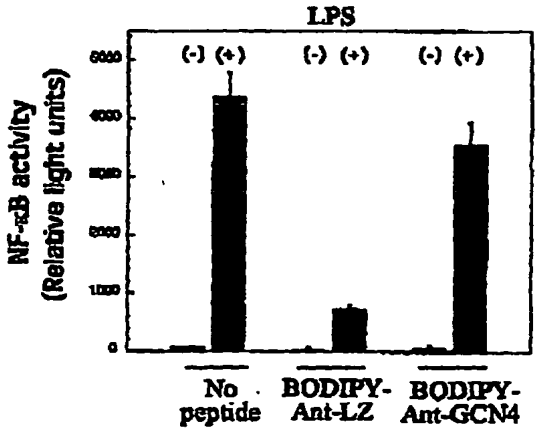
LPS
(-) (+) (-) (+) (-) (+)
NF-κB activity
(Relative light units)
No peptide
BODIPY-Ant-LZ
BODIPY-Ant-GCN4

Figure 6

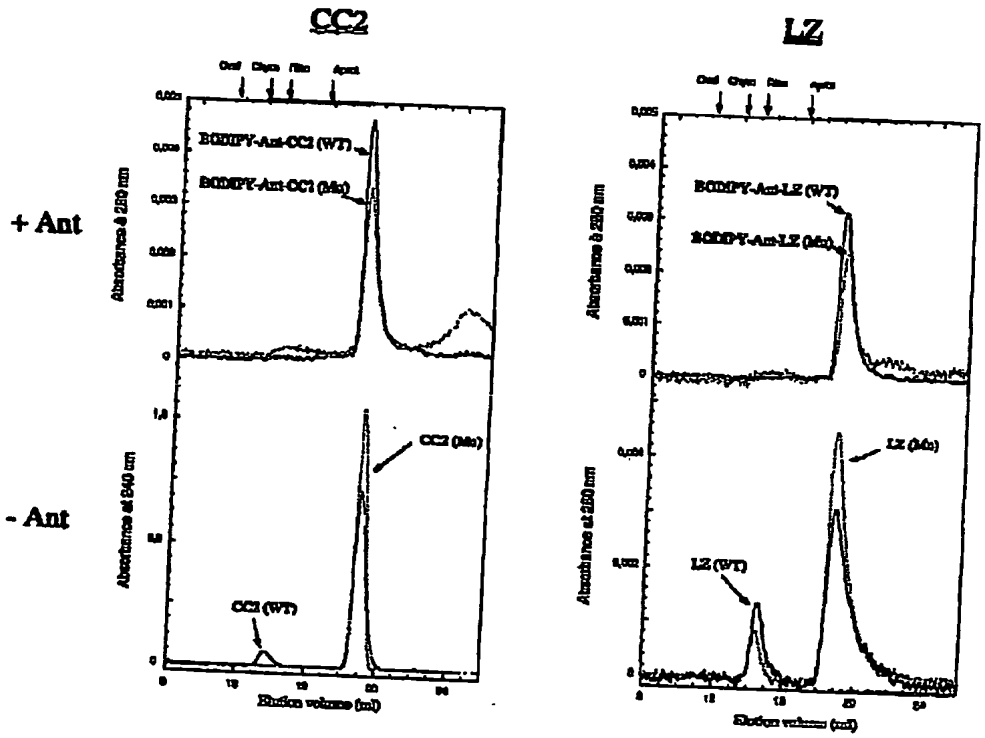
CC2
LZ
+ Ant
- Ant
BODIPY-Ant-CC2 (WT)
BODIPY-Ant-CC2 (Mu)
CC2 (Mu)
CC2 (WT)
BODIPY-Ant-LZ (WT)
BODIPY-Ant-LZ (Mu)
LZ (Mu)
LZ (WT)

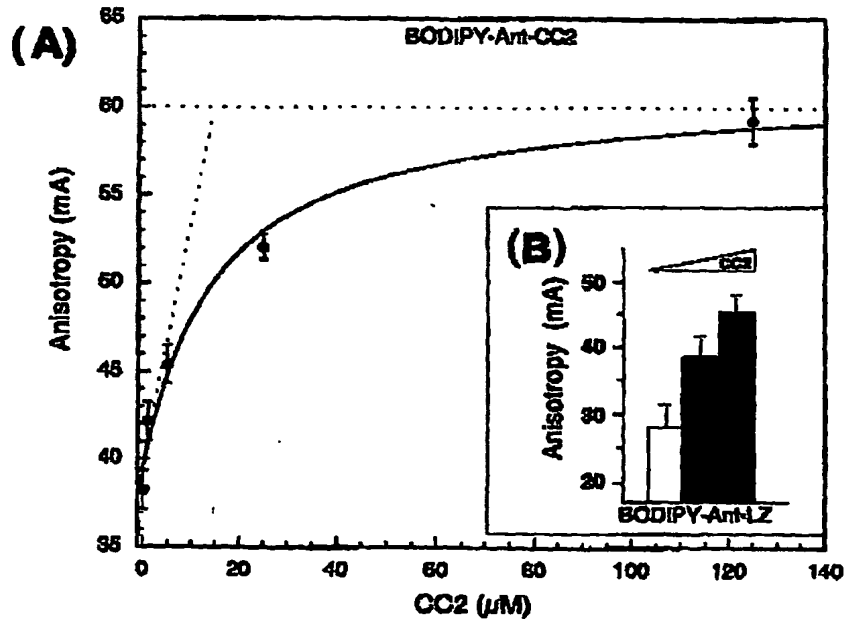
(A)
BODIPY-Ant-CC2
Anisotropy (mA)
CC2 (μM)
65
60
55
50
45
40
35
0
20
40
60
80
100
120
140
(B)
CC2
Anisotropy (mA)
50
40
30
20
BODIPY-Ant-LZ

Figure 8

(A)

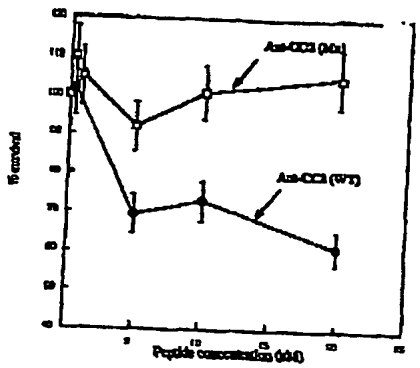

(B)

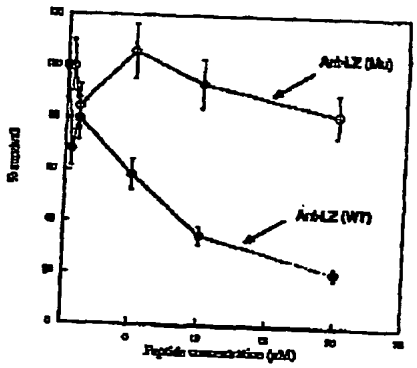

(C)

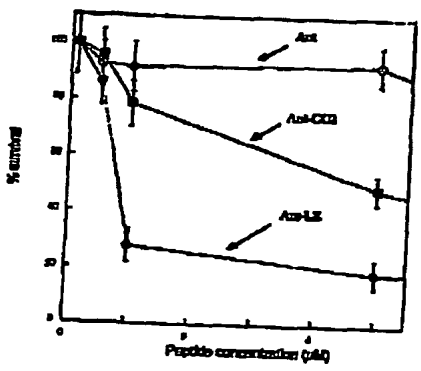

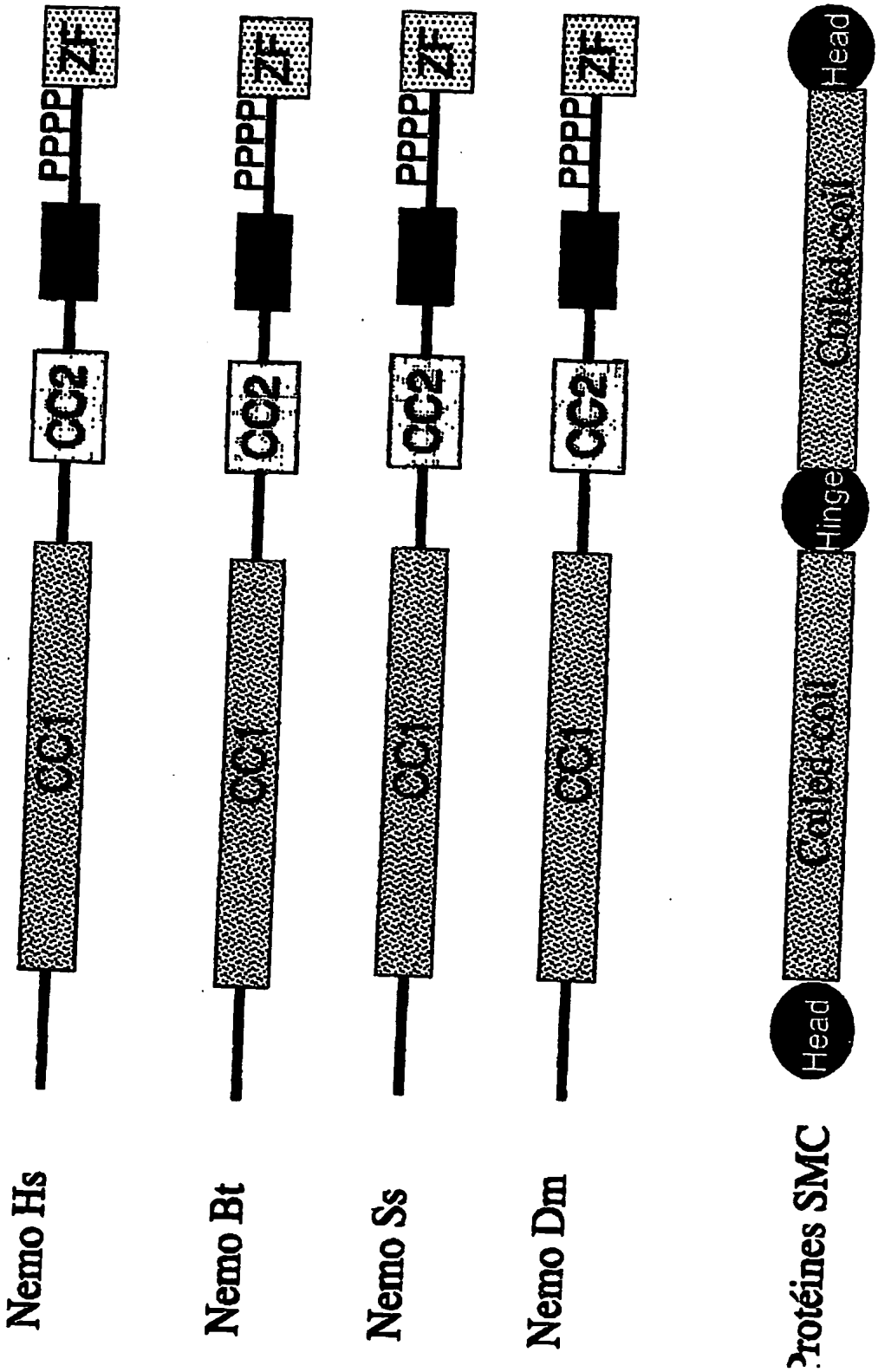
Nemo Hs
Nemo Bt
Nemo Ss
Nemo Dm
Protéines SMC
PPPP
Zn
CC2
CC1
Head
Coiled-coil
Hinge
Coiled-coil
Head

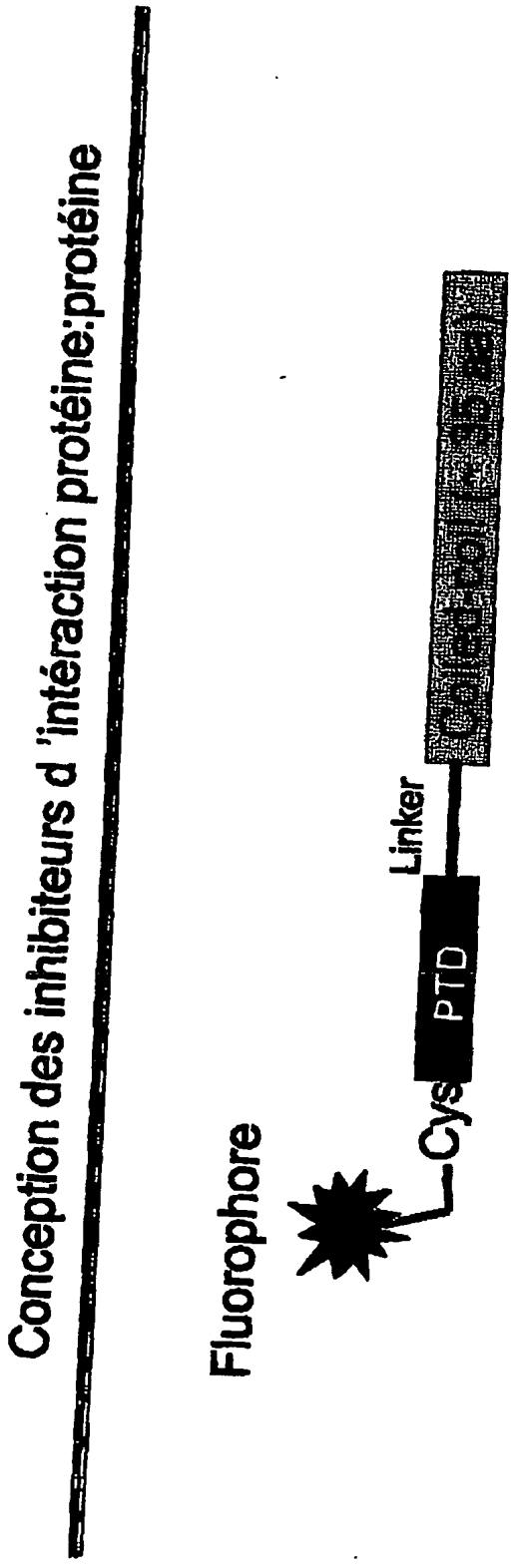
Conception des inhibiteurs d 'intéraction protéine:protéine
Fluorophore
Cys
PTD
Linker

Protein transduction domain (PTD) ou Membrane permeable sequence (MPS)

Nom	Longueur (aa)	Caractéristiques
Antennapedia /penetratin (43-58)	16	Hélice amphiphile avec une face hydrophile basique
Arg/Trp	16	Produit dérivant d 'antennapedia
TAT (48-58)	11	Motif riche en aa basique. Ne forme pas d 'hélice amphiphile
VP 22	34	MPS le plus long
Transportan	28	Chimère synthétique dérivant de galanin et mastoporan
kFGF	16	Séquence contenant essentiellement des résidus hydrophobes
R7	7	Le plus court et le plus récent !
Homopolymère de citrulline	7-9	Produit dérivant du R7

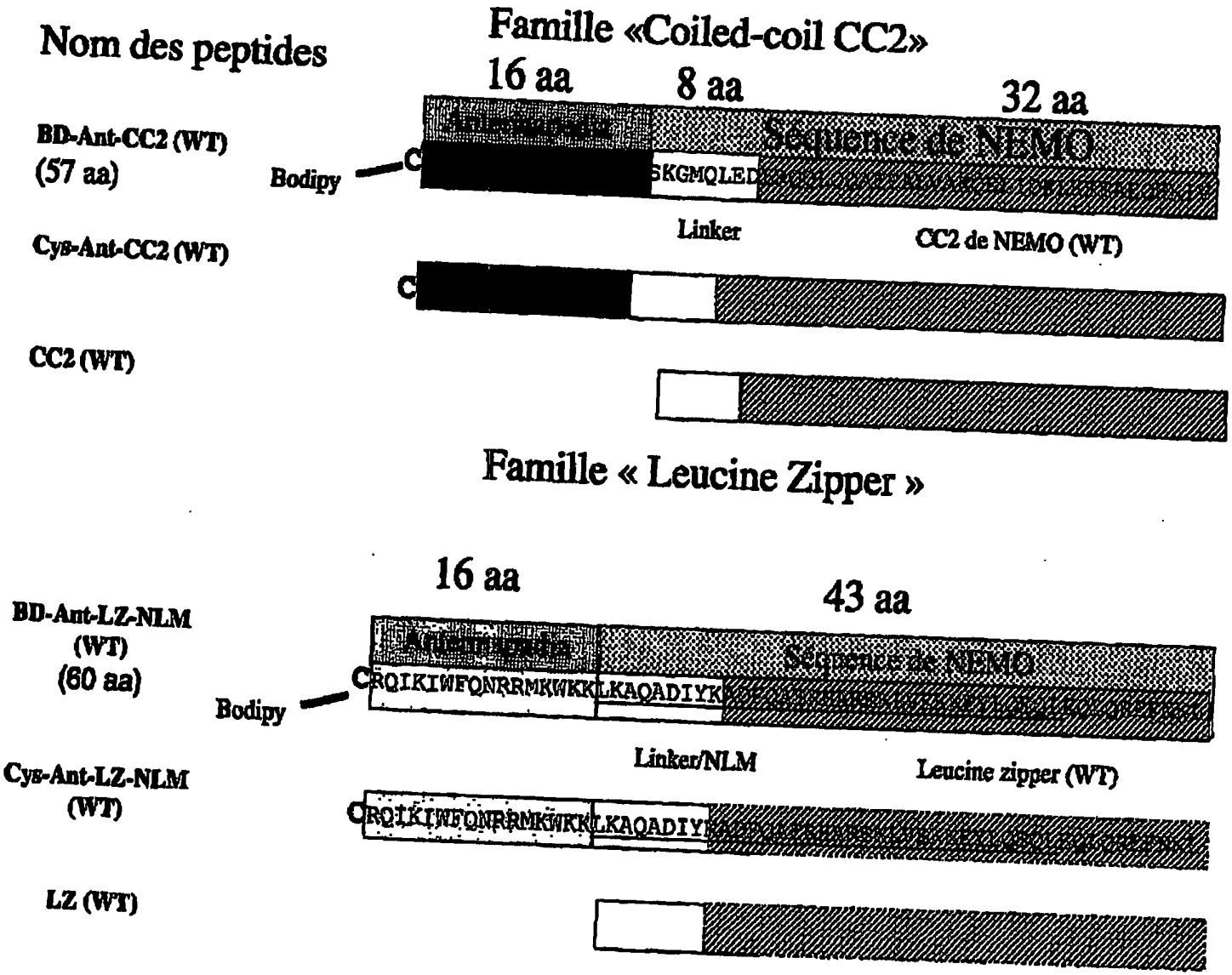

I. Analyse de l 'efficacité d 'internalisation des peptides dans les lymphocytes B par FACS

Effet du sérum, du LPS, de la concentration, du temps d 'incubation

II. Mesures de l 'inhibition de la voie de signalisation NF-kB en réponse au LPS

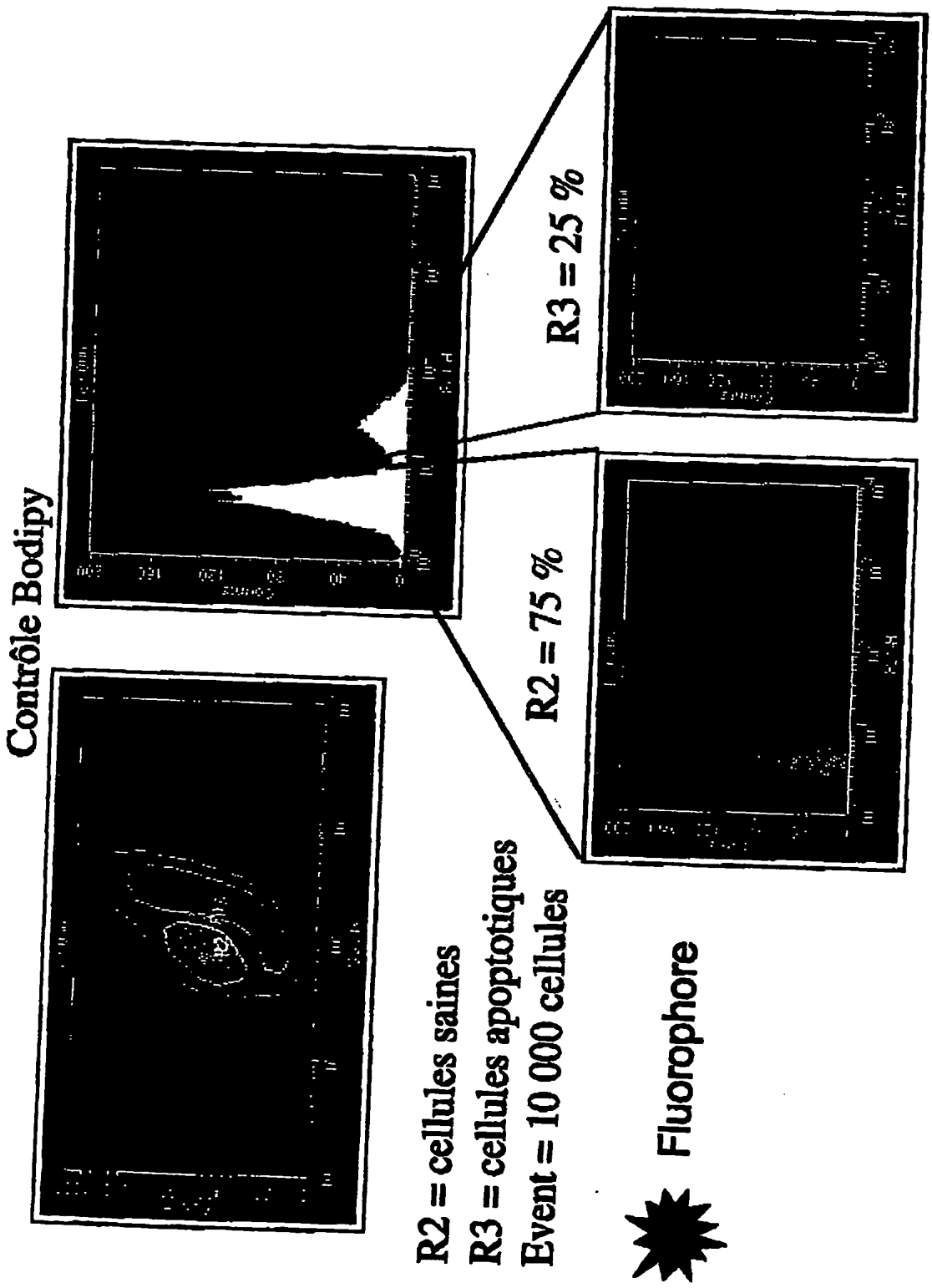
Contrôle Bodipy
R3 = 25 %
R2 = 75 %
R2 = cellules saines
R3 = cellules apoptotiques
Event = 10 000 cellules
Fluorophore

Temps: 2 h15
Conc: 2 µM

Temps: 2 h
de contact
Conc: 2 µM
Contrôle III
(BD-BSA)
Ant-BD-NLM-LZ
(mutant)
Ant-BD-CC2

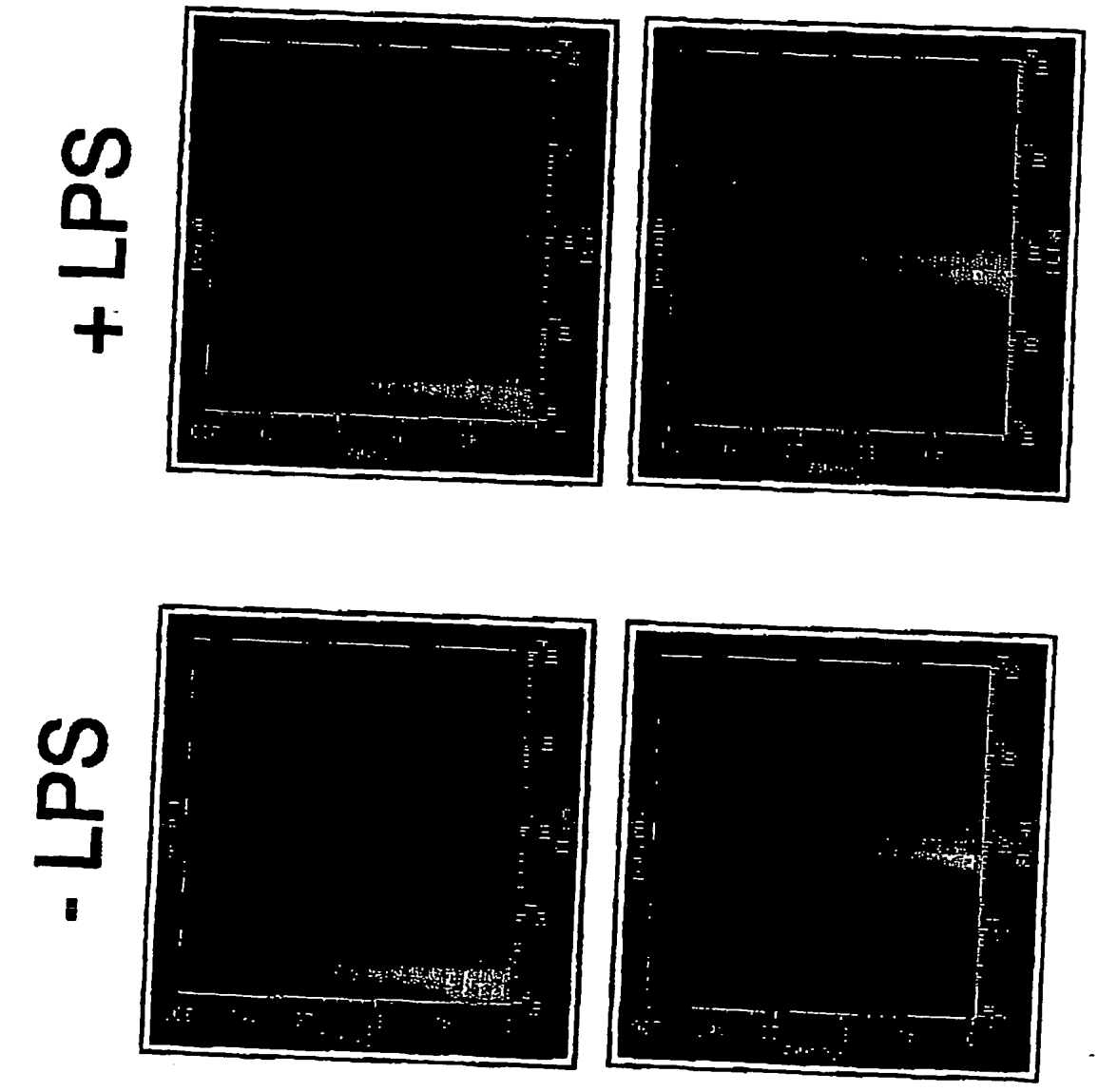
+ LPS
- LPS
Temps : 2 h
de contact
Conc: 2 µM
Stimulation: 2 h
Contrôle
(Bodidy)
Ant-BD-LZ
(WT)

Temps de contact : 2 h
Temps de stimulation : 3 h

Temps de contact : 2 h
Temps de stimulation : 3 h

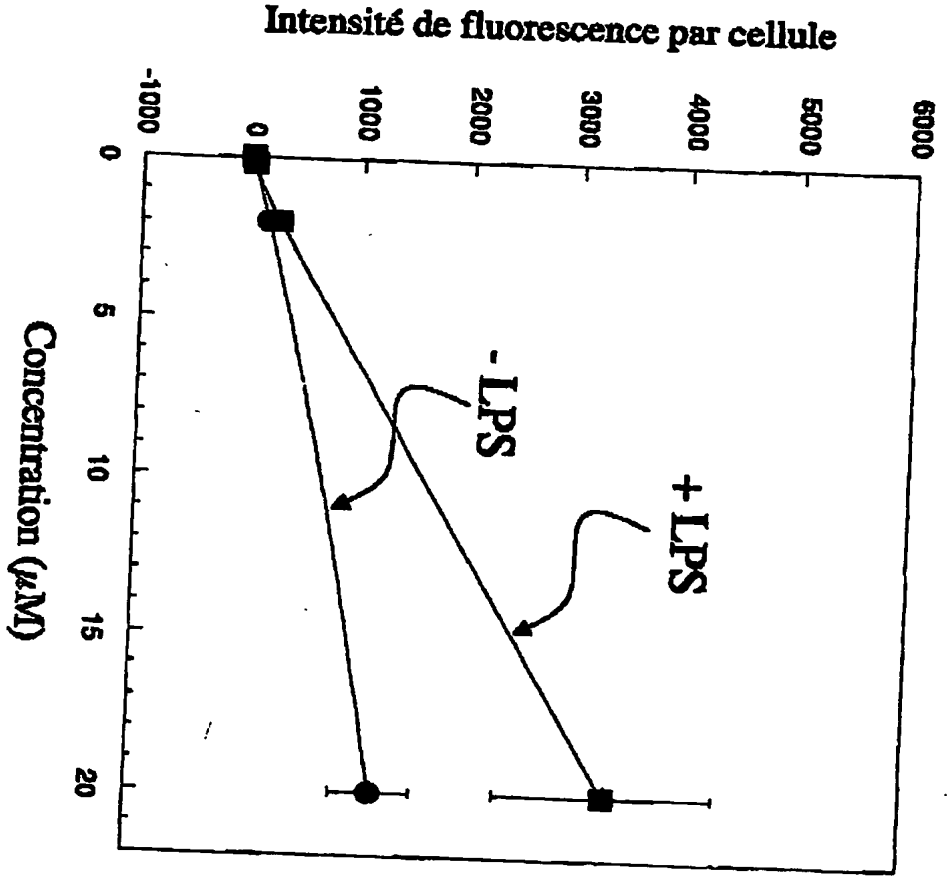

Temps de contact : variable
Ant-BD-CC2] = 20 µM
Avec sérum
Sans sérum
0 min
30 min
120 min

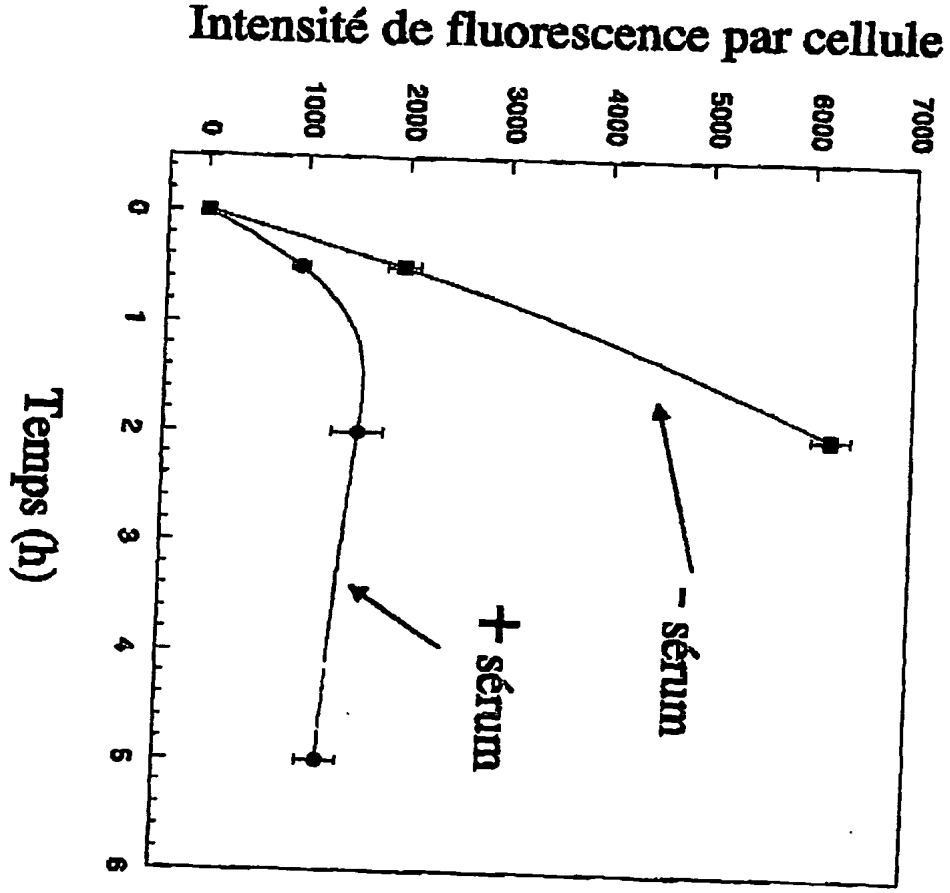
Intensité de fluorescence par cellule
0
1000
2000
3000
4000
5000
6000
7000
Temps (h)
0
1
2
3
4
5
6
+ sérum
- sérum

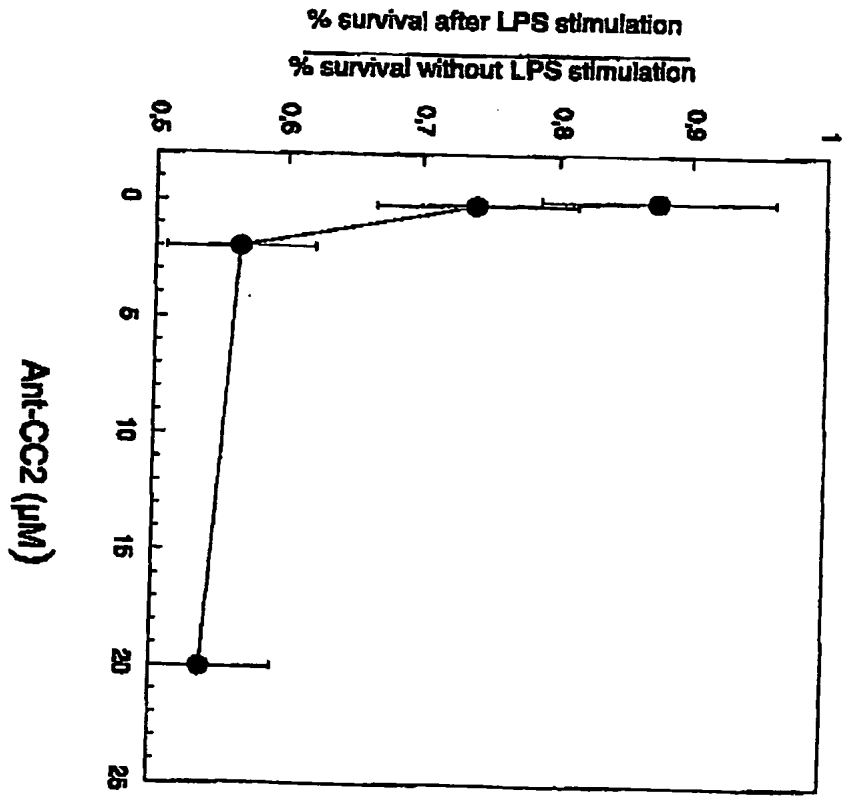
% survival after LPS stimulation
% survival without LPS stimulation
0,5
0,6
0,7
0,8
0,9
1
Ant-CC2 (µM)
0
5
10
15
20
25

Conclusion sur la vectorisation des drogues

- Absence de toxicité pour toutes les drogues peptidiques étudiées
- Le peptide « Antennapedia » assure une excellente internalisation des drogues peptidiques (100 % de cellules transduites)
- La présence de sérum diminue l'efficacité d 'internalisation des peptides mais accroit considérablement la survie cellulaire
- La stimulation des cellules par le lipopolysaccharide bactérien (LPS) n'inhibe pas cette internalisation
- La concentration intracellulaire des peptides vectorisés varie linéairement avec la concentration des peptides incubés dans le milieu extracellulaire
  ($[5\ \mu M]_{extracellulaire} \rightarrow [350\ \mu M]_{intracellulaire}$)
- L 'internalisation des peptides croît avec le temps et atteint un optimum après 2 heures d 'incubation

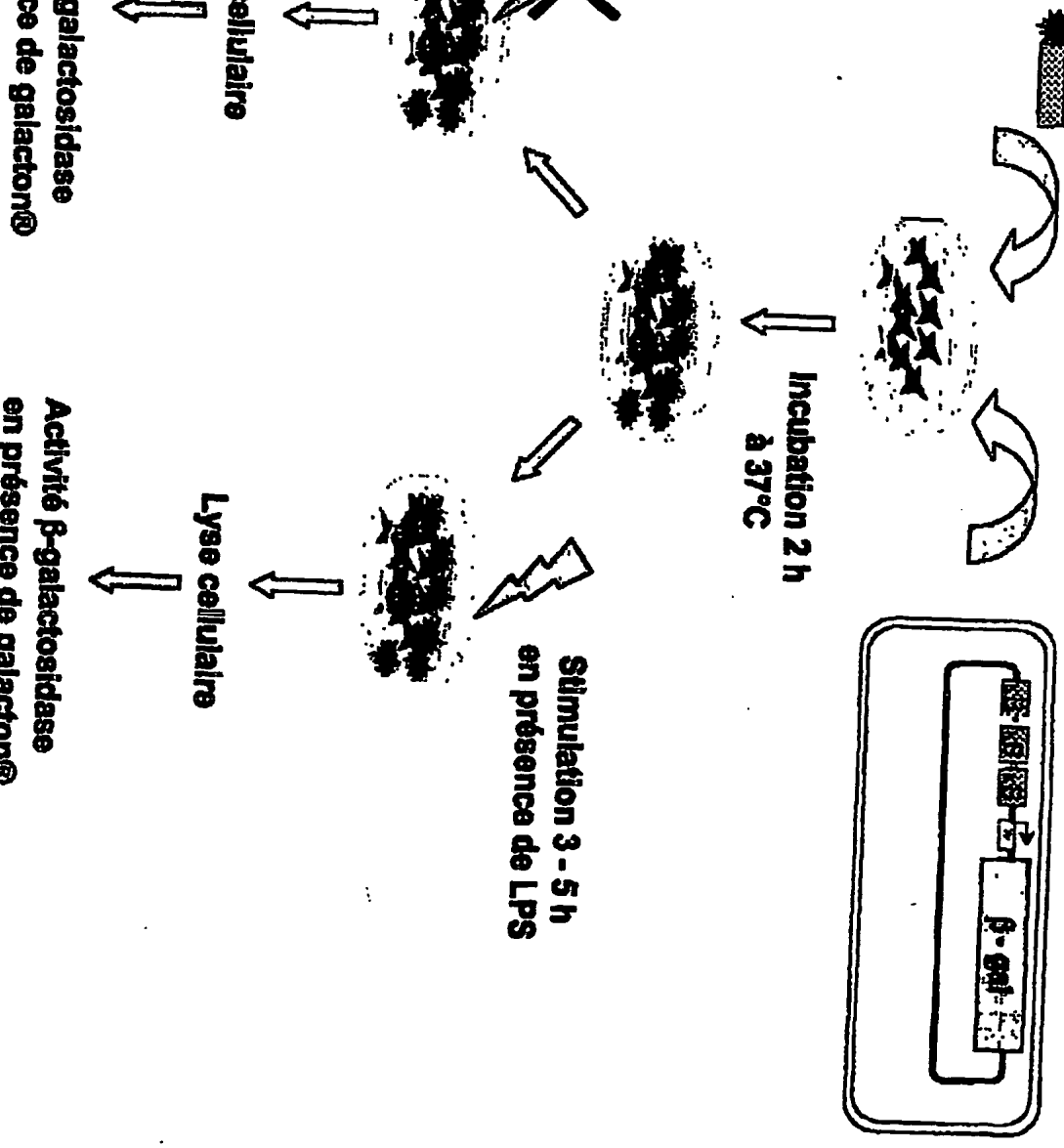
β - gal
Incubation 2 h
à 37°C
Stimulation 3 - 5 h
en présence de LPS
Lyse cellulaire
Activité β-galactosidase
en présence de galacton®
Lyse cellulaire
Activité β-galactosidase
en présence de galacton®

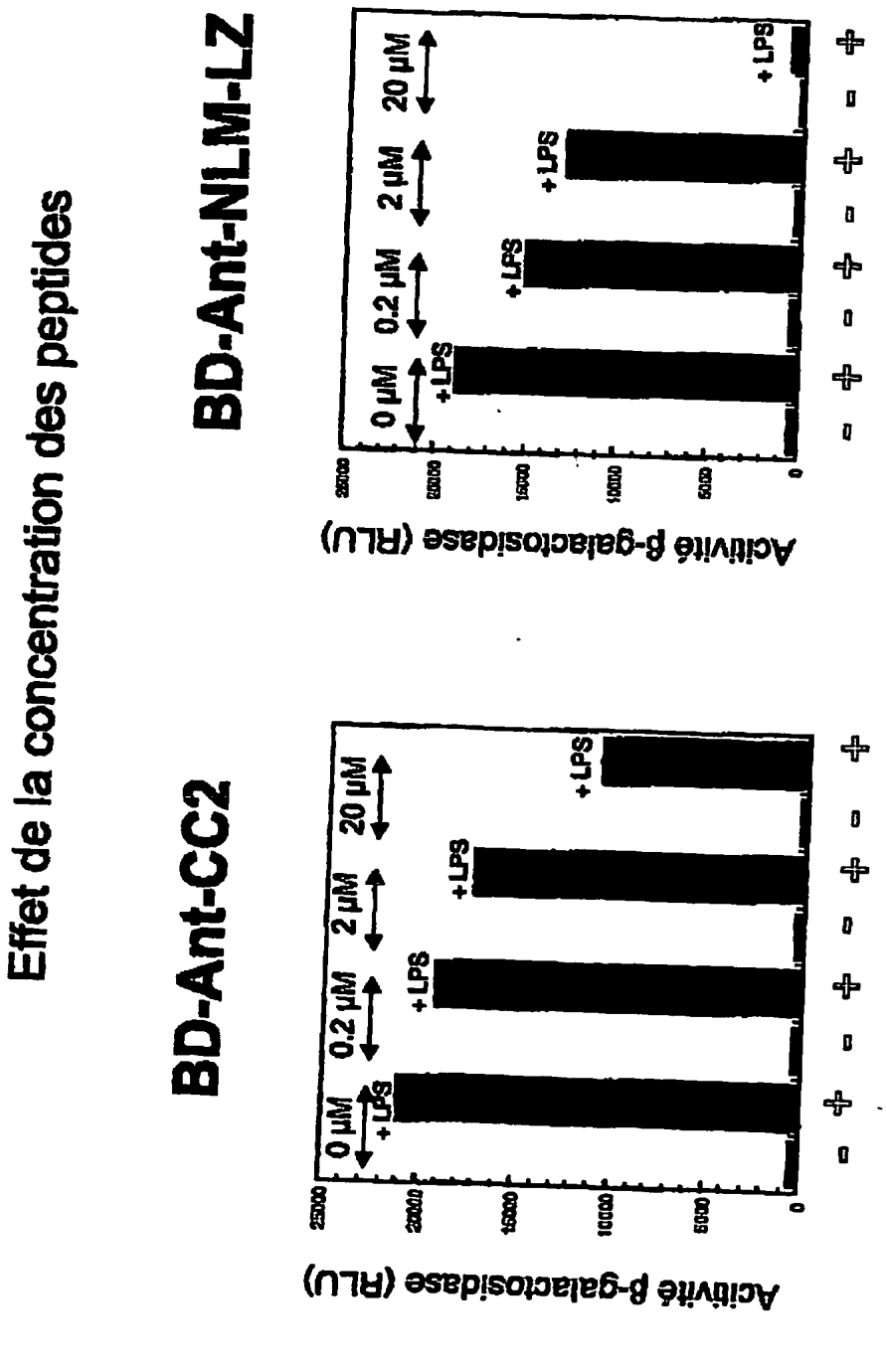
Effet de la concentration des peptides
BD-Ant-NLM-LZ
Activité β-galactosidase (RLU)
0 µM
0.2 µM
2 µM
20 µM
+LPS
BD-Ant-CC2
Activité β-galactosidase (RLU)
Stimulation 5 h par LPS

Effet de la séquence d 'internalisation

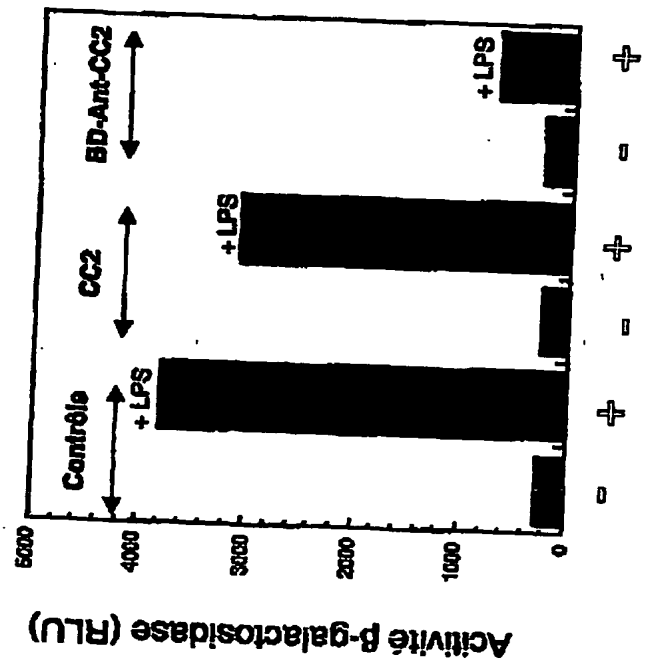

Stimulation 3 h

Quelle est la spécificité de ces drogues ?

Parallel coiled coils (most commonly observed)

Heptad abcdefgabcdefgabcdefg.....

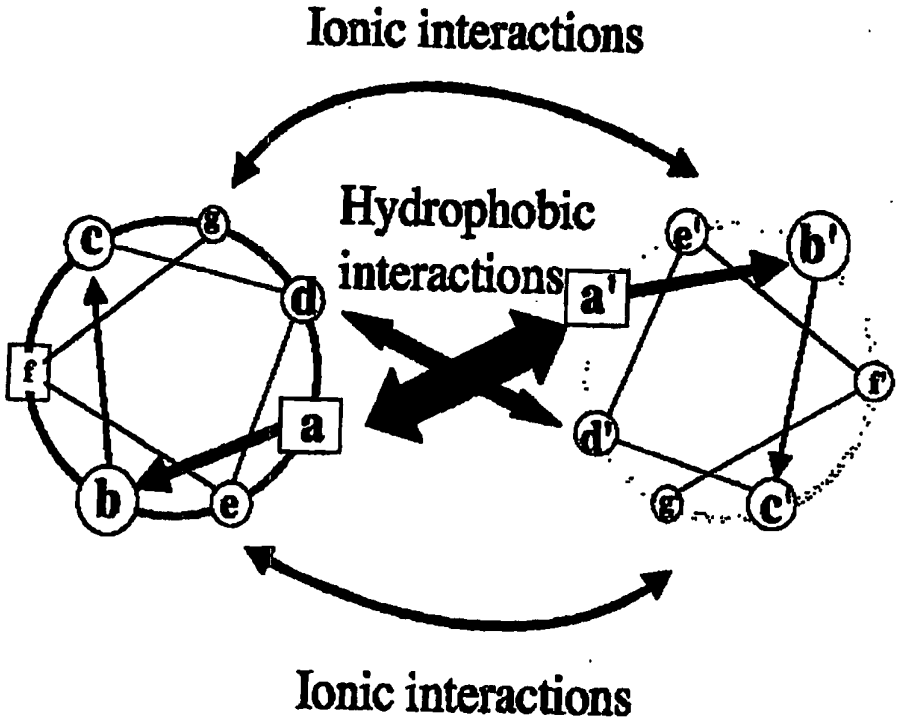

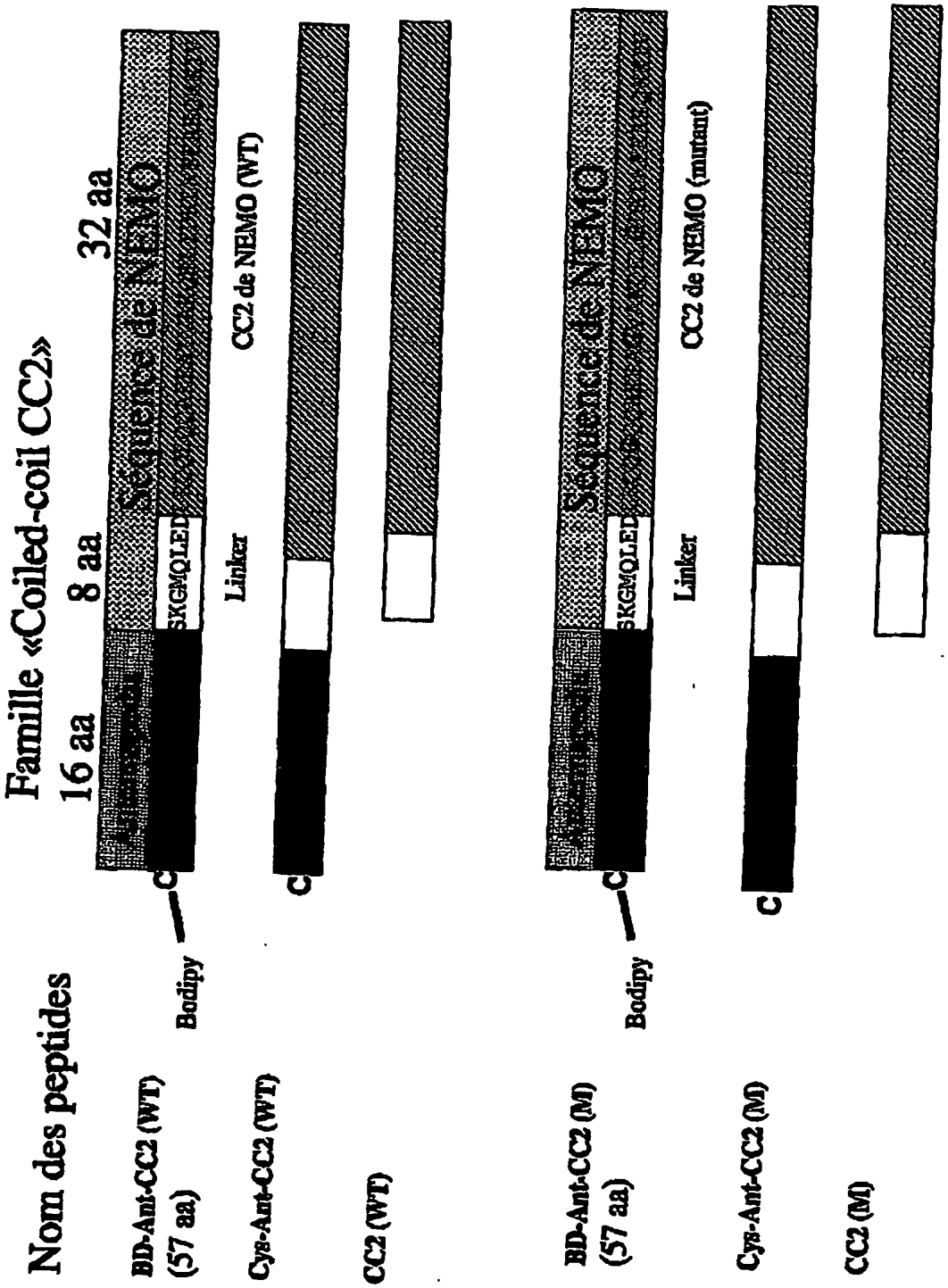
Famille «Coiled-coil CC2»
16 aa
8 aa
32 aa
Nom des peptides
BD-Ant-CC2 (WT) (57 aa)
Bodipy
Séquence de NEMO
SKGMQLED
Linker
CC2 de NEMO (WT)
Cys-Ant-CC2 (WT)
CC2 (WT)
BD-Ant-CC2 (M) (57 aa)
Bodipy
Séquence de NEMO
SKGMQLED
Linker
CC2 de NEMO (mutant)
Cys-Ant-CC2 (M)
CC2 (M)
C

Famille « Leucine Zipper »

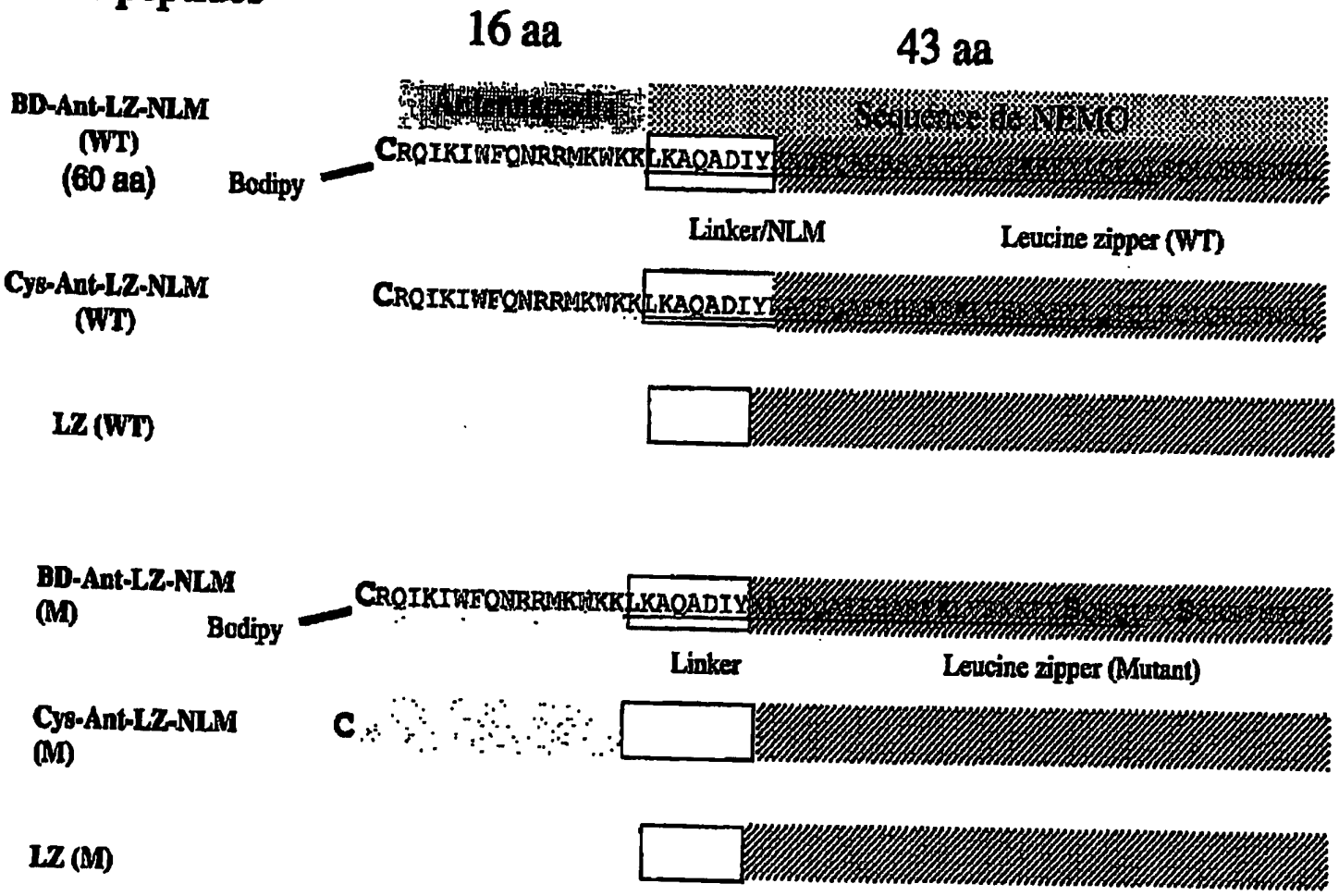

Spécificité des drogues

Famille NLM-LZ

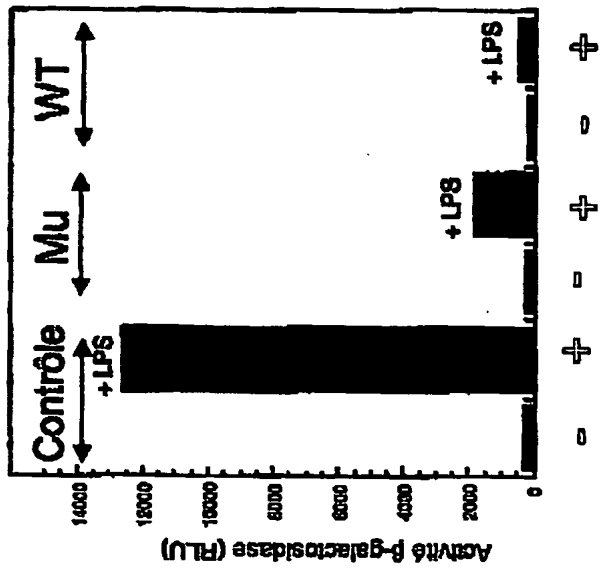

Famille CC2

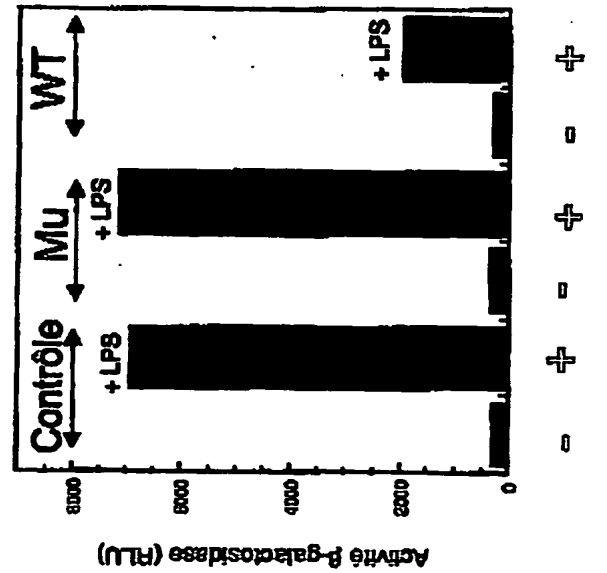

Stimulation 5 h; 20 µM

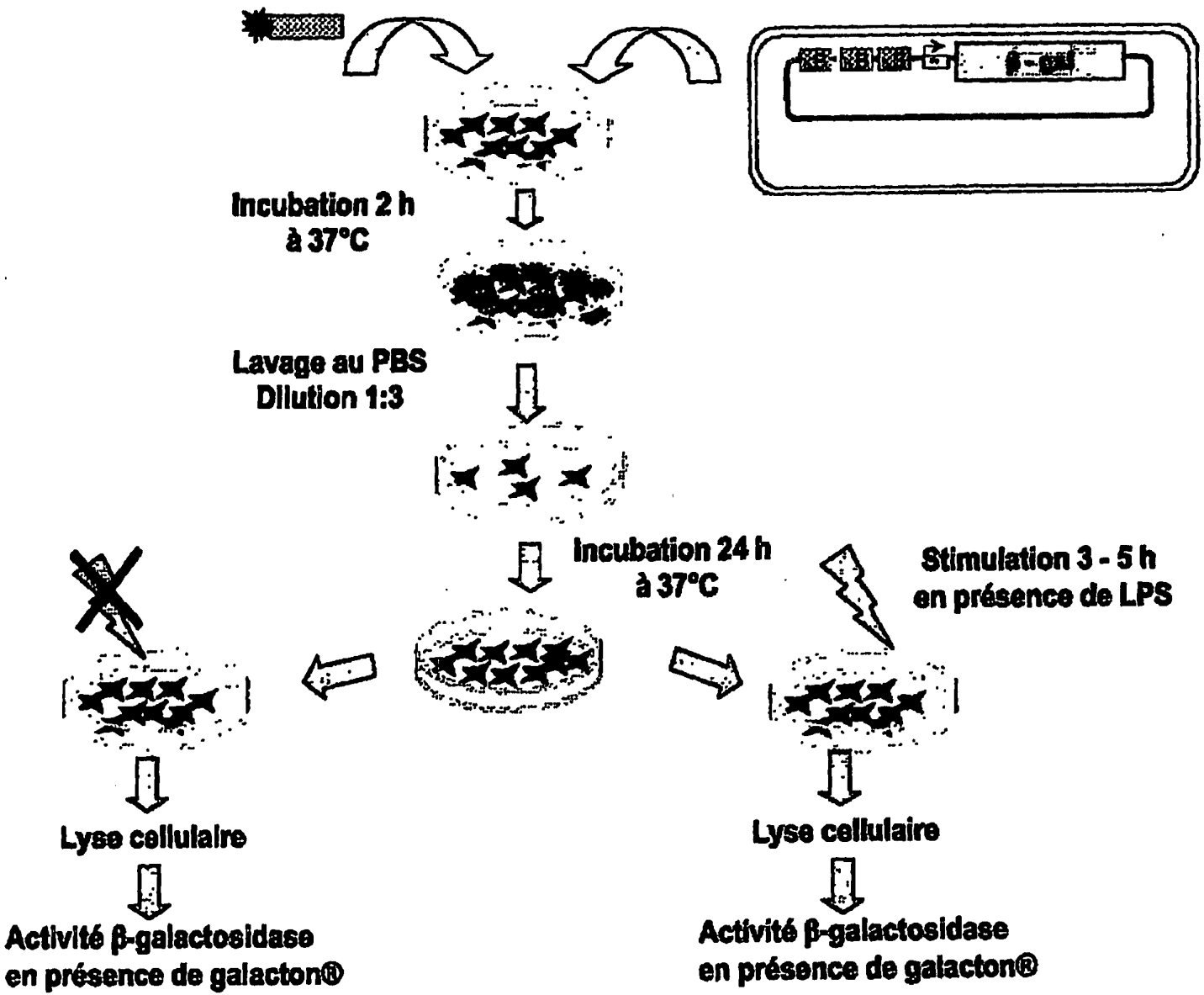

LPS (5 heures)

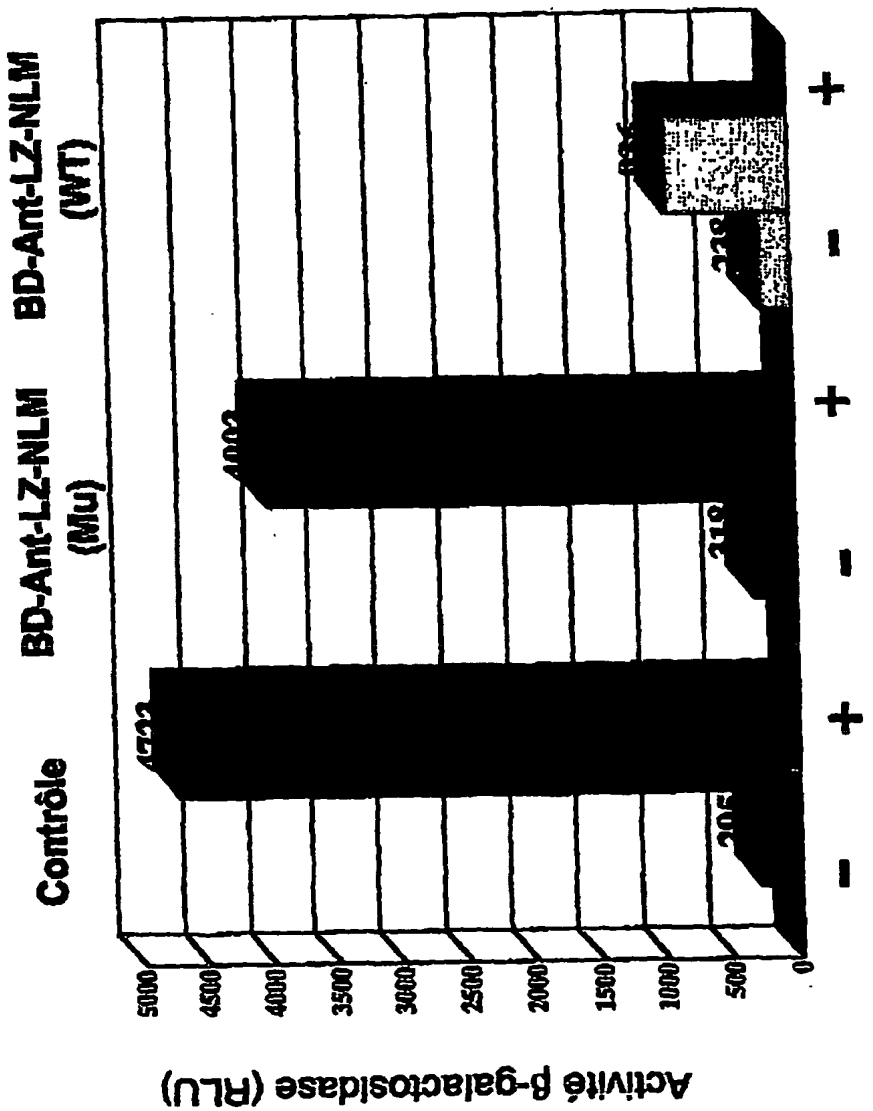
Activité β-galactosidase (RLU)
5000
4500
4000
3500
3000
2500
2000
1500
1000
500
0
Contrôle
BD-Ant-LZ-NLM (Mu)
BD-Ant-LZ-NLM (WT)
+
-
+
-
+
-

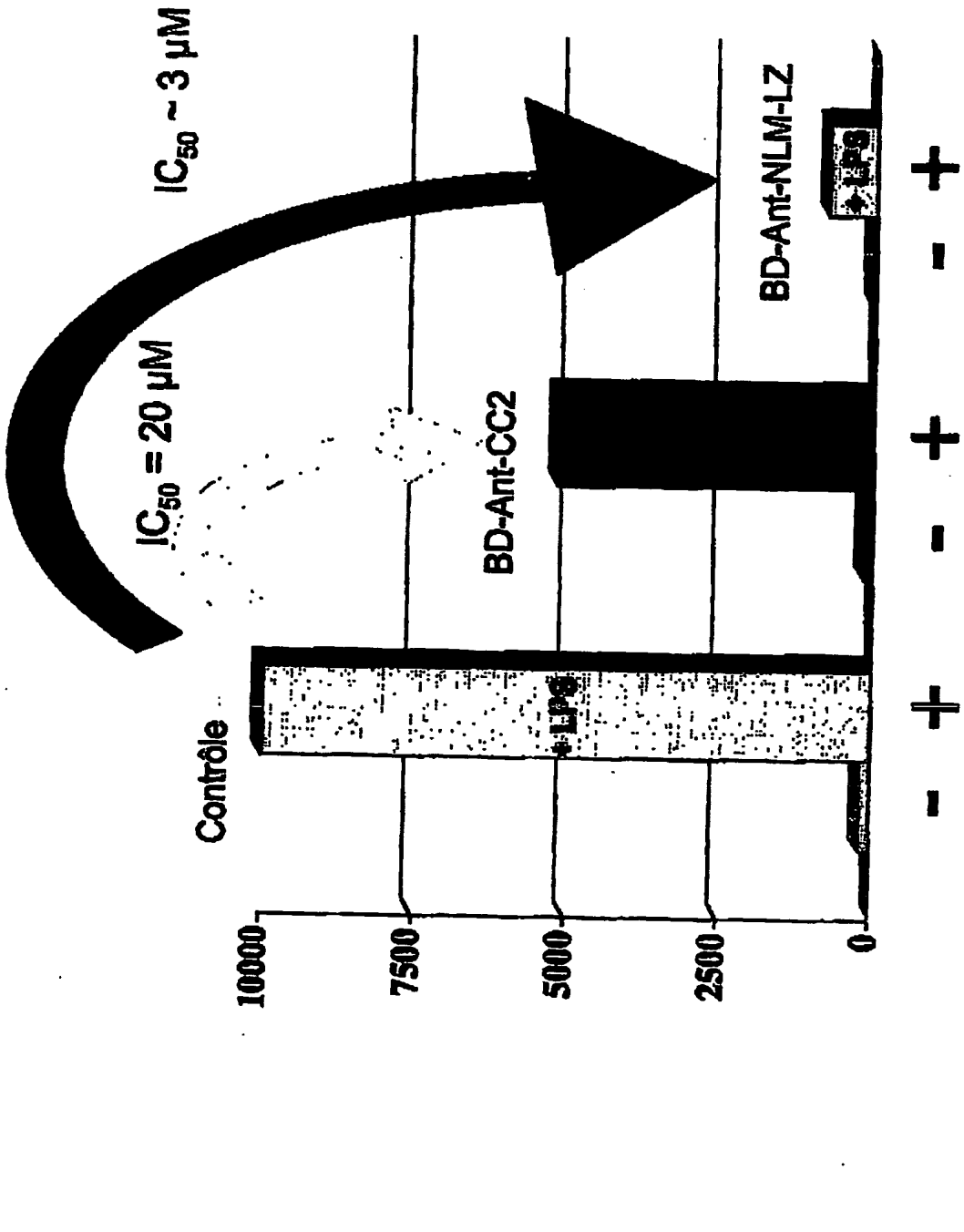
IC50 ~ 3 µM
IC50 = 20 µM
Contrôle
BD-Ant-CC2
BD-Ant-NLM-LZ
LPS
10000
7500
5000
2500
0
- + - + - +
Stimulation par le LPS 5 h, 20 µM

Rappel sur l 'abondance des motifs coiled-coils dans le protéome

- « Approximatively 2 - 4 % of amino acids in proteins are estimated to adopt coiled-coil folds » . T. Alber (2000)

- « Greater than 5 % of all putative ORFs found in sequenced genomes are predicted to contain coiled-coils». P.S. Kim & J.C. Hu (2000)

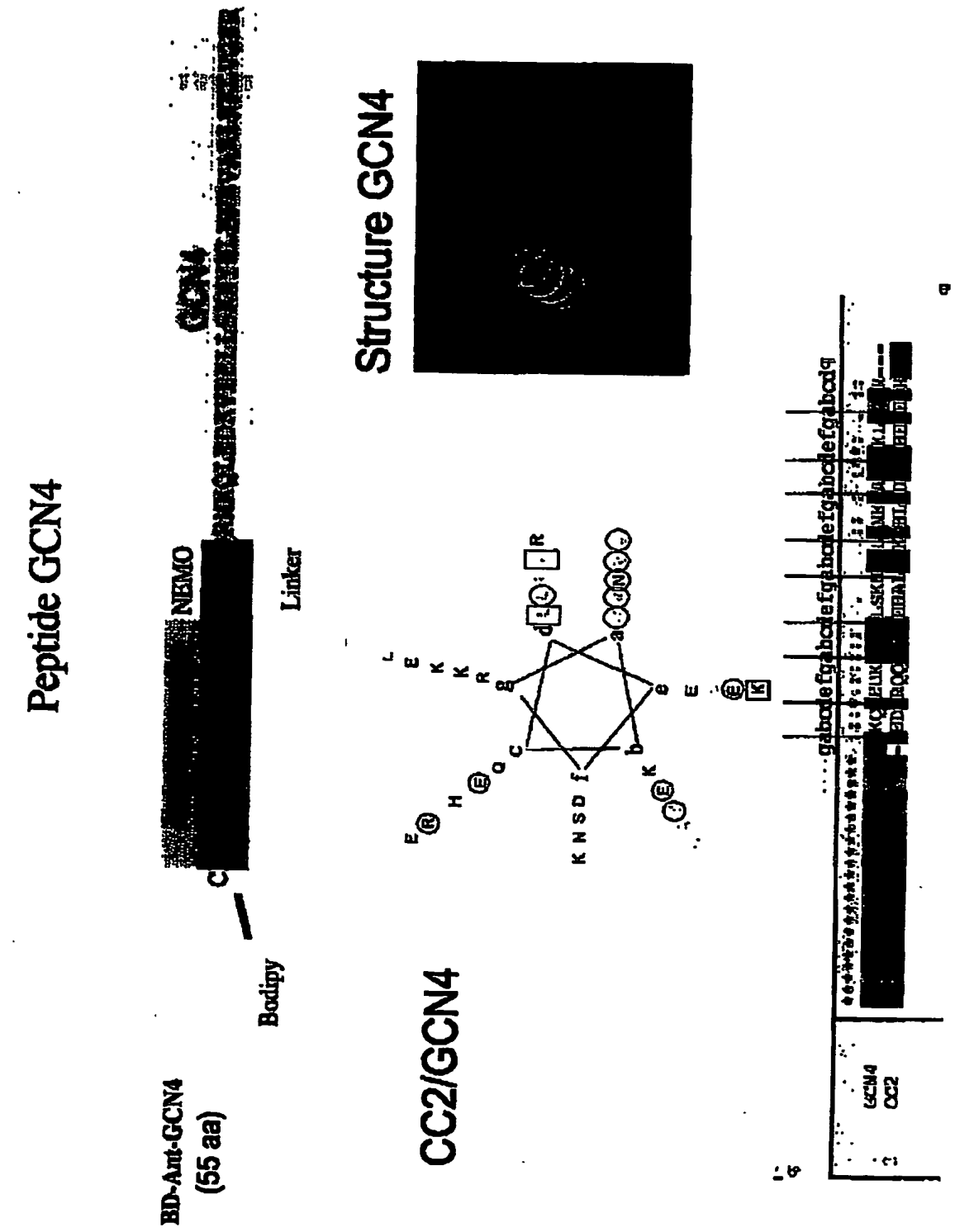
Peptide GCN4
BD-Ant-GCN4
(55 aa)
NBM0
GCN4
Linker
Bodipy
Structure GCN4
CC2/GCN4
GCN4
CC2

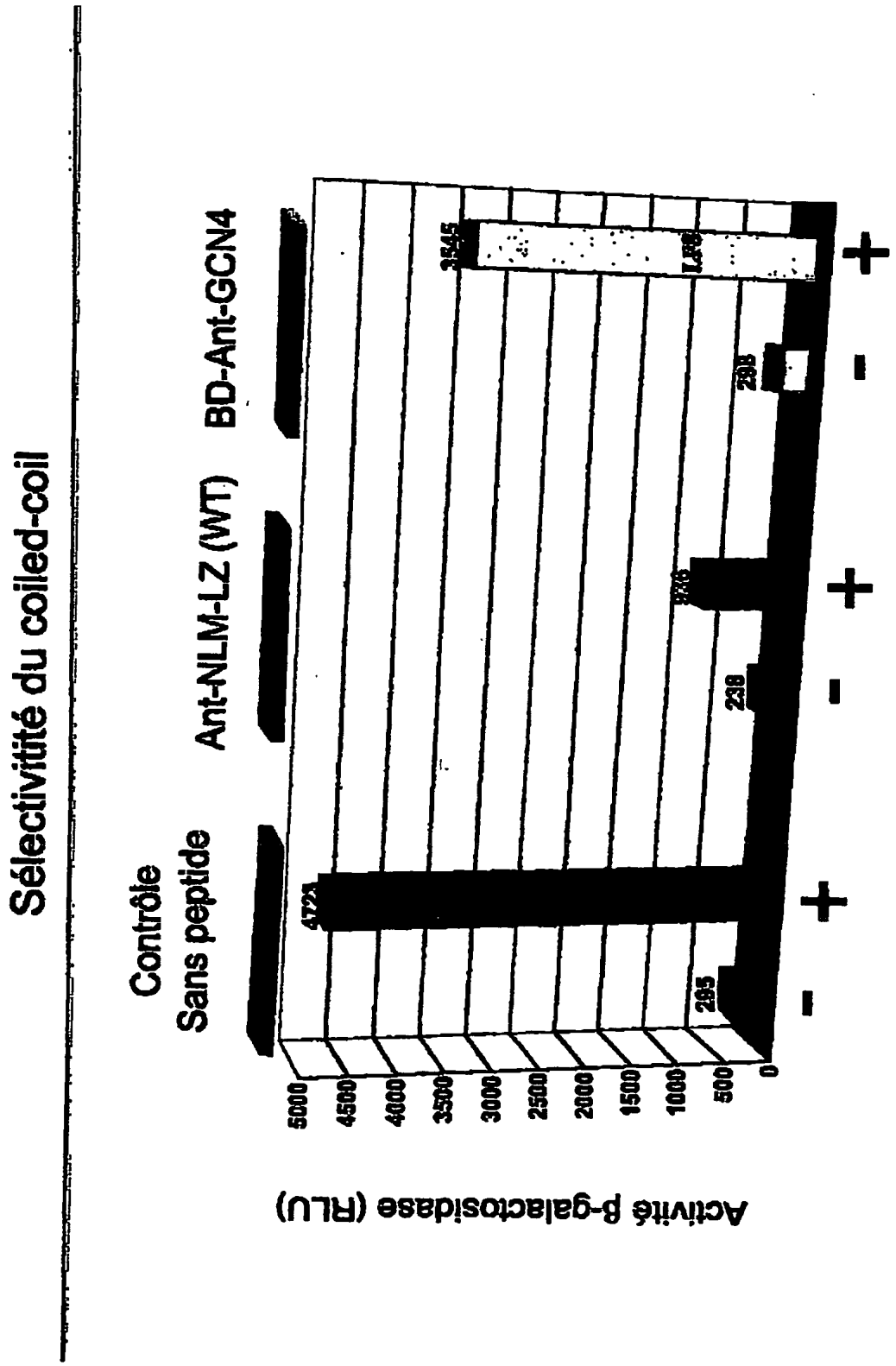
Sélectivitité du coiled-coil
Contrôle
Sans peptide
Ant-NLM-LZ (WT)
BD-Ant-GCN4
Activité β-galactosidase (RLU)
5000
4500
4000
3500
3000
2500
2000
1500
1000
500
0
4723
295
239
1776
293
3545
LPS
- + - + - +
10 µM de peptide)
LPS (5 heures)

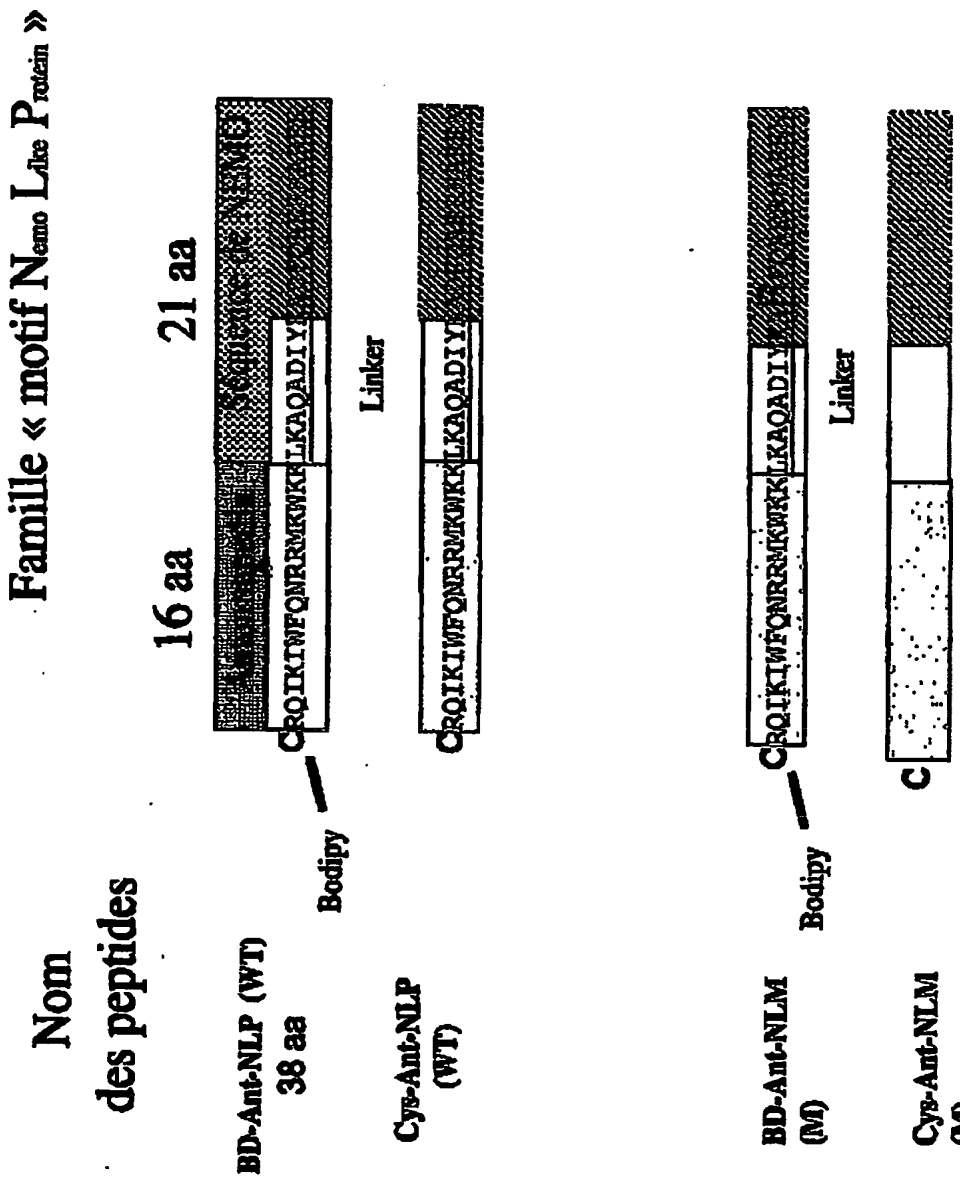
Famille « motif Nemo Like Protein »
Nom des peptides
16 aa
21 aa
BD-Ant-NLP (WT) 38 aa
Bodipy
Linker
Cys-Ant-NLP (WT)
BD-Ant-NLM (M)
Bodipy
Linker
Cys-Ant-NLM (M)

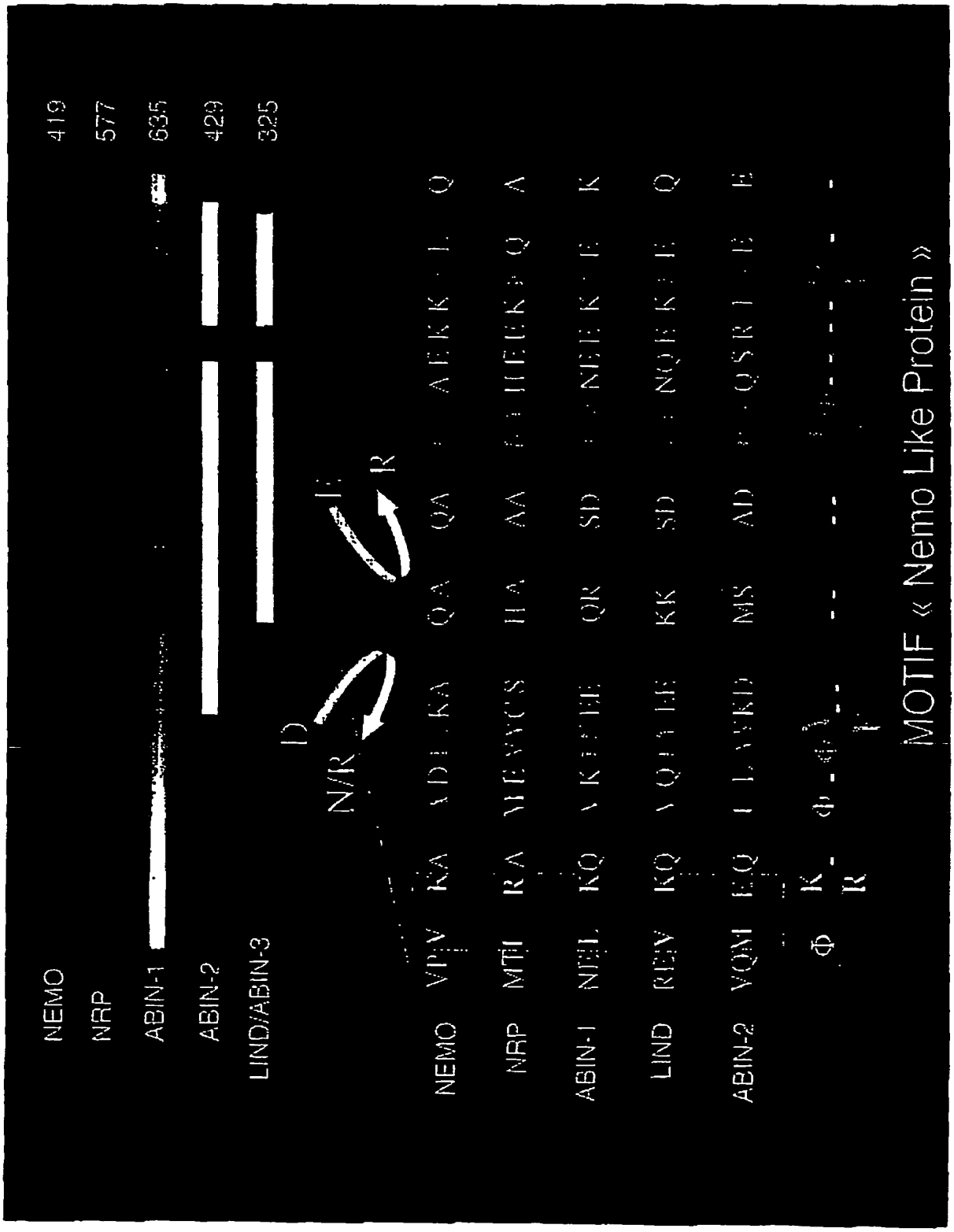
NEMO
NRP
ABIN-1
ABIN-2
LIND/ABIN-3
419
577
635
429
325
D
N/R
E
R
NEMO VPV RA VDLKA QA QA AEKKLQ
NRP MTI RA VEVCS HA AA EIIEEKEQA
ABIN-1 NTL KQ VKEIE QR SD NEEKEK
LIND REV KQ VQIIR KK SD NQRKEQ
ABIN-2 VQM EQ LLAKD MS AD QSRIEE
Φ K - Φ - - - -
R
MOTIF « Nemo Like Protein »

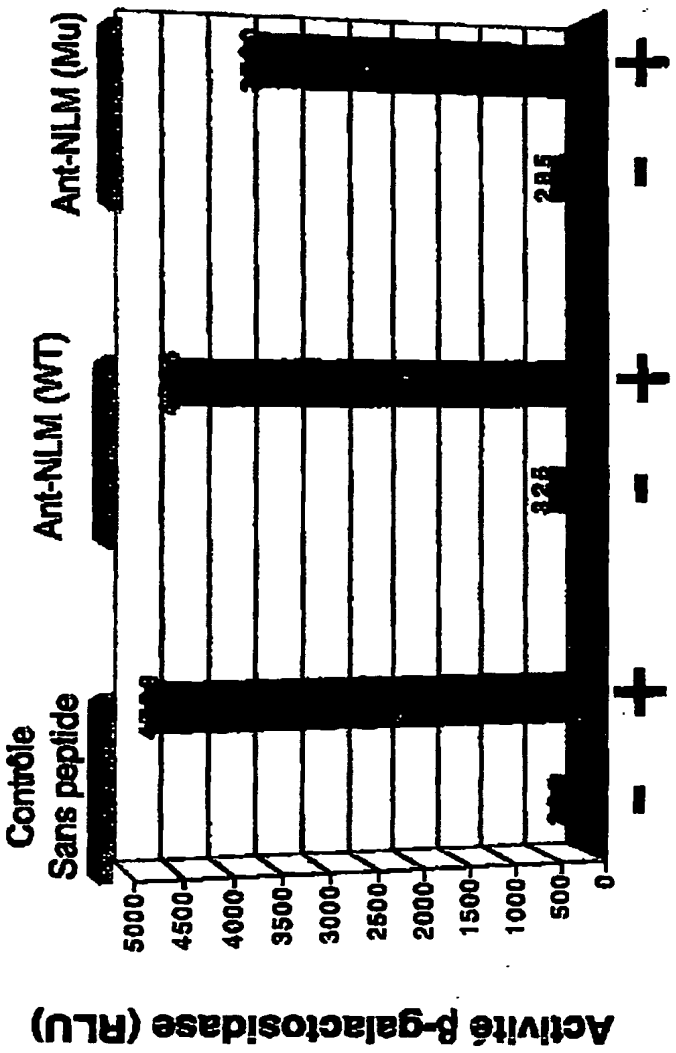
Activité β-galactosidase (RLU)
5000
4500
4000
3500
3000
2500
2000
1500
1000
500
0
Contrôle
Sans peptide
Ant-NLM (WT)
Ant-NLM (Mu)
285
328
+
-
+
-
+
-

POSTER NO: 402

The genetic IP defects: molecular analysis of NEMO gene and NF-kB related genes

Tiziana Bardaro, Geppino Falco, Angela Sparago, Vincenzo Mercadante, Matilde Valeria Ursini, Michele D'Urso
International Institute of Genetics and Biophysics, CNR, Via Marconi, 12 -80125- Naples Italy

In collaboration with International IP Consortium (IPIF) we recently demonstrated that 78% of Incontinentia Pigmenti (IP; MIM 308310) patients show an identical deletion within the NEMO/IKKg (NF-kB Essential MOdulator/IKKgamma) gene that eliminated exons 4 to 10 and consequently abolished protein function, required for the activation of the transcription factor NF-kB. This recurrent rearrangement occurs between two identical, 878-bp MER67B repeats: the first copy is located in intron 3 and the second is approximately 4kb telomeric to the gene. To determine the spectrum of mutations in IP families, we sequenced the complete NEMO locus (AJ271718). The 23 kb gene is composed of 10 exons with three alternative non-coding first exons (1a, 1b, 1c). The NEMO gene partially overlaps the G6PD gene and is transcribed in the opposite direction. Screening of RPCI11 BAC library with the NEMO cDNA we revealed that an incomplete copy of NEMO was present in the genome. deltaNEMO (AL596249) maps 75kb distal to NEMO and lacks exons 1 and 2. Mapping and sequence information bringing the total length of the duplication to 35.5kb and indicated that the duplicated regions are in opposite orientation and only 22 single nucleotide differences are present, making the duplications >99% identical. The high frequency of the rearrangement affecting NEMO locus allows for the molecular diagnosis of IP in the vast majority of cases by a simple PCR assay in the pre and post-natal studies. The complete loss of NF-kB activation is lethal for IP males during embryogenesis while IP females can survive, owing to mosaicism as a result of X-inactivation. However, males showing an IP female-like phenotype are rarely identified and they can be explained by a chromosomal abnormality (47, XXY), a genomic X-chromosomal mosaicism resulting from an early post-zygotic mutation or a gametic half-chromatid mutation. Hypomorphic mutations affecting NEMO gene impair but do not abolish NF-kB signaling and lead also to surviving males showing features of osteopetrosis, lymphoedema, EDA, and immunodeficiency (OL-ED-ID). In our study we performed the molecular genetic studies in 99 IP collected patients: 87 are females and 12 are male. There were 76 Italian, 20 Spanish, 1 Polish, 1 Turkish and 1 Indian patients. Analysing genomic DNA from the proband we revealed that the D4-10 deletion accounts for 56 cases including one 47,XXY and three males patients with X-chromosomal mosaicism. Although one of the three male shows a late post-zygotic mutation he has severe neurological involvement asociated with ocular abnormalities. Interestingly, a preliminary biochemical study revealed an impaired cellular response of proinflammatory cytokine in response to LPS cytokines related to immune modulation and apoptosis. Mutational analysis by DHPLC revealed 5 new small mutations and do not exhibit mutations in NEMO gene in 22 females and 2 male patients, although a typical IP phenotype has been ascertained on clinical presentation. The remaining 14, 6 of them are male with no family history of IP and with normal karyotype, show OL-ED-ID clinical features. Since multiple pathways impinge on the NF-kB transcription system, it is conceivable that combinations of mutations in the upstream and downstream genes could cause a phenotype similar to that produced by specific defects in NEMO. For this purpose, we are identifying and characterizing regulatory regions of the NEMO promoters and search for mutations in IP and OL-ED-ID patients, which still lack a molecular diagnosis. In the meantime, we are searching for other genes through the comparison of gene expression profiles in IP, ED-ID and EDA mice in order to determine the relative regulatory targets and pathological mechanisms. Those genes will be considered and processed as candidate for both IP and other EDs with immunodeficiency. These observations indicate that male individuals can suffer from IP and they have implications for clinical care, genetic counseling and prenatal diagnosis.

Other abstracts in same session

THE JOURNAL OF BIOLOGICAL CHEMISTRY

Vol. 277, No. 20, Issue of May 17, pp. 17464–17470, 2002
Printed in U.S.A.

NEMO Trimerizes through Its Coiled-coil C-terminal Domain*

Received for publication, February 27, 2002
Published, JBC Papers in Press, March 4, 2002, DOI 10.1074/jbc.M201964200

Fabrice Agou‡§, Fei Ye‡, Stéphane Goffinont‡, Gilles Courtois¶, Shoji Yamaoka‖, Alain Israël‡, and Michel Véron‡

From the ‡Unité de Régulation Enzymatique des Activités Cellulaires and ¶Unité de Biologie Moléculaire Expression Génique, CNRS FRE 2384, Institut Pasteur, 25 Rue du Dr. Roux 75724 Paris Cedex 15, France and the ‖Department of Microbiology, Tokyo Medical and Dental University School of Medicine, Yushima 1-5-45 Bunkyo-ku, Tokyo, Japan

NEMO/IκB kinase (IKK) γ is the regulatory component of the IKK complex comprising the two protein kinases, IKKα and IKKβ. To investigate the self-assembly properties of NEMO and to understand further the mechanism of activation of the IKK complex, we purified wild-type and mutant NEMO expressed in *Escherichia coli*. In the absence of its IKK partners, recombinant NEMO (rNEMO) is a metastable functional monomer correctly folded, according to its fluorescence and far-UV CD spectra, which is binding specifically to the IKK complex. A minor fraction of rNEMO was found tightly associated with DnaK (*E. coli* Hsp70). We also examined the interaction of NEMO with prokaryotic and eukaryotic Hsp70, and we showed that the Hsp70-NEMO complex forms a supramolecular structure probably corresponding to an assembly intermediate. *In vivo* cross-linking experiments indicate that native NEMO in association with IKK is in equilibrium between a dimeric and a trimeric form. Similarly to native NEMO, a NEMO mutant deleted from its IKK binding N-terminal domain (residues 249–338) forms a stable trimeric coiled-coil, suggesting that the association of NEMO with IKK or with Hsp70 prevents incorrect interdomain pairing reactions that could lead to aggregation or to an non-native oligomeric state of rNEMO. We propose a model in which the activation of the IKK complex occurs through the trimerization of NEMO upon binding to a not yet identified upstream activator.

Among the signaling pathways known to date, the transcription factor NF-κB is one of the most intensely studied regulators of gene expression, playing a crucial role in inflammatory responses, cell proliferation, and apoptosis (1–4). NF-κB transcription factors activate groups of genes in response to various stimuli, including the proinflammatory cytokine tumor necrosis factor (TNF),[1] interleukin 1β, bacterial lipopolysaccharide, and viral products. The most common form of NF-κB transcription factor consists of RelA (p65) and p50 subunits (5, 6). In most non-induced cell types it is sequestered in the cytoplasm in an inactive state through its association with members of a family of inhibitory proteins known as IκB. After cell stimulation, IκB proteins are rapidly phosphorylated by the IκB kinase complex (IKK) and are then degraded by the 26 S proteasome upon polyubiquitination (7). This degradation allows NF-κB to move to the nucleus to switch on its target genes.

Three components were identified as constituents of the IKK complex (~700 kDa): IKKα, IKKβ, and NF-κB essential modulator (NEMO, also called IKKγ). IKKα and IKKβ sharing 52% identity possess a similar organization in functional domains including a kinase, a leucine zipper, and a helix-loop-helix domain (8–11). Although in cells IKKα and IKKβ are active both as homo- or as heterodimers promoted by their leucine zipper motifs, the heterodimer is the predominant form (12). The recent generation of IKKα- and IKKβ-deficient mice showed different phenotypes assigning different functional roles to each catalytic subunit. Thus, whereas IKKβ is required for the activation of NF-κB, IKKα but not IKKβ seems rather involved in keratinocyte differentiation (13).

NEMO, the third component of the IKK complex, was originally identified by functional complementation of cells that did not respond to a variety of stimuli (14). It associates preferentially with IKKβ, and its presence is crucial for the stimuli-dependent activation of the IKK complex. NEMO, which has no known catalytic activity, contains at least four structural motifs as deduced from the primary structure analysis. The N-terminal domain contains a large coiled-coil domain (CC1, residues 93–231) carrying most of the essential peptidic determinants required for binding to IKKβ (15). The C-terminal domain is composed of three sub-domains including a coiled-coil (CC2, residues 246–286), leucine zipper (LZ, residues 303–337), and zinc finger motifs (ZF, residues 380–412). Consistent with an essential role for NEMO in the activation of the NF-κB pathway, two human pathologies, Incontinentia Pigmenti and Anhidrotic Ectodermal Dysplasia with Immunodeficiency (EDA-ID), were recently shown to be associated with a partial or total loss-of-function of NEMO (16, 17). Interestingly, mutations responsible for EDA-ID were mainly found in the C-terminal part of the molecule. To date the molecular mechanism by which the IKK complex is activated remains unclear. It has been proposed that NEMO activates the IKK complex by recruiting the IKK kinase to a receptor. However, IKKβ alone is sufficient for the recruitment of IKK to TNF receptor 1 after TNFα stimulation in NEMO-deficient cells, indicating that NEMO is not essential for TNF-induced IKK recruitment (18). Co-immunoprecipitation experiments and *in vitro* cross-linking (19) showed the ability of NEMO to self-associate. NEMO oligomerization has also been shown to be crucial for IKK activa-

* This work was supported in part by grants from the Ligue Nationale contre le Cancer équipe labellisée (to A. I.) and the Association pour la Recherche sur le Cancer. The costs of publication of this article were defrayed in part by the payment of page charges. This article must therefore be hereby marked "*advertisement*" in accordance with 18 U.S.C. Section 1734 solely to indicate this fact.

§ To whom correspondence should be addressed: Unité de Régulation Enzymatique des Activités Cellulaires, Institut Pasteur, 25 Rue du Docteur Roux, 75724 Paris Cedex 15, France. Tel.: 33-1-45 68 88 80; Fax: 33-1-45 68 89 99; E-mail: fagou@pasteur.fr.

[1] The abbreviations used are: TNF, tumor necrosis factor; Ni-NTA, nickel-nitrilotriacetic acid; OG, octyl glucoside; DDM, *dodecyl* maltoside; TGME, tetraethylene glycol monooctyl ether; BMH, bis(maleimido)hexane; BMOE, bis(maleimido)ethane; WT, wild-type; rNEMO, recombinant NEMO; IKK, IκB kinase; LZ, leucine zipper; ZF, zinc finger; EDA-ID, Anhidrotic Ectodermal Dysplasia with Immunodeficiency; cmc, critical micelle concentration.

tion (19, 20) and probably for recruitment by upstream activators. Mutagenesis experiments mapped the region of NEMO responsible for its self-association (21), but no correlation with its oligomeric state could be established.

To understand further the molecular role of NEMO in the activation of the IKK complex, we have studied the biochemical properties of purified murine NEMO recombinant protein (rNEMO) as well as of a truncated C-terminal domain produced in *Escherichia coli*. The homologous Hsp70 of *E. coli*, DnaK, was found tightly associated to rNEMO, and we characterized this association by gel filtration and analytical ultracentrifugation methods. As the Hsp70 protein family is relatively well conserved, the *in vitro* and *in vivo* association of NEMO with human Hsp70 was examined. We also investigated the oligomeric state of NEMO *in vivo* by protein cross-linking experiments. Consistent with our results a model was proposed in which the bipartite function of the C-terminal of NEMO modulates the activation of the IKK complex.

EXPERIMENTAL PROCEDURES

Materials—Octyl glucoside (OG) and dodecyl maltoside (DDM) were from Roche Molecular Biochemicals. Tetraethylene glycol monooctyl ether (TGME) and Brij 35 were from Sigma, and the zwitterion detergent, zwittergent 3-16, was from Calbiochem. Bis(maleimido)hexane (BMH) and bis(maleimido)ethane (BMOE) were from Pierce.

Expression and Purification of rNEMO and of Its C-terminal Domain—Murine NEMO was expressed in *E. coli* with the pRSETa expression system (Invitrogen). The NEMO cDNA (14) was cloned *in-frame* with the vector into *Bam*HI and *Pvu*II sites to give plasmid pRSETa/NEMO. The encoded polypeptide (rNEMO) contains an N-terminal extension of 34 residues (MRGS(H)$_6$GMASMTGGQQMGRDLYDDDDKDRW) inserted at position 2 in NEMO. This sequence contains a His tag and a site of proteolysis by enterokinase.

A truncated mutant of NEMO corresponding to a part of its C-terminal domain (amino acids 249–339) was made by PCR mutagenesis using the plasmid pRSETa/NEMO as template. Briefly, NEMO cDNA was amplified between the 5′ primer oligonucleotide 5′- GCACCCTAGCTAGGACAGCGACATTAAGAGC and the 3′ primer oligonucleotide 5′- GCACGGATCCCTAGTCAGGAGGTTCTTCAGGAGG. This introduced *Nhe*I and *Bam*HI sites (*underlined*) and a stop codon (*bold*) at position 338 in the polypeptide sequence. After amplification, the fragment was digested with *Nhe*I and *Bam*HI and cloned into a pET-28b expression vector (Novagen). The nucleotide sequences of NEMO and of the D249-F338Stop fragment were verified by DNA sequencing.

Purification of rNEMO was performed starting from a 2-liter culture of BL21(DE3) cells transformed with pRSETa/NEMO grown at 22 °C in 2× YT/ampicillin (50 μg/ml) medium to A_{600} = 1, and 1 mM isopropyl-1-thio-β-D-galactopyranoside was then added to the medium for 5 h. All subsequent steps were conducted at 4 °C. After harvesting by centrifugation, the cells were washed twice in a buffer, 100 mM Tris-HCl, pH 8, containing 10 mM $MgCl_2$ and 1 mM dithioerythritol, resuspended in extraction buffer (50 mM Tris-HCl, pH 7.5, 20 mM KCl, 5% glycerol, 1 mM dithioerythritol) containing a protease inhibitor mixture (Sigma), and broken in a French press at 1,500 pounds/square inch. The lysate was then diluted 2.5-fold with the equilibrium buffer of the Ni-NTA column (50 mM Tris-HCl, pH 8.0, 500 mM NaCl, 0.1 mM DDM) and centrifuged at 12,000 × *g* for 30 min. The supernatant was loaded on a 25-ml Ni-NTA-agarose column (Qiagen, 1.6 × 12.5 cm) charged with Ni^{2+}. After washing with the equilibrium buffer containing 10 mM imidazole, the bound material was eluted at 110 mM imidazole by a 400-ml linear gradient (10–400 mM imidazole) in 50 mM Tris-HCl, pH 7.5, 500 mM NaCl, 0.1 mM DDM. Fractions containing rNEMO were pooled (70 ml) according to optical density profile and SDS-PAGE, and dialyzed twice against 50 mM Tris-HCl, pH 8.0, 50 mM KCl, 1 mM EDTA, 1 mM dithioerythritol, and 1 mM DDM (buffer A). An rNEMO sample was then applied to a Resource Q column (6 ml, Amersham Biosciences) equilibrated in the buffer A and eluted with a 150-ml linear gradient 50–500 mM KCl. Fractions containing rNEMO (according to the OD profile and to SDS-PAGE) were pooled (15 ml) and dialyzed against 1 liter of 10 mM potassium phosphate, pH 7.0, 1 mM dithioerythritol, and 1 mM DDM. The solution was then applied onto a ceramic hydroxyapatite column (1.6 cm × 15 cm, Bio-Rad) and eluted with a 600-ml linear gradient (10–400 mM) of potassium phosphate. The peak of rNEMO was pooled (65 ml), concentrated by ultrafiltration (Millipore), and dialyzed twice against 50 mM Tris-HCl, pH 7.5, 1 mM dithioerythritol, 150 mM KCl, 1 mM DDM, and 50% glycerol before freezing at −80 °C at a concentration of 4.9 mg/ml.

The first purification steps of the C-terminal fragment (D249-F338Stop fragment) were the same as described above for rNEMO except that the recombinant protein was produced at 37 °C from 1 liter of culture, and 0.1 mM DDM was used instead of 1 mM in all buffers. The elution from the Ni-NTA column was performed using a higher concentration of imidazole (250 mM) as compared with rNEMO. Fractions (5 ml) containing the C-terminal domain were pooled and dialyzed against buffer 50 mM Tris-HCl, pH 7.5, containing 50 mM KCl, 1 mM dithioerythritol, and 0.1 mM DDM (buffer B). The protein sample (~15 mg) was then loaded on a Resource Q column (6 ml, Amersham Biosciences) equilibrated in the buffer B. A majority of the protein sample (80%) passed through the column and corresponded to homogeneous D249-F338Stop fragment (see *Fig. 5*). 20% was bound to the matrix and eluted with a 120-ml gradient (50 mM to 1 M) of KCl. This fraction contained truncated rNEMO associated to DnaK with a stoichiometry of 1:1 as judged by SDS-PAGE. Both fractions were dialyzed twice against 50 mM Tris-HCl, pH 7.5, 100 mM KCl, 1 mM dithioerythritol, 50% glycerol, and 1 mM DDM and stored at −20 °C. Protein concentrations were determined either by the method of Bradford or by absorbance at 280 nm using an extinction coefficient of 0.353 unit·mg^{-1}·cm^2 for rNEMO and of 0.181 unit·mg^{-1}·cm^2 for the truncated rNEMO. Microsequencing of an internal peptide of the DnaK protein was performed as described previously (22), and the amino acid sequence comparisons were carried out using the protein data base *Calibri*.

In Vitro Binding Assay with Prokaryotic and Eukaryotic Hsp70s and Co-immunoprecipitation—Ni-NTA magnetic agarose beads suspensions (25 μl, Qiagen) equilibrated with the buffer C (20 mM Tris-HCl, pH 8.0, 20 mM imidazole, 300 mM NaCl, 1 mM DDM, 5% glycerol, and 0.1 mM dithioerythritol) were incubated for 30 min at 4 °C with the purified His-tagged NEMO. After separation of beads with a magnet, the excess protein was removed, and beads captured with His-NEMO were washed twice with a 100-μl volume of buffer D (20 mM $NaPO_4$, pH 7.0, 20 mM imidazole, 150 mM NaCl, 1 mM DDM, 5% glycerol, and 0.1 mM dithioerythritol). DnaK (StressGen) or human Hsp70 (Sigma) was then added and incubated for 1 h at 4 °C in buffer C containing 0.1 mM phenylmethylsulfonyl fluoride. Magnetic beads were separated and washed 3 times with buffer D (100 μl). Hsp70 proteins trapped by His-tagged NEMO were recovered by elution with buffer D containing 300 mM imidazole followed by SDS-PAGE with silver staining. Cell culture, transfection of 293T cells, and co-immunoprecipitation were carried out as described previously (14). Western blotting was performed using anti-Hsp70 antibodies provided by Sigma.

Functional Interaction Assay of rNEMO with the IKK Complex—Cell culture and preparation of S100 extracts from 70Z/3 murine pre-B cell and the NF-κB unresponsive mutant 1.3E2 were carried out as described previously (14). His-tagged NEMO or His-tagged C-terminal domains (0.15 mg/ml, 200 μl), which were used as bait, were incubated with Ni-NTA magnetic agarose beads (100 μl, Qiagen) equilibrated in buffer C. After separation with a magnet, the supernatant containing His-tagged proteins in excess was removed, and the beads saturated with His proteins were washed twice with buffer D (200 μl) and incubated in a 200-μl volume of buffer D at 4 °C for 1 h with S100 extracts from 70Z/3 and 1.3E2 cells containing 0.8 and 1 mg/ml of proteins, respectively. After extensive washing in buffer D, His-tagged proteins were recovered by elution with buffer D containing 300 mM imidazole (100 μl). The IKK complex trapped (pellet) or not trapped (supernatant) was detected by Western blotting using anti-IKKα antibodies (Imgenex). The amount of His-tagged protein immobilized by Ni-NTA beads was evaluated by SDS-PAGE analysis with Coomassie staining.

Circular Dichroism and Fluorescence Spectroscopy—The CD spectrum of rNEMO (1.5 μM) or of the truncated C-terminal domain (38 μM) was recorded from 182 to 260 nm at 20 °C and pH 7.0 in a buffer 20 mM potassium phosphate containing 1 mM DDM and 1 mM dithioerythritol (buffer E) using a Jobin-Yvon CD6 spectrodichrograph (Longjumeau, France). Cells (20 μl) with a path length of 0.1 mm were used, and the product of the time constant and the rate of scanning were below 0.33 nm (23). Each spectrum was the result of the average of three scans taken from the same sample minus the average of three scans from the reference buffer. Deconvolution of CD spectra was performed according to the method of Chang *et al.* (24) using the MDFITT program as described previously (25). The fluorescence spectrum was recorded in buffer E at 20 °C on a PTI spectrofluorometer Quantamaster™. The excitation wavelength was 295 nm to minimize the contribution of tyrosyl residues to the total fluorescence. The excitation and emission bandwidths were both set to 2 nm. The fluorescence yield was determined as described previously (25).

Analytical Gel Filtration—The apparent Stokes radius of rNEMO was determined both at 20 and 4 °C by filtration of 400-μl samples on a Superdex 200 HR 10/30 column (Amersham Biosciences) equilibrated in 50 mM Tris-HCl, pH 7.5, containing 200 mM KCl, 0.2 mM DDM, and 1 mM dithioerythritol (buffer F), developed at a constant flow rate of 0.4 ml/min. The respective elution of standard globular protein or rNEMO was described in terms of $V_e - V_0$ (ml) corresponding to the product of K_{av} and $V_T - V_0$ where V_e is the elution volume of the particular protein; V_0 and V_T are void and total volumes of the column determined with blue dextran 2000 and dithioerythritol, respectively. Thyroglobulin (669 kDa, R_S = 89.3 Å), ferritin (440 kDa, R_S = 69.1 Å), catalase (232 kDa, R_S = 52.4 Å), aldolase (158 kDa, R_S = 46.4 Å), bovine serum albumin (67 kDa, R_S = 35.2 Å), ovalbumin (43 kDa, R_S = 27.5 Å), chymotrypsinogen A (25 kDa, R_S = 21.1 Å), and ribonuclease A (13.7 kDa, R_S = 16.4 Å) were used for calibration.

Sedimentation Velocity—Prior to sedimentation, rNEMO was injected on a Superdex 200 HR 10/30 column equilibrated in buffer F at 4 °C. The fraction (0.8 mg/ml in 500 μl) corresponding to the median of the elution peak was analyzed by centrifugation, using the equilibrium buffer of the column as reference. Sedimentation velocity experiments were performed at 10 °C to minimize protein aggregation on a Beckman Optima XL-A analytical ultracentrifuge equipped with an An-Ti60 titanium four-hole rotor with two-channel 12-mm path length centerpieces. Samples of 400 μl were centrifuged at 50,000 rpm, and radial scans of absorbance at 280 nm were taken at 1-min intervals. Data were analyzed using the computer programs Svedberg (37), kindly provided by John Philo (Amgen, Inc.). The first scans with incomplete clearing of the meniscus were not taken into account for the fitting function. The XLA-VELOC program supplied by Beckman was used for the calculation of the apparent sedimentation coefficient $g(s^*)$, from the time derivative of the sedimentation velocity concentration profile as described previously (28). The sedimentation coefficient of species M_1 determined using two species model with Svedberg corresponded to the peak position in the $g(s^*)$ profiles. Sedimentation and diffusion coefficients were corrected to standard conditions, $s_{20,w}$ and $D_{20,w}$. A partial specific volume of 0.730 cm^3/g at 10 °C for rNEMO was calculated from its amino acid composition according to Ref. 29. Solvent density and viscosity at 10 °C were 1.003 g/cm^3 and 1.3×10^{-2} cp, respectively, determined from published tables (29). Hydrodynamic parameters such as frictional ratio f/f_0 and Stokes radius were deduced from the Teller method (30) using the SEDNTERP program provided by John Philo.

Equilibrium Sedimentation—Sedimentation equilibrium experiments with rNEMO were carried out at 10 °C at 8,000 or 12,000 rpm in a Beckman Optima XL-A analytical ultracentrifuge. Initial loading concentrations (120 μl) were either 0.34 mg/ml in a buffer 20 mM potassium phosphate, pH 7.0, containing 100 mM KCl, 10 mM OG, and 1 mM dithioerythritol or 0.23 mg/ml in a buffer 20 mM potassium phosphate, pH 7.0, containing 150 mM KCl, 10 mM TGME, and 1 mM dithioerythritol. In the study of the C-terminal fragment, experiments were performed using two loading concentrations (1 and 1.9 mg/ml in 120 μl) and two rotor speeds (12,000 and 18,000 rpm) in a single run as described in Table II. Protein samples were allowed to equilibrate for 20 h, and duplicate scans (2 h apart) were overlaid to determine that there were no further changes in the sample cell. After collecting data at equilibrium, the samples were centrifuged at 50,000 rpm for 12 h to sediment the protein, and radial scans were again collected to obtain a base-line correction for each cell. To determine the buoyant molecular mass, we followed the formalism of Reynolds and Tanford (31) in which the contribution of the bound detergent δ_{bd} in g/g can be written by the relation

$$M^*(1 - \Phi'\rho) = M_p[(1 - \bar{\nu}_p\rho) + \delta_{bd}(1 - \bar{\nu}_{bd}\rho)] \qquad \text{(Eq. 1)}$$

where M^* is the molecular mass of the anhydrous protein-detergent complex, Φ' its partial specific volume, M_p is the molecular mass of the anhydrous protein, $\bar{\nu}_p$ its partial specific volume, ρ is the buffer density, and $\bar{\nu}_{bd}$ the partial specific volume of detergent. Because the density of the detergent TGME (C_8E_3) was close to that of buffer, the second term in the second member of Equation 1 was negligible. In contrast, the $\bar{\nu}_{bd}$ of detergent micelle OG was low (0.92 ± 0.004 ml/g at 20 °C (32)) and a densifier such as the sucrose is often added to the buffer to match with the detergent density ($\rho_{bd} = 1/\bar{\nu}_{bd}$). However, the addition of sucrose can change dramatically the oligomer equilibrium or the protein heteroassociation. We rather used an OG concentration of 10 mM below its critical micelle concentration (20 mM) to prevent detergent micelle formation such that the second term becomes negligible due to a low δ_{bd}. At 10 °C the densities were 1.009 and 1.007 g/ml in the buffers containing 10 mM TGME and 10 mM OG, respectively. The partial specific volumes of DnaK and of DnaK-rNEMO complex calculated from their amino acid composition were 0.731 and 0.726 ml/g, respectively, at 10 °C. All data were fitted with one, two, or three species models as described previously (33, 34).

In Vivo Chemical Cross-linking—HeLa cells were purchased from American Type Culture Collection and were grown in Dulbecco's modified Eagle's medium supplemented with 10% fetal calf serum. Chemical cross-linkings *in vivo* were performed with a homobifunctional cross-linker as described previously (35, 36). We used BMH or BMOE which is very similar to BMH except that the two carbodiimide groups are linked by a shorter spacer arm (8 Å). BMH and BMOE were purchased from Pierce and were stored in Me_2SO at −20 °C at 20 mM. The *in vivo* cross-linking with BMH gave the same results as BMOE except that the efficiency of cross-linking was lower. Briefly, cells (8×10^7) were concentrated into 1 ml, resuspended twice with fresh medium by successive centrifugations (100 × *g* for 10 min), and incubated on ice for 30 min. 25 μl of stock BMOE (20 mM) was then added to half of cells (4×10^7 cells in 500 μl) at 37 °C to give a final concentration of BMOE of 1 mM. The other half were mock-treated by 25 μl of Me_2SO added as control. 100 μl of cells were withdrawn either immediately after adding BMOE or after 10 min or 2 h, incubated for 10 min at 37 °C, and mixed with 20 μl of 180 mM dithioerythritol (final concentration 20 mM) to quench the cross-linking reaction. Cells were then pelleted at 4 °C and washed twice with cold phosphate-buffered saline. The Laemmli loading buffer supplemented with 6 M urea (100 μl) was added to cell pellets (40 μl), and the mixtures were boiled for 10 min. The precipitates were removed by centrifugation at 20,000 × *g* at 4 °C for 20 min. Supernatants (40 mg/ml) were diluted 50-fold with Laemmli buffer so that 16 μg of protein were loaded in each well. Western blots were performed as described previously (37) using a final antibody concentration of 0.5 μg/ml with polyclonal anti-NEMO (14) or with monoclonal anti-IKKβ (PharMingen).

RESULTS

Expression and Purification of Recombinant NEMO—Recombinant His-tagged NEMO (rNEMO) was expressed in *E. coli* at 22 °C to prevent the formation of inclusion bodies and purified following the protocol under "Experimental Procedures." The analysis by SDS-PAGE of each chromatographic step is presented in Fig. 1*A*. The specific binding on chromatographic matrix bearing a nitrilotriacetic group charged with nickel (Ni-NTA) was strictly dependent on the presence of a neutral detergent such as dodecyl maltoside (DDM), which prevented the formation of aggregates. Despite the addition of protease inhibitors, a partial proteolysis of rNEMO protein was detected by Western blot. This partial degradation occurred even if the bacteria were directly boiled in SDS/urea lysis buffer (data not shown) and was likely due to *in vivo* endogenous proteases, possibly fostered by the lack of interaction with IKKα or -β kinases. The proteolyzed fragments were easily removed using ion exchangers (compare *lanes Ni* and *HA* in Fig. 1*A*). The analysis of the Ni-NTA pool by SDS-PAGE also revealed the presence of 40- (p40) and 70-kDa (p70) proteins (*lanes Ni* and *Q*). These proteins were not found in the eluate when extracts without tagged NEMO were loaded onto Ni-NTA columns (data not shown). Their co-elution with rNEMO at the high imidazole concentration used suggests that both proteins were bound to the column via their association with rNEMO. Whereas p40 could be separated by chromatography on ceramic hydroxyapatite column (*lane HA*), p70 remained associated with rNEMO throughout all purification steps (compare *lanes Ni* and *HA* in Fig. 1*A*) as well as in additional gel filtration and hydrophobic chromatographies (not shown). These results support the view that p70 forms a protein complex with rNEMO. Two additional minor bands with molecular masses of 110 and 160 kDa, respectively, were observed in SDS-PAGE (*lane HA*, asterisks) and recognized by anti-NEMO antibodies in Western blotting (data not shown). Incomplete dissociation of oligomeric proteins upon SDS-PAGE can be observed when a neutral detergent is present in the loading buffer, and these two polypeptides could correspond to dimeric and trimeric forms of

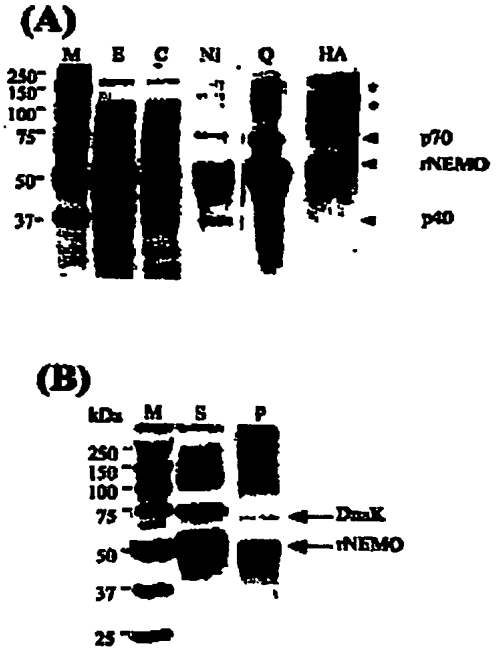

FIG. 1. Purification of recombinant NEMO and effect of DnaK on rNEMO. *A*, analysis by SDS-PAGE of the purification steps of NEMO. The crude extracts from transformed *E. coli* cells expressing (*lane E*) or not expressing NEMO (null plasmid) (*lane C*) were analyzed by SDS-PAGE. An *arrowhead* indicates the polypeptide corresponding to recombinant NEMO. The analysis of the pooled fractions from each purification step is shown as follows: *lanes Ni*, *Q*, and *HA* are the pools of Ni-NTA, POROS HQ, and ceramic hydroxyapatite columns, respectively (see "Experimental Procedures"). *Lane M* corresponds to protein markers. *Arrows* indicate rNEMO and co-eluting p40 and p70 proteins. *Asterisks* indicate 110- and 150-kDa protein bands that are specifically recognized by rNEMO antibodies. *B*, chaperone role of DnaK on the recombinant NEMO. Purified rNEMO containing 1 mM DDM was diluted in a buffer containing 0.2 mM DDM. After centrifugation at 18,000 rpm, the supernatant (*lane S*) and the pellet (*lane P*) were analyzed by SDS-PAGE, and the ratio DnaK/rNEMO was determined by densitometry after Coomassie staining.

rNEMO as judged by their apparent molecular mass. Because rNEMO with a calculated molecular mass of 51,796 Da carried an N-terminal extension of 33 residues, it exhibited a slightly slower electrophoretic mobility as compared with the native NEMO (compare *lanes M* and *HA* in Fig. 1*A*). The purification procedure yielded 15 mg of purified rNEMO starting from a 2-liter culture (10 g of cell pellet) with a global recovery of 28%. As judged by densitometry, rNEMO was at least 95% homogeneous, with p70 representing less than 5% of the material. The ability of several other detergents like OG, Brij 35 ($C_{12}E_{23}$), zwittergent 3-16, or tetraethylene glycol monooctyl ether (C_8E_4, TOME) to preserve rNEMO from aggregation was evaluated using each detergent at a concentration above its critical micelle concentration (cmc). DDM was found as the most efficient and was used in all further experiments unless otherwise indicated.

In order to identify the p70 protein co-purifying with rNEMO, the N-terminal sequence of an internal peptide was obtained after a trypsin digestion performed directly on the polyacrylamide matrix. The sequence KRRINE found identified unambiguously the molecular chaperone Hsp70 of *E. coli*, also called DnaK, in the *E. coli* protein data bank. Lowering the DDM concentration from 1 to 0.2 mM induced immediate protein precipitation. Fig. 1*B* shows a change in the DnaK/rNEMO ratio at this lower detergent concentration. Very little DnaK was found in the pellet fraction (*lane P*, DnaK/rNEMO ratio of 1:20), whereas the two proteins were in a ratio of 1:3 in the supernatant (*lane S*). Because DnaK co-elutes with rNEMO in all chromatographic columns used, reflecting the formation of a protein complex, these data indicate that DnaK can act as a molecular chaperone protecting rNEMO from aggregation. DnaK-rNEMO complex was further characterized by developing an *in vitro* assay using the purified rNEMO as bait and the commercially available pure DnaK. His-tagged rNEMO was captured on magnetic beads (Ni-NTA). After incubation with a variable amount of DnaK, the protein complex was detected by silver staining of the SDS-PAGE analysis after elution of His-tagged rNEMO (Fig. 2). Ni-NTA beads not saturated with His-NEMO were used as control. As shown in Fig. 2*a* the addition of DnaK induces an increase of a specific DnaK-rNEMO complex with 1:1 stoichiometry. Note that although the interaction was weaker in the presence of ATP/Mg^{2+}, it was not abolished (compare *4th* and *5th lanes*).

As Hsp70 protein family has been conserved in evolution, we next examined whether the human counterpart of DnaK could also interact specifically with rNEMO, using a similar *in vitro* assay. As shown in Fig. 2*b*, the His-tagged NEMO interacts specifically with Hsp70 forming a protein complex with 1:1 stoichiometry. The *in vivo* association of Hsp70 was also investigated using co-immunoprecipitation experiments. In these experiments NEMO was transiently expressed in human 293 cells, and crude extracts were used for immunoprecipitation with anti-NEMO antibodies. The immunoprecipitates were then analyzed by Western blotting using anti-Hsp70 antibody. The preimmune serum was used as negative control. As shown in Fig. 2*c* both constitutive (73 kDa) and inducible (72 kDa) forms of Hsp70 were detected in the immunoprecipitate, indicating that human Hsp70-like DnaK interacts specifically with NEMO *in vivo*.

Intrinsic Fluorescence and Secondary Structure of rNEMO—Because NEMO has no enzymatic activity, we checked whether the recombinant protein was correctly folded by recording its CD spectra (Fig. 3*A*) and by measuring its fluorescence yield (Fig. 3*B*). Far-UV CD and fluorescence spectra of rNEMO were recorded in the presence of 1 mM DDM. Under these conditions, the signal contribution of DnaK was negligible. The CD profile exhibited two negative dichroic bands with minima at 208 and 222 nm and a positive dichroic band with a maximum at 193 nm characteristic of a protein with a high α-helix content. Deconvolution of CD spectra using the method of Chang *et al.* (24) estimated the fractions of the α-helix, β-form, and unordered form to 44, 0, and 56%, respectively. This result is in agreement with the secondary structure prediction derived from the amino acid sequence using the DSC software (38).

Recombinant NEMO contains two Trp residues (Trp-34 and Trp-39), located in the N-terminal part of the protein. To minimize the contribution of the 6 Tyr, the fluorescence spectrum was recorded with an excitation at 295 nm (Fig. 2*b*). The emission spectrum displayed a maximum at 345 nm indicating that at least one of the two Trp was accessible to the solvent. In addition, the fluorescence quantum yield of 0.3 was high as compared with that of *N*-acetyl-L-tryptophanamide ($\phi_F = 0.14$) indicating that rNEMO is correctly folded.

rNEMO Binds Specifically to the IKK Complex—The structural integrity of rNEMO was also checked by determining whether the pure His-tagged recombinant protein could bind specifically to the IKK complex through the interaction with

17468

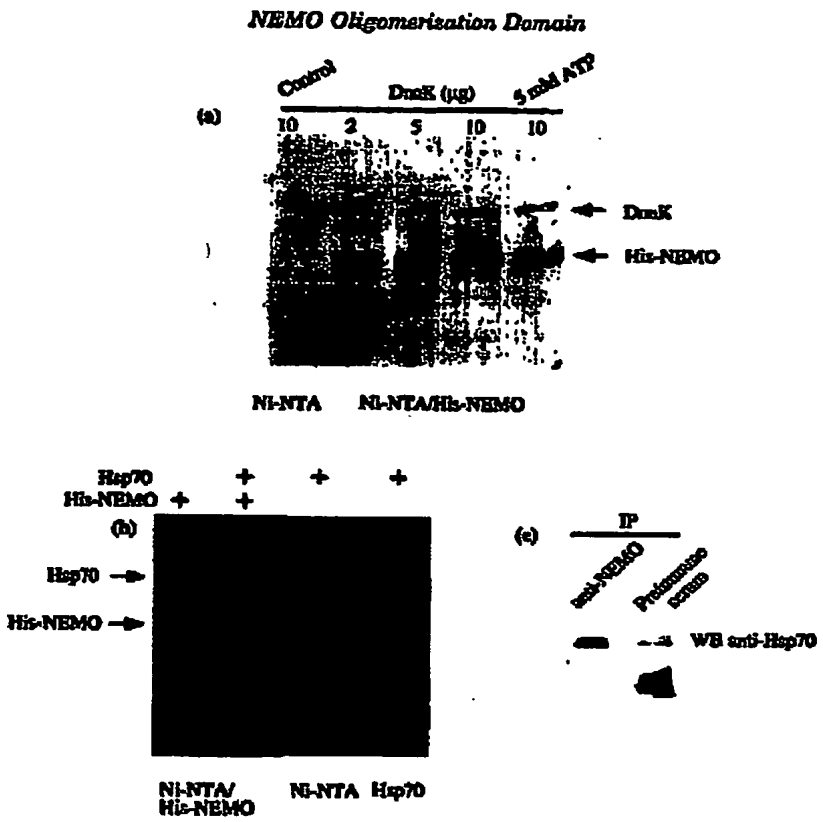

FIG. 2. Association of NEMO with Hsp70. *a*, *in vitro* association with *E. coli* DnaK. Ni-NTA beads (25 μl) saturated with (Ni-NTA/His-NEMO) or without (Ni-NTA) His-tagged rNEMO were incubated with variable amounts of DnaK in the absence or in the presence of 5 mM ATP as indicated. After thorough washing, His-tagged rNEMO was eluted, and the protein complex was analyzed by SDS-PAGE and visualized by silver staining as described under "Experimental Procedures." *b*, *in vitro* association with human Hsp70. Similar experiment as *a* except that Ni-NTA beads with or without bound His-NEMO were incubated with a saturating concentration of Hsp70 (10 μg, 0.2 mg/ml). In the *right lane* (Hsp70) 1 μg was loaded alone to show purity. *c*, *in vivo* association with human Hsp70. Extracts from 293 cells transiently expressing NEMO were immunoprecipitated with anti-NEMO antibodies or a preimmune serum (control). Immunoprecipitates (*IP*) were then analyzed by Western blot (*WB*) with anti-Hsp70 as described under "Experimental Procedures."

the IKKα kinase (Fig. 4). S100 extracts were prepared either from a parental pre-B cell line (70Z/3) which contains the native endogenous NEMO associated to IKK complex or from a NEMO-deficient mutant pre-B cell line (1.3E2) (14). The His-tagged NEMO captured on Ni-NTA beads was then incubated in extracts from both cell types, and the interaction with IKK complex was detected by Western blotting after elution of the His-tagged NEMO. The purified His-tagged C terminus mutant of rNEMO lacking the N-terminal IKK binding domain was used as control (see below). As shown in Fig. 4*a*, a specific interaction of rNEMO with the IKK complex was detected in 1.3E2 cells (*lane 2*), whereas no association with IKK complex was observed with His-tagged rNEMO to 70Z/3 cells nor with His-tagged C terminus mutant in 1.3E2 cells (*1st* and *3rd lanes*). To determine the recovery of IKK complex bound, we analyzed by Western blotting unbound materials in different extracts (Fig. 4*b*). About 50% of IKK complex in the 1.3E2 extract were captured by Ni-NTA beads saturated with His-NEMO, indicating that the interaction is highly specific. Taken together, CD and fluorescence spectra as well as the interaction assay showed that rNEMO is a functional recombinant protein that is correctly folded with a high α-helical content.

Quaternary Structure of rNEMO and of the DnaK-rNEMO Complex—The states of association of the recombinant rNEMO and the DnaK-rNEMO complex were analyzed by a combination of gel filtration and ultracentrifugation experiments. To increase the fraction of DnaK-rNEMO complex in solution, a part of free rNEMO was removed by precipitation using a lower concentration of DDM (0.2 mM) (see Fig. 1*B*, *lane 5*). Fig. 5*A* shows the analysis by gel filtration of the DnaK/rNEMO mixture at 20 °C on a Superdex 200 HR10/30 column in a buffer containing 0.2 mM DDM. All of rNEMO eluted in a single symmetrical peak both at 20 and at 4 °C. SDS-PAGE analysis showed that each fraction contained both rNEMO and DnaK proteins in a ratio 3:1 (data not shown). The elution volume, between that of ferritin and thyroglobulin, corresponds to a very high Stokes radius (R_S = 78 Å) (*inset* of Fig. 5*A*), corresponding to an apparent mass of 600 kDa for a globular protein that could indicate the presence of multimeric species.

The fraction corresponding to the median peak of the column shown in Fig. 5*A* (0.8 mg/ml) was analyzed in sedimentation velocity in the same buffer (Fig. 5*B*). Using the Svedberg software (27), the data were poorly fitted with a single species, and the best fit was obtained with a two species model, M_1 and M_2,

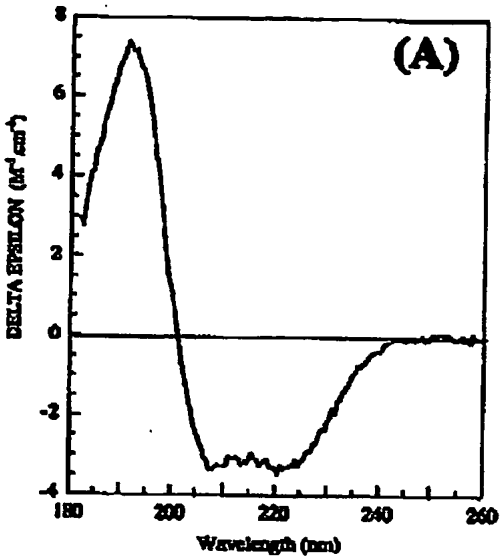

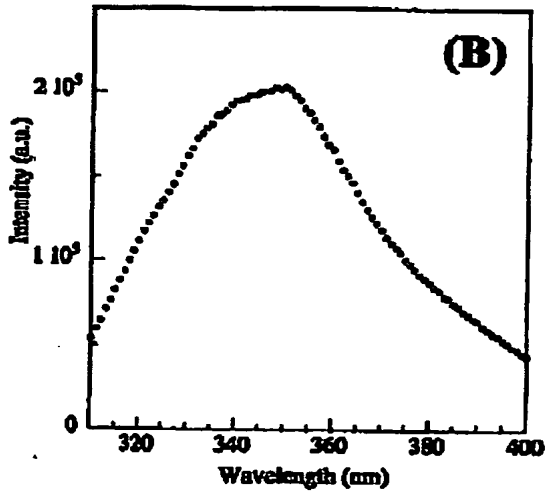

FIG. 3. CD and fluorescence spectra of the rNEMO. The CD spectrum of rNEMO (15 μM) (*A*) or the intrinsic fluorescence emission spectrum of rNEMO (1.5 μM) (*B*) were recorded at 20 °C in 20 mM potassium phosphate buffer, pH 7.0, containing 1 mM DDM and 1 mM dithioerythritol. Excitation wavelength was 295 nm.

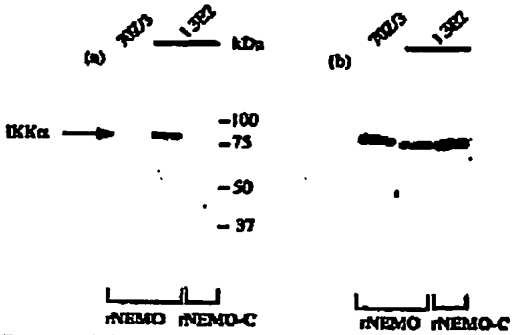

FIG. 4. rNEMO binds specifically to IKK complex. Ni-NTA magnetic beads (100 μl) saturated with pure His-tagged NEMO (rNEMO) or with pure His-tagged C-terminal fragment (rNEMO-C) were incubated for 1 h at 4 °C with S100 extracts from NEMO-deficient cell lines (1.3E2) or parental cell lines (70Z/3). After thorough washing, bound (*a*) and unbound (*b*) IKK complex was detected by Western blotting using anti-IKKα antibodies as described under "Experimental Procedures." The His-tagged C-terminal fragment, which does not contain the IKK binding domain, was used as control.

representing 75 and 25% of the material, respectively. The sedimentation and diffusion coefficients of species M_1 ($s_{20,w}$ = 4.1 S and $D_{20,w} = 7.0 \times 10^{-7}$ cm²/s, Table I) and the corresponding molecular mass calculated from the Svedberg relation (mass = 53,000 Da) indicated that it corresponded to monomeric rNEMO (calculated mass = 51,796 Da). Moreover, its Stokes radius (R_S = 29.7 Å) and frictional ratio (f/f_0 = 1.20) indicated that it behaved as a globular molecule. These results contrast strongly with the data from size-exclusion chromatography experiments where all of rNEMO was eluted as a single peak with a R_S of 78 Å (see "Discussion"). The proportion of species M_2 relative to M_1 (25 and 75%, respectively) strongly suggests that M_2 may correspond to the DnaK-rNEMO complex. Both the values of the average sedimentation coefficient ($s_{20,w}$ = 5.5 S) and the very large diffusion coefficient ($D_{20,w}$ = 10.9×10^{-7} cm²/s) reflect an equilibrium between rNEMO and DnaK-rNEMO complex. The apparent sedimentation coefficient distribution function, $g(s^*)$ *versus* s^*, supports this analysis because the distribution profile exhibited a large asymmetric peak toward the high s^* with a maximum at 4.1 S (*Inset of Fig. 3B*).

To obtain additional information on species M_2 and to confirm the monomeric state of rNEMO, we next analyzed the mixture DnaK/rNEMO by equilibrium sedimentation (*Fig. 6* and Table I). For this experiment, the detergent used could not be DDM because its high density would require the presence of a densifier such as sucrose to make the detergent transparent in equilibrium sedimentation (see "Experimental Procedures"). To minimize the possible contribution of the detergent to the calculated mass of the protein, we chose two different approaches. *First*, we used the detergent TCME (cmc of 7 mM in 0.1 M NaCl) with a density close to that of the buffer in order to achieve gravitational transparency (31). *Second*, we used the detergent OG with a high cmc (cmc of 25 mM in 0.1 M NaCl) so that its working concentration was below its cmc to minimize micelle formation. *Fig. 6* shows a sedimentation equilibrium experiment of the mixture DnaK/rNEMO with a ratio 1:2 in a buffer containing 10 mM OG. Again, the radial distribution was poorly fitted with a single species model, and the best fitting, represented by the *curved line* in Fig. 6, was obtained with a two species model. As shown in Table I the values found (49,000 ± 3,000 Da for M_1 (55%) and 340,000 ± 20,000 Da for M_2 (45%)) corresponded to monomeric rNEMO and to a heavy protein complex between DnaK and rNEMO. No significant improvement was obtained when fitting was performed using a three-component model either in fixing the masses of protein partners or in allowing them to float. This indicated that no

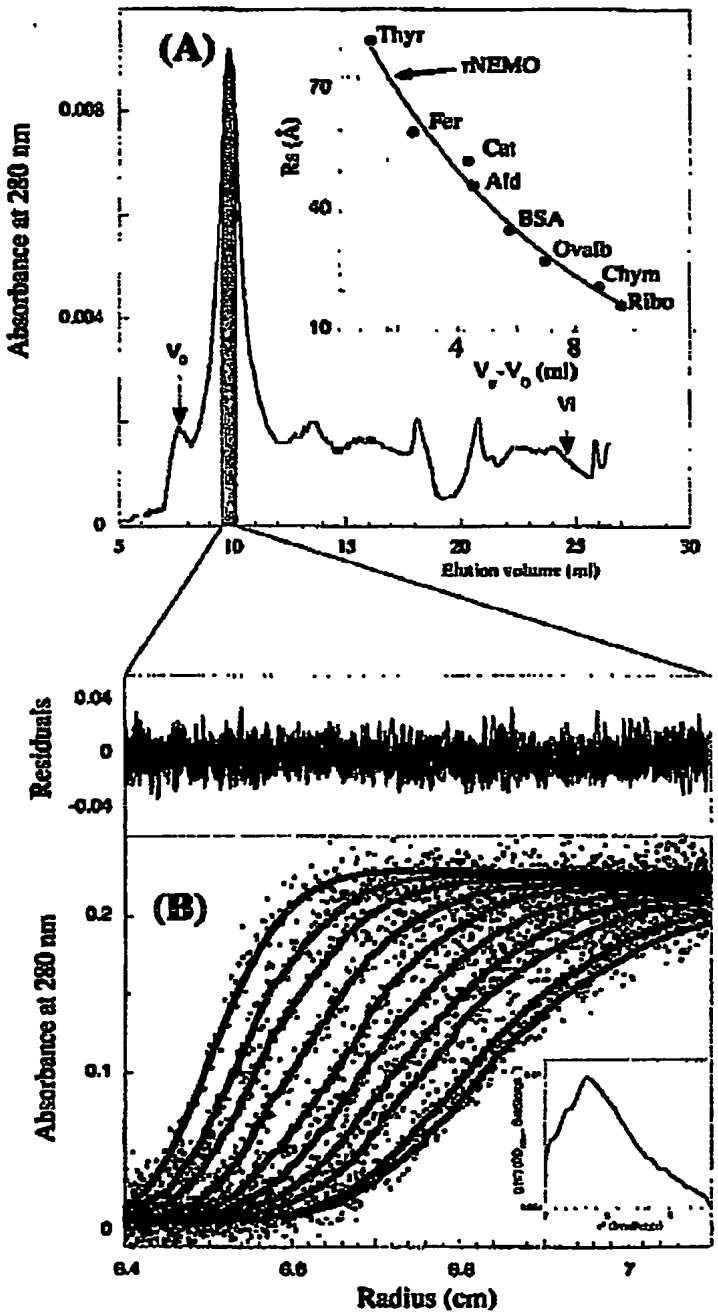

FIG. 5. Analysis of rNEMO by size-exclusion chromatography and by sedimentation velocity. *A*, distribution profile of rNEMO obtained by size-exclusion chromatography. The gel filtration was performed as described under "Experimental Procedures" in loading 2.8 mg/ml rNEMO in equilibrium buffer F (50 mM Tris-HCl, pH 7.5, 200 mM potassium chloride, 0.2 mM DDM, and 1 mM dithioerythritol). *Inset*, calibration curve for globular proteins measured in the same equilibrium buffer (see "Experimental Procedures"). *Thyr*, thyroglobulin; *Fer*, ferritin; *Cat*, catalase; *Ald*, aldolase; *Ovalb*, ovalbumin; *Chym*, chymotrypsinogen A; and *Ribo*, Ribonuclease. V_0 and V_t represent the void and total volumes of the column, respectively. *B*, analysis of rNEMO by sedimentation velocity. Fraction 10 from the size-exclusion chromatography (0.8 mg/ml) was sedimented at 50,000 rpm. Sedimentation profiles (*synthetic*) were recorded at 280 nm, and the sedimentation data were fitted (*curves*) using a two-species model as described under "Experimental Procedures." Residuals calculated for each sedimentation profile are indicated above. *Inset*, sedimentation coefficient distribution analysis. The sedimentation velocity data were analyzed for the sedimentation distribution, $g(s^*)$, as described under "Experimental Procedures."

free DnaK was detectable during the centrifugation, implying again a tight binding between DnaK and rNEMO. Similar results were obtained when the experiments were performed with a buffer containing 10 mM TGME. In this case, the molecular masses of M_1 and M_2 were 85,000 ± 3,000 Da (66%) and 360,000 ± 10,000 Da (34%), respectively. Given a complex

TABLE I

Structural parameters of recombinant NEMO as deduced from size-exclusion chromatography and analytical ultracentrifugation

	Molecular species	
	M_1 (rNEMO)	M_2 (complex DnaK-rNEMO)
Sedimentation velocity data[a]		
Distribution of molecular species (%)[b]	75	25
$s_{20,w}$ (10^{-13} s)	4.1 ± 0.1	5.5 ± 0.2
$D_{20,w}$ (× 10^{-7} cm^2/s)	7.0 ± 0.5	10.9[c] ± 0.9
R_g (Å)	29.7	
f/f_0	1.20	
Molecular mass (Da) from Svedberg's equation	53,000 ± 700	
Sedimentation equilibrium data[d]		
Detergent CC		
Distribution of molecular species (%)	55	45
Molecular mass (Da)	49,000 ± 3,000	340,000 ± 20,000
Detergent TGME		
Molar fraction (%)	66	34
Molecular mass (Da)	55,000 ± 3,000	360,000 ± 10,000
Protein sequence data		
Molecular mass of rNEMO (Da)	51,795	
Molecular mass of DnaK (Da)	68,934	

[a] Data were analyzed in the same buffer using DDM as detergent as described under "Experimental Procedures." The size-exclusion chromatography data R_g for M_1 and M_2 was 78 Å.
[b] Fraction of each species contributing of the total absorbance at 280 nm.
[c] Hydrodynamic parameters from sedimentation velocity were obtained by fitting the approximate solutions of the lamm equation using the Svedberg software (see text for more details).
[d] Experiments were done at 10 °C using a detergent concentration of 10 mM as described under "Experimental Procedures."

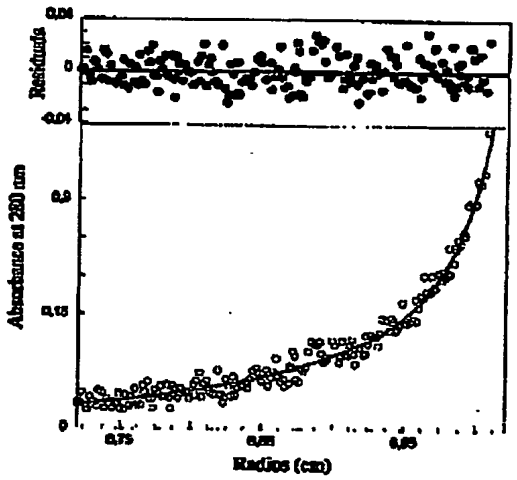

FIG. 6. Sedimentation equilibrium of rNEMO. Equilibrium distribution of rNEMO monitored by its absorbance at 280 nm is plotted as a function of radial distance at 12,000 rpm and 10 °C. Initial protein concentration was 0.35 mg/ml with DnaK/rNEMO ratio of 1:3 in a 50 mM Tris-HCl, pH 7.5, containing 100 mM potassium chloride, 1 mM dithioerythritol, and 10 mM β-OG. Data (*symbols*) were fitted (*curves*) as described under "Experimental Procedures." The *line* shows the best-fitting curve for an ideal two-species model with a molecular mass of 49,000 ± 3,000 Da for species M_1 and 340,000 ± 2,000 Da for species M_2 (see also Table I). The random distribution of residuals as function of radial distance is shown above.

stoichiometry of 1:1 (see Fig. 2), this mass matches with the mass of a DnaK-rNEMO complex containing 3 molecules of DnaK bound to 3 rNEMO molecules (theoretical mass of 360,540 Da).

Altogether, our ultracentrifugation experiments show that a fraction of the recombinant rNEMO is present as a monomer while the remainder is tightly associated to the chaperone DnaK. The DnaK-rNEMO complex forms a supramolecular structure (3:3) that may correspond to an assembly intermediate of rNEMO trapped in its trimeric state.

The C-terminal Domain of rNEMO Forms a Trimeric Coiled-coil—In order to understand which region of NEMO mediates its oligomerisation, we compared the sequences of NEMO and of the related proteins NRP/TIP-2 (39, 40). The best conserved C-terminal half (amino acids 240–412 in NEMO) includes both the coiled-coil CC2 and the LZ domains, as well as the ZF motif (Fig. 7). The analysis of the 7-residue repeat composing each coiled-coil domain using the MultiCoil program (41) predicts that the CC2 shows a propensity to form trimeric coiled-coils, whereas LZ, similar to the wild-type GCN4 LZ (42), is likely to self-associate into dimer. To determine which type of oligomer can be formed with the C-terminal part of NEMO, we tried to express the C-terminal domain in *E. coli*. Unfortunately the complete fragment was poorly produced in *E. coli*, making its purification difficult. We next decided to express a fragment corresponding to the C-terminal part of NEMO devoid of the 24 C-terminal amino acids composing the zinc finger motif (residues 242–383). This fragment was well expressed in *E. coli*, and the use of the purification procedure, described under "Experimental Procedures," resulted in 6 mg of homogeneous protein from 1 liter of culture. As the mutant protein also showed a propensity to form aggregates, all buffers were also supplemented with DDM (0.1 mM). The apparent molecular mass observed by SDS-PAGE (*inset* of Fig. 8*a*) was in agreement with the calculated molecular mass of purified truncated mutant of 19,625 Da. During the last chromatographic step, the fraction of the truncated mutant protein which passed through the Q-column (80%) was homogeneous (*inset* of Fig. 8*a*), whereas the part (20%) eluted with a salt linear gradient was associated to DnaK in a stoichiometry of 1:1 (data not shown).

The CD spectrum of the purified truncated mutant is shown in Fig. 8*a*. It is similar to that of WT rNEMO with a maximum at 192 nm and two minima at 208 and 222 nm, but the amplitude of each dichroic band is significantly higher, yielding an α-helix content of 53% instead of 45% in the case of WT rNEMO. In contrast to the WT rNEMO where the same α-helical content was detected over a large protein concentration

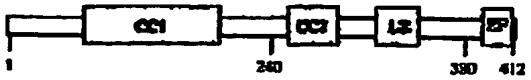

FIG. 7. Schematic structural organization of NEMO. The boxes indicate the major structural motifs as follows: coiled-coil (*CC1* and *CC2*), leucine zipper (*LZ*), and zinc finger motifs (*ZF*).

range (3–40 μs) (data not shown), molar dichroic absorption of the C-terminal fragment showed a strong concentration dependence. As shown in Fig. 8*b*, the increase of protein concentration induced a significant increase in helicity with a plateau at 10–11 μM, consistent with the formation of intermolecular coiled-coils induced by the oligomerization of the C-terminal fragment.

The quaternary structure of the C-terminal fragment was determined by equilibrium sedimentation. Table II summarizes the results of two fits using either a monospecies model or a monomer-dimer-trimer model. All radial distributions obtained at 12,000 or 18,000 rpm with a loading concentration of either 1 or 1.2 mg/ml were poorly fitted with the one-component model (average molecular mass of about 35,000 Da) well above the 19,625 mass of monomer indicating oligomerization of the C-terminal fragment. The best fit at 18,000 rpm was obtained with a monomer-dimer-trimer model which gave a significant improvement of χ^2 and a random distribution of residuals as compared with monospecies or bispecies models (monomer-trimer or dimer-trimer). Therefore, in a protein concentration range of 0.5 to 2.1 mg/ml, the average distribution of the C-terminal fragment present in solution was monomer (54%), dimer (16%), and trimer (30%) with dissociation constants $K_{M\rightarrow D}$, $K_{D\rightarrow T}$, and $K_{M\rightarrow T}$ equal to 117, 17.6, and 8.6 μM, respectively, indicating that the affinity of the homotrimer is 13-fold higher than that for the homodimer.

Quaternary Structure of Native NEMO—Previous experiments (14) using gel filtration analysis of S100 extracts in different cell lines showed that native NEMO is always present in association with IKK kinases and that no free form of the protein could be detected. In order to determine the oligomeric state of the NEMO in these complexes, *in vivo* chemical cross-linking experiments in HeLa cells were performed using the permeable homobifunctional cross-linker, BMOE, which reacts specifically with the cysteine residues (see "Experimental Procedures"). The extent of total protein cross-linking was probed by the SDS-PAGE analysis of crude extracts, either treated or mock-treated with 1 mM BMOE. As shown in Fig. 9*A*, the pattern of treated cells only slightly differed from that of the control, indicating that only a small number of cellular proteins were cross-linked. When the cross-linked cells were compared with the mock-treated cells by immunoblotting with either NEMO antibodies or with anti-IKKβ antibodies, specific cross-links were detected for both proteins (Fig. 9*B*). Note that no band corresponding to either NEMO (48,200 Da) or IKKβ (86,564 Da) was observed in cells treated with BMOE, indicating that the cross-linking reaction was complete. Three species specifically reacted with anti-NEMO antibodies, with masses of 110, 160, and about 350 kDa, respectively. The 110- and 160-kDa species matched the masses of the cross-linked dimer and trimer of NEMO. The slightly slower migration as compared with the theoretical masses of NEMO dimer (96 kDa) and trimer (144 kDa) was probably due to the cross-linker molecules that may affect the electrophoretic migration. The detection of the cross-linked dimer of NEMO could reflect a partial cross-linking of the NEMO trimer. This was not the case because extended incubation of the cross-linker with HeLa (2 h) did not change the relative proportions of cross-linked dimer and cross-linked trimer (data not shown). When using anti-

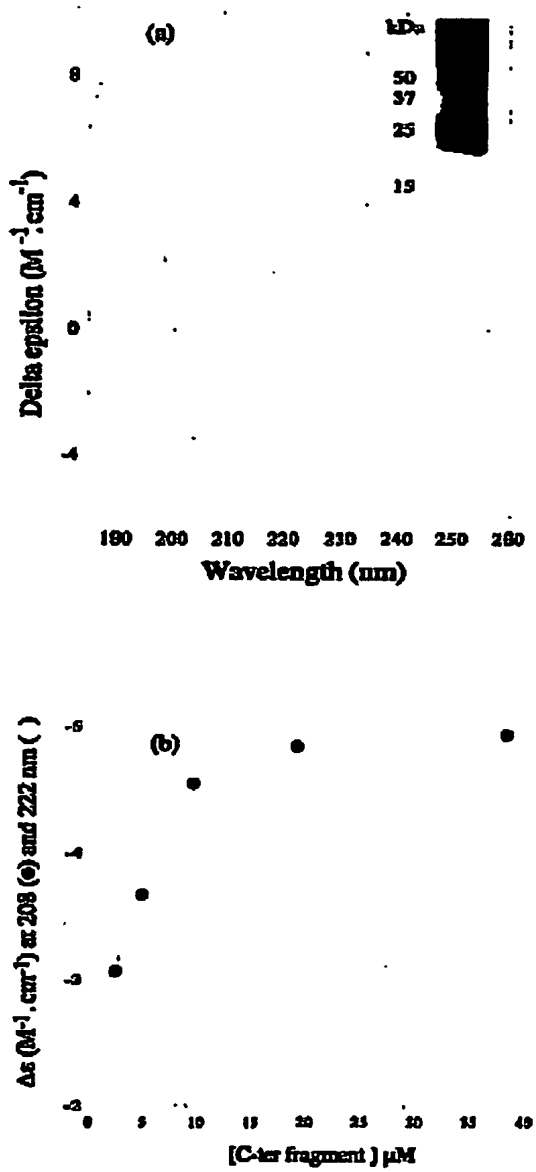

FIG. 8. CD spectrum and SDS-PAGE analysis of purified C-terminal fragment of NEMO. *a*, CD spectrum of the C-terminal domain (0.8 mg/ml) was recorded at 20 °C in 20 mM potassium phosphate, pH 7.0, containing 1 mM dithioerythritol and 0.2 mM DDM. *Inset*, the purified truncated C-terminal domain of NEMO (2 μg of protein in lane) was analyzed on a 15% SDS-PAGE and revealed by Coomassie staining. The positions of size markers are shown. *b*, concentration dependence at 20 °C of the CD signal at 222 nm (○ and 208 nm (●) of the C-terminal fragment of NEMO.

IKKβ antibodies, only one species of about 350 kDa was detected in treated cells. This 350-kDa species, which co-migrated with the third cross-linked species generated with anti-NEMO

TABLE II

Sedimentation equilibrium experiments with recombinant C-terminal truncated form of NEMO-(341–388)

All experiments were performed in the presence of 10 mM OG at 10 °C as described under "Experimental Procedures."

Initial protein concentration	Speed	Single species	χ^2	Monomer-dimer-trimer equilibrium		
				Distribution of molecular species	Deduced mass of monomer	χ^2
mg/ml	*rpm*	*Da*				
1.2	12,000	34,500 ± 1,000	31	65% α; 35% (α_2 + α_3)[a]	22,000 ± 3,000	28
	18,000	37,500 ± 1,000	47	53% α; 16% α_2; 31% α_3[a]	21,000 ± 2,000	20
1.0	12,000	33,500 ± 1,500	30	66% α; 34% (α_2 + α_3)[a]	23,000 ± 4,000	24
	18,000	36,200 ± 2,000	49	54% α; 16% α_2; 30% α_3[a]	22,000 ± 3,000	33

[a] No improvement of the fit was observed by a trispecies model (monomer-dimer-trimer). See text and "Experimental Procedures" for further details.

[b] Distribution of molecular species was calculated for a protein concentration range from 0.3 to 2.1 mg/ml.

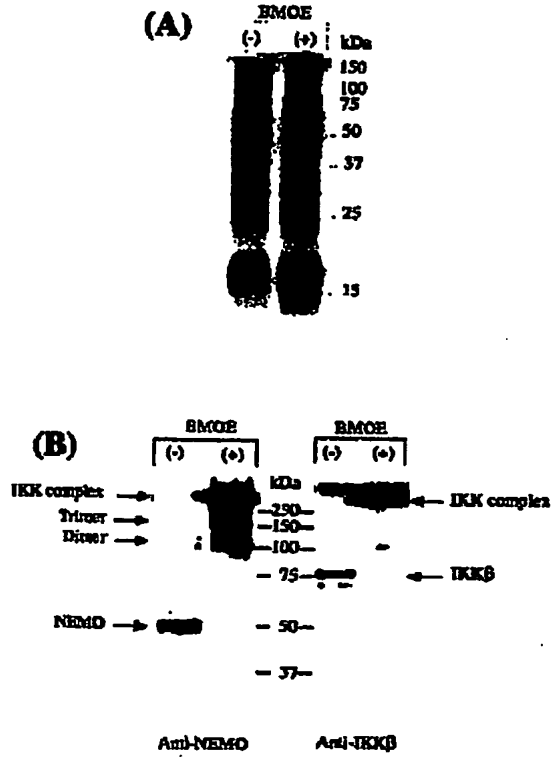

FIG. 9. **Chemical cross-linking of NEMO *in vivo*.** *A*, HeLa cells were either treated (*lane +*) with the BMOE cross-linker or mock-treated (*lane −*). The reaction was quenched by adding a molar excess of dithioerythritol as described under "Experimental Procedures." The total protein content (5 μg), corresponding to soluble and insoluble proteins, was prepared by directly boiling the cells in SDS buffer containing 6 M urea followed by analysis by 15% PAGE and Coomassie staining. *B*, similar experiments were performed as described for *A* except that Western blottings were performed with anti-NEMO (*left*) or with anti-IKKβ (*right*).

antibodies (Fig. 9*B*), is likely to correspond to the cross-linked IKK complex.

DISCUSSION

In the present study, the oligomeric state of native and recombinant NEMO purified from *E. coli* was investigated leading to the identification of a domain responsible for its self-association as a trimer. A variety of biochemical methods showed that most of rNEMO is in a monomeric state. This demonstration mainly relies on ultracentrifugation experiments. The data deduced from the sedimentation velocity were best interpreted using a two-species model which identified unambiguously the presence of monomer (species M_1) in the rNEMO protein preparation. The fits of sedimentation profiles for species M_2 yielded an average sedimentation coefficient of 5.5 S and a diffusion coefficient of 10.9 10^{-7} cm^2/s. This very large diffusion coefficient reflected an equilibrium with a heavier species whose presence was confirmed by the equilibrium sedimentation experiments. Monomeric rNEMO displays an aberrant retarded elution in gel permeation. This suggests that the molecular mass of the IKK complex previously determined by gel filtration (~700–800 kDa) was overestimated (14, 20, 48). This very high aberrant Stokes radius of the rNEMO monomer (73 Å) along with the poor resolution of the gel filtration made it impossible to separate the free form of rNEMO from that bound to DnaK. It should be noted that, in general, the early elution of a protein from a gel permeation column is either due to a denatured state, to a very elongated shape, or to a protein/detergent micellar structure. However, our data from velocity and equilibrium sedimentation experiments demonstrate that rNEMO monomer behaves as a globular protein. In addition the far-UV CD spectrum of rNEMO as well as the interaction assay with IKK show that this monomer is in a native state. It thus appears that interference with the matrix combined with the presence of some detergent molecules bound to rNEMO is the cause for the aberrant elution of the monomer from the gel permeation.

The presence of a DnaK-rNEMO complex was best seen in equilibrium sedimentation (Fig. 6) showing that rNEMO can form a high molecular weight complex (360 kDa) with DnaK comprising 3 molecules of each protein. Neither free DnaK, which exists in a monomer-dimer-trimer equilibrium (44), nor a DnaK-rNEMO complex with a stoichiometry of 1:1 could be detected. This was probably due to the presence of a molar excess of rNEMO in all experiments and to the high propensity of the DnaK-rNEMO complex to self-assemble at the concentration used (0.1–1.25 mg/ml). Because we showed that DnaK binds to NEMO in a stoichiometric ratio of 1:1 (see Fig. 2*a*), the DnaK-rNEMO complex is likely formed via the trimerization of rNEMO. Thus, the fraction of rNEMO bound to DnaK may represent an assembly intermediate of rNEMO in *E. coli*. It is usually thought that DnaK recognizes with high affinity proteins exposing locally short hydrophobic segments either in an extended conformation or as elements with no secondary structure such as loops (45, 46). We showed that the C-terminal fragment of rNEMO also binds to DnaK, although it was correctly folded forming a stable trimeric coiled-coil (data not shown). We hypothesize that the association with DnaK could occur with the monomer of the C-terminal fragment which

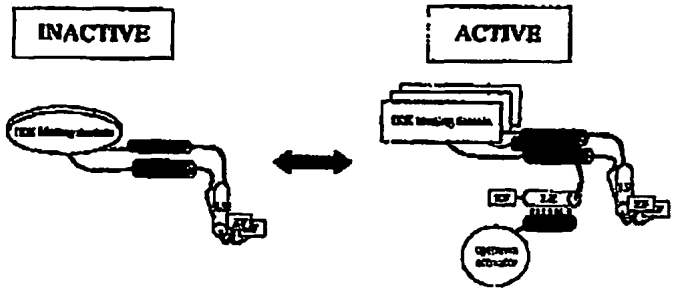

FIG. 10. **A plausible model for the activation of the IKK complex upon a change of NEMO oligomerization.** The N-terminal domain of NEMO containing the IKK kinase binding domain and the C-terminal domain including the CC2 coiled-coil (*CC2, gray areas*), the leucine zipper (*LZ, light gray areas*), and the zinc finger (*ZF*) motifs are shown. In non-stimulated cells NEMO may form a dimer through its CC2 coiled-coil motif leading to a stable inactive IKK complex. Upon stimulation trimerization of NEMO may occur through its CC2 domain providing a monomeric LZ suitable for a specific hetero-association with an upstream inducer containing a specific complementary LZ (*black area*). The ZF motif may have a concerted action with the NEMO LZ to form a specific activator binding domain. This oligomerization switch of NEMO would induce a conformation change to IKK kinases triggering the IKK activity by phosphorylation.

contains at least two coiled-coils motifs with a suitable hydrophobic α-helical interface. Indeed, the motif EEALVAKIQE (positions 263–271) composing the CC2 coiled-coil was predicted to be a DnaK-binding site with a very high score (47). The question then arises why the rNEMO behaves mainly as a monomer, whereas the endogenous form in association with its IKK partners is in equilibrium between a dimer and a trimer. Our hypothesis is that the interactions of IKK partners through the N-terminal domain of rNEMO have a coupling effect in its self-assembly which is impaired in the absence of this interaction. Consistent with this hypothesis, the C-terminal fragment of NEMO deleted of the IKK binding domain forms a stable trimeric coiled-coil structure that was significantly stabilized upon oligomerization as shown by CD (see Fig. 8*b*).

We demonstrate an association of NEMO with the human protein Hsp70 homologous to DnaK. Previous work (48, 49) showed a role for eukaryotic Hsp70 and Hsp90 in the conformational maturation of signal transduction molecules, and recently, the requirements of Hsp70 and Hsp90 proteins in the NF-κB activation of lipopolysaccharide-induced cells were reported (50, 51). It is likely that Hsp70 alone or in association with Hsp90 is involved in maintaining the monomeric metastable NEMO in a state competent to bind to IKKα or IKKβ kinases. This association may facilitate the correct oligomeric assembly of NEMO through stabilization of its N-terminal domain. Our data also suggest that NEMO is more sensitive to proteolytic degradation in the absence of this interaction. We propose that Hsp70 and Hsp90 proteins may play a key role in controlling the biological activity of NEMO and thereby in the activation of NF-κB.

Even though there is strong genetic evidence that NEMO is essential for the activation of the IKK complex, the molecular mechanism by which it activates IKK kinases is poorly understood. It has been proposed that NEMO activates the IKK complex by recruiting it to a receptor, but this mechanism was recently questioned by results showing that the IKK complex was still recruited to tumor necrosis factor R1 in response to TNF in NEMO-deficient cells (18). In contrast the results by others (19–21) indicate that the oligomerization of NEMO plays a key role in the activation of IKK kinases. The biochemical characterization of the purified C-terminal fragment of NEMO shown in this paper suggests that it is based on a coiled-coil trimer rather than on coiled-coil dimers. The C-terminal domain contains both an LZ motif, well known to form stable homo- or heterodimers, and a CC2 coiled-coil motif, which is predicted to form a coiled-coil trimer. Thus, the trimeric assembly of NEMO is likely governed by the CC2 coiled-coil motif and not by the LZ motif, the latter being probably rather involved in a specific hetero-association. The expression of NEMO lacking only the CC2 domain does not restore the NF-κB activation in NEMO-deficient 1.3E2 cells after lipopolysaccharide stimulation,[3] indicating that the trimerization is crucial for activation of IKK complex. Furthermore, the CC2 domain is a key element for NEMO biological function because a point mutation Ala→Gly within this domain leads to EDA-ID syndrome (17).

Fig. 10 shows a model for the regulation of NEMO function upon its oligomerization. In this model, the NEMO LZ forms heterodimers with upstream activators corresponding either to viral proteins (52) or to signaling proteins belonging to the interleukin-1/lipopolysaccharide or TNF pathways, for example the receptor-interacting protein involved in the response to TNF-α. We propose that the association of NEMO with these upstream regulatory components triggers the activation of the IKK complex by a conformational change via its trimerization. The formation of a homodimer through the leucine zipper would then prevent this association. Thus, different oligomeric states of NEMO (α_2 or α_3) shown in this study may correspond to inactive or active states of the IKK complex, respectively. Experiments attempting to correlate the dimer or trimer oligomerization of NEMO with the inactive or active state of IKK complex are in progress.

Acknowledgments—We thank J. P. Waller for critical review of this manuscript, M. Goldberg for expert advice in the ultracentrifugation experiments, and Alain Chaffotte for advice in CD measurements. We are indebted to Roland Nagaotte for performing the velocity sedimentation experiments.

Addendum—While this paper was being revised, the role of the Hsp90 in the assembly of NEMO to the IKK complex was reported (53).

REFERENCES

1. Rothwarf, D. M., and Karin, M. (1999) *Sci. STKE* 1999, RE1
2. Ghosh, S., May, M. J., and Kopp, E. B. (1998) *Annu. Rev. Immunol.* 16, 225–260
3. Karin, M. (1999) *J. Biol. Chem.* 274, 27339–27342
4. Israël, A. (2000) *Trends Cell Biol.* 10, 129–133
5. Rothwarf, D. M., and Karin, M. (1999) *Sci. STKE* 1999, RE1
6. Ghosh, S., Gifford, A. M., Moriarty, L. R., Temple, P., Nolan, G. P., and Baltimore, D. (1998) *Cell* 95, 121–132
7. Karin, M., and Ben-Neriah, Y. (2000) *Annu. Rev. Immunol.* 18, 621–663
8. Ullmann, J. A., Hayakawa, M., Rothwarf, D. M., Zandi, E., and Karin, M. (1997) *Nature* 389, 750–753
9. Mercurio, F., Zhu, H., Murray, B. W., Shevchenko, A., Bennett, B. L., Li, J.,

[3] C. Courtois, unpublished results.

Received at: 11:47AM, 9/24/2003

24. SEP. 2003 16:44 BUREAU DES BREVETS Nº1143 P. 175

Young, D. B., Barbosa, M., Mann, M., Manning, A., and Rao, A. (1997) *Science* 278, 860–866

10. Regnier, C. H., Song, H. Y., Gao, X., Goeddel, D. V., Cao, Z., and Rothe, M. (1997) *Cell* 90, 373–383

11. Woronicz, J. D., Gao, X., Cao, Z., Rothe, M., and Goeddel, D. V. (1997) *Science* 278, 866–869

12. Rothwarf, D. M., Zandi, E., Natoli, G., and Karin, M. (1998) *Nature* 395, 297–300

13. Hu, Y., Baud, V., Oga, T., Kim, K. I., Yoshida, K., and Karin, M. (2001) *Nature* 410, 710–714

14. Yamaoka, S., Courtois, G., Bessia, C., Whiteside, S. T., Weil, R., Agou, F., Kirk, H. E., Kay, R. J., and Israel, A. (1998) *Cell* 93, 1231–1240

15. May, M. J., D'Acquisto, F., Madge, L. A., Glockner, J., Pober, J. S., and Ghosh, S. (2000) *Science* 289, 1550–1554

16. Smahi, A., Courtois, G., Vabres, P., Yamaoka, S., Heuertz, S., Munnich, A., Israel, A., Heiss, N. S., Klauck, S. M., Kioschis, P., Wiemann, S., Poustka, A., Esposito, T., Bardaro, T., Gianfrancesco, F., Ciccodicola, A., D'Urso, M., Woffendin, H., Jakins, T., Donnai, D., Stewart, H., Kenwrick, S. J., Aradhya, S., Yamagata, T., Levy, M., Lewis, R. A., and Nelson, D. L. (2000) *Nature* 405, 466–472

17. Döffinger, R., Smahi, A., Bessia, C., Geissmann, F., Feinberg, J., Durandy, A., Bodemer, C., Kenwrick, S., Dupuis-Girod, S., Blanche, S., Wood, P., Rabia, S. H., Headon, D. J., Overbeek, P. A., Le Deist, F., Holland, S. M., Belani, K., Kumararatne, D. S., Fischer, A., Shapiro, R., Conley, M. E., Reimund, E., Kalhoff, H., Abinun, M., Munnich, A., Israel, A., Courtois, G., and Casanova, J. L. (2001) *Nat. Genet.* 27, 277–285

18. Devin, A., Lin, Y., Yamaoka, S., Li, Z. W., Karin, M., and Liu, Z. G. (2001) *Mol. Cell. Biol.* 21, 3986–3994

19. Poyet, J. L., Srinivasula, S. M., Lin, J. H., Fernandes-Alnemri, T., Yamaoka, S., Tsichlis, P. N., and Alnemri, E. S. (2000) *J. Biol. Chem.* 275, 37966–37977

20. Li, X. H., Fang, X. Q., and Gaynor, R. B. (2001) *J. Biol. Chem.* 276, 4494–4500

21. Ye, J., Xie, X., Tarassishin, L., and Horwitz, M. S. (2000) *J. Biol. Chem.* 275, 9882–9889

22. Fontan, E., Briend, E., Saklani-Jusforgues, H., d'Alayer, J., Vandekerckhove, J., and Fauve, R. M. (1994) *Proc. Natl. Acad. Sci. U. S. A.* 91, 8353–8357

23. Hennessey, J. P., and Johnson, W. C. (1982) *Anal. Biochem.* 125, 177–188

24. Chang, C. T., Wu, C. S., and Yang, J. T. (1978) *Anal. Biochem.* 91, 13–31

25. Agou, F., Yang, Y. S., Gesquiere, J. C., Waller, J. P., and Guittet, E. (1995) *Biochemistry* 34, 569–576

26. Deville-Bonne, D., Sellam, O., Merola, F., Lascu, I., Desmadril, M., and Veron, M. (1996) *Biochemistry* 35, 14643–14650

27. Philo, J. S. (1994) in *Modern Analytical Ultracentrifugation* (Schuster, T. M., and Laue, T., eds) pp. 156–170, Birkhauser Boston, Inc., Cambridge, MA

28. Stafford, W. F. (1994) *Methods Enzymol.* 240, 478–501

29. Laue, T. M., Shah, B. D., Ridgeway, T. M., and Pelletier, S. L. (1992) in *Analytical Ultracentrifugation in Biochemistry and Polymer Science* (Harding, S. E., Rowe, A. J., and Horton, J. C., eds) pp. 90–125, Royal Society of Chemistry, Cambridge, UK

30. Teller, D. C. (1976) *Nature* 260, 729–731

31. Reynolds, J. A., and Tanford, C. (1976) *Proc. Natl. Acad. Sci. U. S. A.* 73, 4467–4470

32. Lustig, A., Engel, A., Tsiotis, G., Landau, E. M., and Baschong, W. (2000) *Biochim. Biophys. Acta* 5, 199–206

33. Johnson, M., and Straume, M. (1994) in *Modern Analytical Ultracentrifugation* (Schuster, T. M., and Laue, T., eds) pp. 37–65, Birkhauser Boston, Inc., Cambridge, MA

34. Agou, F., Waller, J. P., and Mirande, M. (1996) *J. Biol. Chem.* 271, 29295–29303

35. Taggart, A. K., and Pugh, B. F. (1996) *Science* 272, 1331–1333

36. Jackson-Fisher, A. J., Chitikila, C., Mitra, M., and Pugh, B. F. (1999) *Mol. Cell* 3, 717–727

37. Agou, F., Quevillon, S., Kerjan, P., Latreille, M. T., and Mirande, M. (1996) *Biochemistry* 35, 15322–15331

38. King, R. D., and Sternberg, M. J. (1996) *Protein Sci.* 5, 2298–2310

39. Li, Y., Kang, J., and Horwitz, M. S. (1998) *Mol. Cell. Biol.* 18, 1601–1610

40. Schwarzenberg, K., Weil, R., Courtois, G., Whiteside, S. T., and Israel, A. (2000) *J. Biol. Chem.* 275, 22780–22789

41. Wolf, E., Kim, P. S., and Berger, B. (1997) *Protein Sci.* 6, 1179–1189

42. O'Shea, E. K., Klemm, J. D., Kim, P. S., and Alber, T. (1991) *Science* 254, 539–544

43. Miller, B. S., and Zandi, E. (2001) *J. Biol. Chem.* 276, 36320–36326

44. Schonfeld, H. J., Schmidt, D., Schroder, H., and Bukau, B. (1995) *J. Biol. Chem.* 270, 2183–2189

45. Schmid, D., Baici, A., Gehring, H., and Christen, P. (1994) *Science* 263, 971–973

46. Zhu, X., Zhao, X., Burkholder, W. F., Gragerov, A., Ogata, C. M., Gottesman, M. E., and Hendrickson, W. A. (1996) *Science* 272, 1606–1614

47. Rudiger, S., Germeroth, L., Schneider-Mergener, J., and Bukau, B. (1997) *EMBO J.* 16, 1501–1507

48. Freeman, B. C., Toft, D. O., and Morimoto, R. I. (1996) *Science* 274, 1718–1720

49. Nathan, D. F., and Lindquist, S. (1995) *Mol. Cell. Biol.* 15, 3917–3925

50. Byrd, C. A., Bornmann, W., Erdjument-Bromage, H., Tempst, P., Pavletich, N., Rosen, N., Nathan, C. F., and Ding, A. (1999) *Proc. Natl. Acad. Sci. U. S. A.* 96, 5645–5650

51. Triantafilou, K., Triantafilou, M., and Dedrick, R. L. (2001) *Nat. Immunol.* 2, 338–345

52. Xiao, G., Harhaj, E. W., and Sun, S. C. (2000) *J. Biol. Chem.* 275, 34060–34067

53. Chen, G., Cao, P., and Goeddel, D. V. (2002) *Mol. Cell* 9, 401–410

Cell, Vol. 93, 1231–1240, June 26, 1998, Copyright ©1998 by Cell Press

Complementation Cloning of NEMO, a Component of the IκB Kinase Complex Essential for NF-κB Activation

Shuji Yamaoka,*‖# Gilles Courtois,*‖ Christine Bessia,* Simon T. Whiteside,* Robert Weil,* Fabrice Agou,† Heather E. Kirk,† Robert J. Kay,§ and Alain Israel*
*Unité de Biologie Moléculaire de l'Expression Génique
†Unité de Régulation Enzymatique des Activités Cellulaires
URA 1773 CNRS
Institut Pasteur
25 rue du Dr Roux
75724 Paris Cedex 15
France
§Terry Fox Laboratory
British Columbia Cancer Agency
Vancouver, British Columbia
Canada V5Z 4E6

Summary

We have characterized a flat cellular variant of HTLV-1 Tax-transformed rat fibroblasts, 5R, which is unresponsive to all tested NF-κB activating stimuli, and we report here its genetic complementation. The recovered full-length cDNA encodes a 48 kDa protein, NEMO (*NF-κB Essential MOdulator*), which contains a putative leucine zipper motif. This protein is absent from 5R cells, is part of the high molecular weight IκB kinase complex, and is required for its formation. In vitro, NEMO can homodimerize and directly interacts with IKK-2. The NEMO cDNA was also able to complement another NF-κB–unresponsive cell line, 1.3E2, in which the protein is also absent, allowing us to demonstrate that this factor is required not only for Tax but also for LPS, PMA, and IL-1 stimulation of NF-κB activity.

Introduction

The Rel/NF-κB family of transcription factors plays important roles in immune and stress responses, in inflammation, and in apoptosis, regulating the expression of numerous cellular and viral genes (for recent reviews, see Verma et al., 1995; Baldwin, 1996; May and Ghosh, 1998). The NF-κB activity is composed of homodimers or heterodimers of related proteins that share a conserved DNA-binding and dimerization domain called the Rel homology domain. In most cell types, NF-κB is sequestered in the cytoplasm bound to inhibitory proteins called IκB-α, IκB-β, and IκB-ε. In response to diverse stimuli, including inflammatory cytokines, mitogens, bacterial lipopolysaccharide (LPS), or some viral products, active NF-κB is released and translocated to the nucleus as a result of the proteolytic degradation of IκB proteins. Phosphorylation of IκBα on Ser-32 and Ser-36 targets the molecule for degradation by the ubiquitin-26S proteasome pathway. While the processes leading to the degradation of the IκB proteins are relatively well understood, the mechanism by which a variety of distinct signals initiated from the cell membrane are transduced to their common targets, the IκB proteins, remains to be elucidated. A protein kinase activity was identified as a large multisubunit complex that can phosphorylate IκBα at Ser-32 and Ser-36 (Chen et al., 1996; Lee et al., 1997). Most recently, two related kinases have been cloned that contain a catalytic domain at the amino terminus and a leucine zipper (LZ) as well as a helix-loop-helix (HLH) motif at the carboxy terminus (Didonato et al., 1997; Mercurio et al., 1997; Regnier et al., 1997; Woronicz et al., 1997; Zandi et al., 1997). Although both of them have been shown to be essential contributors to cytokine-mediated NF-κB activation, understanding of the precise nature of the IκB kinase activity and its regulatory mechanisms awaits further investigation and identification of the other subunits of the kinase complex. Another important issue still unanswered is how discrete activation signals triggered by a variety of known stimulators are integrated to give rise to IκB kinase activity.

One attractive approach to such questions would be the use of somatic cell genetics. Although the diploidy of the mammalian genome presents a major hurdle to a genetic approach, successful establishment of recessive mutants has provided helpful informations on a signaling pathway and a reliable way to identify relevant gene(s) by complementation. Indeed, the *Janus* kinase family of tyrosine kinases was identified as essential signal transducers for the interferons through a genetic approach (Velazquez et al., 1992; Darnell et al., 1994). Concerning the NF-κB signaling pathways, we have previously reported the characterization of a mutant of the murine pre-B cell line 70Z/3, 1.3E2, which had been isolated by selecting cells unable to express surface IgM following lipopolysaccharide stimulation (Courtois et al., 1997). We have proposed that the 1.3E2 cell line was deficient in a step that is required by several different stimuli to activate NF-κB.

In this report, we present another mutant cell line, 5R, originally isolated as a cellular flat variant of Rat-1 fibroblasts transformed by the Tax protein of human T cell leukemia virus type 1 (HTLV-1). Tax is known to activate transcription from the HTLV-1 long terminal repeat, to cause permanent activation of many cellular transcription factors including NF-κB, and to give rise to cellular transformation (for a review, see Yoshida et al., 1995). 5R cells carry a recessive cellular mutation that abolishes Tax-induced constitutive NF-κB activity, therefore providing a potential means of identifying a critical molecule involved in Tax-mediated NF-κB activation. Interestingly, 5R cells were found to be resistant to multiple NF-κB activating stimuli besides Tax, suggesting they carried a mutation at a converging regulatory step. We decided to use 5R cells for a genetic

‖To whom correspondence should be addressed.
‖These two authors contributed equally to this work.
#Permanent address: Institute for Virus Research, Kyoto University, Shogoin, Sakyo-ku, Kyoto 606, Japan.

Cmf
1252

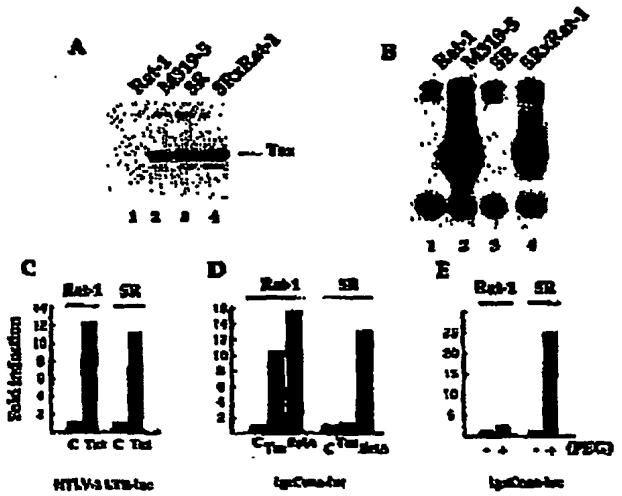

Figure 1. Characterization of 5R Cells

(A) Fifty micrograms of whole-cell extracts derived from wild-type Rat-1 cells (lane 1), the Tax-transformed clone M319-6 (lane 2), the 5R flat revertant (lane 3), and a pool of hybrids between 5R and a Rat-1 derived clone bearing an integrated hygromycin resistance gene (lane 4) were analyzed by immunoblotting using anti-Tax mAb M72.

(B) Five micrograms of nuclear extracts derived from the same cells (as indicated above the lanes) were analyzed by bandshift assay using the κB site derived from the H-2 K^b promoter as a probe. The NF-κB complex is indicated by a square dot on the right. (C and D) Rat-1 or 5R cells were cotransfected with 0.25 μg of HTLV-1 LTR-luciferase (C) or IgκCmv-luciferase (D) and 1 μg of either empty vector (C) or Tax or RelA expression vectors. Luciferase activity was measured after 40 hr. Fold induction over basal level is shown.

(E) Rat-1 or 5R cells (as indicated) were cocultured with Rat-1 cells carrying an integrated IgκCmv-luciferase plasmid, treated with (+) or without (−) 50% PEG for 1 min, and harvested 12 hr later. Equivalent amount of protein extract was used for the luciferase assay.

complementation approach for the following reasons. First, as the screen we decided to use was based on the NF-κB–dependent expression of a drug resistance gene, the presence of Tax would ensure restoration of a permanent high NF-κB activity following complementation. Second, Rat-1–derived cells grow well in the presence of a high NF-κB activity. Third, 5R cells are expected to show a transformed phenotype following complementation. Here, we describe the genetic complementation of 5R cells by infection with a cDNA expression library cloned into a retroviral vector, demonstrate that expression of the cloned gene, *nemo*, also complements the defect in the 1.3E3 cell line, and show that NEMO is part of the high molecular weight IKK complex and is required for its formation.

Results

Characterization of the Mutant Cell Line 5R

Spontaneous flat revertant cells were isolated from M319-6 cells, a clone of Rat-1 fibroblasts transformed by a mutant Tax protein competent to activate NF-κB but unable to stimulate HTLV-1 long terminal repeat (LTR)–directed transcription (Yamaoka et al., 1995). All of them except one (clone 5R) had lost Tax expression (data not shown). 5R cells express Tax at a level comparable with the parental cells (Figure 1A, lane 3) but are defective in Tax-induced NF-κB DNA binding activity (Figure 1B, lane 3). Stable expression of wild-type Tax failed to retransform 5R cells, while forced expression of constitutively active c-Ha-Ras or v-Src protein transformed 5R cells as efficiently as the parental Rat-1 cells (data not shown). Transient expression of wild-type Tax fully activated HTLV-1 LTR-directed, but not NF-κB–dependent, transcription in 5R cells (Figures 1C and 1D). On the other hand, transient expression of RelA or activated c-Ha-Ras strongly stimulated NF-κB– or serum-responsive element–dependent transcription, respectively, in 5R as well as in Rat-1 cells (Figure 1D and data not shown). These results suggest that 5R cells carry a mutation(s) that abrogates Tax-mediated NF-κB activation.

We next analyzed the phenotype of the mutation by somatic cell hybridization. Since 5R cells express Tax, they are expected to restore Tax-induced NF-κB activity after hybridization with parental cells if the mutation is recessive. Hybridization of 5R cells with Rat-1 cells carrying an integrated NF-κB–dependent reporter gene induced a strong transcriptional activity when compared with the control hybridization (Figure 1E). We also established a pooled population of stable hybrids between 5R and Rat-1 cells and found that they exhibited a transformed phenotype (data not shown) and contained high NF-κB DNA binding activity (Figure 1B, lane 4). These results indicate that the phenotype of the mutation in 5R cells is recessive and therefore should be amenable to genetic complementation.

Rat-1 cells normally activate NF-κB in response to diverse external stimuli, including tumor necrosis factor α (TNFα), interleukin-1 (IL-1), lipopolysaccharide (LPS), or double-stranded RNA (dsRNA). Interestingly, none of these stimuli was able to induce NF-κB DNA binding activity in 5R cells (Figure 2A). This result was further confirmed by transient transfection with an NF-κB–dependent reporter gene (Figure 2B). To identify the step at which NF-κB signaling is affected, we examined the levels of IκB proteins in cells stimulated with LPS. As shown in Figure 2C, LPS stimulation led to a complete loss of IκBα and of IκBβ in Rat-1 cells followed by reappearance of IκBα 60 min after stimulation. In contrast, the levels of the two IκB proteins in 5R cells were virtually unaffected by LPS treatment. Taken together, we can conclude that 5R cells carry a recessive mutation(s) at

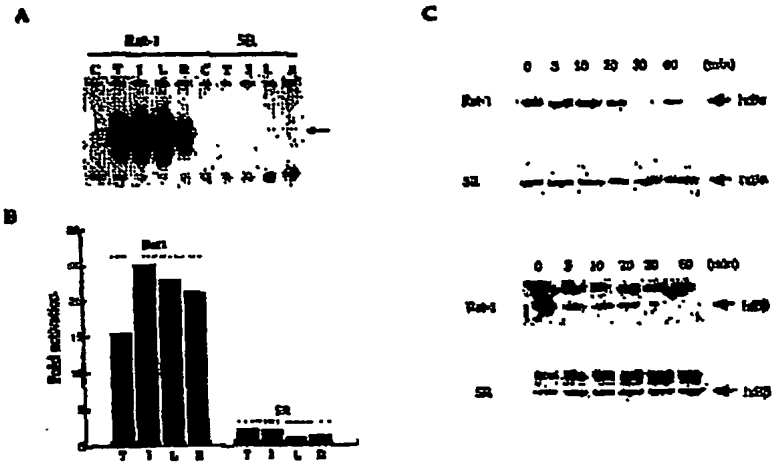

Figure 2. Response of Rat-1 and 5R Cells to NF-κB Activating Signals

(A) Bandshift assay of nuclear extracts from Rat-1 or 5R cells either untreated (none) or stimulated as indicated above the lanes. Stimulation was for 20 min with 10 ng/ml of TNFα, 20 ng/ml of IL-1, 15 μg/ml of LPS, or 0.1 mg/ml of dsRNA. The arrow marks NF-κB complex.

(B) Transactivation of Igκ-luciferase transfected Rat-1 or 5R cells by TNFα (T), IL-1 (I), LPS (L), or dsRNA (R). Stimulation was for 3 hr.

(C) Immunoblotting analysis of extracts derived from LPS-treated Rat-1 or 5R cells. Cytoplasmic extracts were prepared at the indicated times and 50 μg analyzed by Western blotting.

a converging regulatory step leading to inducible degradation of IκB proteins. Finally, we addressed the possibility that 5R cells might be defective in one of the functional IκB kinases. Stable transfection of 5R cells with plasmids encoding either IKK-1 or IKK-2 did not restore NF-κB activity (data not shown).

Molecular Cloning of NEMO

For complementation experiments, we first established a selection system by preparing sublines of 5R cells capable of expressing an NF-κB-dependent inducible drug resistance gene. A conditional drug resistance gene, pκB2bsrH, contains both a hygromycin resistance gene under the control of the HSV1 thymidine kinase gene promoter and the blasticidin deaminase gene (Izumi et al., 1991) linked to a minimal IL-2 promoter following three repeats of the immunoglobulin κ light chain NF-κB-binding site. Stable transfection of the parental Tax transformed cells with this construct using hygromycin selection followed by selection with blasticidin S resulted in numerous surviving colonies, whereas none could be observed for 5R cells. Hygromycin-resistant 5R clones were tested for survival in the presence of blasticidin S following simple coculture or hybridization with normal Rat-1 cells. One of the 5R clones, h12, was chosen at random for further experiments as being able to survive a high dose of blasticidin S selection after the hybridization but showing absolutely no survival at a low concentration of the drug without the hybridization step. A high NF-κB DNA binding activity was detected in stable h12/Rat-1 hybrids, a result of activation by Tax following complementation of the defect of h12 cells (data not shown).

Approximately 30×10^6 h12 cells were infected with retroviruses carrying a cDNA expression library derived from the TaB murine T cell hybridoma cell line (Whitehead et al., 1995). Viral supernatants were produced by transient transfection of Phoenix cells with the retroviral constructs giving titers in the range of 2×10^5 to 3×10^5/ml. Selection with blasticidin S was started 36 hr after viral infection. In 20–30 days, a total of more than 60 independent clones was obtained, and 20 were tested for their NF-κB DNA binding activity. All clones except one contained high levels of DNA binding activity and clearly showed a transformed phenotype (Figure 4B, lanes 5–6). Polymerase chain reaction–mediated amplification of genomic DNAs from seven clones resulted in a provirus-derived specific band with a size of 9.2 kb. While 33 other clones carried a 2.8 kb insert. Southern blot analysis of the 9.2 kb insert showed cross-hybridization with the 2.8 kb fragment. Sequencing analysis of the amplified 2.8 kb cDNA showed that it contained an open reading frame predicted to encode a previously unknown 48 kDa polypeptide, which we have named NEMO (NF-κB Essential MODulator) (Figure 3). This molecule is acidic (pI 5.88) and unusually rich in glutamic acid and glutamine (13% each). In addition, it contains a putative leucine zipper motif (amino acids 315–342). To characterize its function, we first transfected Rat-1 or 5R cells with a mammalian expression vector capable of expressing NEMO. Cotransfection of 5R cells with a very small amount of NEMO and an NF-κB–dependent reporter gene resulted in a strong

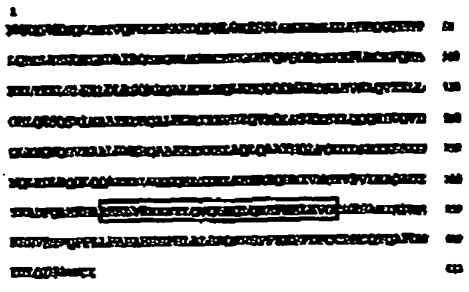

Figure 3. Sequence of the NEMO Protein
The putative leucine zipper is boxed.

reporter gene activation by endogenous Tax, whereas its overexpression in Rat-1 cells barely activated the reporter construct (Figure 4A). We then established Rat-1 or 5R cells stably expressing NEMO. As expected, stable expression of NEMO (under the control of the strong CMV promoter) in wild-type Rat-1 cells did not give rise to detectable NF-κB activity (Figure 4B, lane 2). On the other hand, two pooled populations derived from NEMO-transformed 5R cells and two isolated clones showed high levels of NF-κB DNA binding activity (lanes 7–10), indicating that stable NEMO expression can complement the defect in 5R cells.

A polyclonal antibody was raised against the region encompassing amino acids 60–328 of NEMO and used to analyze its expression in 5R cells. Whereas the protein could be readily detected as a single 48 kDa band in Rat1 cytoplasmic extracts (Figure 4C), no NEMO band could be observed in 5R cells. In addition, we were not able to detect any truncated form of the protein. Thus, the defective phenotype of 5R cells results from the absence of the NEMO protein.

Complementation of the 1.3E2 Mutant Cell Line by NEMO

We have recently reported the characterization of another mutant cell line, the 70Z/3-derived mutant 1.3E2, that exhibits a defect in NF-κB activation (Courtois et al., 1997). In this cell line NF-κB is not activated in response to a large set of stimuli, among them LPS, IL-1, PMA, dsRNA, or TNF. This is due to a lack of IκBα, IκBβ, and IκBε degradation. Since phosphorylation of IκBα on Ser-32 and Ser-36 is not observed after stimulation, we proposed that a converging step preceding the IκB phosphorylation step or the phosphorylation step itself was deficient in 1.3E2.

Since the 1.3E2 phenotype shares many similarities with the 5R phenotype, we tested whether NEMO could

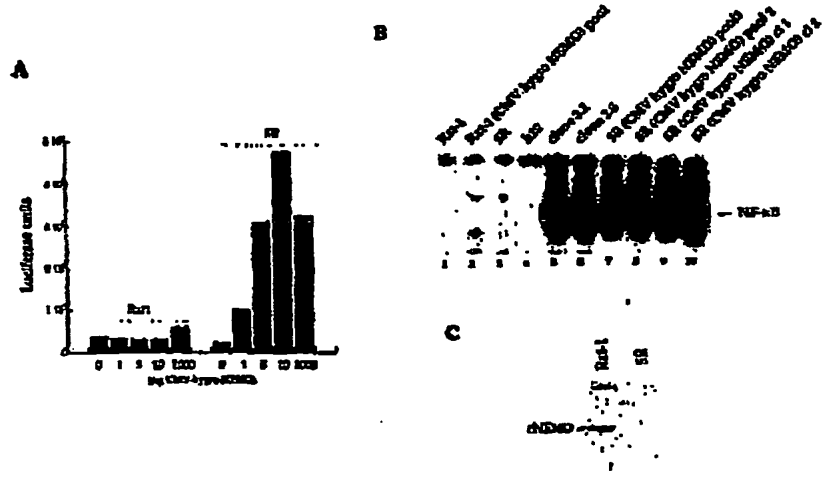

Figure 4. NEMO Complements the Defect in 5R Cells
(A) Rat-1 or 5R cells were transiently transfected with 0.25 μg of tax-luciferase and the indicated amount of CMV-hygro-NEMO. Luciferase assays were performed as described in Figure 2.
(B) Band shift assay of Rat-1- or 5R-derived cell lines stably expressing NEMO. Five micrograms of nuclear extracts derived from the following cell lines were analyzed as in Figure 1. Lane 1, wild-type Rat-1 cells. Lane 2, a pool of Rat-1 cells transfected with CMV-hygro-NEMO. Lane 3, 5R cells. Lane 4, h12 cells (5R cells containing the inducible blasticidin S resistance gene). Lanes 5 and 6, cDNA library infected h12 clones that survived the blasticidin S selection. The size of the cDNA amplified from each clone is indicated. Lanes 7 and 8, independent pools of 5R cells stably transfected with CMV-hygro-NEMO. Lanes 9 and 10, two representative 5R cell clones obtained by stable transfection with CMV-hygro-NEMO.
(C) Immunoblotting analysis of cytoplasmic extracts (100 μg) derived from Rat-1 or 5R cells was carried out with an antibody specific for NEMO. rNEMO, rat NEMO.

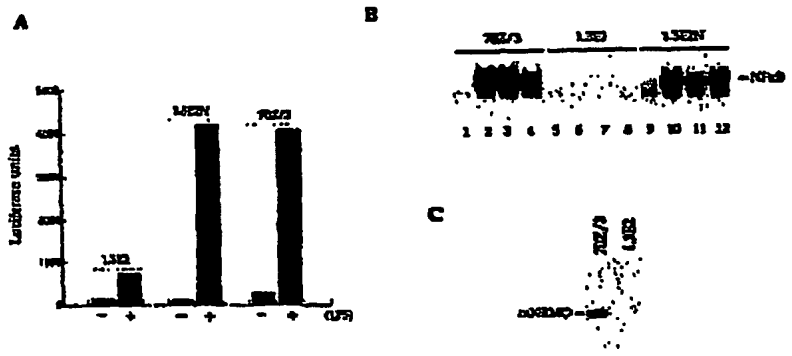

Figure 6. NEMO Complements the Defect in 1.3E2 Cells

(A) 1.3E2, 1.3E2 stably transfected with NEMO (1.3E2N), and 70Z/3 cells were transiently cotransfected with 3 μg of Igκ-luciferase and 6 μg of CMV-hygro-NEMO. After 24 hr, cells were split in two and left untreated (−) or stimulated (+) with 15 μg/ml LPS. Luciferase assays were performed as described in Figure 2.

(B) Bandshift assay of complemented 1.3E2 cells. 70Z/3 (lanes 1–4), 1.3E2 (lanes 5–8), or a pool of 1.3E2 cells stably transfected with CMV-hygro-NEMO (1.3E2N, lanes 9–12) were left untreated (lanes 1, 5, and 9) or stimulated with 15 μg/ml LPS (lanes 2, 6, and 10), 100 ng/ml PMA (lanes 3, 7, and 11), or 20 ng/ml IL-1 (lanes 4, 8, and 12). Five micrograms of nuclear extracts were then analyzed by bandshift using the H-2 Kᵇ derived κB site.

(C) Immunoblotting analysis of cytoplasmic extracts (100 μg) derived from 70Z/3 or 1.3E2 cells was carried out with the NEMO antiserum. mNEMO, mouse NEMO.

complement 1.3E2. Strikingly, as shown in Figure 5A, transient transfection of 1.3E2 with a vector expressing NEMO allowed the recovery of a wild-type NF-κB activation level after LPS stimulation. Such an effect was clearly stimulus-specific, indicating that NEMO overexpression by itself was unable to activate NF-κB. Complementation was also observed in the case of two other stimuli, IL-1 and PMA, although with less efficiency in the latter case (data not shown).

1.3E2 cells stably expressing NEMO (1.3E2N) were also prepared and tested for complementation. A mobility shift experiment presented in Figure 5B confirmed the results of the transient transfection experiments described above. NF-κB activation in response to LPS, IL-1, or PMA was found to be similar in wild-type 70Z/3 and 1.3E2N. Moreover, an immunoblot analysis revealed that NEMO is undetectable in 1.3E2 cells (Figure 5C). These results demonstrate that, as for 5R cells, the phenotype of the 1.3E2 mutant cell line is due to the absence of NEMO.

NEMO Is Part of the IκB Kinase Complex

Since NEMO appears to be critically involved in NF-κB activation by a large set of stimuli and complements cells defective in IκB phosphorylation, an attractive possibility would be that it constitutes a subunit of the 600–800 kDa kinase complex that phosphorylates IκB. Therefore, we investigated whether NEMO is associated with the inducible IκB kinase activity (Figure 6). To demonstrate this point, we carried out immune complex kinase assays on Rat-1 or 5R cells. The antiserum against NEMO immunoprecipitated a specific endogenous IκBα kinase activity from wild-type cells stimulated with TNFα. Absence of kinase activity in NEMO immunoprecipitates from 5R cells and lack of phosphorylation of a mutant IκBα polypeptide (S32A, S36A) established the specificity of the antiserum and kinase activity, respectively. Thus, NEMO is associated with an inducible endogenous IκBα kinase activity. As reported previously, an anti-IKK-1 antibody brought down a specific IκBα kinase activity from wild-type cells stimulated with TNFα for 5 min. Interestingly, no inducible IκBα kinase activity was observed in IKK-1 precipitates from 5R cell extracts.

To confirm that NEMO is an integral part of the IκB kinase complex and to determine whether it is stably associated with it before stimulation, S100 extracts were prepared from Rat-1 cells and fractionated on a Superose 6 gel filtration column. Elution of the IκB kinase, monitored with an anti-IKK-1 antibody, was mostly observed in fractions containing proteins of 600–800 kDa, as previously reported (Figure 7A). When we looked for NEMO elution, an identical profile was obtained. Immunoprecipitation of the NEMO-containing fractions with an anti-NEMO antibody allowed us to coimmunoprecipitate IKK-1 (Figure 7B). NEMO is therefore a stable component of the 600–800 kDa IκB kinase complex.

Quite remarkably, when 5R extracts were analyzed with the IKK-1 antibody, the elution peak appeared shifted toward fractions containing proteins of 300–450 kDa instead of 600–800 kDa (Figure 7A). Since the overall elution profile, as checked either by silver staining (Figure 7A, top panel) or by Western blotting against RelA (Figure 7A, bottom panel) or p105 (data not shown), was identical between Rat-1 and 5R, this observation demonstrated the requirement of NEMO for building a high molecular weight IκB kinase complex. Moreover,

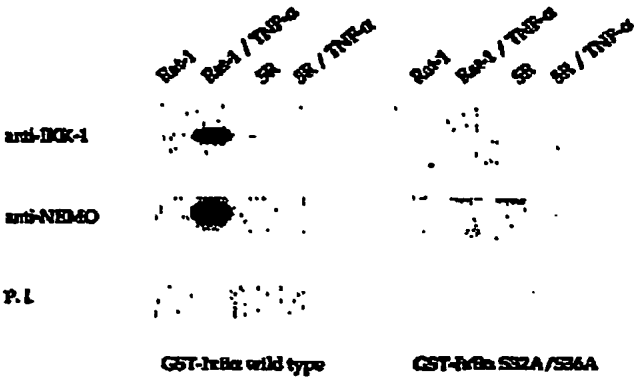

Figure 6. NEMO Is Associated with an Inducible Endogenous IκBα Kinase Activity

Rat-1 or 5R cells were treated for 5 min with or without TNFα (10 ng/ml). Cytoplasmic extracts were immunoprecipitated with either preimmune serum (P.I.), anti-IKK-1 antibody (anti-IKK-1), or NEMO antiserum (anti-NEMO), and specific IκBα kinase activity was determined by an in vitro immune complex kinase assay with GST-IκBα (1–72) wild-type or GST-IκBα (1–72) S32A/S36A mutant protein as substrates.

the absence of IκB kinase activity in 5R cells after stimulation (see above) indicates that the lower molecular weight kinase complex is refractory to activation.

NEMO Can Form Homodimers and Interacts Directly with IKK-2

The presence of a leucine zipper-like motif in NEMO led us to ask whether this molecule could dimerize. Glutaraldehyde cross-linking experiments (Figure 7C) demonstrated that NEMO was indeed able to form homodimers. The possible role of the leucine zipper-like region in this dimerization is currently under investigation.

Since NEMO is part of the IκB kinase complex, we also looked for direct interactions with known components of the complex, namely the two catalytic subunits IKK-1 and IKK-2. We carried out an in vitro analysis using ^{35}S-labeled proteins translated in wheat germ extracts (WGE). After cotranslation of VSV-IKK-2 and NEMO followed by anti-VSV immunoprecipitation, we readily detected NEMO in the immunoprecipitate (Figure 7D). The converse experiment, using NEMO plus VSV-IKK-2 and immunoprecipitating with anti-NEMO allowed the detection of VSV-IKK-2 in the immunoprecipitate (data not shown). Interestingly, such an interaction could barely be observed with IKK-1, suggesting a potential functional divergence between the two IKKs (data not shown).

Discussion

The recent description of a high molecular weight cytoplasmic complex able to phosphorylate IκBα on Ser-32 and Ser-36 (Chen et al., 1996; Lee et al., 1997) has prompted intense studies, which culminated a few months ago with the cloning of two kinases, named IKK-1 and IKK-2, or IKKα and IKKβ (Didonato et al., 1997; Mercurio et al., 1997; Regnier et al., 1997; Woronicz et al., 1997; Zandi et al., 1997). Two approaches were used to this end: one involved biochemical purification from a cytoplasmic extract derived from TNF-treated HeLa cells (Didonato et al., 1997; Mercurio et al., 1997; Zandi et al., 1997), while the other used a two-hybrid screen using as a bait NIK, a protein kinase previously shown to be involved in TNF- and IL-1–induced NF-κB activation (Regnier et al., 1997; Woronicz et al., 1997). The cloned kinases were postulated to directly phosphorylate Ser-32 and Ser-36 of IκBα, although this has not been formally demonstrated. The reason for this uncertainty is that all kinase assays reported so far rely on immunoprecipitation of transfected or in vitro translated IKK, therefore leaving open the possibility that the "true" IκB kinase is coprecipitated together with IKK and the rest of the high molecular weight complex. Immunoprecipitation of one kinase from extracts of cells transfected with the two kinases results in the coprecipitation of the second kinase, and a more detailed study has demonstrated that heteroassociation was favored over homoassociation. The sequence of IKK-1 and IKK-2 has revealed two interesting features: a leucine zipper and a HLH motif. Deletion of the LZ in one of the kinases results in the abrogation of coimmunoprecipitation with either itself or the other kinase and a strong reduction in the resulting kinase activity. However, it is unclear whether the LZ motif is required for direct interaction between the kinase subunits or between the kinase(s) and some other component of the complex. Deletion of the HLH motif leaves the coimmunoprecipitation of the two kinases intact, but it strongly reduces the resulting kinase activity. In the assays used in the above mentioned papers, transfected IKK-2 seems to exhibit a stronger basal kinase activity when compared to IKK-1 (Mercurio et al., 1997; Zandi et al., 1997). Zandi et al. (1997) also observed that cotranslation of the two kinases in wheat germ extracts resulted in no IκB kinase activity, suggesting that either posttranslational modifications or additional components of the complex (or both) are required. We also observed that cotranslation of the two kinases in wheat germ extracts precluded their association (S. T. W., unpublished data). One possibility is that the kinase subunits need to be incorporated into the 600–800 kDa complex in order to be fully active and that some critical components of the complex are absent in wheat germ extracts. In any case, all these data emphasize the importance of identifying additional components of the complex.

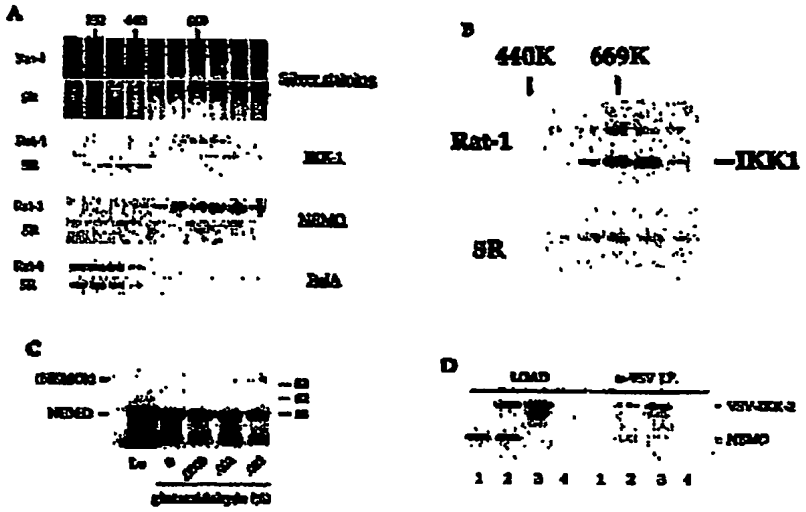

Figure 7. NEMO Is a Subunit of the IκB Kinase Complex

(A) Gel filtration analysis of NEMO and IκB kinase complex in Rat-1 and 5R cells. S100 extracts were prepared as described in Experimental Procedures and fractionated through a Superose 6 column. Fractions were analyzed by Western blotting, using antibodies specific for IKK-1 or NEMO. Analysis of NF-κB/IκB elution, using an anti-relA antibody, is also shown. To demonstrate identical elution of Rat-1 and 5R extracts, the protein profile from each fraction was analyzed by silver staining (upper panel).

(B) Coimmunoprecipitation of IKK-1 with NEMO. Positive NEMO fractions from Rat-1 and the equivalent fractions from 5R cells were immunoprecipitated with anti-NEMO, run through a 7.5% SDS-Laemmli gel, and immunoblotted with anti-IKK-1.

(C) NEMO forms homodimers. The NEMO protein was in vitro synthesized in wheat germ extract and treated with the indicated concentrations of glutaraldehyde. The reactions were immunoprecipitated with NEMO antiserum and analyzed on a 9% SDS-polyacrylamide gel. The positions of the NEMO monomer and NEMO dimer ([NEMO]$_2$) are indicated. Lo, in vitro translated product.

(D) In vitro interaction between NEMO and IKK-2. Untagged NEMO (lane 1), VSV-IKK-2 (lane 2), or both molecules (lane 3) were in vitro translated in wheat germ extract (Load). The ^{35}S-labeled products were then precipitated with anti-VSV antibody (VSV-IP). Lane 4 represents unprogrammed wheat germ extract. The relevant proteins are indicated on the right.

One approach aimed at identifying components of the NF-κB signaling pathway that has not been widely used so far is to generate mutant cell lines which are unresponsive to one or several NF-κB activating signals and to try and complement these cell lines with genomic or cDNA libraries (Ting et al., 1995). We have used here a spontaneous mutant (called 5R) of a HTLV-1 transformed Rat-1 fibroblastic cell line, which had lost its transformed morphology. This mutation was accompanied by disappearance of Tax-induced NF-κB activity, as measured by bandshift and transactivation assays. In addition, LPS-, IL-1-, dsRNA-, or TNF-induced NF-κB DNA binding activity could not be observed in the 5R cell line. However, other signaling pathways seemed to be still functional. Importantly, cell fusion experiments demonstrated that the mutation was recessive. All these observations prompted us to try to complement this cell line. The selection was based on introduction into these cells, prior to complementation, of a gene encoding resistance to the antibiotic blasticidin S driven by multimerized NF-κB–binding sites. Only the complemented cells would be expected to become resistant to blasticidin S treatment, a result of transactivation of the blasticidin S resistance gene by endogenous Tax. More than 40 independent blasticidin S–resistant clones were isolated, and bandshift analysis demonstrated the presence of a p50/relA complex in 19 analyzed clones out of 20, with an intensity similar to that observed following stimulation of wild-type Rat-1 cells with LPS or TNF. PCR amplification of DNA from 40 independent clones using primers localized in the flanking regions of the retroviral vector yielded two cross-hybridizing fragments of 2.8 and 3.2 kb. Sequencing of the amplified cDNA revealed that the 2.8 kb insert contains an open reading frame encoding a previously undescribed 412 amino acid protein, which we call NEMO. This protein is acidic (pI 5.68), unusually rich in glutamic acid and glutamine (13% each), and also contains a putative leucine zipper motif (amino acids 315–342).

Transfection of NEMO complemented the mutation in 5R cells. This led us to conclude that NEMO is necessary for activation of NF-κB by Tax. However, the presence of endogenous Tax in the 5R cell line precluded the analysis of NEMO involvement in other NF-κB activation pathways. This problem was circumvented by the use of 1.3B2, another mutant cell line that we previously characterized (Courtois et al., 1997). NF-κB activation, degradation of the three known IκB inhibitors, as well as

induced phosphorylation of IκBα could not be observed following PMA, LPS, IL-1, or dsRNA treatment of this cell line. We stably introduced the NEMO cDNA into 1.3E2 and observed that NF-κB activation by at least three of these stimuli (LPS, PMA, and IL-1) was restored. Therefore the NEMO protein is involved in the response to at least four NF-κB activating stimuli.

An interesting conclusion we can draw from complementation of the 5R cells, which regain a transformed phenotype when stably transfected with NEMO, is that NF-κB activity seems to be required for cell transformation by Tax (at least in this cell system). There have been conflicting data in the literature concerning the actual involvement of NF-κB in Tax-induced transformation (Smith and Greene, 1991; Kibajima et al., 1992; Yamaoka et al., 1995), and the formal possibility exists that NEMO is involved in another signaling pathway, beside that of NF-κB, which would be required for transformation. Clearly more work is needed to unambiguously answer this question.

The next question concerned the actual function of NEMO. Since this molecule appears to be involved in all tested NF-κB activating pathways, an obvious possibility was that it constituted one subunit of the high molecular weight IκB kinase complex. We obtained three types of arguments in favor of this hypothesis. First, immunoprecipitation of NEMO from Rat-1 cells pulled down a bona fide IκBα kinase activity, specific for the two N-terminal serines. Second, NEMO elutes as a 600–800 kDa peak from a gel filtration column performed on extracts from unstimulated Rat-1 cells, as does IKK-1. Third, immunoprecipitation of NEMO from Rat-1 fractions ranging from 600–800 kDa brings down IKK-1.

We then tested the possible interaction of NEMO with the two catalytic subunits of the complex, IKK-1 and IKK-2. In vitro cotranslation of IKK-2 and NEMO in wheat germ extract followed by immunoprecipitation demonstrated that the two proteins could interact with each other. In contrast, an interaction between NEMO and IKK-1 could barely be detected under these conditions. We also demonstrated that NEMO can form homodimers.

The fact that NEMO interacts with IKK-2 and apparently not with IKK-1 introduces an asymmetry between the two kinases. The respective functions of these two molecules, however, are still unclear; in particular, the question of whether the two serines in the N-terminal regions of the three inhibitors are phosphorylated by the same or different kinases is currently unknown. Similarly, the three inhibitors might be phosphorylated by the same complexes or by different ones. The issue of the actual function of NEMO in the complexes will be addressed by a detailed molecular analysis of the IκB kinase complex in 5R and 1.3E2 cells, as well as by a mutational analysis of NEMO followed by reintroduction of the mutated molecules into 5R or 1.3E2 cells. These points are currently under investigation.

Another intriguing question concerns the actual defects in 5R and 1.3E2 cells. Immunoblot analysis indicates that the NEMO protein is absent from both 5R and 1.3E2 cells and that in 5R cells, which exhibit no IKK-1–associated kinase activity, the high molecular weight complex does not seem to exist. Although unlikely, the formal possibility exists that a complex which would not contain IKK-1 exists in these cells, but in any case they exhibit no inducible phosphorylation of IκB. Interestingly, IKK-1 can be detected in a 300–450 kDa complex in 5R cells, therefore indicating that NEMO is required for the formation of a 500–800 kDa functional IKK complex, and probably plays a role as a structural component of this complex. Further work will be needed to determine which components of the functional complex (besides NEMO) are missing from this smaller nonfunctional complex and which components of the complex (besides IKK-2) already interact with NEMO.

It was unexpected that two independently isolated mutant cell lines could be complemented by the same cDNA. The selection for LPS-unresponsive derivatives of 70Z/3 yielded several types of mutant cell lines, but only 1.3E2 was also unresponsive to other NF-κB activating stimuli, and the fact that it grows faster than the wild-type 70Z/3 probably facilitated its isolation. In Tax-transformed Rat-1 cells, 5R was the only NF-κB–defective cellular revertant that could be isolated. This leads to the intriguing possibility that mutating the *nemo* gene might be the only means of knocking out NF-κB activation by a single gene mutation. Future inactivation experiments of the other components of the complex (including IKK-1 and IKK-2) will tell whether this hypothesis is correct and whether NEMO is a relevant target for future drugs aimed at blocking NF-κB activation.

Experimental Procedures

Cells and Transfections

The 70Z/3 murine pro-B cell line and the NF-κB unresponsive mutant 1.3E2 were maintained in RPMI medium supplemented with 10% fetal calf serum and 50 μM β-mercaptoethanol. 70Z/3 and 1.3E2 cells were transiently transfected as described (Courtois et al., 1997). Isolated stable clones were prepared as described (Whiteside et al., 1995). Rat-1 and 5R cells were grown in DMEM supplemented with 10% fetal calf serum and transfected using the calcium phosphate coprecipitation method. For measurement of luciferase activity in transiently transfected Rat-1 or 5R cells, approximately 2×10^5 cells were transfected with 0.25 μg of a reporter plasmid, 0.25 μg of EF1-lacZ plasmid, and 1 μg of either vector or effector plasmid. Cells were harvested 40–45 hr after transfection. The amount of lysate used for luciferase assay was determined on the basis of β-galactosidase activity. The results shown are representative of one experiment carried out in duplicate and averaged. Each experiment was repeated at least three times, with similar results.

Phoenix-Eco packaging cells were a kind gift of G. Nolan (Stanford University).

Plasmids

A BLAST search of GenBank with the human IKK-1 cDNA sequence revealed the presence of an EST clones encoding for a single IKK-1–related cDNA. This clone was obtained from the UK HGMP, and the cDNA insert was used to screen an adult human liver cDNA library. Positively hybridizing phage were isolated, and both strands of the largest insert obtained were sequenced by the dideoxy termination method (Sequenase, USB). IKK-2 coding sequences were amplified by PCR and inserted into vectors that allowed the in vitro and in vivo expression of proteins fused to the VSV epitope. Rat IKK-1 was amplified by PCR from an EST clone and subcloned into the same vector. The plasmids Igκ-luciferase and SRE-luciferase have been described previously (Courtois et al., 1997); HTLV-1 LTR-luciferase was a kind gift of P. Jalinot (Ecole Normale Superieure de Lyon).

The plasmid Igκ2barH was constructed by ligating a 1.5 kb HindIII/

BamHI fragment of the plasmid pSV2bsr (Izumi et al., 1991) with a 5.1 kb HindIII/BamHI fragment of the plasmid conA*lacZ*-κB (Fiering et al., 1990), which contains three tandem copies of the NF-κB oligonucleotide derived from the Igκ sequence (TCAGAGGGGACTTTCCGAG) followed by a minimal IL-2 promoter.

A Tax expression vector, pC*rtax*, was constructed by inserting a BamHI fragment of the plasmid pUC*wtax* (Yamaoka et al., 1996) containing the entire coding sequence of Tax to the unique BamHI site of pCMV-Neo-Bam vector (Baker et al., 1990).

A 2.8 kb PCR product derived from genomic DNA of a blasticidin S-resistant 5R clone was obtained using primers located in the retroviral vector pCTV1 (Whitehead et al., 1995). This PCR product was then digested with SalI, subcloned into pBluescript for sequencing, or into the XhoI site of the CMV-hygro vector (a kind gift of F. Aurade, Institut Pasteur). Full construction details are available on request.

Reagents

LPS, PMA, poly (I-C), chloroquine, and polybrene were from Sigma. Recombinant hIL-1β was from Biogen (Geneva, Switzerland). Recombinant TNFα was from Genzyme. Blasticidin S was purchased from ICN. Absence of endotoxin contamination in all these reagents, except LPS, was checked with a polymyxin B assay (Shapiro and Dinarello, 1995).

Antisera

Rabbit antiserum against IκBα was a kind gift of J. DiDonato and M. Karin (UCSD). Anti-VSV was mouse monoclonal P5D4. Anti-Tax was mouse monoclonal MI73 (Mori et al., 1987). Anti-IKK-1 antibody was from Santa Cruz. Anti NEMO rabbit polyclonal antiserum (serum 44106) was raised against a TrpE fusion of a fragment encompassing amino acids 30–329 of murine NEMO in the Path11 vector (Spindler et al., 1984).

Preparation of Cell Extracts

Cells were washed with PBS and resuspended at 10^6 cells/10 μl in hypotonic solution (10 mM HEPES [pH 7.6], 10 mM KCl, 2 mM $MgCl_2$, 1 mM DTT, 0.1 mM EDTA supplemented with a protease inhibitor cocktail [Boehringer]). After 10 min at 4°C, NP40 was added to 1% and the cells centrifuged in a microfuge for 20 s. The supernatant, containing the cytoplasmic fraction, was recovered. One volume of 2× Laemmli buffer containing 20% β-mercaptoethanol was added, and the sample was boiled for 5 min. The nuclear pellet was briefly washed with hypotonic buffer and resuspended in 40 μl of extraction buffer (50 mM HEPES [pH 7.6], 50 mM KCl, 350 mM NaCl, 0.1 mM EDTA, 1 mM DTT, 0.1 mM PMSF, 10% glycerol). After a 30 min incubation on ice, with occasional agitation, the DNA was pelleted by centrifuging at 14000 rpm for 10 min. The supernatant, containing the nuclear fraction, was recovered and quickly frozen on dry ice. Samples were stored at −80°C.

Preparation of S100 Extracts and Gel Filtration Analysis

Fifty million cells were washed in PBS and resuspended in 600 μl of 50 mM Tris (pH 7.5), 1 mM EGTA. Cells were lysed by thirty passages through a 26-gauge needle. After centrifugation for 10 min at 15000 rpm, the supernatant was recovered and complemented with 1 mM DTT, 0.025% Brij 35, and a cocktail of proteases and phosphatases inhibitors. S100 were prepared by centrifuging the cytoplasmic extracts for 30 min at 62000 rpm in a TLA 100.2 rotor (Beckman). After adding 10% glycerol, the S100 extracts were quickly frozen in dry ice and stored in liquid nitrogen. Gel filtration chromatography was carried out on a Superose 6 column (Pharmacia) precalibrated with aldolase (158 kDa), catalase (232 kDa), ferritin (440 kDa), and thyroglobulin (669 kDa). Five hundred microliter fractions were recovered and directly analyzed by Western blotting or immunoprecipitated with anti-NEMO. Silver staining of the fractions was performed with a Silver Stain Plus Kit (Biorad).

Western Blot Analysis

Proteins from cytoplasmic extracts were fractionated on 10% SDS-polyacrylamide gels, transferred onto Immobilon membranes (Millipore), and blots were revealed with an enhanced chemiluminescence detection system (ECL, Amersham).

In Vitro Translation and Cross-Linking

Translations and coimmunoprecipitation experiments were performed as described previously using TNT kits (Promega) (Kieran et al., 1990). For dimerization experiments, translation reactions were diluted thirty times with phosphate buffered saline, treated with glutaraldehyde at room temperature for 20 min, with 100 mM of Tris-HCl (pH 7.4) for 20 min, and subjected to immunoprecipitation after addition of an equal volume of TNT buffer (NaCl 200 mM, Tris-HCl 20 mM [pH 7.5], Triton X-100 1% supplemented with protease and phosphatase inhibitors).

Immunoprecipitations and Kinase Assays

Cytoplasmic extracts were subjected to immunoprecipitation with anti-IKK-1 antibody, anti-NEMO, or preimmune serum in TNT buffer and collected on protein A-Sepharose beads, which were then washed three times with TNT buffer and three times with kinase buffer (20 mM HEPES, 10 mM $MgCl_2$, 100 μM Na_3VO_4, 20 mM β-glycerophosphate, 2 mM DTT, 50 mM NaCl [pH 7.6]). Kinase reactions were for 30 min at 30°C using 5 μCi of [γ-^{32}P]-ATP and GST-IκBα (1–72) wild type or GST-IκBα (1–72) S32A/S36A mutant protein as substrates. The reaction products were analyzed on 10% SDS-polyacrylamide gels and revealed by autoradiography for 3 hr at room temperature.

Electrophoretic Mobility Shift Assays

Five micrograms of nuclear extracts were added to 15 μl of binding buffer (10 mM HEPES [pH 7.6], 100 mM NaCl, 1 mM EDTA, 10% glycerol final), 1 μg poly (dI-dC), and 0.5 ng ^{32}P-labeled κB probe derived from the H-2K^b promoter (Kieran et al., 1990), and incubated for 30 min at room temperature. Samples were run on a 5% polyacrylamide gel in 0.5× TBE.

Viral Stocks and Infection

T28 cells, a murine T cell hybridoma (Pysaniak et al., 1994), were cultured in Dulbecco's modified Eagle's medium supplemented with 10% fetal bovine serum. Total mRNA from exponentially growing T28 cells was used as template for cDNA synthesis, using random hexamer primers. Procedures for cDNA synthesis and cloning were as described previously (Whitehead et al., 1995). The cDNA was ligated into pCTV1 (Whitehead et al., 1995), yielding 3.8×10^6 cDNA clones. Complexities of the libraries were as follows: L35, 470,000 clones (0.9 kb and up); L36, 600,000 clones (2.2–3.5 kb). The Phoenix-Eco packaging cell line was used for transient transfection with DNA from the L35 or L36 libraries. To determine the virus titer on 5R cells, a cDNA library (L20) cloned into the pCTV3 vector (Whitehead et al., 1995), which carries a hygromycin resistance gene, was transfected by the calcium phosphate method into Phoenix-Eco cells, and the resultant supernatants were titered by the appearance of hygromycin resistant 5R cells. This library produced viral titers of ~2–3×10^5/ml. We produced viral supernatants for complementation experiments by transfecting approximately 1.5×10^7 Phoenix cells plated 24 hr before with 20 μg of the L35 or L36 library DNA in the presence of 25 μM chloroquine. Supernatants were recovered every 12 hr from 36–72 hr after transfection and either immediately used for infection of h12 cells or snap frozen in dry ice and stored at −80°C. Approximately 10^6 h12 cells were plated 12–15 hr before infection on a 100 mm petri dish and exposed to 3 ml of viral supernatant in the presence of 3 ml of conditioned medium and 10 μg/ml of polybrene. Twelve hours after starting the infection, the viral supernatant was removed and cells were cultured for an additional 24 hr in normal growth medium. Blasticidin S was added to a final concentration of 10 μg/ml 36 hr after infection. The selection medium was replaced at least every 5 days, and the resultant cell clones were isolated with cloning cylinders. We used a total of 30×10^6 h12 cells for infection with virus stock obtained using 20 μg of L35 or L36 library DNA and finally isolated a similar number of independent cell clones for the two cDNA libraries.

Acknowledgments

We would like to thank S. Memet (Institut Pasteur) for the gift of the EF1-lacZ construct, F. Aurade (Institut Pasteur) for the gift of the CMV-hygro vector, P. Jalinot (Ecole Normale Superieure de Lyon)

for the gift of the HTLV-1-LTR-luc vector, A. Veillette (McGill University) for the gift of the Path11 vector, J. A. DiDonato and M. Karin (UCSD) for the gift of anti-IκBα antibodies, G. R. Crabtree (Stanford University) for the gift of the cx16lacZ-κB plasmid, G. P. Nolan (Stanford University) for the gift of the Phenix-Eco cell line, and M. Veron (Institut Pasteur) for helpful discussions. S. Y. would like to thank Dr. Masakazu Hatanaka for his support during isolation of 5R cells. G. C. wishes to thank J.-C. Epinat for constant support throughout this project. S. T. W. is the recipient of a fellowship from Association Nationale de Recherches sur le Sida (ANRS), and R. W. is the recipient of a fellowship from Sidaction. This work was supported in part by grants from the Medical Research Council of Canada, the British Columbia Health Research Foundation, and the Leukemia Research Fund of Canada to R. K., and from ANRS, Association pour la recherche sur le cancer, Ligue Nationale contre le Cancer, and European Community to A. I.

Received February 17, 1998; revised May 7, 1998.

References

Baker, S.J., Markowitz, S., Fearon, E.R., Willson, J.K., and Vogelstein, B. (1990). Suppression of human colorectal carcinoma cell growth by wild-type p53. Science 249, 912–915.

Baldwin, A.S. (1996). The NF-κB and IκB proteins: new discoveries and insights. Annu. Rev. Immunol. 14, 649–683.

Chen, Z.J., Parent, L., and Maniatis, T. (1996). Site-specific phosphorylation of IκBα by a novel ubiquitination-dependent protein kinase activity. Cell 84, 853–862.

Courtois, G., Whiteside, S.T., Sibley, C.H., and Israel, A. (1997). Characterization of a mutant cell line that does not activate NF-κB in response to multiple stimuli. Mol. Cell. Biol. 17, 1441–1449.

Darnell, J.E., Jr., Kerr, I.M., and Stark, G.R. (1994). Jak-STAT pathways and transcriptional activation in response to IFNs and other extracellular signaling proteins. Science 264, 1415–1421.

DiDonato, J.A., Hayakawa, M., Rothwarf, D.M., Zandi, E., and Karin, M. (1997). A cytokine-responsive IκB kinase that activates the transcription factor NF-κB. Nature 388, 548–554.

Fiering, S., Northrop, J.P., Nolan, G.P., Mattila, P.S., Crabtree, G.R., and Herzenberg, L.A. (1990). Single cell assay of a transcription factor reveals a threshold in transcription activated by signals emanating from the T-cell antigen receptor. Genes Dev. 4, 1823–1834.

Izumi, M., Miyazawa, H., Kamakura, T., Yamaguchi, I., Endo, T., and Hanaoka, F. (1991). Blasticidin S-resistance gene (bsr): a novel selectable marker for mammalian cells. Exp. Cell Res. 197, 229–233.

Kieran, M., Blank, V., Logeat, F., Vandekerckhove, J., Lottspeich, F., LeBail, O., Urban, M.B., Kourilsky, P., Baeuerle, P.A., and Israel, A. (1990). The DNA binding subunit of NF-κB is identical to factor KBF1 and homologous to the rel oncogene product. Cell 62, 1007–1018.

Kitajima, I., Shinohara, T., Bilakovics, J., Brown, D.A., Xu, X., and Nerenberg, M. (1992). Ablation of transplanted HTLV-I Tax-transformed tumors in mice by antisense inhibition of NF-κB. Science 258, 1792–1795.

Lee, F.S., Hagler, J., Chen, Z.J., and Maniatis, T. (1997). Activation of the IκBα kinase complex by MEKK1, a kinase of the JNK pathway. Cell 88, 213–222.

May, M.J., and Ghosh, S. (1998). Signal transduction through NF-κB. Immunol. Today 19, 80–88.

Mercurio, F., Zhu, H.Y., Murray, B.W., Shevchenko, A., Bennett, B.L., Li, J.W., Young, D.B., Barbosa, M., and Mann, M. (1997). IKK-1 and IKK-2: cytokine-activated IκB kinases essential for NF-κB activation. Science 278, 860–866.

Mori, K., Sabe, H., Siomi, H., Iino, T., Tanaka, A., Takeuchi, K., Hirayoshi, K., and Hatanaka, M. (1987). Expression of a provirus of human T cell leukaemia virus type I by DNA transfection. J. Gen. Virol. 68, 499–506.

Pyszniak, A.M., Welder, C.A., and Takei, F. (1994). Cell surface distribution of high-avidity LFA-1 detected by soluble ICAM-1-coated microspheres. J. Immunol. 152, 5241–5249.

Regnier, C.H., Song, H.Y., Gao, X., Goeddel, D.V., Cao, Z., and Rothe, M. (1997). Identification and characterization of an IκB kinase. Cell 90, 373–383.

Shapiro, L., and Dinarello, C.A. (1995). Osmotic regulation of cytokine synthesis in vitro. Proc. Natl. Acad. Sci. USA 92, 12230–12234.

Smith, M.R., and Greene, W.C. (1991). Type I human T cell leukemia virus tax protein transforms rat fibroblasts through the cyclic adenosine monophosphate response element binding protein/activating transcription factor pathway. J. Clin. Invest. 88, 1038–1042.

Spindler, K.R., Rosser, D.S., and Berk, A.J. (1984). Analysis of adenovirus transforming proteins from early regions 1A and 1B with antisera to inducible fusion antigens produced in Escherichia coli. J. Virol. 49, 132–141.

Ting, A.T., Pimentel-Muiños, F.X., and Seed, B. (1996). RIP mediates tumor necrosis factor receptor 1 activation of NF-κB but not Fas/APO-1-initiated apoptosis. EMBO J. 15, 6189–6196.

Velazquez, L., Fellous, M., Stark, G.R., and Pellegrini, S. (1992). A protein tyrosine kinase in the interferon α/β signaling pathway. Cell 70, 313–322.

Verma, I.M., Stevenson, J.K., Schwarz, E.M., Van Antwerp, D., and Miyamoto, S. (1995). Rel/NF-κB/IκB family: intimate tales of association and dissociation. Genes Dev. 9, 2723–2735.

Whitehead, I., Kirk, H., and Kay, R. (1995). Expression cloning of oncogenes by retroviral transfer of cDNA libraries. Mol. Cell. Biol. 15, 704–710.

Whiteside, S.T., Ernst, M.K., LeBail, O., Laurent-Winter, C., Rice, N.R., and Israel, A. (1995). N- and C-terminal sequences control degradation of MAD3/IκBα in response to inducers of NF-κB activity. Mol. Cell. Biol. 15, 5339–5345.

Woronicz, J.D., Gao, X., Cao, Z., Rothe, M., and Goeddel, D.V. (1997). IκB kinase-β: NF-κB activation and complex formation with IκB kinase-α and NIK. Science 278, 866–869.

Yamaoka, S., Inoue, H., Sakurai, M., Sugiyama, T., Hazama, M., Yamada, T., and Hatanaka, M. (1996). Constitutive activation of NF-κB is essential for transformation of rat fibroblasts by the human T-cell leukemia virus type I Tax protein. EMBO J. 15, 873–887.

Yoshida, M., Suzuki, T., Fujisawa, J., and Hirai, H. (1995). HTLV-1 oncoprotein Tax and cellular transcription factors. Curr. Topics Microbiol. Immunol. 193, 79–89.

Zandi, E., Rothwarf, D.M., Delhase, M., Hayakawa, M., and Karin, M. (1997). The IκB kinase complex (IKK) contains two kinase subunits, IKK-α and IKK-β, necessary for IκB phosphorylation and NF-κB activation. Cell 91, 243–252.

GenBank Accession Number

The accession number for the partial mouse nemo cDNA sequence reported in this paper is AF069542.

HSF. No significant decrease of the absorption at 800 nm was detected within 8 hours.
19. T. J. Kleen and V. J. Dwarkas, Biochemistry 32, 5177 (1993).
20. N. H. Horowitz, Proc. Natl. Acad. Sci. U.S.A. 31, 153 (1945).
21. L. Holm and C. Sander, Nucleic Acids Res. 26, 316 (1998).
22. J. A. Cerli and P. C. Babbitt, Curr. Opin. Chem. Biol. 2, 607 (1998).
23. M. S. Hasson et al., Proc. Natl. Acad. Sci. U.S.A. 95, 10396 (1998).
24. C. Jürgens et al., Proc. Natl. Acad. Sci. U.S.A. 97, 9925 (2000).
25. E. M. Marcotte et al., Science 285, 751 (1999).
26. R. F. Doolittle, Annu. Rev. Biochem. 64, 287 (1995).
27. B. Morgenstern and W. R. Atchley, Mol. Biol. Evol. 16, 1654 (1999).
28. G. E. Cohen, J. Appl. Crystallogr. 30, 1160 (1997).
29. The figures were prepared using the graphics software MOLSCRIPT version 2.1 [P. J. Kraulis, J. Appl. Crystallogr. 24, 946 (1991)] and GRASP version 1.3 [A. Nicholls, K. A. Sharp, N. Honig, Proteins 11, 281 (1991)].

30. We thank K. Kirschner for discussions, V. Lamzin for comments on the manuscript, and S. Beismann-Driemeyer for the provision of Hsf mutants. M.H.-S. is a fellow of the Hans-Böckler-Stiftung. The atomic coordinates have been deposited in the Protein Data Bank (code for HisA: 1QO2; code for HisF: 1THF). This work was supported by the Deutsche Forschungsgemeinschaft (grants STE 691/2-1, STE 691/2-2, and STE 691/3-1 to R.S., WI 1058/5-1 and WI 1058/5-2 to M.W., and a Heisenberg Fellowship to R.S.).

29 April 2000; accepted 6 July 2000

Selective Inhibition of NF-κB Activation by a Peptide That Blocks the Interaction of NEMO with the IκB Kinase Complex

Michael J. May,[1] Fulvio D'Acquisto,[1] Lisa A. Madge,[2] Judith Glöckner,[1] Jordan S. Pober,[2] Sankar Ghosh[1]*

Activation of the transcription factor nuclear factor (NF)–κB by proinflammatory stimuli leads to increased expression of genes involved in inflammation. Activation of NF-κB requires the activity of an inhibitor of κB (IκB)-kinase (IKK) complex containing two kinases (IKKα and IKKβ) and the regulatory protein NEMO (NF-κB essential modifier). An amino-terminal α-helical region of NEMO associated with a carboxyl-terminal segment of IKKα and IKKβ that we term the NEMO-binding domain (NBD). A cell-permeable NBD peptide blocked association of NEMO with the IKK complex and inhibited cytokine-induced NF-κB activation and NF-κB–dependent gene expression. The peptide also ameliorated inflammatory responses in two experimental mouse models of acute inflammation. The NBD provides a target for the development of drugs that would block proinflammatory activation of the IKK complex without inhibiting basal NF-κB activity.

The regulatory protein NEMO (also named IKK-γ) is required for proinflammatory activation of the IκB-kinase (IKK) complex (*1–5*). We surmised that prevention of the NEMO-IKK interaction would inhibit signal-induced NF-κB activation and, therefore, attempted to identify the mechanism of interaction between NEMO and IKKβ. We analyzed the interaction of NEMO fused at its NH_2-terminus to glutathione *S*-transferase (GST-NEMO, see Fig. 1A) with IKKβ mutants lacking the catalytic, leucine zipper, and helix-loop-helix (HLH) domains [Fig. 1A and (*6*)]. None of the mutants interacted with GST, whereas all three COOH-terminal fragments (307–756, 458–756, and 486–756) interacted with GST-NEMO [Fig. 1A and (*7*)]. None of the NH_2-terminal fragments (1–458, 1–605, or 1–644) precipitated with GST-NEMO, demonstrating that NEMO interacts with the COOH-terminus of IKKβ distal to the HLH. An IKKβ mutant consisting of only residues 644 to 756 associated with GST-NEMO, confirming that this region mediates interaction between the molecules (Fig. 1B). Furthermore, IKKβ(644–756) dose-dependently inhibited cytokine-induced NF-κB activation in transfected HeLa cells [Fig. 1C and (*6*, *8*)]. The most likely explanation for this result is that overexpressed IKKβ(644–756) associates with endogenous NEMO and prevents recruitment of regulatory proteins to the IKK-complex.

To identify the domain of NEMO (*1–3*, *9*) required for association with IKKβ, we analyzed the interaction of GST-IKKβ(644–756) with truncation mutants of NEMO (Fig. 1D). IKKβ(644–756) associated with NEMO fragments 1–196, 1–302, and 44–419 but not 197–419 or 86–419, indicating that the interaction domain lies between residues 44 and 86. A deletion mutant lacking this α-helical region (residues 50–93, delαH) did not interact with IKKβ(644–756) (Fig. 1E) and inhibited tumor necrosis factor–α (TNF-α)–induced NF-κB activity (Fig. 1F), confirming the dominant-negative effects of the NEMO COOH-terminus (*2*, *3*). These findings suggest that the NH_2-terminus of NEMO anchors it to the IKK-complex, leaving the remainder of the molecule accessible for interacting with regulatory proteins.

The IKKβ COOH-terminus contains a region with identity to IKKα (denoted α_1), a serine-rich domain (*10*), and a serine-free region (Fig. 2A). Analysis of IKKβ mutants omitting each of these segments indicated that NEMO associates with the COOH-terminus after residue 734 (Fig. 2A). The region of IKKβ from F734 to T744 [α_2 in Fig. 2B (*11*)] contains a segment that is identical to the equivalent sequence in IKKα. The IKKβ sequence then extends for 12 residues forming a glutamate-rich region (Fig. 2B) that we speculated would be the NEMO interaction domain. However, a truncation mutant omitting this region (1–744) associated with GST-NEMO (Fig. 2C). Thus, the NEMO-interaction domain of IKKβ appears to be within the α_2-region of the COOH-terminus.

We next used the IKKβ(1–744) and (1–733) mutants to determine the effects of NEMO association on IKKβ activity and found that IKKβ(1–733) induced NF-κB activation that was approximately 1.5 to 2 times that induced by wild-type IKKβ (Fig. 2D). Furthermore, NF-κB activity induced by IKKβ(1–744) was identical to that induced by wild-type IKKβ. Thus, NEMO may maintain basal IKKβ activity as well as regulate its signal-induced activation.

Because the α_2-region of IKKβ resembles the COOH-terminus of IKKα (Fig. 2B), we tested the ability of IKKα to interact with NEMO (*7*). IKKα and IKKβ expressed in wheat germ extract both associated with GST-NEMO demonstrating that the individual interactions are direct (Fig. 3A). Further analysis revealed that IKKα interacts with NEMO through the COOH-terminal region containing the six amino

[1]Section of Immunobiology and Department of Molecular Biophysics and Biochemistry, Howard Hughes Medical Institute, Yale University School of Medicine, New Haven, CT 06510, USA. [2]Interdepartmental Program in Vascular Biology and Transplantation, Boyer Center for Molecular Medicine, Yale University School of Medicine, New Haven, CT 06536, USA.

*To whom correspondence should be addressed. E-mail: sankar.ghosh@yale.edu

acids shared with the α_2-region of IKKβ (Fig. 3B). In contrast, the IKK-related kinase IKKi (*12*), which does not contain an α_2-homologous region, failed to interact with NEMO (*7*). Gene-targeting has demonstrated a profound difference between IKKα and IKKβ activation by TNF-α (*13*). Our findings suggest that this difference is not due to differential interaction with NEMO.

A mutant of IKKβ lacking the six α_2 region residues did not associate with GST-NEMO (Fig. 3C). Therefore, we have named this sequence the NEMO-binding domain (NBD) (*7*). We examined the effects of point mutations within the NBD and found that replacement of D738, W739, or W741 with alanine prevented association with NEMO (Fig. 3D). In contrast, replacement of L737, S740, or L742 with alanine did not affect NEMO binding (Fig. 3D). To test the effects of these mutations on IKKβ function, we measured NF-κB activation in transfected HeLa cells. Consistent with previous results (Fig. 2D), mutants that did not bind NEMO activated NF-κB to a greater extent than did wild-type IKKβ or IKKβ(1–744), whereas NEMO-binding mutants activated to the same level as the controls (Fig. 3E). These data strongly support the hypothesis that NEMO plays a role in the down-regulation of IKKβ activity.

The ability to selectively inhibit NF-κB activation induced by proinflammatory cytokines may be crucial for the treatment of inflammation. However, inhibition of the catalytic activity of the IKKs may block basal NF-κB activity and impair its function as a survival factor, leading to potentially toxic side effects. We reasoned that a more effective anti-inflammatory drug might result from blocking the interaction of NEMO with the IKK complex. Therefore, we designed cell-permeable peptides (*11*, *14*) spanning the IKKβ NBD and determined their ability to disrupt the IKKβ-NEMO interaction. The wild-type NBD peptide (Fig. 4A) consisted of the region from T735 to E745 of IKKβ fused with a sequence derived from the Antennapedia homeodomain that mediates membrane translocation (*15*). The mutant peptide was identical except that W739 and W741 in the NBD were mutated to alanines (Fig. 4A). Only the wild-type NBD peptide dose-dependently inhibited in vitro interaction of IKKβ with NEMO (Fig. 4B). Furthermore, after incubating HeLa cells with the peptides, the wild-type, but not the mutant, NBD peptide disrupted formation of the endogenous IKK complex (Fig. 4C).

The effects of the NBD peptides on IKK activation were determined by immune-complex kinase assays (*16*) by using IKK complexes precipitated from TNF-α–stimulated HeLa cells pretreated with peptides. The wild-type, but not the mutant, peptide de-

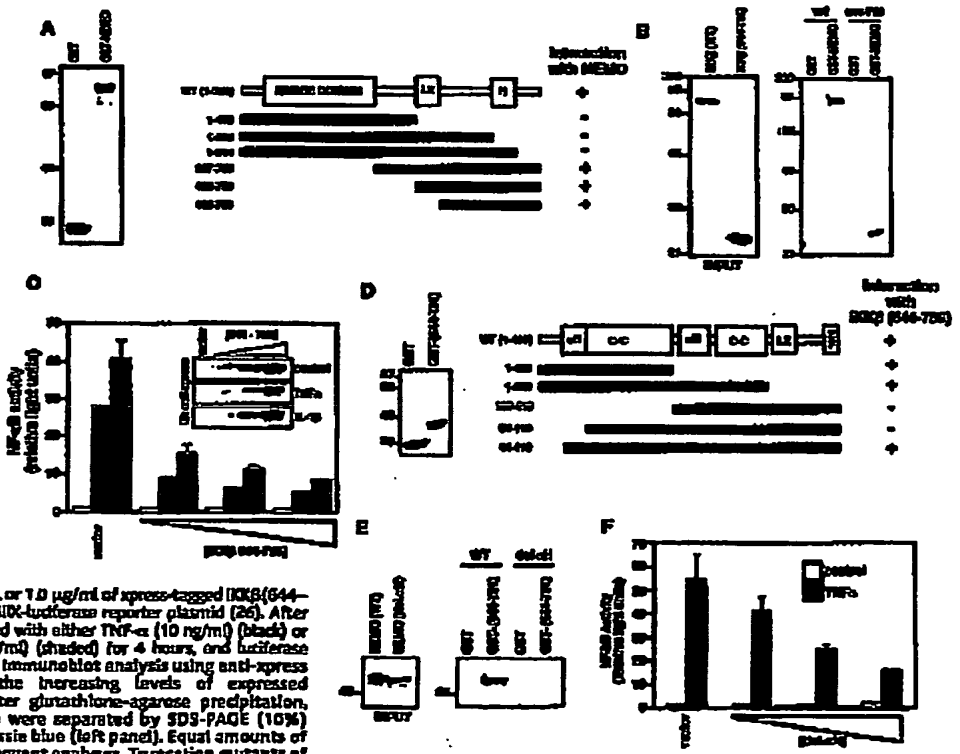

Fig. 1. Interaction of the COOH-terminus of IKKβ with the first α-helical region of NEMO. (A) GST and GST-NEMO were precipitated with glutathione-agarose, separated by SDS-PAGE (10%), and stained with Coomassie blue (left panel). Equal amounts of each were used in subsequent pull-down experiments. The truncation mutants of IKKβ (WT, wild-type; LZ, leucine zipper; H, HLH) were expressed (*6*) and used for GST pull-down (right panel, see (*7*)) as previously reported (*26*). NEMO-interacting mutants are indicated (+). (B) In vitro translated IKKβ and IKKβ(644–756) (left panel) were used for pull-down analysis (right panel). (C) HeLa cells were transiently transfected (*8*) with pcDNA-3.1-xpress (vector) or 0.25, 0.5, or 1.0 μg/ml of xpress-tagged IKKβ(644–756) together with the pBIIX-luciferase reporter plasmid (*26*). After 48 hours, cells were treated with either TNF-α (10 ng/ml) (black) or interleukin (IL)-1β (10 ng/ml) (shaded) for 4 hours, and luciferase activity was measured (*8*). Immunoblot analysis using anti-xpress (inset) demonstrates the increasing levels of expressed IKKβ(644–756). (D) After glutathione-agarose precipitation, GST and GST(644–756) were separated by SDS-PAGE (10%) and stained with Coomassie blue (left panel). Equal amounts of each were used for subsequent analyses. Truncation mutants of NEMO were constructed (C-C, coiled coil; LZ, leucine zipper), expressed, and used for pull-down analysis (right panel, see (*6*, *24*)), and interacting mutants are indicated (+). None of the mutants interacted with GST (*17*). (E) Wild-type NEMO and a mutant lacking the first α-helical region (delLH) were expressed (input) and used for pull-down analysis by using the proteins in (D, left). (F) NF-κB activity (*8*) in HeLa cells transfected with pBIIX-luciferase and either pcDNA-3 (vector) or delLH (0.25, 0.5, or 1.0 μg/ml) for 48 hours then treated for 4 hours with TNF-α (10 ng/ml).

ceased TNF-α–induced IKK activity [Fig. 4D and (7)], whereas neither peptide inhibited TNF-α–induced phosphorylation of c-Jun (7). Electrophoretic mobility shift analysis (EMSA) demonstrated that only the wild-type peptide inhibited TNF-α–stimulated nuclear translocation of NF-κB in HeLa cells (Fig. 4E), whereas neither peptide affected DNA binding of the transcription factor Oct-1 (17). Furthermore, the wild-type NBD peptide inhibited TNF-α–induced NF-κB activity (Fig. 4F, upper panel). Basal NF-κB activity was enhanced approximately twofold by the wild-type peptide (Fig. 4F, lower panel), suggesting that removal of NEMO slightly increases the basal, intrinsic activity of the IKK complex while abolishing its responsiveness to TNF-α.

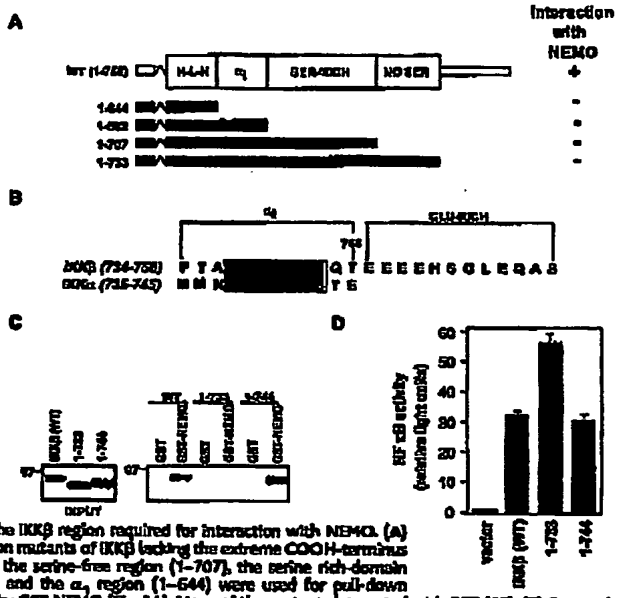

Fig. 2. The IKKβ region required for interaction with NEMO. (A) Truncation mutants of IKKβ lacking the extreme COOH-terminus (1–733), the serine-free region (1–707), the serine rich-domain (1–662), and the α_2 region (1–644) were used for pull-down analysis by GST-NEMO (Fig. 1A). None of the mutants interacted with GST (17). (B) Comparison of the COOH-termini of IKKα and IKKβ indicating the α_2 and glutamate-rich regions and the six identical amino acids (shaded). (C) Wild-type IKKβ and the truncation mutants (1–733 and 1–744, input) were used for in vitro pull-down analysis with either GST or GST-NEMO. (D) NF-κB activity in HeLa cells transfected with 1 μg/ml of the indicated constructs or vector (pcDNA-3) together with pBIIX-luciferase (8).

Many genes involved in inflammation are regulated by NF-κB (18). E-selectin is a leukocyte adhesion molecule expressed by vascular endothelial cells after activation by proinflammatory cytokines (19). To assess the anti-inflammatory potential of the NBD peptides, we pretreated human umbilical vein endothelial cells with the peptides then induced E-selectin expression with TNF-α. The wild-type peptide caused low-level expression of E-selectin (Fig. 5A). However, TNF-α–induced E-selectin was diminished in cells treated with wild-type, but not mutant, peptide (Fig. 5A). The wild-type NBD peptide also inhibited LPS-induced nitric oxide (NO) release from a macrophage cell line (7).

The effects of the NBD peptides in vivo were tested in two distinct experimental mouse models of acute inflammation. Ear edema induced with phorbol 12-myristate 13-acetate (PMA) (20, 21) was reduced by the wild-type peptide (77 ± 3% inhibition) as effectively as dexamethasone (82 ± 9% inhibition), whereas the mutant was less effective (27 ± 9%) (Fig. 5C). Neither peptide had

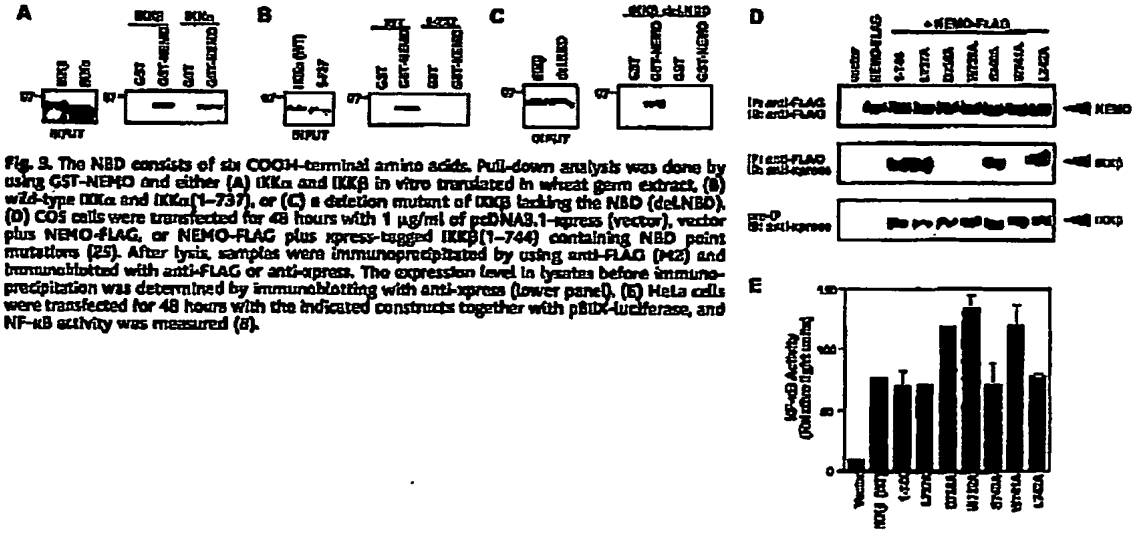

Fig. 3. The NBD consists of six COOH-terminal amino acids. Pull-down analysis was done by using GST-NEMO and either (A) IKKα and IKKβ in vitro translated in wheat germ extract, (B) wild-type IKKα and IKKα(1–737), or (C) a deletion mutant of IKKβ lacking the NBD (delNBD). (D) COS cells were transfected for 48 hours with 1 μg/ml of pcDNA3.1-xpress (vector), vector plus NEMO-FLAG, or NEMO-FLAG plus xpress-tagged IKKβ(1–744) containing NBD point mutations (25). After lysis, samples were immunoprecipitated by using anti-FLAG (M2) and immunoblotted with anti-FLAG or anti-xpress. The expression level in lysates before immunoprecipitation was determined by immunoblotting with anti-xpress (lower panel). (E) HeLa cells were transfected for 48 hours with the indicated constructs together with pBIIX-luciferase, and NF-κB activity was measured (8).

any effect in the absence of PMA (*17*). In another model, peritonitis was induced in mice by intraperitoneal injection of zymosan, either alone or in combination with dexamethasone or the NBD peptides (*22*, *23*). Zymosan injection caused accumulation of inflammatory exudate fluids and migration of polymorphonuclear cells into the peritoneum that was inhibited by dexamethasone and the wild-type, but not the mutant, NBD peptide (Fig. 5D). Dexamethasone and wild-type peptide also reduced NO accumulation in the peritoneum of these animals (*7*). We therefore conclude that the wild-type NBD peptide is an effective inhibitor of inflammation in these experimental models.

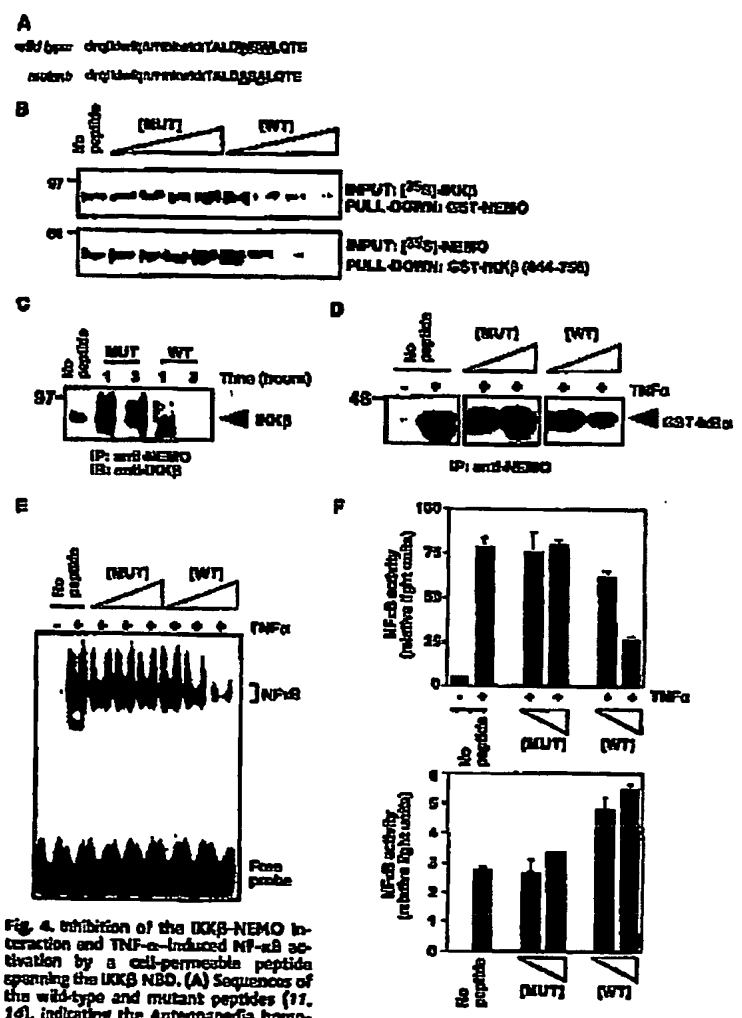

Fig. 4. Inhibition of the IKKβ-NEMO interaction and TNF-α–induced NF-κB activation by a cell-permeable peptide spanning the IKKβ NBD. (**A**) Sequences of the wild-type and mutant peptides (*11*, *14*), indicating the Antennapedia homeodomain (*15*) (lower case) and IKKβ (upper case) segments. Positions of the W⇒A mutations are underlined. (**B**) GST pull-down analysis was done with either GST-NEMO with in vitro translated IKKβ (upper panel) or GST-IKKβ(644–756) with in vitro translated NEMO (lower panel) in the absence (no peptide) or presence of 125, 250, 500, or 1000 μM of either mutant (MUT) or wild-type (WT) NBD peptide. (**C**) HeLa cells were incubated with either peptide (200 μM) for the times indicated and the IKK complex was immunoprecipitated by using anti-NEMO. The resulting immunoblot was probed with anti-IKKβ. (**D**) The IKK complex was immunoprecipitated by using anti-NEMO from HeLa cells treated with the peptides (100 or 200 μM) for 3 hours followed by incubation with TNF-α (10 ng/ml) (+) for 5 min and used for immune-complex kinase assay (*16*). (**E**) HeLa cells were incubated for 3 hours with 50, 100, or 200 μM of each peptide followed by treatment for 15 min with TNF-α (10 ng/ml) (+). EMSA was performed by using nuclear extracts and a specific κB-site probe as previously described (*26*). (**F**) NF-κB activity (*5*) in HeLa cells transfected with pBIIX-luciferase and incubated for 2 hours in the absence or presence of NBD peptides (100 and 200 μM) then treated for 4 hours with TNF-α (+ in upper panel) or untreated (lower panel).

In summary, we have identified the structural requirements for the association of NEMO with the IKKs and revealed that NEMO not only functions in the activation of IKKβ (*1*–*5*), but may also suppress the intrinsic, basal activity of the IKK complex. Drugs targeting the IKK-NEMO interaction may be of clinical importance for the control of inflammation, and as the NBD is only six amino acids long, it should be possible to design peptidomimetic compounds that disrupt the NEMO-IKK interaction. Such drugs would prevent activating signals from reaching the IKK complex, yet maintain a low level of NF-κB activity that may be required to avoid potential toxic side effects.

References and Notes

1. S. Yamaoka *et al.*, *Cell* **93**, 1231 (1998).
2. D. M. Rothwarf, E. Zandi, G. Natoli, M. Karin, *Nature* **395**, 297 (1998).
3. F. Mercurio *et al.*, *Mol. Cell. Biol.* **19**, 1526 (1999).
4. E. W. Hanhoj and S. C. Sun, *J. Biol. Chem.* **274**, 22911 (1999); Z. L. Chu, Y. A. Shin, J. M. Yang, J. A. DiDonato, D. W. Ballard, *J. Biol. Chem.* **274**, 15297 (1999); D.-Y. Jin, V. Giordano, K. V. Kibler, H. Nakano, K.-T. Jeang, *J. Biol. Chem.* **274**, 17402 (1999). S. Q. Zhang, A. Kovalenko, G. Cantarella, D. Wallach, *Immunity* **12**, 301 (2000).
5. D. Rudolph *et al.*, *Genes Dev.* **14**, 854 (2000).
6. IKKα and IKKβ were gifts from M. Karin (University of California, San Diego). All subcloning and mutagenesis were done by polymerase chain reaction (PCR) using cloned *Pfu* DNA polymerase (Stratagene, La Jolla, CA) (*7*). Human NEMO cDNA was obtained by reverse transcriptase (RT)–PCR from HeLa cell mRNA using the Expand Long Template PCR System (Boehringer Mannheim, Mannheim, Germany) (*7*). For in vitro pull-down assays (*24*), proteins were expressed and [^{35}S]methionine-labeled by in vitro transcription and translation using rabbit reticulocyte lysates or wheat germ extracts (Promega, Madison, WI).
7. Supplementary material is available to Science Online subscribers www.sciencemag.org/feature/data/1052581.shl.
8. HeLa and COS cells were seeded into either 24-well (16-mm, 1 × 10^5 cells/well) or 6-well (35-mm, 5 × 10^5 cells/well) plates and grown for 24 hours before transfection of DNA (1 μg/ml) by using Fugene6 (Roche, Basel, Switzerland). After 48 hours, cells were lysed with TNT (200 mM NaCl, 20 mM Tris, pH 8.0, 1% Triton X-100), and samples were used for immunoprecipitation (*25*) or luciferase assay (Promega luciferase assay system).
9. J. Ye, X. Xie, L. Tarassishin, M. S. Horwitz, *J. Biol. Chem.* **275**, 9882 (2000).
10. M. Delhase, M. Hayakawa, Y. Chen, M. Karin, *Science* **284**, 309 (1999).
11. Single-letter abbreviations for the amino acid residues are as follows: A, Ala; C, Cys; D, Asp; E, Glu; F, Phe; G, Gly; K, Lys; L, Leu; M, Met; N, Asn; Q, Gln; R, Arg; S, Ser; T, Thr; V, Val; and W, Trp.
12. Y. Shimada *et al.*, *Int. Immunol.* **11**, 1357 (1999).
13. K. Takeda *et al.*, *Science* **284**, 313 (1999); Y. Hu *et al.*, *Science* **284**, 316 (1999); Q. Li *et al.*, *Genes Dev.* **13**,

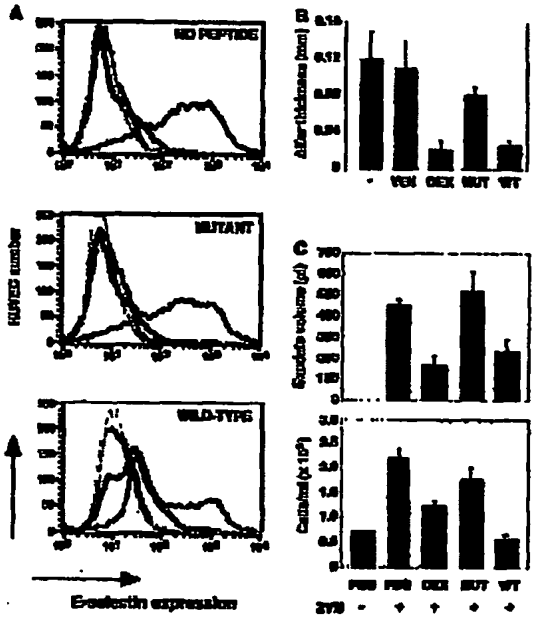

Fig. 5. The wild-type NBD peptide inhibits NF-κB–induced gene expression and experimentally induced inflammation. (A) Human umbilical vein endothelial cells were incubated for 2 hours with mutant (middle) or wild-type (bottom) NBD peptides (100 μM) then stimulated with TNF-α (10 ng/ml) for 6 hours. Control cells (top) received no peptide. Cells were stained with either anti–E-selectin (1.2B6/16) and expression was measured by FACS [FACSort, Becton Dickinson, Paramus, NJ (27)]. The profiles show E-selectin staining in the absence (black) and presence (red) of TNF-α and control antibody staining under the same conditions (blue, no TNF-α; green, +TNF-α). (B) PMA-induced ear edema in mice topically treated with vehicle (VEH), dexamethasone (DEX) or NBD peptides was measured as described (20, 27). (C) The effects of the NBD peptides and dexamethasone (DEX) on Zymosan (ZYM)–induced peritonitis in mice were determined as described (22). Control mice were injected with phosphate-buffered saline (PBS).

1222 (1999); Q. Li, D. Van Antwerp, F. Mercurio, K. F. Lee, I. M. Verma, *Science* 284, 321 (1999); Z. W. Li *et al.*, *J. Exp. Med.* 189, 1839 (1999); M. Takeda *et al.*, *Immunity* 10, 421 (1999).

14. The sequences of the NBD peptides are shown in Fig. 5A (17). Both peptides were dissolved in dimethyl sulfoxide (DMSO) to a stock concentration of 20 mM. Unless shown, DMSO controls were no different from no peptide controls.

15. D. Devaux, A. H. Joliot, G. Chassaing, A. Prochiantz, *J. Biol. Chem.* 268, 10444 (1994); H. Hall *et al.*, *Curr. Biol.* 6, 580 (1996); E. Hälbt and S. Ozes, *J. Exp. Med.* 189, 1707 (1999).

16. Precipitated immune complexes were washed with TNT and kinase buffer (20 mM Hepes, pH 7.5, 20 mM $MgCl_2$, 1 mM EDTA, 2 mM NaF, 2 mM β-glycerophosphate, 1 mM dithiothreitol, 10 μM ATP) then incubated for 15 min at 30°C in 20 μl of kinase buffer containing GST-IκBα(1–90) and 10 μCi [γ-^{32}P]ATP (Amersham Pharmacia Biotech, Uppsala, Sweden). The phosphorylated substrate was precipitated by using glutathione-agarose (Amersham Pharmacia Biotech), separated by SDS–polyacrylamide gel electrophoresis (SDS-PAGE, 10%) and visualized by autoradiography.

17. M. J. May *et al.*, unpublished data.

18. M. J. May and S. Ghosh, *Semin. Cancer Biol.* 9, 63 (1997); S. Ghosh, M. J. May, E. B. Kopp, *Annu. Rev. Immunol.* 16, 225 (1998).

19. J. S. Pober *et al.*, *J. Immunol.* 136, 1680 (1986); M. P. Bevilacqua *et al.*, *Proc. Natl. Acad. Sci. U.S.A.* 84, 9238 (1987); T. Collins *et al.*, *FASEB J.* 9, 899 (1995).

20. Ear edema was induced in replicate groups of mice (C57BL/6NCR) as described previously (27). Briefly, 20 μl of either NBD peptide (200 μg/ear), dexamethasone (40 μg/ear) or vehicle (DMSO:ethanol, 13:79 v/v) was applied to the right ear of mice 30 min before and 15 min after the application of 20 μl of PMA (5 μg/ear) dissolved in ethanol. Swelling was measured 6 hours after PMA application by using a micrometer (Mitutoyo America, Aurora, IL) and expressed as the mean difference in thickness between the treated and untreated ears.

21. J. Chang, E. Staub, M. Shamonki, L. Marinaki, R. P. Carlson, *Eur. J. Pharmacol.* 142, 197 (1987).

22. Zymosan-induced peritonitis, measurement of peritoneal exudates and inflammatory cell collections from replicate groups mice (C57BL/6NCR) were performed as described previously (23). Animals were injected concomitantly with 1 ml zymosan (1 mg/ml) and either dexamethasone (100 μg/ml) or the NBD peptides (200 μg/ml).

23. S. J. Getting, R. J. Flower, M. Perretti, *Br. J. Pharmacol.* 120, 1073; M. N. Ajuebor, L. Virag, R. J. Flower, M. Perretti, C. Szabo, *Immunology* 95, 625 (1998).

24. H. Zhang, H. Sun-Wang, H. Erdjument-Bromage, P. Tempst, S. Ghosh, *Cell* 89, 413 (1997).

25. For immunoprecipitations, HeLa or COS cells grown in 6-well (35 mm) trays were lysed in 500 μl TNT. Transfected FLAG-tagged proteins were precipitated for 2 hours at 4°C by using 20 μl of anti-FLAG (M2)-conjugated agarose beads (Sigma). Endogenous IKKβ or NEMO were immunoprecipitated by using 1 μg of specific polyclonal antibodies (Santa Cruz Biotechnology, Santa Cruz, CA) plus 20 μl of Protein-A Sepharose (Amersham Pharmacia Biotech). For immunoblotting, precipitates were washed with TNT twice, and PBS then suspended in SDS-sample buffer. Proteins were separated by SDS-PAGE (10%), transferred to polyvinylidene difluoride membranes, and visualized by enhanced chemiluminescence (Amersham Pharmacia Biotech).

26. E. B. Kopp and S. Ghosh, *Science* 265, 956 (1994).

27. L. A. Madge, M. R. Sierra-Honigmann, J. S. Pober, *J. Biol. Chem.* 274, 15643 (1999).

28. Supported by the Howard Hughes Medical Institute and NIH (AI 43443), the Irvington Institute for Immunological Research (M.J.M), and a grant from ISIS Pharmaceuticals (L.A.M). We thank D. Schatz, M. Solomon, and A. Horwich for critically reading the manuscript.

23 May 2000; accepted 29 June 2000

Predictions of Biodiversity Response to Genetically Modified Herbicide-Tolerant Crops

A. R. Watkinson,[1]* R. P. Freckleton,[1]† R. A. Robinson,[2] W. J. Sutherland[1]

We simulated the effects of the introduction of genetically modified herbicide-tolerant (GMHT) crops on weed populations and the consequences for seed-eating birds. We predict that weed populations might be reduced to low levels or practically eradicated, depending on the exact form of management. Consequent effects on the local use of fields by birds might be severe, because such reductions represent a major loss of food resources. The regional impacts of GMHT crops are shown to depend on whether the adoption of GMHT crops by farmers covaries with current weed levels.

There is a growing research interest in the potential effects of the release of genetically modified (GM) crops (*1*) on biodiversity. This is prompted by concerns relating to the direct impact of GM crops on target organisms and the indirect effects on the wider environment. The environmental debate has to be set within a biodiversity landscape that is already affected by the intensification of agriculture (*2*). Although, in some senses, the introduction of GM crops may be no different than the introduction of any other technology that leads to the further intensification of agriculture, this new technology might offer a

APPLICATION DATA SHEET

APPLICATION INFORMATION

Application Type::	PROVISIONAL
Subject Matter::	UTILITY
CD-ROM or CD-R?::	NONE
Title::	SELECTIVE INHIBITION OF NF-KB ACTIVATION BY PEPTIDES DESIGNED TO DISRUPT NEMO OLIGOMERIZATION
Attorney Docket Number::	243238US0PROV
Total Drawing Sheets::	45

INVENTOR INFORMATION

Applicant Authority Type::	INVENTOR
Primary Citizenship Country::	France
Status::	FULL CAPACITY
Given Name::	Fabrice
Family Name::	Agou
City of Residence::	Paris
Country of Residence::	France
Street of Mailing Address::	21, avenue du Bel-Air
City of Mailing Address::	Paris
Country of Mailing Address::	France
Postal or Zip Code of Mailing Address::	75012

Applicant Authority Type::	INVENTOR
Primary Citizenship Country::	France
Status::	FULL CAPACITY
Given Name::	Gilles
Family Name::	Courtois
City of Residence::	Paris
Country of Residence::	France
Street of Mailing Address::	157, rue de Menilmontant
City of Mailing Address::	Paris
Country of Mailing Address::	France
Postal or Zip Code of Mailing Address::	75020

Applicant Authority Type::	INVENTOR
Primary Citizenship Country::	France
Status::	FULL CAPACITY
Given Name::	Alain
Family Name::	Isreal
City of Residence::	Paris
Country of Residence::	France
Street of Mailing Address::	20, rue Daguerre
City of Mailing Address::	Paris
Country of Mailing Address::	France
Postal or Zip Code of Mailing Address::	75014

Applicant Authority Type::	INVENTOR
Primary Citizenship Country::	France
Status::	FULL CAPACITY
Given Name::	Michel
Family Name::	Veron
City of Residence::	Paris
Country of Residence::	France
Street of Mailing Address::	16, rue de Fourcy
City of Mailing Address::	Paris
Country of Mailing Address::	France
Postal or Zip Code of Mailing Address::	75004

Applicant Authority Type::	INVENTOR
Primary Citizenship Country::	France
Status::	FULL CAPACITY
Given Name::	Francois
Family Name::	Traincard
City of Residence::	Issy-les-Moulineaux
Country of Residence::	France
Street of Mailing Address::	21, rue Jules Guesde
City of Mailing Address::	Issy-les-Moulineaux
Country of Mailing Address::	France
Postal or Zip Code of Mailing Address::	92130

Applicant Authority Type::	INVENTOR
Primary Citizenship Country::	Japan
Status::	FULL CAPACITY
Given Name::	Shoji
Family Name::	Yamaoka
State or Province of Residence::	Tokyo
Country of Residence::	Japan
Street of Mailing Address::	Yushima 1-5-45 Bunkyo-ku
State or Province of Mailing Address::	Tokyo
Country of Mailing Address::	Japan

CORRESPONDENCE INFORMATION

Correspondence Customer Number::	22850

REPRESENTATIVE INFORMATION

Representative Customer Number::	22850

This Page is Inserted by IFW Indexing and Scanning Operations and is not part of the Official Record

BEST AVAILABLE IMAGES

Defective images within this document are accurate representations of the original documents submitted by the applicant.

Defects in the images include but are not limited to the items checked:

- ☑ BLACK BORDERS
- ☑ IMAGE CUT OFF AT TOP, BOTTOM OR SIDES
- ☑ FADED TEXT OR DRAWING
- ☑ BLURRED OR ILLEGIBLE TEXT OR DRAWING
- ☐ SKEWED/SLANTED IMAGES
- ☐ COLOR OR BLACK AND WHITE PHOTOGRAPHS
- ☐ GRAY SCALE DOCUMENTS
- ☑ LINES OR MARKS ON ORIGINAL DOCUMENT
- ☐ REFERENCE(S) OR EXHIBIT(S) SUBMITTED ARE POOR QUALITY
- ☐ OTHER: _____

IMAGES ARE BEST AVAILABLE COPY.
As rescanning these documents will not correct the image problems checked, please do not report these problems to the IFW Image Problem Mailbox.